INL/EXT-09-16857

Transmutation Dynamics: Impacts of Multi-Recycling on Fuel Cycle Performances

S. Bays
S. Piet
M. Pope
G. Youinou
A. Dumontier
D. Hawn

September 2009

The INL is a U.S. Department of Energy National Laboratory
operated by Battelle Energy Alliance

INL/EXT-09-16857
AFCI-SYSA-PMO-MI-DV-2009-000185

Transmutation Dynamics: Impacts of Multi-Recycling on Fuel Cycle Performances

S. Bays
S. Piet
M. Pope
G. Youinou
A. Dumontier
D. Hawn

September 2009

Idaho National Laboratory
Idaho Falls, Idaho 83415

http://www.inl.gov

Prepared for the
U.S. Department of Energy
Office of Nuclear Energy
Under DOE Idaho Operations Office
Contract DE-AC07-05ID14517

SUMMARY

From a physics standpoint, it is feasible to sustain continuous multi-recycle in either thermal or fast reactors. In Fiscal Year 2009, transmutation work at INL provided important new insight, caveats, and tools on multi-recycle. This work entails new data and calculation methods for systematic evaluation of fuel cycle options, allowing comparison of key physics related in-core and out-of-core performances.

Multi-recycle of MOX, even with all the transuranics, is possible provided continuous enrichment of the uranium phase to ~6.5% while limiting the transuranic enrichment to slightly less than 8% to satisfy the expected void reactivity constraint. Multi-recycle of heterogeneous-IMF assemblies is possible with continuous enrichment of the UOX pins to ~4.95% and having ≤60 of the 264 fuel pins being inter-matrix. A new tool enables quick assessment of the impact of different cooling times on isotopic evolution. The effect of cooling time was found to be almost as controlling on higher mass actinide concentrations in fuel as the selection of thermal versus fast neutron spectra. A new dataset was built which provides on-the-fly estimates of gamma and neutron dose in MOX fuels as a function of the isotopic evolution. All studies this year focused on the impact of dynamic feedback due to choices made in option space. Both the equilibrium fuel cycle concentrations and the transient time to reach equilibrium for each isotope were evaluated over a range of reactor, reprocessing and cooling time combinations. New bounding cases and analysis methods for evaluating both reactor void reactivity and radiation worker safety were established. This holistic collection of physics analyses and methods gives improved resolution of fuel cycle options, and impacts thereof, over that of previous ad-hoc and single-point analyses.

The buildup of problem isotopes in both thermal and fast systems was found to be controlled by the presence of gateway isotopes in the fuel. Gateway isotopes are governed by similar transmutation physics as U-238 but instead of breeding Pu-239, they breed curium and the higher mass actinides. It is the buildup of these transmutation products, Cm, Bk, and Cf, which pose an issue to out-of-core fuel handling operations because of their associated intense decay heat and radiation fields. Gateway Pu-242 and Am-243 are formed in Light Water Reactors (LWR) and then are externally fed to the burner reactor as its make-up fuel. The external supply of these gateway isotopes behaves as an external driving force towards the creation and buildup of Cm-Bk-Cf in the fuel cycle, analogous to plutonium breeding from uranium. The lower the burner reactor's conversion ratio, the higher the external feed of LWR TRU and therefore the gateway isotopes. Hence, the Cm-Bk-Cf buildup over successive recycles is greater for lower conversion ratio. In this report, the authors consider the dynamic transmutation feedback caused by gateway isotopes in burner reactors: MOX-UE, heterogeneous-IMF and Sodium cooled Fast Reactor (SFR). The principle findings are:

- The equilibrium concentration and equilibration time of key problem isotopes in the fuel cycle is strongly dictated by whether or not curium, and americium to a lesser extent, are recycled or discarded during reprocessing.
- The post-irradiation cooling time can be nearly as controlling a parameter on the buildup performances of some isotopes as the energy of neutrons used in the transmutation reactor. The alpha, gamma and neutron radiologic source intensities per assembly of MOX-UE and SFR are generally within one order of magnitude of each other for the first 50-75 years of recycling.
- Increasing decay time can significantly delay the buildup of certain problem isotopes at the expense of degrading the fuel value due to loss of fissile Pu-241, resulting in a front-end versus back-end economic trade-off that requires further trade studies to quantify.
- Sustained recycle of MOX-UE and heterogeneous-IMF is feasible, from a physics perspective, with enriched uranium support. The fleet average support ratio between MOX-UE and UOX

fuels was found to be comparable for analogous scenarios using fast reactors. The MOX-UE support ratio varied from ~30% to ~70% for Pu-only to all-TRU recycling, respectively. A complimentary study of heterogeneous-IMF support ratios is recommended for future work.

- The void coefficient calculations highlighted the importance of the MAs on this safety-related parameter. Indeed the void coefficient limits the Pu content at about 10% when only this element is recycled whereas when Np, Am and Cm are recycled as well the PuNpAmCm content should be ≤8%, and possibly slightly smaller if recycling Am and Cm. To relax the void performance limitations caused by Am and Cm (i.e., the minor actinides, MA) in LWR fuel, a study on the lumping of MAs into target pins is recommended for future work. A target pin approach could also have dual benefit as a burnable poison, which gives a potential for economic benefit.

- A methodology was developed for quick investigations of impacts to reactor coolant void worth associated with multi-recycle of americium and curium in SFRs. This method was only tested for a single SFR scenario. A comprehensive study of void coefficients contrasting multiple conversion ratios and MA-to-plutonium ratios is recommended for future work.

- The expected radiation dose to fuel fabrication workers of MOX-UE was evaluated. An isotope-by-isotope dose contribution library for MOX-UE was also generated for future dose-calculator purposes. This tabulation method was able to accurately represent the spontaneous fission and alpha,n, (and gamma with limitations) contributions to dose. A complimentary SFR study is recommended for future work. This information will ultimately prove useful for demonstrating bounding cases that indicate when glove-box or hot-cell fuel handling operations are more applicable.

This work also supported parallel research efforts. The Losses study is a task undertaken to understand the reactivity penalties and associated detriment of fuel value by tolerating imperfect removal of fission products during recycling resulting in neutron poison isotopes in the fresh fuel. The Minor Actinide study compared the reactivity penalty of irradiating TRU in MOX prior to being introduced to SFRs versus simply allowing the TRU to sit for the equivalent amount of time.

In support of the Losses study, the fission product production, neutron capture, and differential reactivity was examined for fast reactor metal fuel (CR=0.50), fast reactor oxide fuel (CR=0.50), and LWR MOX-Pu. Current Fuel Campaign working limits were extended by chemical element analogy to all elements from H to Th and Fuel limits for groups of elements were evenly divided among elements in that group for exploratory assessments. The fission yield of elements Se through Dy are sufficiently high that they must be removed before subsequent recycle. The tolerable fraction of these fission products remaining in recycled fuel is lower than 0.1% for some individual elements. Other participants in the Losses study show the upper bound reactivity impact of impurities if kept at Fuel Campaign working limits is below 1% in fast reactors and below 4% for LWR MOX-Pu.

In support of the Minor Actinide study, the fuel value of MA recovery from UOX separation was assessed via three scenarios: 1) discard MA from UOX, use MOX-Pu, 2) keep all MA, use MOX-Pu, 3) keep all MA, no MOX. Each scenario is taken through to equilibrium. The MOX scenarios produce more 5-7% more electricity and the advantage is front loaded in time because the MOX recycle starts before the SFR recycle. However, the higher SFR fuel burnup causes the MOX scenarios to require 3-4% more separation flow per electricity produced. The FR disadvantage arises because it is operating at a transuranic conversion ratio of 0.5, whereas MOX is 0.70-0.75. In this instance the UOX-MOX-SFR have the benefit of consuming all the transuranics plus a slightly higher global transuranic conversion ratio due to one MOX recycle. Of course, this conclusion would be reversed if the fast reactor had a higher conversion ratio than that of MOX.

CONTENTS

FIGURES

TABLES

ACRONYMS

AFCI	Advanced Fuel Cycle Initiative
BU	Burnup, measure of fission energy produced per initial heavy metal of nuclear fuel
CR	Transuranic Conversion Ratio (TRU produced/TRU destroyed)
CY	Calendar Year
DU	Depleted uranium, the low U-235 content tailings from uranium enrichment
E-chem	Electrochemical separation, also known as pyroprocessing
EU	Enriched uranium, the high U-235 content uranium produced by uranium enrichment
FPY	Full Power Year
GWe	Gigawatt-electric
GWth	Gigawatt-thermal
GW-day/tonne	Gigawatt-thermal – Day per Metric Ton, a unit of nuclear fuel burnup
HM	Heavy Metal
I_∞	Fresh fuel concentration of an isotope in the equilibrium fuel cycle
IMF	Inert Matrix Fuel (thermal reactor fuel without uranium)
INL	Idaho National Laboratory
kt	Kilotonne
LMFBR	Liquid Metal cooled Fast Breeder Reactor
LWR	Light Water Reactor
LWR MOX	MOX fuel in Light Water Reactors
MA	Minor Actinide (All non-plutonium transuranics)
MOX	Mixed Oxide fuel, a mixture of uranium oxide and one or more transuranic element oxides, e.g. MOX-Pu or MOX-TRU
MOX-UE	MOX fuel with the uranium phase being enriched in the U-235 isotope
MRS	Managed Retrievable Storage
MRTAU	Multi-Reactor Transmutation Analysis Utility
MT	Montana, sometimes used as metric ton (1000 kg)
NRC	Nuclear Regulatory Commission
pcm	Reactivity unit – percent milli-rho ($\rho \times 10^5$)
R_{95}	Number of recycles for the fresh fuel concentration of an isotope to reach 95% of its equilibrium fuel cycle value
RU	Recovered uranium from a separation process
SFR	Sodium cooled Fast Reactor
SNF	Spent Nuclear Fuel, also called used fuel
t	Tonne (metric ton)
t_{95}	Time for the fresh fuel concentration of an isotope to reach 95% of its equilibrium fuel cycle value (i.e., over multiple recycles)
T&P	Transmutation and Partitioning
TRU	Transuranics
UOX	Uranium Oxide
VHTR	Very High Temperature Reactor
VISION	Verifiable Fuel Cycle Simulation

TERMINOLOGY

Adjusted composition	The input/output composition resulting from the Winery adjustment methods described in this report. During the time period that the adjusted composition is in force, it is used in the simulation as a replacement to the initial composition. Initially, the plan is for the input and output compositions to be adjusted every 5 years, in conjunction with changes to the initial recipes. Compare: adjusted, available, initial, real composition.
Available composition	The input composition available in the simulation in a given time step. Compare: adjusted, available, initial, real composition.
Burnup-dependent	Cross-section and flux data that is a function of fuel burnup
Burnup-step	A set of unique 1-group cross-section, flux, power level and actinide losses efficiency corresponding to a discretized period of time within a recycle-period, used by the MRTAU code
Criticality	An indication of growth, decline or sustainability of a chain reaction
Decay products	Decay products of uranium, specifically Pb, Bi, Ra, Ac, Th, Pa
Transuranic Burner, Fast burner or converter reactor	A fast reactor with conversion ratio < 1
Fast breeder reactor	A fast reactor with conversion ratio > 1
Fertile	Any isotope considered to be transmutable into a fissile isotope
Fissile	Capable of fission by absorption of a neutron of zero added kinetic energy
Fissile breeding ratio	The ratio of creation of fissile isotopes divided by the loss of fissile isotopes from all processes. Sometimes in literature, all-transuranics has been classified as a fissile species used in this definition. Compare with transuranic conversion ratio.
Fission	A type of actinide isotope transmutation that converts an isotope into at least two lighter isotopes, releasing energy and neutrons. Compare with neutron capture, radioactive decay.
Fuel value	Alternative measures of reactivity required to sustain a fuel burnup, used to contrast different fuel recipes (e.g., uranium resource saved)
Gain	The ratio of isotope concentration in the fuel at the end divided by that at the beginning of a recycle-period; also common nomenclature in dynamic mechanical and electrical systems analysis
Gateway isotope	Isotope of central importance in a given transmutation chain such that its partitioning during recycle results in greatly reduced buildup of its transmutation daughters in the fuel cycle
Group 1A/2A	Alkali/Alkali earths, specifically Rb, Sr, Cs, Ba. For fuel cycle management, the most important radioactive Group 1A/2A are Sr-90, Cs-134, Cs-135, Cs-137.
Halogens	Group VII of the Periodic Table, specifically Br and I. For fuel cycle management, the most important radioactive halogen is I-129.
Inert gases	Group O of the Periodic Table, specifically Kr and Xe. For fuel cycle management, the most important radioactive inert gases are Kr-81 and Kr-85.
Initial composition	The input/output composition recipes corresponding to the case being simulated in VISION, e.g., uranium oxide at 51 GW-day/tonne-HM burnup (UOX-51) or metal fast reactor fuel for TRU conversation ratio=0.50 based on 5-year old feed from UOX-51. Compare: adjusted, available, initial, real composition.
Lanthanides	Elements La through Lu. For fuel cycle management, the most important isotopes are Ce-144, Pm-147, Sm-146, Sm-147, Sm-151, Eu-154, Eu-155, Ho-166m.
Minor actinides	Transuranic isotopes other than plutonium, specifically Np, Am, Cm, Bk, Cf.
Neutron absorption	The sum of neutron capture, fission, and other neutron multiplication reactions

	such as n,2n, n,3n, etc.
Neutron capture	A type of isotope transmutation that converts an isotope into a heavier isotope, typically releasing a gamma-ray. Compare with fission, radioactive decay, and neutron multiplication.
Partitioning	Separation of one actinide mass flow from another via reprocessing
Phantom	Computational or experimental model equivalent of a human being for the purposes of measuring radiation deposition in human tissue
Pyroprocessing	A type of electrochemical spent fuel reprocessing involving high temperature and molten salt solutions
Radioactive decay	A type of isotope transmutation in which a nucleus seeks a more stable or non-radioactive condition by emitting an alpha, beta particle, gamma, or neutron. Compare with transmutation via fission or neutron capture.
Radiotoxicity	Is a measure of the radiation hazard toxicity due to the radiation from isotopes that are ingested, inhaled, or absorbed
Reactivity	The fractional difference between two neutron criticality states
Real composition	An actual set of input/output recipes corresponding to an adjusted composition. For example, to test the methods, consider a initial composition with TRU conversion ratio = 0.50. Then, using these methods, estimate the recipe for ratio = 0.75 and then compare with the actual input/output recipes for 0.75. Compare: adjusted, available, initial, real composition.
Recipe	A fresh fuel or spent fuel fractional composition containing sufficient isotope and lumped isotope information to represent all relevant mass flows in the nuclear fuel cycle as modeled by VISION
Recycle-frequency	One divided by the recycle-period
Recycle-loop	One iteration of the recycle-period in the MRTAU multi-recycle scheme
Recycle-period	Time duration from fresh fuel creation to spent fuel recycle defined for the MRTAU code
Threshold-fission	A property of even-neutron numbered actinides; a fission process requiring an energy barrier to be overcome by the added kinetic energy of the incident neutron.
Transition metals	In this report, literally elements not otherwise categorized, including Se, Mo, Ru, Pd, Pd, Cd, Sn, Sb, Te.
Time-step	Discretization of time used in numerical computer methods
Transuranic	Isotopes above uranium in the Periodic Table, specifically Np, Pu, Am, Cm, Bk, Cf, (i.e., greater proton number than uranium)
Transmutation	The conversion of one thing into another
TRU conversion ratio (CR)	Ratio of transuranic material created divided by that destroyed by fission. Compare with transuranic conversion ratio.
VISION	The suite of Excel input files, Powersim core, and Excel output files that models the nuclear fuel cycle system., developed at INL
Worksheet (or page)	Worksheets within a spreadsheet file, worksheet names are in **bold** in this document

TRANSMUTATION DYNAMICS: IMPACTS OF MULTI-RECYCLING ON FUEL CYCLE PERFORMANCES

1. INTRODUCTION

Transmutation and partitioning (T&P) of actinide materials and fission products in nuclear reactors is the fundamentally governing process of operating a closed nuclear fuel cycle. In the nuclear fuel cycle, transmutation means the conversion of one isotope into another, typically by means of adding a neutron to an actinide atom to make a new isotope (i.e., physics: controlled by atomic neutron number). Partitioning typically is described as a process devised for dividing a spent fuel into single or groups of elemental constituents. As a general statement, partitioning employs chemical manipulation, capitalizing on properties associated with the element (i.e., chemistry: controlled by atomic proton number) classification of atoms in the spent fuel. With the exception of a few developmental industrial processes, such as laser enrichment, there is no isotopic manipulation during partitioning[a]. The compatibility of transmutation related processes with partitioning related processes creates complexity in the nuclear fuel cycle, particularly in a closed nuclear fuel cycle.

1.1 Background

There are essentially three types of transmutation: (1) fission, which converts an actinide into a lighter non-actinide, (2) neutron capture reaction, which converts an isotope into a heavier isotope, (3) radioactive decay, which is the property of an atom to seek a more stable or non-radioactive condition. Fission and capture transmutation are sensitive to the neutron energy spectrum specific to the reactor type. The third is a fundamental property belonging to each isotope. The neutron energy of Light Water Reactors (LWR) is *thermal* and thus has a higher probability for neutron capture than for fission. This leads to the buildup of plutonium isotopes heavier than Pu-239 in the fuel by the end of its life in the reactor. Similarly, fission-less transmutation of U-235 leads to the formation of U-236 and ultimately Np-237 which is a radiotoxicity burden for Spent Nuclear Fuel (SNF) disposal in a repository. Fission-less transmutation reactions in fissile atoms are undesirable from the standpoint of uranium resource utilization because they convert a fissile isotope into a non-fissile isotope. Once this occurs, typically many neutron capture transmutations are necessary to create a new fissile isotope. The reason for successive neutron captures follows from combinatory transmutation and decay paths leading to non-fissile minor actinides (MA). The need for many neutron capture transmutations favors a *fast* neutron energy reactor system with sufficient surplus neutrons to do the work of transmuting minor actinides into fissile isotopes where they can be ultimately destroyed by fission.

Fission-less transmutation of fissile isotopes are also undesirable from the standpoint of transuranic waste minimization. Fission-less transmutation of Pu-239 leads to formation of Pu-240 which is not fissile and thus readily capture transmutes into Pu-241. Pu-241 is fissile but is short-lived to the extent that it can not be effectively recovered for recycle into new fuel. Instead, much is lost by radioactive decay during the prerequisite cooling time before the SNF can be transported and recycled into new fuel. This isotopic decay loss of Pu-241 not only removes fissile material from the fuel cycle but creates an additional element, americium, with an isotope, Am-241, that negatively impacts repository storage. The amount of

[a] Elements are groups of atoms with the same proton number. Isotopes of elements have the same proton number but different neutron number. Isotopes belonging to the same element exhibit chemical properties specific to the element.

Pu-241 loss into Am-241 is dictated by decay time due to its relatively short 14.1 year half-life, which is on the order of the reactor charge-to-discharge period (i.e., in-core plus out-of-core times). Therefore, after multiple recycles, not only is the balance of Pu-241 and Am-241 in the fuel cycle affected by the reactor type but also the out-of-core time allowing for decay. Because Am-241 takes the form of an element separate from plutonium, partitioning it from plutonium adds complexity to fuel recycling processes. Because of its heat and radiotoxicity contributions to a geologic repository, it adds complexity to the repository design if not recycled.

Fission-less transmutation of Pu-241 forms the non-fissile isotope, Pu-242. Recycle and repository storage of this isotope is fairly benign. However, recycle and re-irradiation leads to successive fission-less transmutations and decays leading to Cm-244 via Am-243. Thus, Pu-242 and Am-243 are considered gateway isotopes leading to elements of curium and heavier. Cm-244 and the higher mass actinide elements, contribute significantly more radioactivity to the fuel cycle than the other lower-mass actinides. Elemental partitioning of americium can greatly reduce the accumulation of Cm-244 and higher mass actinides because it removes the *gateway*, Am-243. However, this brings about the issues of Am-241 disposal in a repository.

Loss of fissile isotopes either by fission-less transmutation or decay decreases the fissile worth of the fuel composition. Therefore, the economic *fuel value* is also reduced, requiring either a higher concentration of the fissile element or enrichment of the fertile element or both (e.g., MOX-UE). Thus, the loss of fuel value has an associated front-end economic cost. This would lead one to want to reduce the decay time as much as possible while at the same time making the spectrum as hard as possible in order to get the maximum fuel value. However, decreasing the decay time also decreases the amount of time for Cm-244 and higher mass actinides such as Cf-252 to decay away prior to back-end recycle processes. Increasing out-of-core decay time becomes a significant compromise in terms of the radiation fields associated with an increasing presence of un-decayed curium and higher mass actinides with successive recycle passes.

1.2 Report Organization

In order to explore the physics aspects of the aforementioned trade-off, this report is organized as follows. Chapter 1 is the Introduction. Chapter 2 discusses T&P effects of different fuel, reactor, and recycle options. Chapter 3 discusses the out-of-core decay time and reactor spectrum dependency effect on the magnitude and time-scale for achieving fuel cycle equilibrium. Chapter 4 discusses the affect on fuel value of 1-tier versus 2-tier recycle strategies as well as fuel value penalties associated with imperfect fission product removal during reprocessing. Chapter 5 gives results of an initial investigation into the sensitivity of reactor coolant reactivity void worth (an important parameter in gauging reactor safety) for both LWR MOX-UE fuel assemblies and fast burner reactor cores. Chapter 6 gives results for an initial investigation of fuel handler dose as a function of recycle/reactor-pass. Here the results are given for MOX but the methodology could easily be expanded to include fast reactor fuels. Chapter 7 is the report conclusion and provides summary comments.

2. Dynamic Fuel Cycle Analyses

This section summarizes understanding and comparisons among multi-recycle MOX [1], multi-recycle IMF [2,3], and fast reactors [4,5,6]. Though these are not the only transmutation options available, these particular fuel cycle systems have been the subject of intent study over the past several years for sustainable recycle of the TRU waste produced by conventional UOX fuels. Multiple previous studies have indicated that variations in the fuel isotopic composition for various actinide grouping options (i.e., partitioning scenarios), as well as variations due to multi-recycling, affect the out-of-core radiologic source terms, reactor safety and fuel performance. A comprehensive comparison of these different behaviors is made with some preliminary discussion on the isotopic dependencies of each effect.

2.1 Multi-Recycle of MOX-UE in LWRs

A goal this year was to improve the understanding of what LWRs can do with regard to recycling. In particular, we wanted to clarify the impact of recycling Np, Am, Cm-Bk-Cf versus just recycling Pu. For both MOX and IMF, we studied four MA partitioning strategies – Pu-only, PuNp, PuNpAm, and all-TRU. Each was calculated for 10 recycles and then an estimate made of the equilibrium input and output compositions. TRU elements are sent to waste only if deliberately left out of recycled material.

The report [1] presents the results of a neutronic analysis related to the homogeneous recycling of different TRU mixtures (Pu, PuNp, PuNpAm, PuNpAmCm or PuNpAmCmBkCf) in Pressurized Water Reactors (PWR) using MOX-UE fuel, i.e. MOX fuel with a U-235 enriched uranium support instead of the depleted uranium typical of standard MOX fuel today. It focuses mainly on reactor physics issues and does not deal with other issues like economics, fuel fabrication, transportation or reprocessing that are essential to assess a system as a whole.

With this in mind, and from a neutron physics point of view, the MOX-UE approach allows sustained multi-recycling of TRU as long as U-235 is available. The key caveat to this sustainable recycle is keeping the TRU content per heavy metal at a value that ensures a negative moderator void coefficient. Once this value is determined, the U-235 enrichment of the MOX-UE fuel is adjusted in order to reach the target burnup (51 GW-day/tonne in this study).

2.1.1 Method of Calculation

The calculations are carried out using the lattice physics capabilities of the SCALE5.1 code systems, i.e. the discrete-ordinates code NEWT coupled to the depletion code ORIGEN-S via the TRITON control module [7,8]. Using the discrete-ordinates approximation to the transport equation on an arbitrary grid, together with a 238-group neutron cross-section library based on ENDFB-VI, NEWT provides a robust and rigorous deterministic solution for non-orthogonal configurations.

The calculations carried out simulate the fuel cycle represented on the Figure 2-1 (example of Pu recycling). After each cycle, the amount of TRU initially loaded that disappeared by either fission, capture or decay is replaced by the same amount of TRU coming from UOX spent fuels. In other words, the TRU content at the MOX-UE fuel fabrication stage is the same at each cycle and the U-235 enrichment is adjusted in order to maintain a constant cycle length irrespective of degradation of the transuranic isotopes' fissile worth after multiple recycles. This can be expressed as follows for the different recycling strategies:

$$m_{X-fab}^{n+1} = m_{X-rep}^{n} + m_{X}^{SNF} = m_{X-fab}^{n} = m_{X-fab}^{n-1} = ... = K \qquad \text{Eqn 2-1}$$

Where: m^n_{X-fab} and m^n_{X-rep} are respectively the masses of TRU per ton of initial HM for the n^{th} fabrication and n^{th} reprocessing of the MOX-UE fuel (X = Pu or PuNp or PuNpAm or PuNpAmCm or PuNpAmCmBkCf depending on the recycling strategy) and m^{SNF}_X is the mass of TRU coming from reprocessed spent UOX (i.e., SNF) from LWRs and that must be blended with m^n_{X-rep} so that $m^{n+1}_{X-fab} = m^n_{X-fab}$.

The ratio $\frac{m^n_{X-rep}}{m^n_{X-fab}}$, which is equal to $\frac{m^n_{X-rep}}{m^{n+1}_{X-fab}}$ since m^{n+1}_{X-fab} is a constant, depends on the kind of TRU being recycled. For Pu or PuNp recycling it is typically around 0.75 whereas for PuNpAm or PuNpAmCm it is typically around 0.9.

We considered a 3-batch core with an average discharge burnup of 51 GW-day/tonne. The time between the end of the irradiation and the separation of the TRU from the SNF is taken to be 10 years and there is another year between the separation and the beginning of the next irradiation in order to take into account the time necessary for the fabrication and transportation. One cycle then corresponds to 1 year + 51 GW-day/tonne (1500 days) + 10 years ≅ 15 years. The losses at reprocessing are taken to be 0.1%, i.e. we consider that 99.9% of the elements being recycled are actually extracted and reused for the next cycle and that only 0.1% goes into the waste stream together with the fission products and the elements that are not recycled (Figure 2-1).

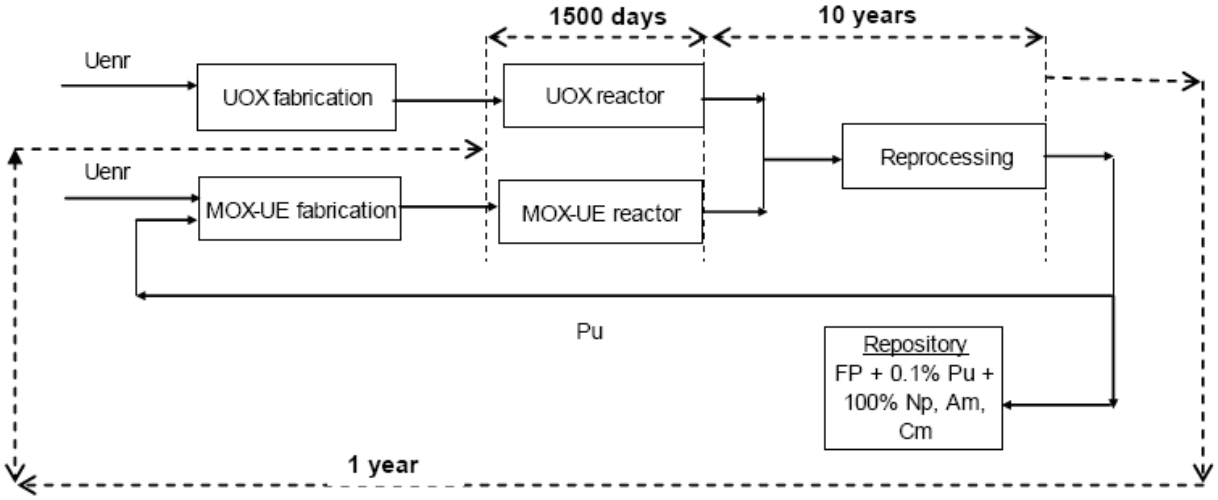

Figure 2-1. Transuranic recycling in a PWR fleet made up of UOX reactors and MOX-UE reactors.

2.1.2 Synopsis of Results

For the Pu only recycling case we chose to keep the Pu content equal to its first cycle value which is 10%. For the other cases (PuNp, PuNpAm, PuNpAmCm and PuNpAmCmBkCf) we chose to lower this value in order to ensure a negative void coefficient (i.e. the loss of the coolant brings imperatively the reactor to

a subcritical state). Since we consider PWRs entirely loaded with MOX-UE, and based on previous studies, we decided to limit the TRU content at 8%[b]. However, for partially loaded MOX-UE cores, i.e. containing for example only 30% or 50% of MOX-UE assemblies, the global void coefficient would be less of an issue and the TRU content in the MOX-UE assemblies could be higher but in this case the concern would lie in the power distribution between the UOX and the MOX-UE assemblies [9]. These aspects were not considered in this study but could be interesting to address in the future.

The first cycle does not require any U-235 enrichment in the case of Pu recycling if the Pu content is set at 10%, hence depleted uranium can be used (0.25% U-235). For the next cycles, the U-235 enrichment must be steadily increased because the Pu contains fewer and fewer of the fissile isotopes Pu-239 and Pu-241. For the Pu-only case the U-235 enrichment in fresh MOX-UE reaches a value equal to 90% of its asymptotic value (which is about 3.6% U-235 enrichment) after about 5 recycles. For the PuNp, PuNpAm, PuNpAmCm and PuNpAmCmBkCf cases, the necessary U-235 enrichments are higher than for the Pu-only case because the Pu enrichment in the Pu-only case was less than that of the other cases, and also because the MAs do not fission appreciably in a PWR neutron spectrum[c]. The U-235 enrichments vary between 0.25% (Pu-only) and 3.7% (all-TRU) for the first cycle depending on the MA that are recycled together with the Pu. The asymptotic values of the U-235 enrichment vary between 4.0% Pu-only and 6.6% (all-TRU). Knowing that the U-235 enrichment for the reference UOX fuel is 4.3%, the necessary MOX-UE U-235 enrichments might seem high. However, the situation is actually not as bad as it looks because the quality of the uranium at reprocessing is still very good. For example, for the PuNpAm recycling case, the necessary MOX-UE enrichment at equilibrium is about 6.6% but the reprocessed Uranium still contains about 3.95% of U-235 and only 0.7% U-236.

Multi-recycling the entirety of the Pu, or PuNp or PuNpAm or PuNpAmCm or PuNpAmCmBkCf necessitates the use of MOX-UE fuel in respectively about 32.5%, 41%, 62% 69% and 69% of the fleet. For a 100 GWe fleet producing 800 TWhe/year it translates into MOX-UE fabrication capacities of between 625 tHM/year (Pu case) and 1325 tHM/year (PuNpAmCm and PuNpAmCmBkCf cases). Since all the fuel assemblies are reprocessed, the reprocessing capacity has to be 1920 tHM/year. Logically, multi-recycling a specific element *drastically reduces* the amount of that element requiring disposal. However, multi-recycling *increases* the amount of heavier elements that require disposal. However, the balance is always positive, that is to say that the decrease in the mass requiring disposal (the element being multi-recycled) is always larger than the increase in the mass of heavier elements requiring disposal.

A preliminary assessment of the impact of recycling the recovered uranium from the MOX-UE fuel shows a clear incentive to investigate this option further. Indeed recycling recovered uranium significantly decreases the need for natural uranium. For the Pu multi-recycling case, relative to the reference UOX reactor fleet, the natural uranium economy goes from 8.5% when recovered uranium is not recycled to 21% when it is recycled. For the PuNpAm case, the differential is even more striking: relative to the same reference UOX reactor fleet, the natural uranium requirement goes from about +28% to -19%. This important information, i.e. multi-recycling Minor Actinides in a PWR fleet consumes less natural uranium than a UOX fleet even though the U-235 enrichment of the MOX-UE is higher than that of the reference UOX fuel, stems from the fact that the U reprocessed from the MOX-UE fuel still contains a lot of U-235.

---

[b] See Chapter 5 to see results of follow-on calculations that were performed to verify this assumption.

[c] The transuranic enrichment of the Pu-only case was 10% per HM, whereas the transuranic enrichment of all the other cases was 8% per HM.

The data presented in this report show that it would be possible to equalize TRU production and consumption in a PWR fleet with, depending on the TRU being recycled, between one third and two thirds of the fleet loaded with MOX-UE fuel. That means that if the whole fleet is loaded with MOX-UE fuel, then it becomes a net TRU burner, i.e. it can recycle its own TRU as well as some TRU coming from SNF accumulated over the past 30 years. A preliminary assessment shows that such a reactor fleet could accommodate about 12 tHM/year of PuNpAm coming from the SNF legacy in addition to its own. This 100% MOX-UE fleet would need about 30% less natural uranium than the reference UOX fleet.

The impact of the different recycling strategies at the fabrication and reprocessing has been evaluated. The most important effect is related to the neutron source at the fabrication when Cm is recycled. Indeed, in the PuNpAmCm case, it is between 50 and 400 times (1st and 10th recycling) higher than that of a standard MOX-Pu fuel that can be fabricated today at MELOX for example. The neutron source of the PuNpAmCmBkCf case is similar to that of the PuNpAmCm case up to the 6th recycling (i.e. 75 years after the beginning of the first recycling), when the build-up of Cf-252, even though present only in minute quantities (9 mg/tHM and 50 mg/tHM at the 6th and 10th recycling) brings about an even larger increase in the neutron source. Hence, the consequences of Cf-252 build-up would start to be noticeable only 75 years after the beginning of the first recycling which leaves time to find a way to flush these few grams of Cf per ton HM if it is deemed necessary (either through chemical extraction or, since Cf-252's half-life is only 2.6 years, simply by letting the fuel cool a few extra years)[d].

The fleet multi-recycling Pu at equilibrium needs about 8.5% less natural uranium than the reference UOX fleet. Multi-recycling Pun brings about an economy of only 2% compared to the reference UOX fleet whereas the PuNpAm and PuNpAmCm cases needs more natural uranium than the reference UOX fleet (respectively about +28% and +23%).

In terms of fuel performances, the presence of americium brings about an increase of the Helium production at 51 GW-day/tonne by about a factor of 2 compared to a standard MOX fuel mainly because of the higher Cm-242 production. Depending on how much of this helium is released, fuel designers will need to make sure the rods internal pressure does not exceed the allowable upper limit.

[d] See Chapter 3 for a detailed analysis of radiologic source term buildups as a function of recycling over multiple centuries

2.1.3 Isotopic Evolution over Multiple Recycles

Figure 2-2 through Figure 2-5 show the evolution of the multi-recycle MOX-UE system for the four scenarios – Pu-only, PuNp, PuNpAm, and all-TRU. The first three Figures show that there is little change, perhaps a factor of two for the higher TRU isotopes. An exception is U-235 and U-236 which climb as recycling starts. Figure 2-5, however, shows considerable evolution in the higher TRU isotopes when Cm, Bk, and Cf are recycled. As will be seen later, this higher mass actinide buildup results in an increase in neutron emission.

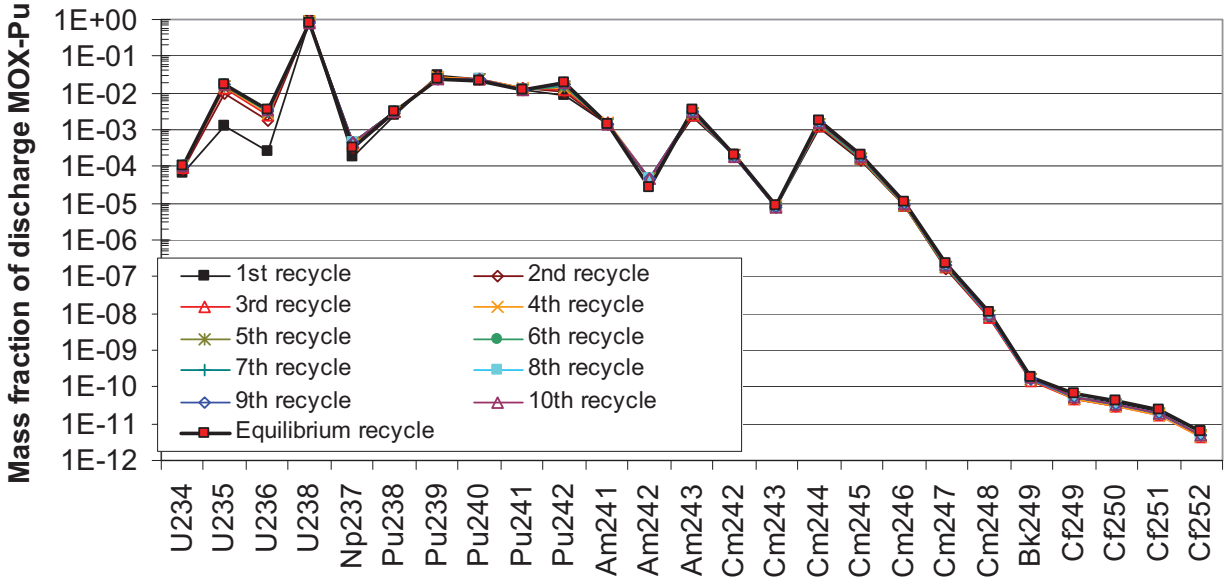

Figure 2-2. Evolution of discharge composition in MOX-UE Pu-only fuel

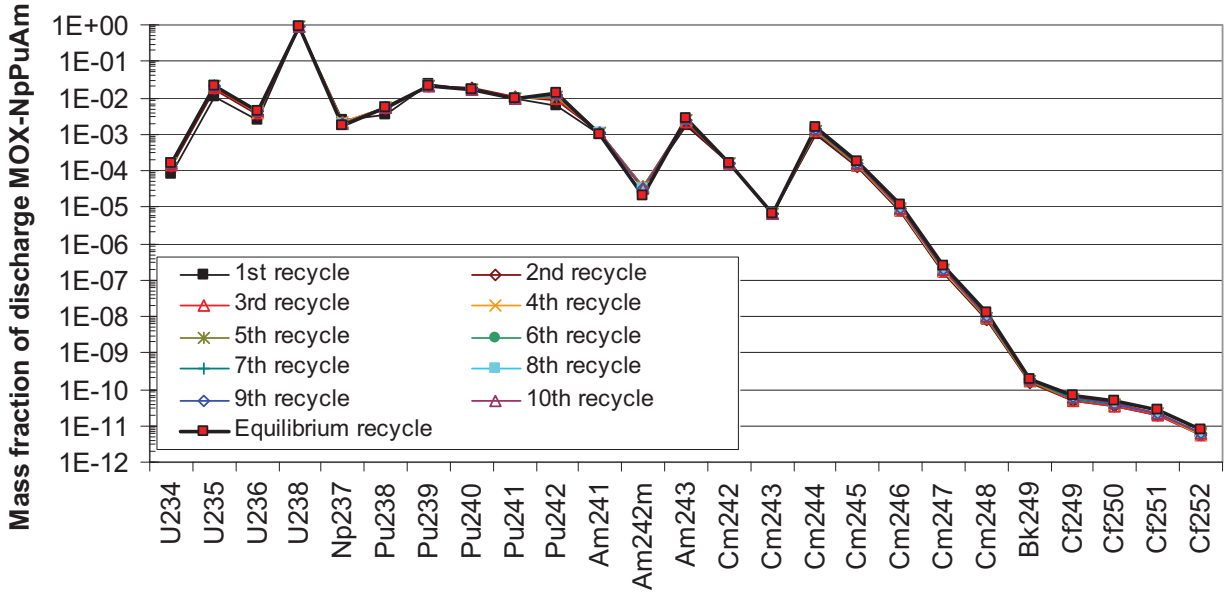

Figure 2-3. Evolution of discharge composition in MOX-UE PuNp fuel

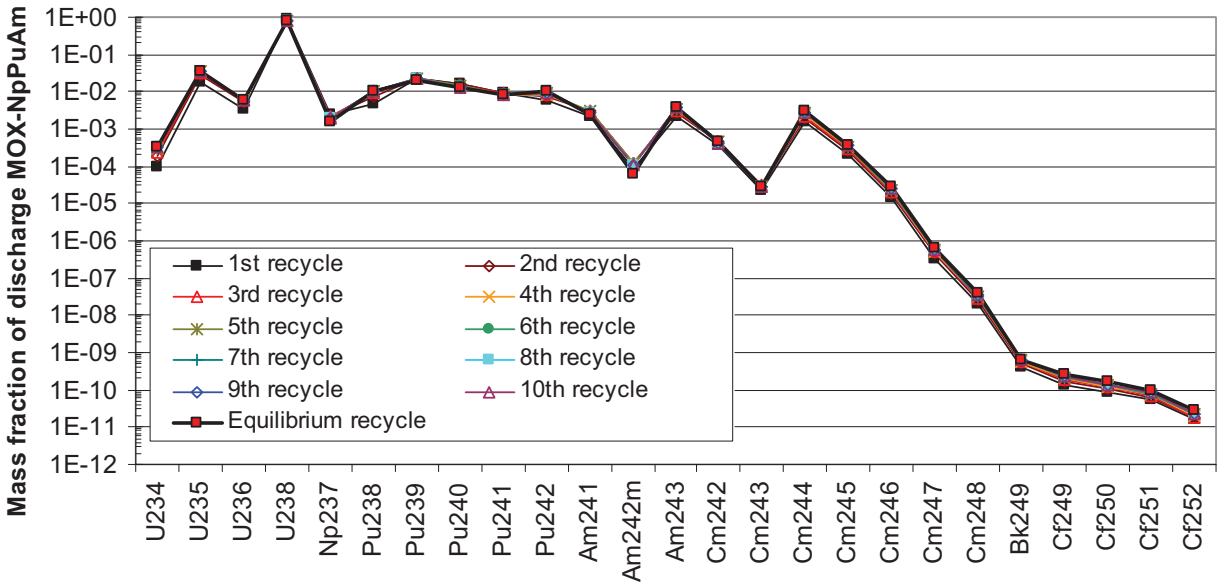

Figure 2-4. Evolution of discharge composition in MOX-UE PuNpAm fuel

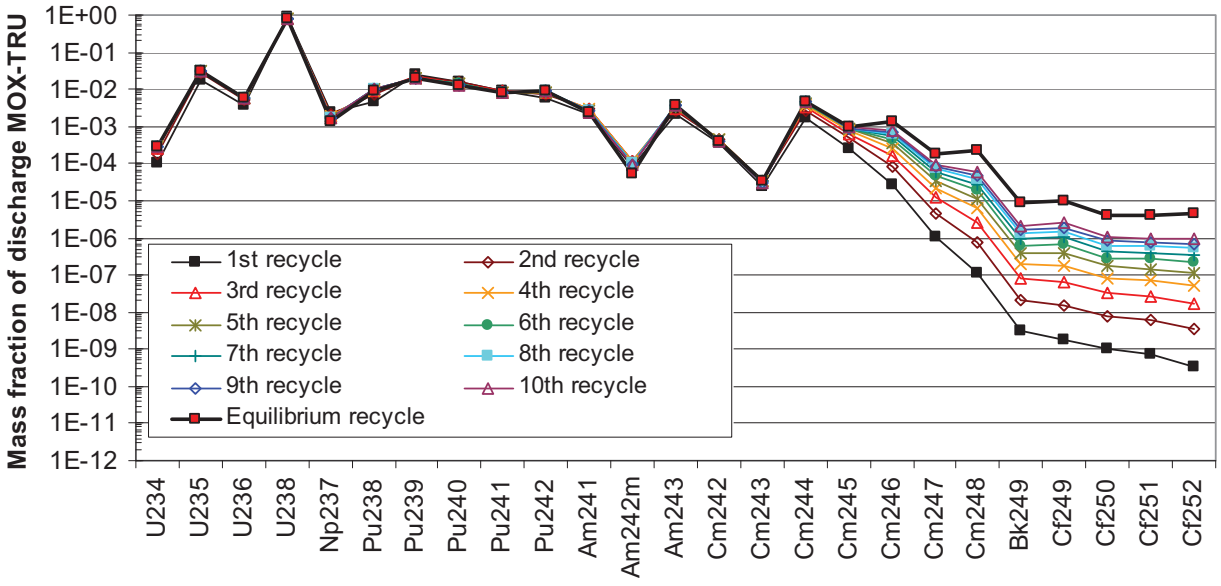

Figure 2-5. Evolution of discharge composition in MOX-UE TRU fuel

2.1.4 Impact of Actinide Partitioning Scenario

The impact of MA partitioning strategy on the discharged fuel composition, alpha, gamma and neutron source terms is shown in Figure 2-6 through Figure 2-9. Figure 2-6 shows dramatically the change in equilibrium composition when the strategy shifts from recycling PuNpAm to all-TRU. The gateway isotope Cm-244 is the lynch pin of the 5 orders of magnitude difference that accumulates at the end of the actinide chain, Cf-252. There is one other composition change worth noting. When shifting from Pu-only to PuNp there is an increase in Np-237 (of course) and the Pu-238 that results from neutron capture by Np-237.

Figure 2-7 shows the heat production from fresh fuel as the four actinide partitioning scenarios evolve as a function of recycle number. They have reached near-equilibrium values after ~5 recycles. Unlike the 12 orders of magnitude in Figure 2-6, there are only two orders of magnitude in Figure 2-7 and at equilibrium only one order of magnitude between Pu-only and all-TRU recycling. Figure 2-8 shows that recycling of Am and Cm-Bk-Cf increase gamma emission is approximately one order of magnitude greater than recycle of Pu or PuNp. Near-equilibrium values have been reached by ~5 recycles.

As would be expected observing the compositions in Figure 2-5, recycle of CmBkCf significantly increases neutron emission. A survey of the transuranic isotopes show that high heat emitters are scattered throughout, which is why Figure 2-7 shows modest change from Pu-only to all-TRU. High gamma emitters are also scattered throughout with some weighting toward the higher TRU, so that there is a jump from PuNp to PuNpAm in Figure 2-8. But, high neutron emitters are very strongly weighted in the higher part of the actinide chain – Cm-244, Cm-248, Cf-252. So, as they accumulate when CmBkCf are recycled, the neutron emission increases substantially in Figure 2-9.

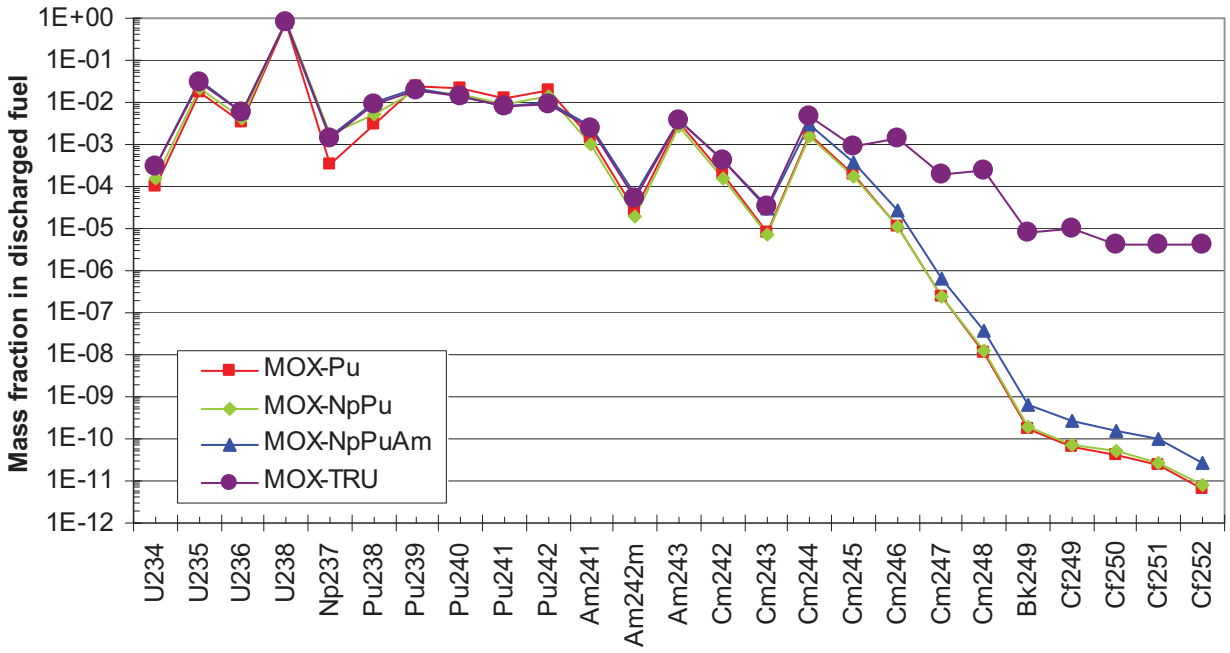

Figure 2-6. Equilibrium fuel cycle isotopic concentration of MOX-UE for the four different MA partitioning strategies

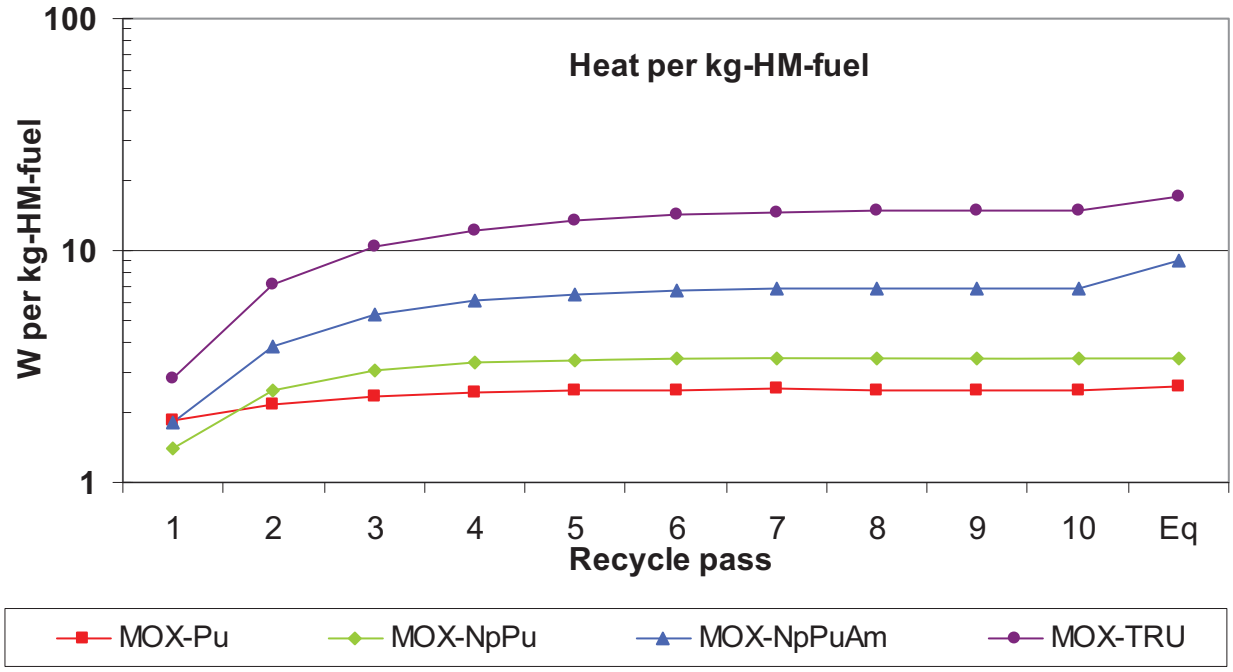

Figure 2-7. Heat from fresh MOX-UE as a function of recycle pass and MA partitioning strategy

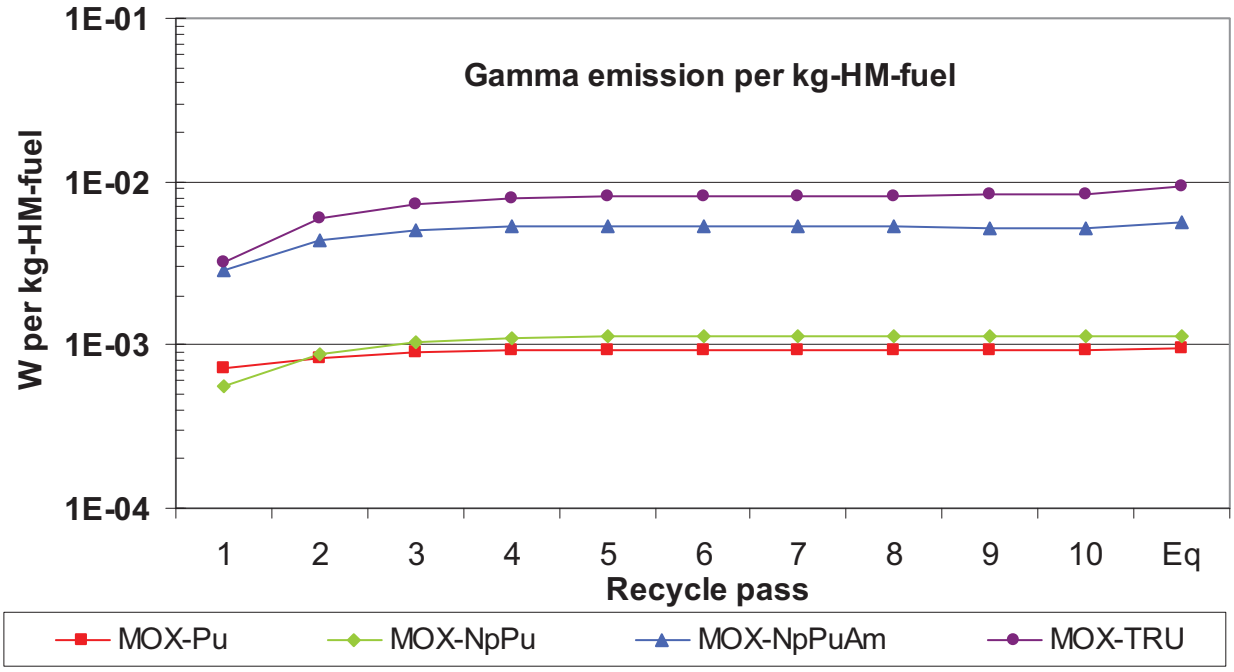

Figure 2-8. Gamma emission from fresh MOX-UE as function of recycle pass and MA partitioning strategy

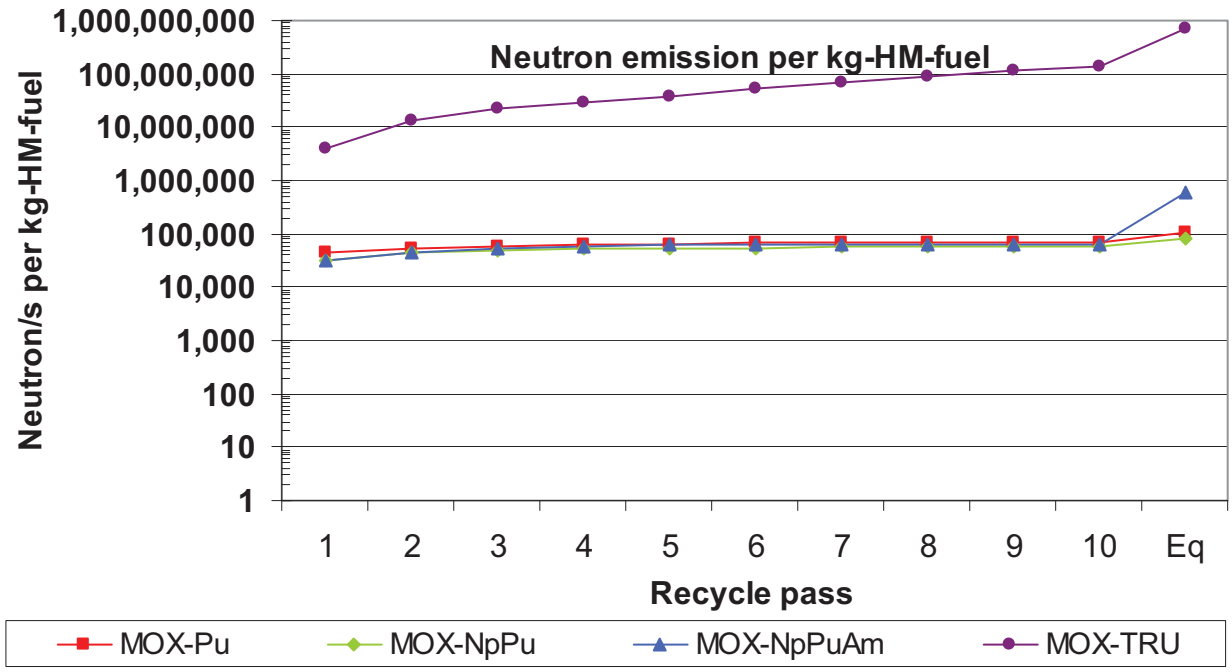

Figure 2-9. Neutron emission from fresh MOX-UE as function of recycle pass and MA partitioning strategy

2.2 Multi-recycle of Heterogeneous IMF/UOX in LWRs

A task was undertaken at INL to perform neutronics analyses in order to further assess several key issues related to the viability of thermal recycling using a heterogeneous Inert Matrix Fuel (IMF) and UOX fuel assembly concept. The initial study was focused on direct thermal recycling of IMF fuels in a heterogeneous PWR 17x17 bundle design in a multi-recycle strategy. These analyses provided comparison of direct thermal recycling of four actinide partitioning options: PuNpAmCmBkCf, PuNpAm, PuNp, and Pu-only.

2.2.1 Method of Calculation

The TRITON depletion code (a component of the SCALE5.1 suite) was used to simulate depletion of a 2-D infinite-lattice PWR fuel assembly, containing both IMF and UOX pins (Figure 2-10). A 44-group neutron cross-section library based on ENDFB-VI was used. The TRU loading in the IMF pins was adjusted to ensure a pin power peaking factor no greater than 1.2. The enrichment of the uranium in the UOX pins was adjusted to achieve a 1500 day fuel life in a 3-batch strategy, which is equivalent to ~50 GW-day/tonne in UOX or MOX. TRU elements of the given partitioning strategy were recycled from UOX and IMF pins in the previous cycle and loaded into IMF pins of the current cycle.

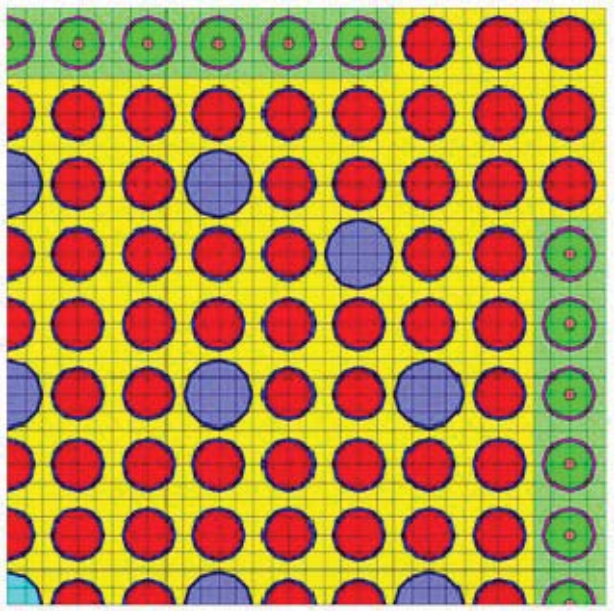

Figure 2-10. Top-Right one-fourth quarter of the 44 pin heterogeneous-IMF bundle design

The pin has an annular design to compensate for the low thermal conductivity of the zirconium oxide. The inner cylinder of the IMF fuel is zirconium oxide only, while the surrounding annulus is a mixture of zirconium oxide and TRU-O2. The key measure for the cycle sustainability was determined by the fuel assembly reactivity at a point equivalent to 2/3 of the discharge burnup. The target assembly reactivity at the 2/3 of the discharged burnup (i.e., 1000 days of irradiation) was selected to be k~1.035 similar to other studies [1,2,3]. This simulates a 3-batch fuel management strategy (if linear reactivity model is assumed) and allows for some neutron leakage which would result in a full-core model rather than the infinite lattice calculations performed here.

Unlike the MOX-UE study, the heterogeneous-IMF symbiosis with SNF TRU is *in-series* as opposed to *in-parallel*. This infinite-series relationship from one recycle pass to the next is shown in Figure 2-11. Thus, it was assumed that only TRU from the previous cycle was available to be introduced into each

subsequent cycle. No external feed of TRU from SNF was provided beyond the first recycle. This infinite-series type of fuel cycle was selected for ease of interpretation in the frame of modeling gross nuclear growth using this fuel concept in the VISION code. However, it is not practical in a real-world frame because it implies a fuel cycle with UOX supporting an infinite series of heterogeneous-IMF fuel assembly designs in order to balance TRU production with TRU consumption. An in-parallel fuel cycle implies that a UOX fleet supports a heterogeneous-IMF fleet. The in-parallel fuel cycle is aimed at stabilizing the TRU inventory produced by the UOX fleet and the heterogeneous-IMF fleet; whereas the in-series fuel cycle stabilizes the TRU in a single fleet of heterogeneous-IMF.

Since the time of this study, VISION has undergone significant revision and should be able to accept a more practical in-parallel fuel relationship between UOX and heterogeneous-IMF just as in the MOX-UE study. Therefore, analysis of heterogeneous-IMF as a dedicated in-parallel burner of the TRU produced by UOX is suggested for future work.

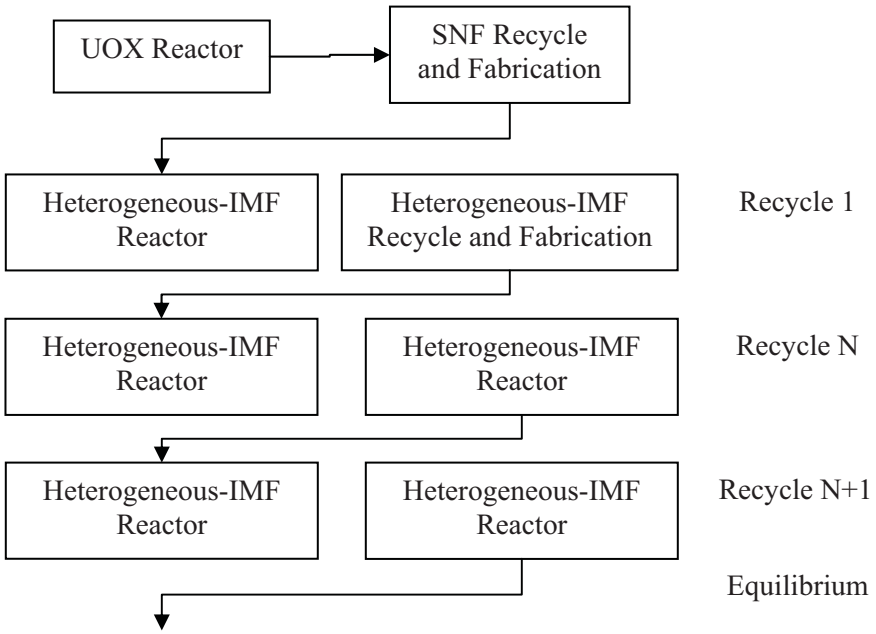

Figure 2-11. Transuranic recycling scheme evaluated in the heterogeneous-IMF study

2.2.2 Synopsis of Results

In a previous work, the bundle design was constrained to have a constant number of IMF pins per assembly (44 of the 264 pins)[e]. With this constraint, some of the partitioning scenarios required that a portion of the transuranic mass be discarded to repository storage. The reasons for this mass expulsion from an otherwise closed fuel cycle was the requirement to maintain a peaking factor no greater than 1.2. For example, in the plutonium-only recycling scheme, the first recycle results in very high reactivity Pu

[e] Note that the accommodation of all TRU mass in subsequent follow-on recycles by adjusting the number of IMF pins per recycle was conducted as part of the scope for this current project. This work stems from a previous endeavor taken in 2007 that assumed a fixed number of 44 pins in the heterogeneous design and then discarded whatever TRU was necessary to meet the 1.2 power peaking requirement.

being placed into the 44 pins resulting in a high peaking factor unless some material is kept out of the pins. At equilibrium cycle, however, the Pu was sufficiently degraded to allow all of it to be placed in the 44 IMF pin locations without violating the peaking limit. Alternately, in the PuNpAmCmBkCf partitioning scenario, the higher mass actinides provided enough poisoning of the reactivity that all of the TRU could be recycled in the first recycle pass, but at equilibrium, some needed to be discarded to respect the peaking factor.

Additional calculations, performed this year, allowed variation of the number of IMF pins between 44 and 60 per assembly as needed in each pass in order to accommodate all TRU in the fuel cycle with no material (aside from separation losses and the actinides not kept in the partitioning scenario) being discarded. This analysis showed that by varying the number of IMF pins between 44 and 60 all of the TRU could be multi-recycled without violating the peaking factor of 1.2. Here are the results for the four different partitioning scenarios investigated.

- IMF-Pu-only: 52 IMF pins were required in the first recycle. This number dropped to 44 after the first recycle of IMF.
- IMF-PuNp: 48 IMF pins were required in the first recycle. This number was dropped to 44 after the first recycle of IMF.
- IMF-PuNpAm: 44 IMF pins were required in the first recycle. This number was increased to 48 before equilibrium was reached.
- IMF-PuNpAmCmBkCf: 44 IMF pins were required in the first recycle. This number was increase to 60 before equilibrium was reached.

Based on the single-assembly infinite lattice calculations performed in this work (i.e., a pure neutronic physics standpoint only), using between 44 and 60 IMF pins within an otherwise typical UOX PWR assembly in order to stabilize the TRU inventory is feasible. Further work is needed, however, to verify this at the full-core level with attention paid to safety characteristics such as delayed neutron fraction, control rod worth, etc. An in depth fuel qualification program would be necessary to establish the integrity of IMF fuel under irradiation. The matrix used in this study was ZrO_2. However, it is expected that a different inert matrix choice would give similar results so long as the transparency to neutron interaction properties were similar.

2.2.3 Isotopic Evolution over Multiple Recycles

The pattern of system evolution is quite similar to that of multi-recycle MOX-UE. Figure 2-12 through Figure 2-15 show the evolution of the multi-recycle heterogeneous-IMF system for the four cases – Pu-only, PuNp, PuNpAm, and all-TRU. The first three Figures show that there is little change, perhaps a factor of two for the higher mass actinides. Figure 2-15, however, shows considerable evolution in the higher mass actinide isotopes when CmBkCf are recycled. As will be seen later, this buildup results in an increase in neutron emission for IMF as it did for MOX-UE.

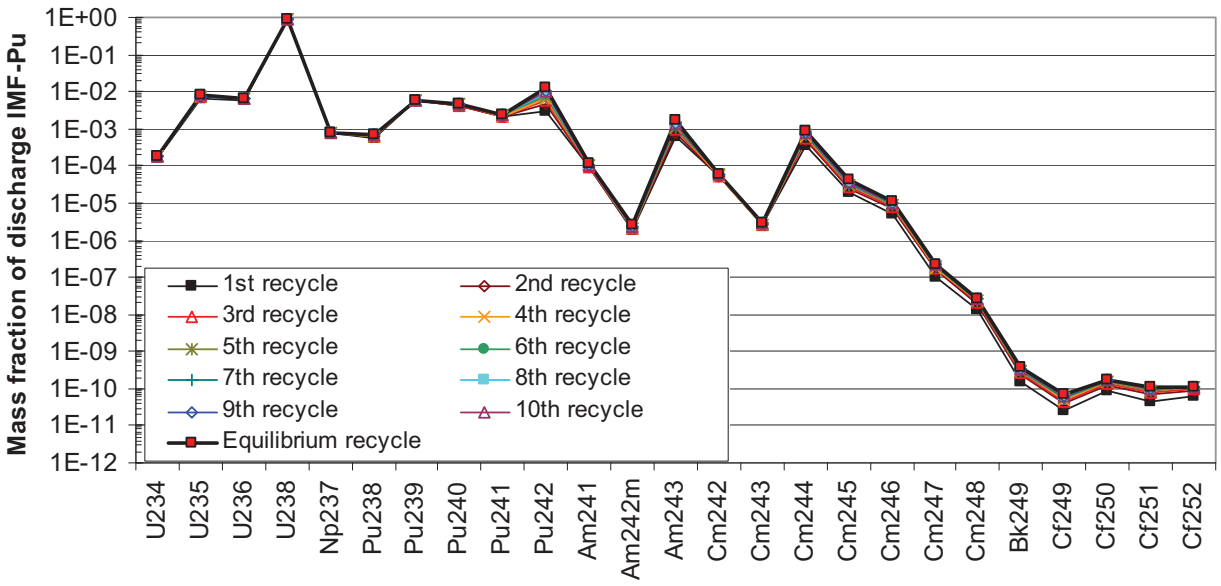

Figure 2-12. Evolution of discharge composition in heterogeneous-IMF Pu-only fuel

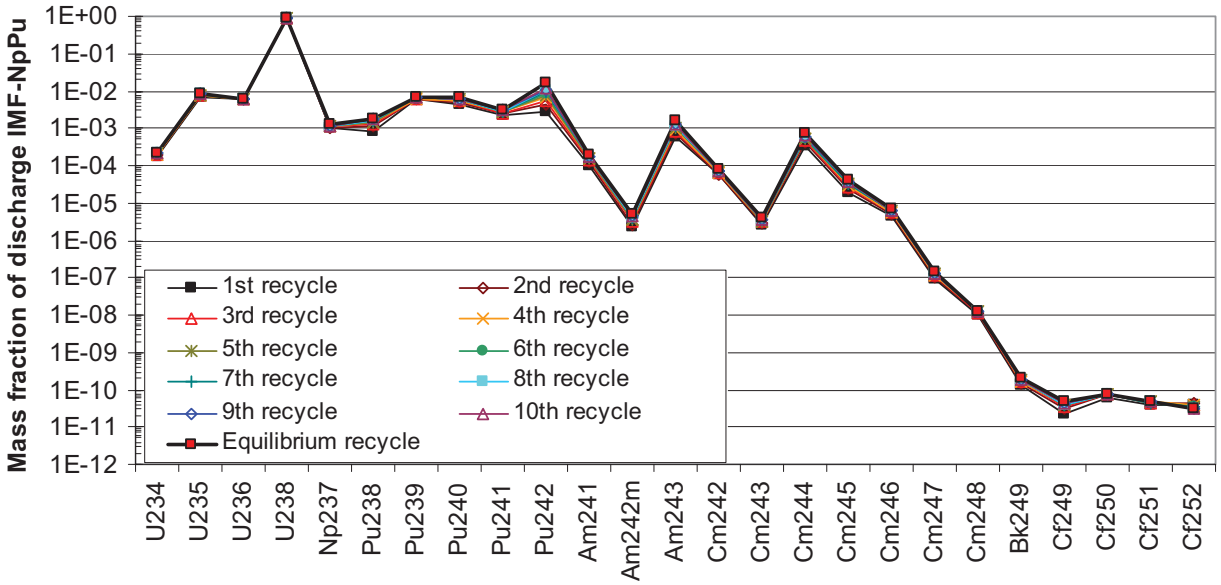

Figure 2-13. Evolution of discharge composition in Heterogeneous-IMF PuNp fuel

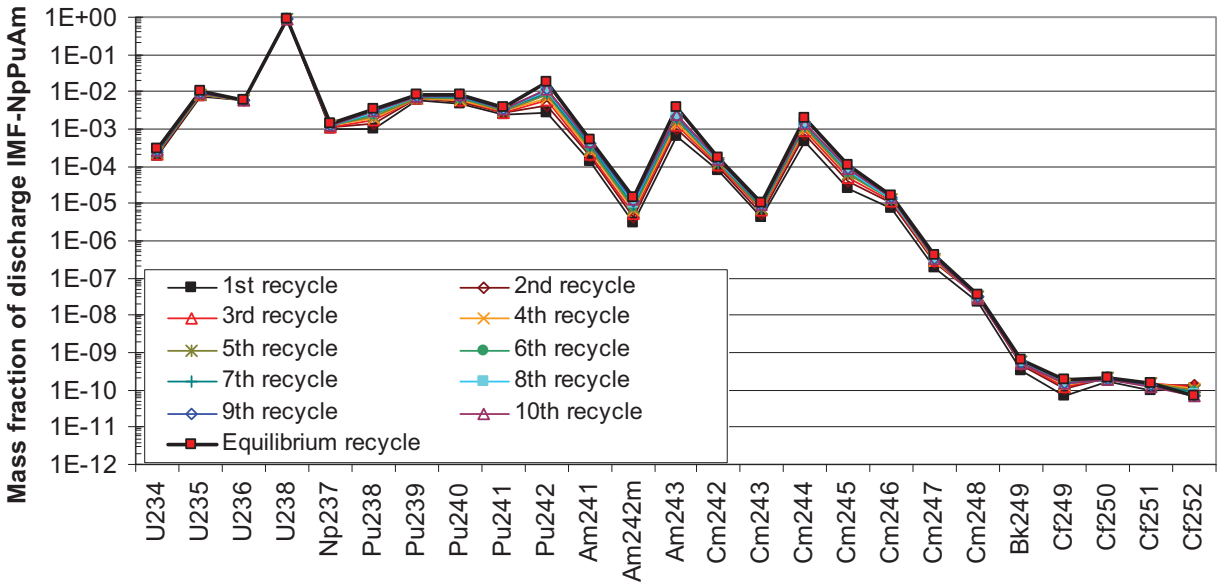

Figure 2-14. Evolution of discharge composition in heterogeneous-IMF PuNpAm fuel

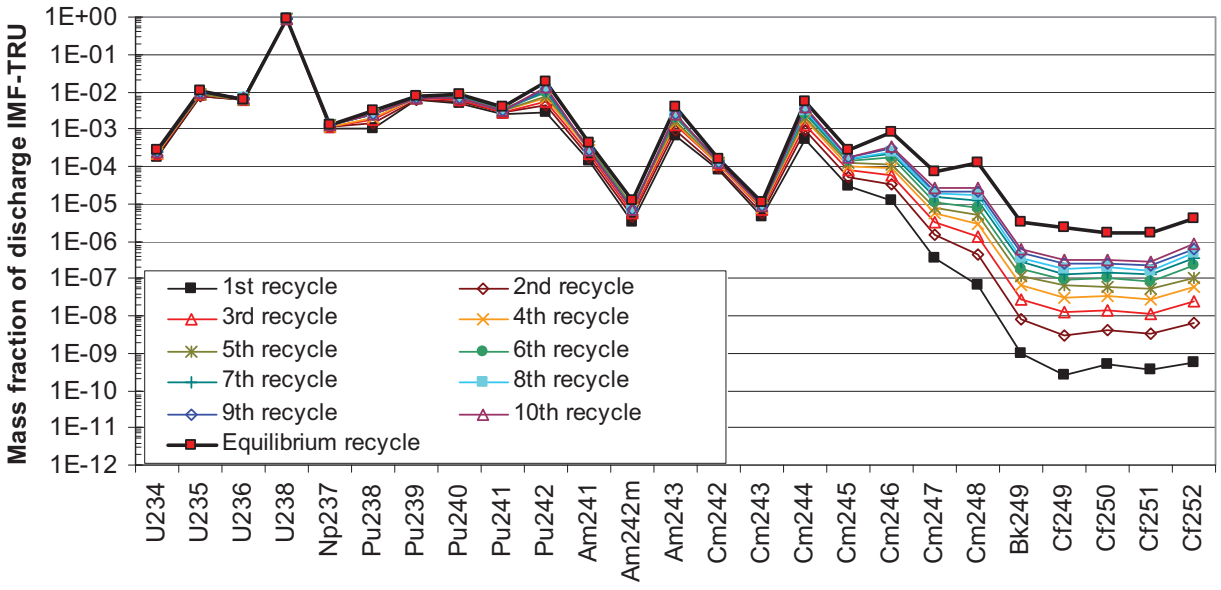

Figure 2-15. Evolution of discharge composition in heterogeneous-IMF TRU fuel

2.2.4 Impact of Actinide Partitioning Scenario

The impact of MA partitioning strategy on the discharged fuel composition, alpha, gamma and neutron source terms is shown in Figure 2-16 through Figure 2-19. Figure 2-16 shows dramatically the change in equilibrium composition when the strategy shifts from recycling PuNpAm to all-TRU. Like MOX-UE, the gateway isotope Cm-244 is the lynch pin of the 5 orders of magnitude difference that accumulates at the end of the actinide chain, Cf-252. Like MOX-UE, Figure 2-17 shows how heat increases as the system evolves and as more actinides are recycled. Figure 2-18 shows the same thing for gamma

emission. The final heterogeneous-IMF graph (Figure 2-19) again shows the dramatic impact of recycling Cm-Bk-Cf.

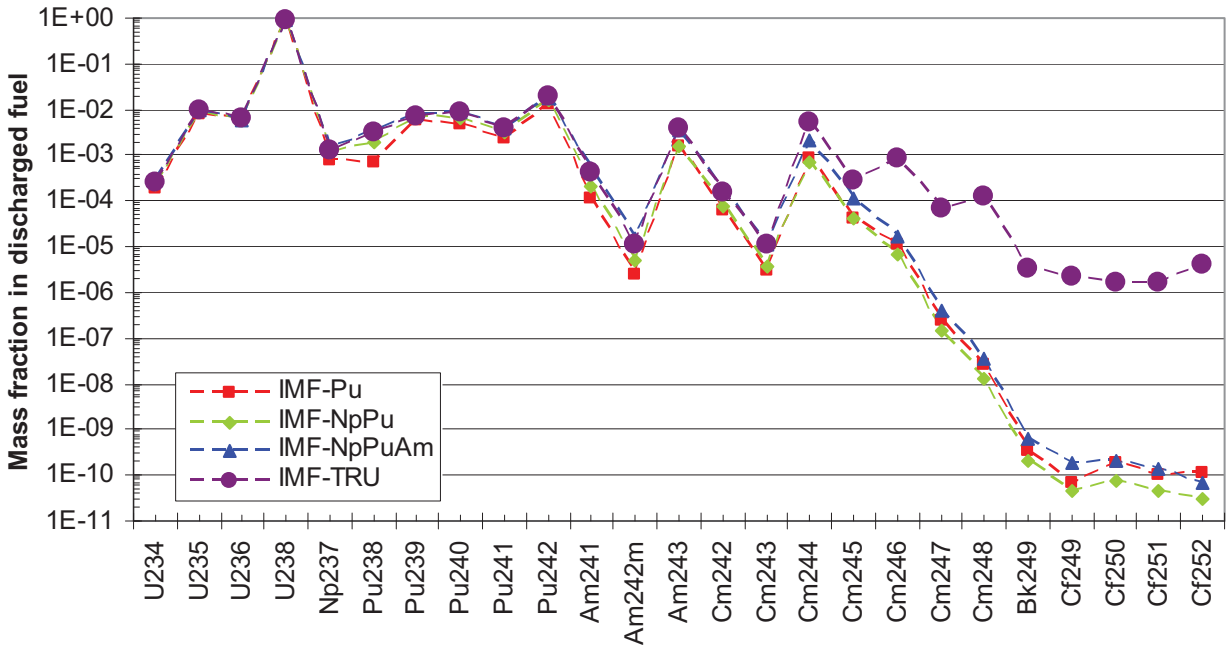

Figure 2-16. Equilibrium fuel cycle isotopic concentration of heterogeneous-IMF for the four different MA partitioning strategies

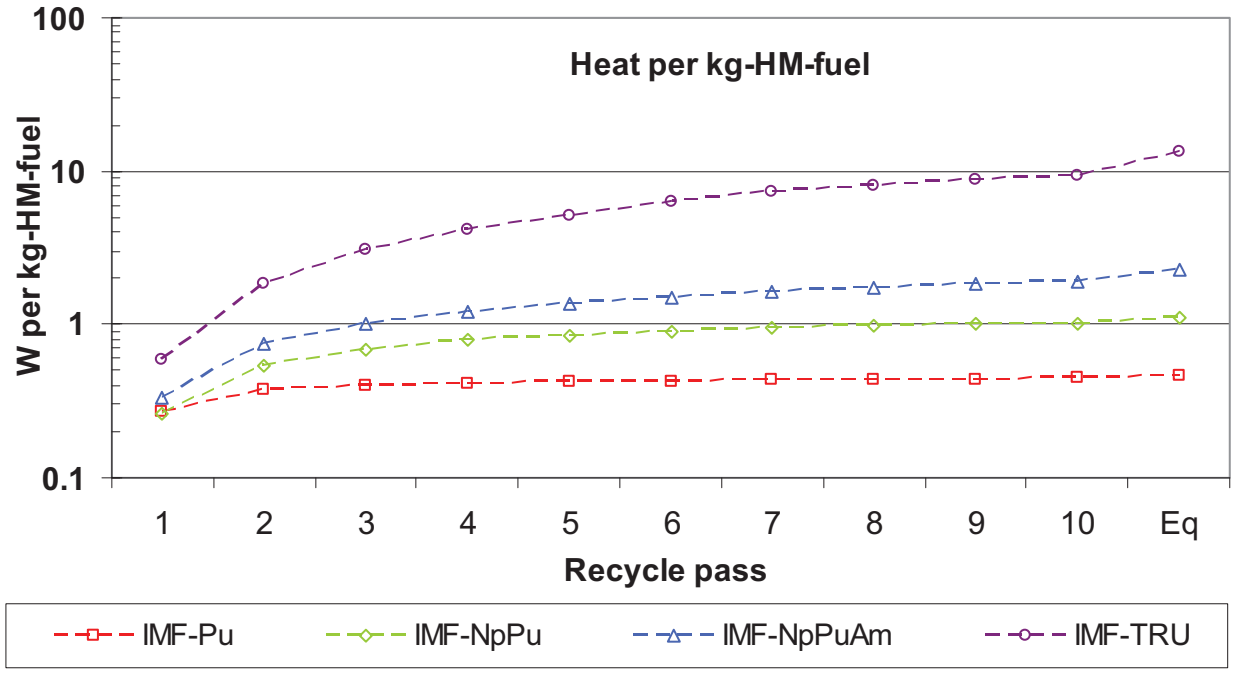

Figure 2-17. Heat from fresh heterogeneous-IMF as function of recycle pass and MA partitioning strategy

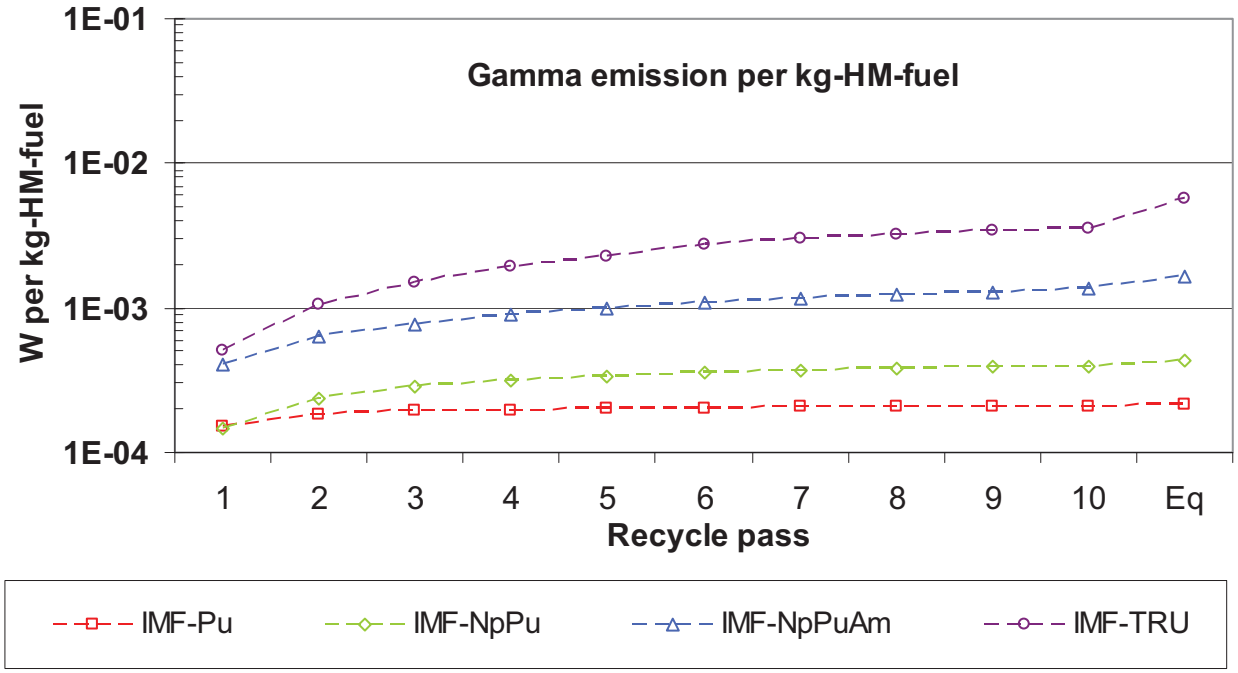

Figure 2-18. Gamma emission from fresh heterogeneous-IMF as function of recycle pass and MA partitioning strategy

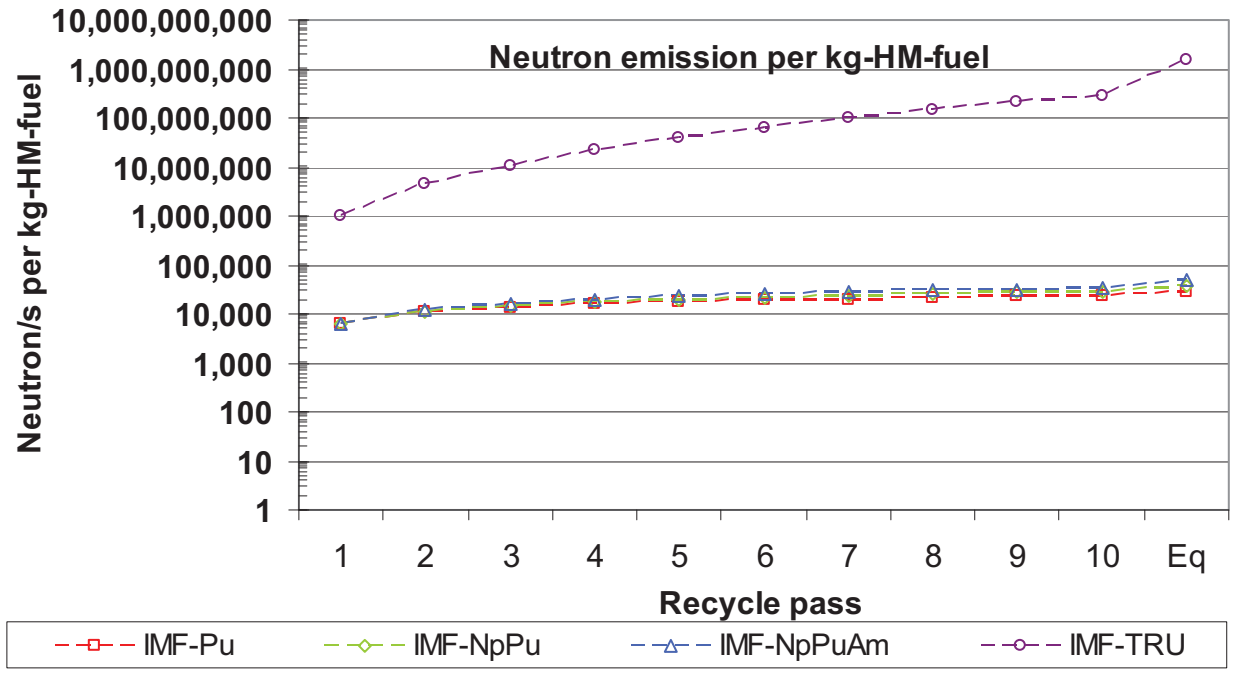

Figure 2-19. Neutron emission from fresh heterogeneous-IMF as function of recycle pass and MA partitioning strategy

2.3 Fast Reactors

To study the impact of conversion ratio, only metal-fueled fast reactors were the focus rather than oxide-fueled because the former has higher fuel density and is believed to be capable of higher TRU conversion ratio. To study the impact of minor actinide recycle strategies, oxide-fueled fast reactors were the focus because of the presumption that aqueous separation (for which separation of one TRU element from the others) would be used whereas the common presumption is that electrochemical separation (for which separation among TRU elements is difficult or impossible) would be used with metal fuel.

2.3.1 Survey of Fast Reactor Scenario Studies

Steadily for the better part of this decade ANL has examined fast reactor transmutation scenarios with respect to the fuel cycle as a whole [4,5,6,10,11,12]. Until recently, the majority of these calculations initially truncated at Cm-246. As with the preceding sections on MOX-UE and heterogeneous-IMF, it is now recognized as important to go to the end of the actinide chain, Cf252. Analysis elsewhere confirms that tracking isotopes to Cf-252 is sufficient to capture all isotope evolution and buildup effects as well as the corresponding influence on radiologic source terms. [13,14,15]. In the following graphs, all the data points, produced by recent work by Hoffman, as a function of fast reactor TRU conversion ratio include all isotopes through Cf-252, except some of the graphs have a Stillman data point (shown in red) at CR=1.07 that truncated at Cm-246 to show for which considerations it matters.

2.3.2 Impact of Fast Reactor TRU Conversion Ratio

Figure 2-20 shows the impact of conversion ratio on burnup. In these calculations, the burnup was allowed to float while holding the maximum fluence to the cladding constant. Since burnup, by definition, is energy per heavy metal in fuel and energy released and fluence scale together, Figure 2-20 is really showing the impact of the composition change. Figure 2-21 shows that as conversion ratio increases there is more uranium (for conversion into TRU). Since total energy (i.e., via a constant fluence) is kept constant, the burnup necessarily decreases with higher conversion ratio and higher initial uranium mass.

Figure 2-22 shows the discharged fuel composition as a function of conversion ratio at equilibrium. All cases except CR~0.00 have high U-238 content and all cases have ~10% Pu-239. Upon close inspection Figure 2-21 and Figure 2-22, the U-238 concentration increases with CR. This increase is offset by the decrease in virtually all the other isotopes as CR increases. As CR increases there is more U-238, less Pu-239 and less of the high-neutron emitting isotopes high on the actinide chain.

Figure 2-23 is the same as Figure 2-22 with one difference, the inclusion of the CR=1.07 dataset for which recycling was truncated at Cm-246. At Cm-247, the new set is marked by red points. The CR=1.07 dataset diverges from the pattern by more than two orders of magnitude by Cf-252.

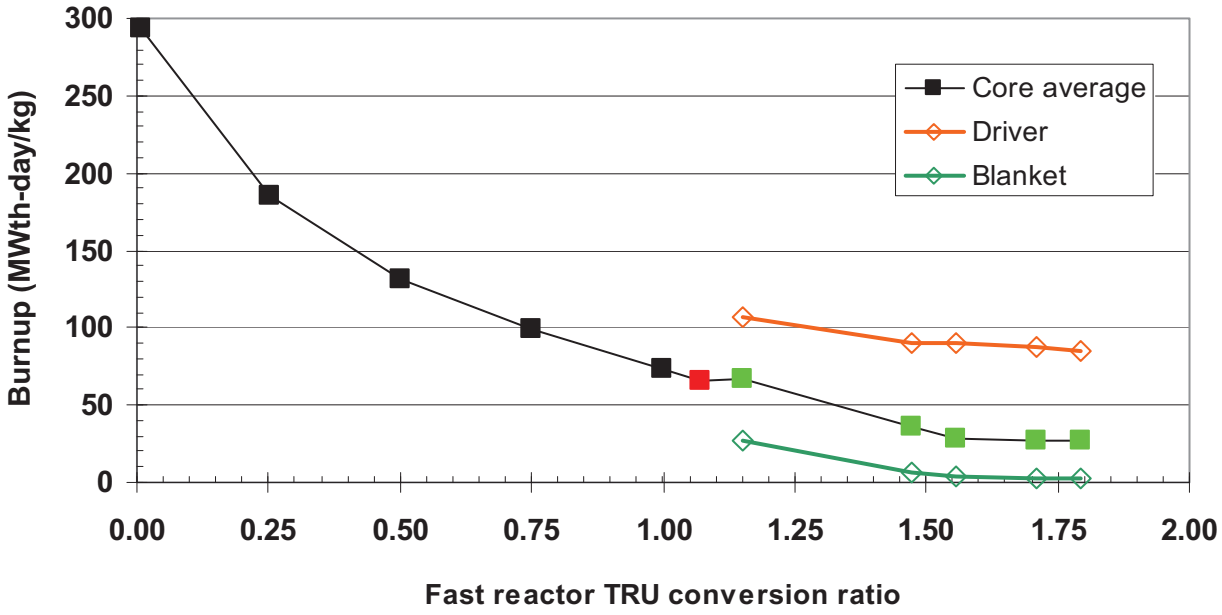

Figure 2-20. Impact of fast reactor TRU conversion ratio on energy produced per mass of total initial HM. (The red curve is the burnup specific to the HM in the driver fuel. The green curve is the burnup specific to the HM in the blanket)

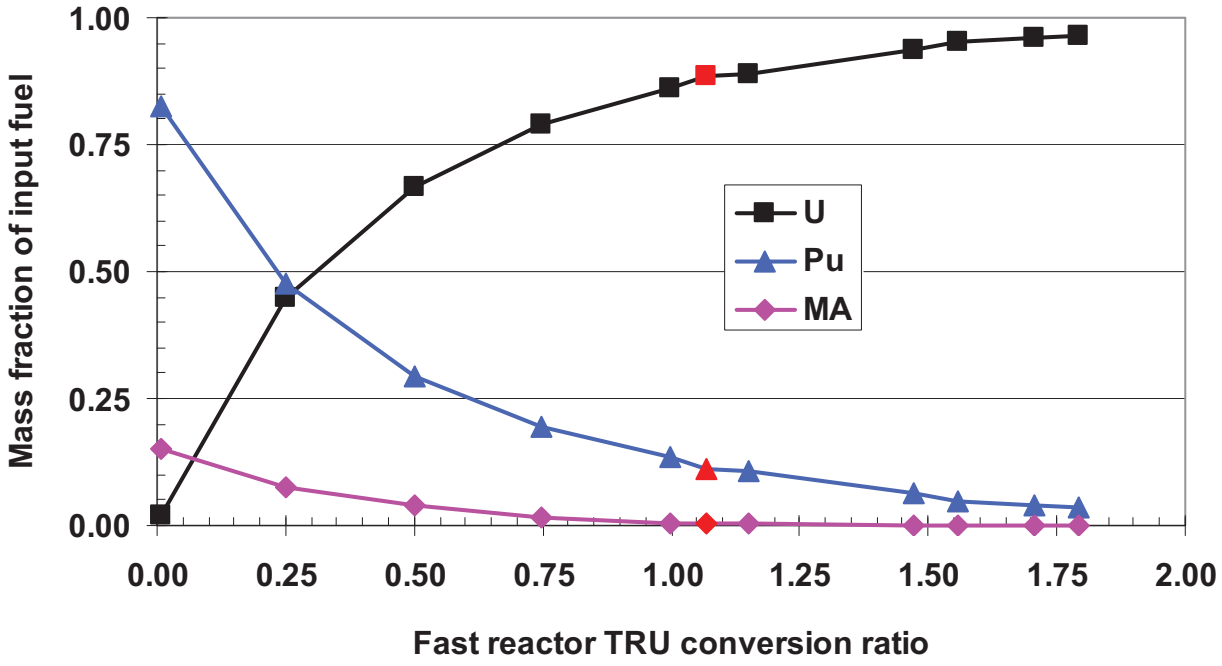

Figure 2-21. Impact of fast reactor TRU conversion ratio on initial HM composition of a fresh fuel batch

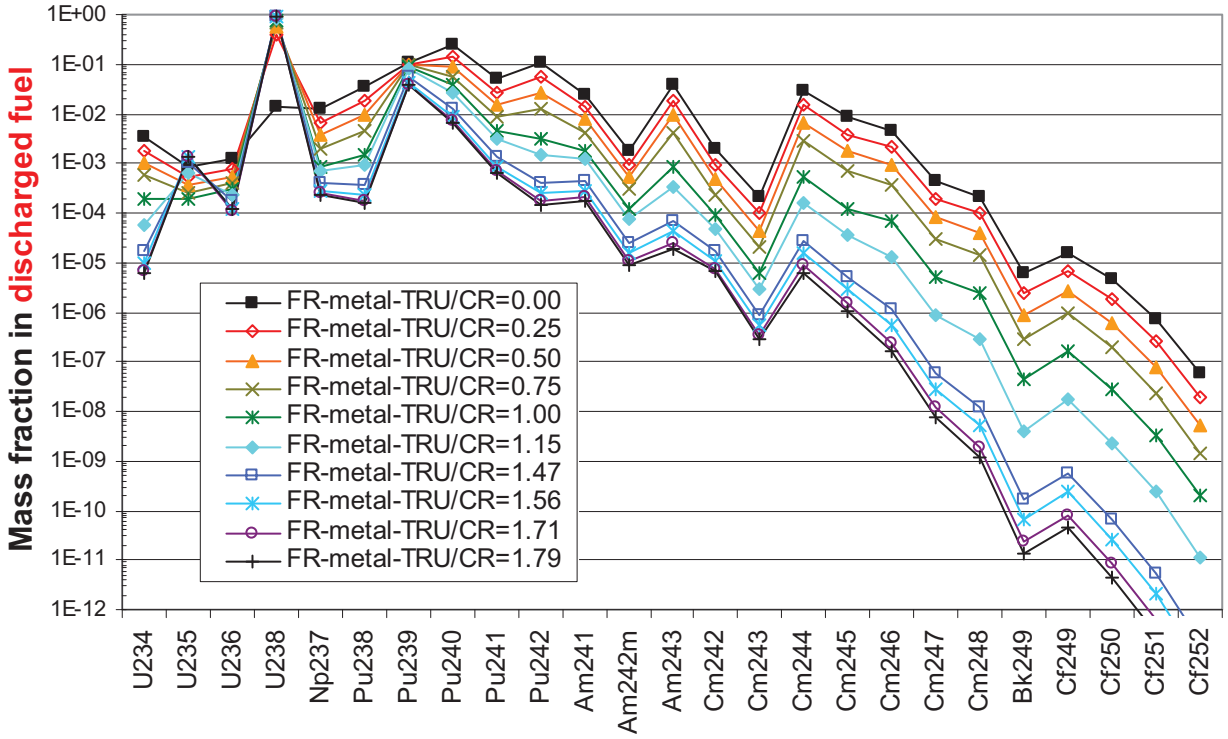

Figure 2-22. Impact of fast reactor TRU conversion ratio on FR-metal fuel discharge composition, all cases recycled isotopes through Cf-252

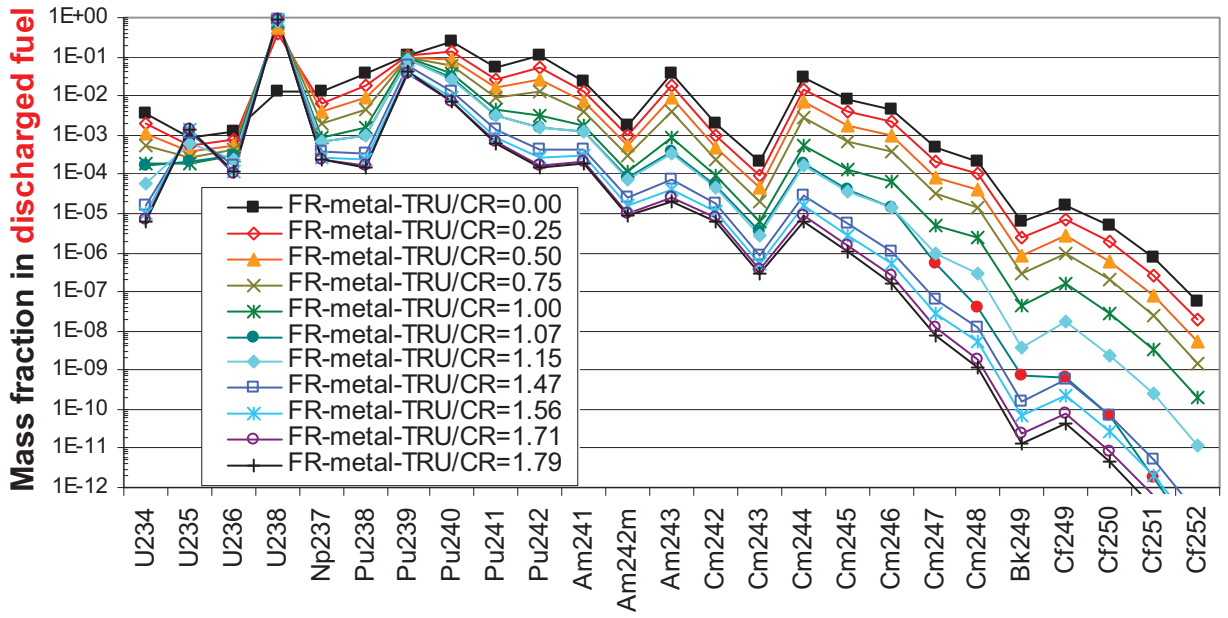

Figure 2-23. Impact of fast reactor TRU conversion ratio on SFR-metal fuel discharge composition, comparing all cases where depletion was tracked to Cf-252 rather than one case study ending in Cm-246 (the bright red data points of the CR=1.07 case)

Figure 2-24 through Figure 2-26 show the heat, gamma, and neutron emission as a function of conversion ratio. The green lines are the first recycle in fast reactors; the black lines are the equilibrium recycle. In the first recycle pass, there is little impact from conversion ratio as TRU content in fuel and burnup generally compensate[f]. As the systems evolve toward equilibrium, the heat, gamma, and neutron emission increases relative to first recycle for decreasing conversion ratio.

The bright red data point in the three Figures at CR=1.07 denotes the case for which recycling of isotopes stopped at Cm-246. The impact on neutron emission is unsurprisingly the largest, about a factor of two away from the pattern, whereas heat and gamma are a factor of 1.2-1.3 away from the line connecting CR=0.00 and CR=1.13.

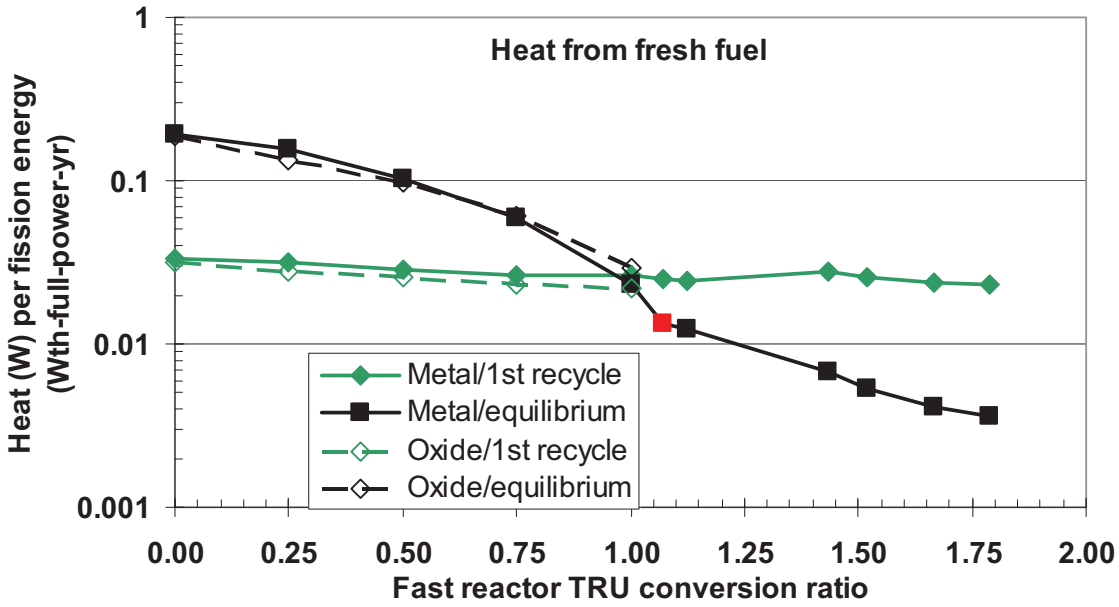

Figure 2-24. Heat from fresh fast reactor metal fuel as function of fast reactor TRU conversion ratio

[f] The units here are per fission energy produced, i.e., inversely proportional to burnup.

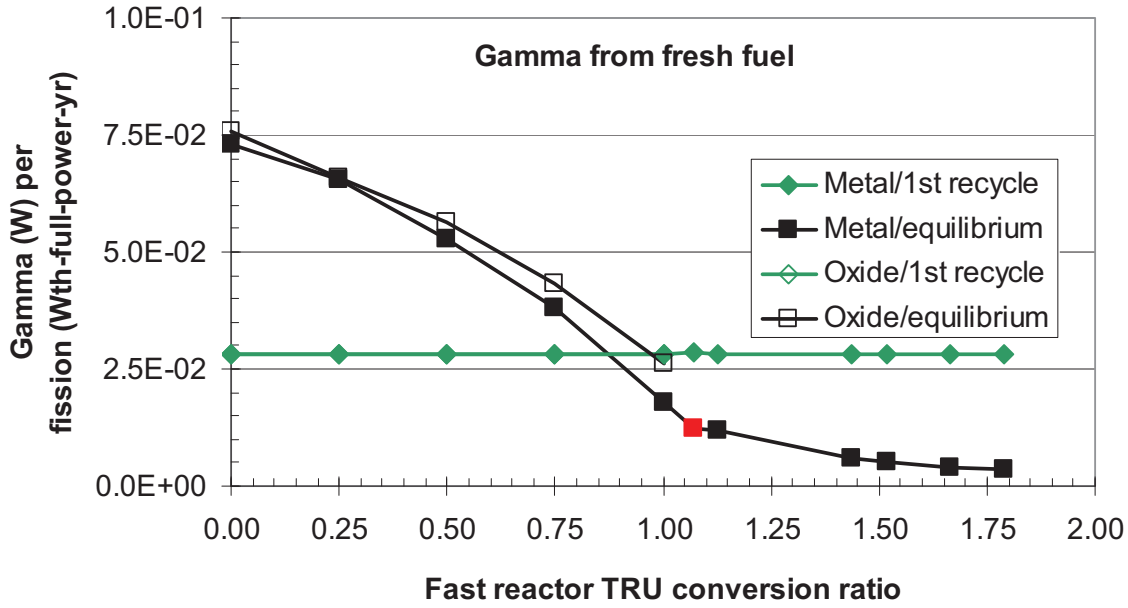

Figure 2-25. Gamma emission from fresh fast reactor metal fuel as function of fast reactor TRU conversion ratio

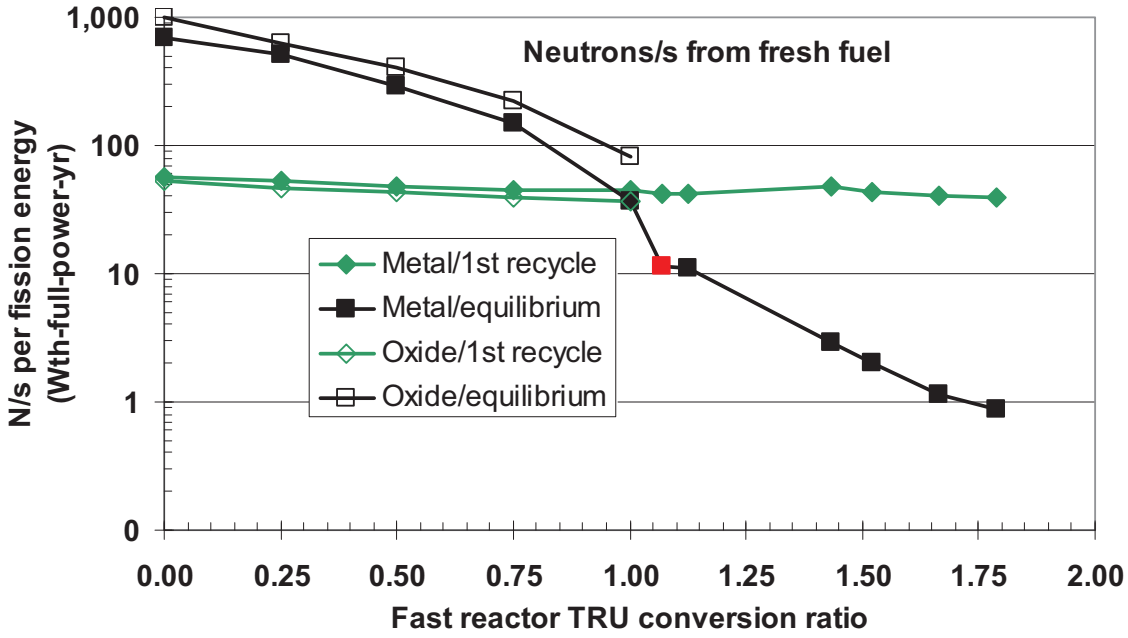

Figure 2-26. Neutron emission from fresh fast reactor metal fuel as function of fast reactor TRU conversion ratio

2.3.3 Impact of Actinide Partitioning Scenario

Figure 2-27 shows the impact of the actinide partitioning strategy on equilibrium composition. The pattern is similar to multi-recycle MOX-UE and heterogeneous-IMF. Significant buildup of the higher mass actinides when CmBkCf are recycled. Recycle-by-recycle data for any of the four strategies - Pu, PuNp, PuNpAm, all-TRU is needed to make a fair comparison with the previous MOX-UE and

heterogeneous-IMF studies. Therefore there are no analogous graphs to those for MOX-UE and heterogeneous-IMF. The equilibrium heat, gamma, and neutron emission for these cases is presented in the next subsection in comparison with MOX-UE and heterogeneous-IMF.

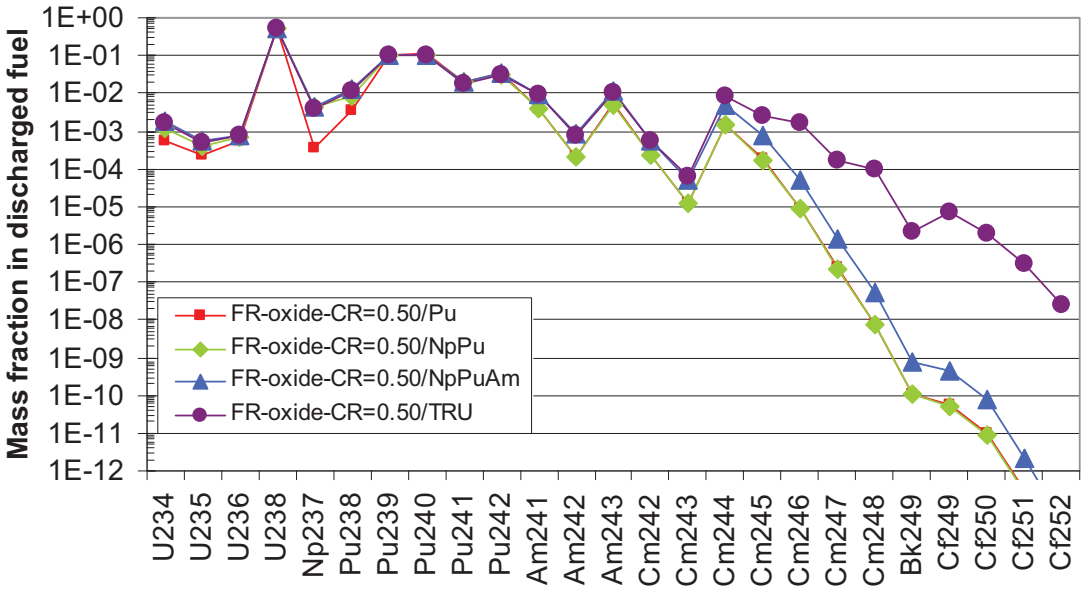

Figure 2-27. Equilibrium fuel cycle isotopic concentration of FR-oxide (CR=0.5) for the four different MA partitioning strategies

2.4 Comparisons

This subsection compares multi-recycle MOX-UE, heterogeneous-IMF, and fast reactor at CR=0.50. This covers the majority of information in the VISION Transmutation Library, which is summarized in Table 2-1 [14]. A "case" is a fixed reactor physics calculation, in which the reactor is in equilibrium with some defined input, operates with some set of parameters, and is calculated to produce an output. For each case, the Library contains key input parameters, purpose of the analysis, citation, and input and output recipes (mass fractions) for 81 isotopes [14,15]. Some of the cases include 1-group cross sections for (n,fission), (n,gamma), and (n,2n).

To provide context, it should be recognize that this year 44 new MOX-UE and 44 new heterogeneous-IMF cases were added to the Library. These new cases include the four actinide partitioning strategies (Pu, PuNp, PuNpAm, all-TRU) carried out over 11 recycles (1-10 recycle passes plus equilibrium).

Table 2-1. Summary of Contents of Transmutation Library

Reactor/Fuel Case	Number of Active Cases	Cases Ready to be Added	Obsolete Cases Retained for Archival Purposes
UOX (PWR)	14	2	
Other once through	2	6	Brand new HWR data ready to enter. Only one VHTR dataset.
MOX	53	33	
IMF	48	27	54 (44 are the previous multi-recycle heterogeneous-IMF data set)
Burner fast reactor (TRU conversion ratio < 1)	112		5
MOX-FR	24		5
IMF-FR	20		
LWR target	0		
FR target	17	TBD	
Breeder FR	25		5 (data sets for the CR=1.07 case described in section 2.3)

2.4.1 Composition

Figure 2-28 compares the composition at equilibrium as a function of which minor actinides are recycled for multi-recycle MOX, multi-recycle IMF, and fast reactor oxide at CR=0.50. As can be seen from the Figure, the recycling of Cm-Bk-Cf is the dominant determinant to higher mass actinide buildup, *not* the reactor/fuel type. A likely explanation of this trend is offered in Section 2.5.

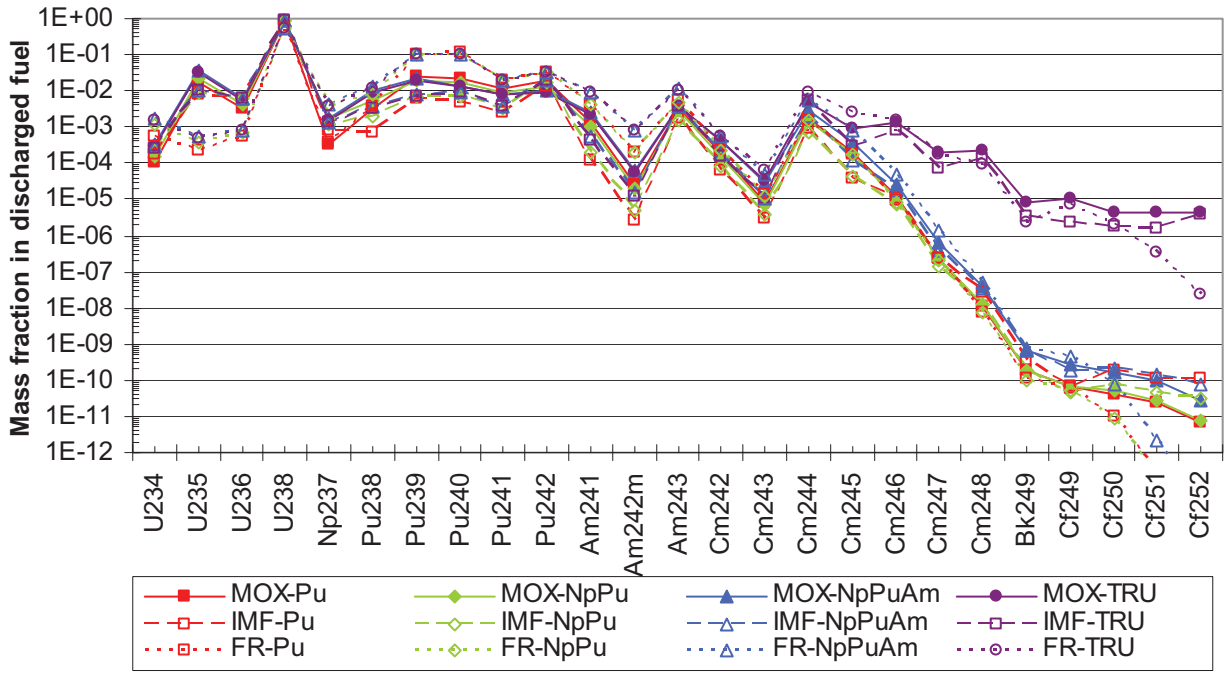

Figure 2-28. Equilibrium fuel cycle isotopic concentration of oxide-FR (CR=0.50), MOX-UE, heterogeneous-IMF

2.4.2 Decay Heat Power

As noted previously, when one is comparing fuels from one reactor type to the next, there are different ways to compare or normalize the values. Throughout the rest of this subsection, two normalizations - per kg-TRU and per kg-heavy metal, are shown. The color and symbols in the graphs are the same and the "TRU" graph always precedes the "heavy metal" graph.

Figure 2-29 and Figure 2-30 compare heat generated as a function of recycle pass and MA recycle strategy. Since fast reactor data by recycle pass is not available, there are only fast reactor points for first and equilibrium recycle. When viewing Figure 2-29 (per kg-TRU), the pattern is clear, heat increases in progressing from Pu to PuNp to PuNpAm to all-TRU. The pattern in Figure 2-30 (per kg-HM) is demonstrates the differences among fuel and reactor types in terms of the TRU content in the fuel. The fast reactor has a higher enrichment by about a factor of three. Thus, its decay power per heavy metal relative to the other scenarios depicted in Figure 2-30 is higher than compared per mass of TRU, shown in Figure 2-29. In the next Chapter it will be shown that when factoring in the mass per assembly, the MOX-UE assembly has a greater decay heat power due to the fact that it is more massive than a typical fast reactor assembly.

Figure 2-31 and Figure 2-32 compare the decay heat power at equilibrium. UOX data is added to Figure 2-32 to provide a frame of reference. Figure 2-31 (per TRU) shows the initial TRU feed for each case from discharged UOX, from which each of the fuel/reactor strategies start. As more MAs are recycled, there is more difference at equilibrium recycle relative to the corresponding initial TRU feed. Figure 2-32 (per HM) shows 30-year old UOX for comparison. (As the fuels have different TRU/HM ratios, showing UOX feed on the HM graph would be meaningless.) All of the fresh fuels at equilibrium are an order of magnitude hotter than 30-year old UOX.

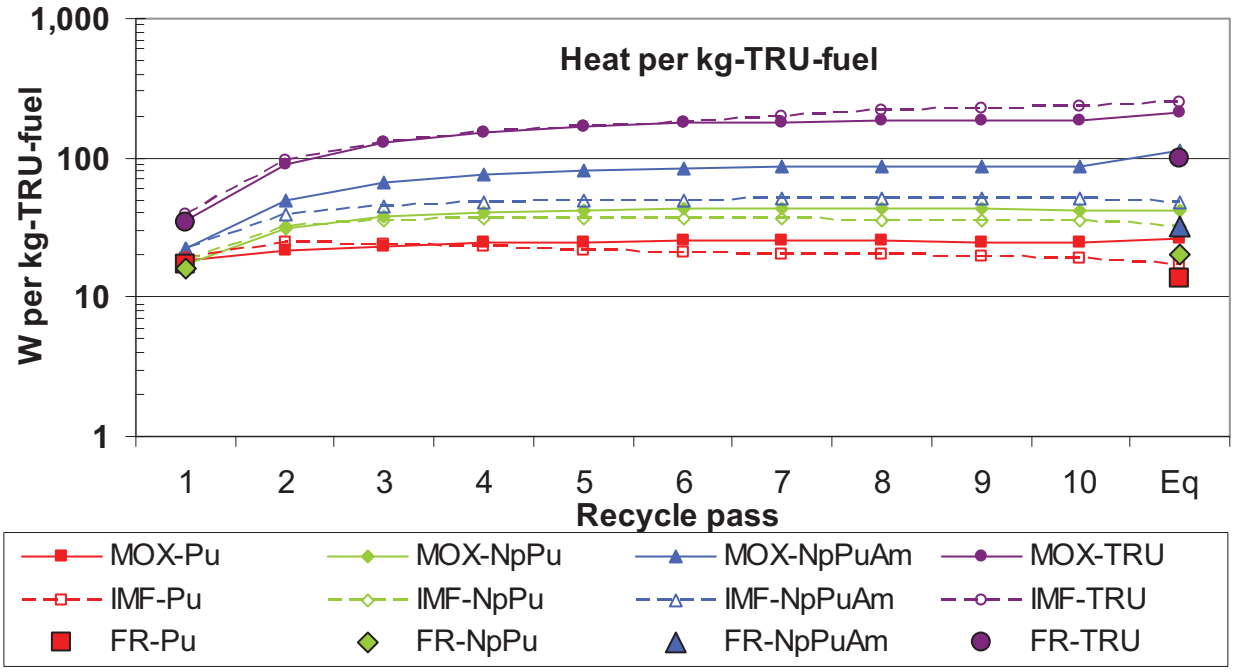

Figure 2-29. Fresh fuel decay heat power as a function of the number of recycles and MA partitioning strategy, per mass of TRU (FR-oxide at CR=0.50, MOX-UE, heterogeneous-IMF)

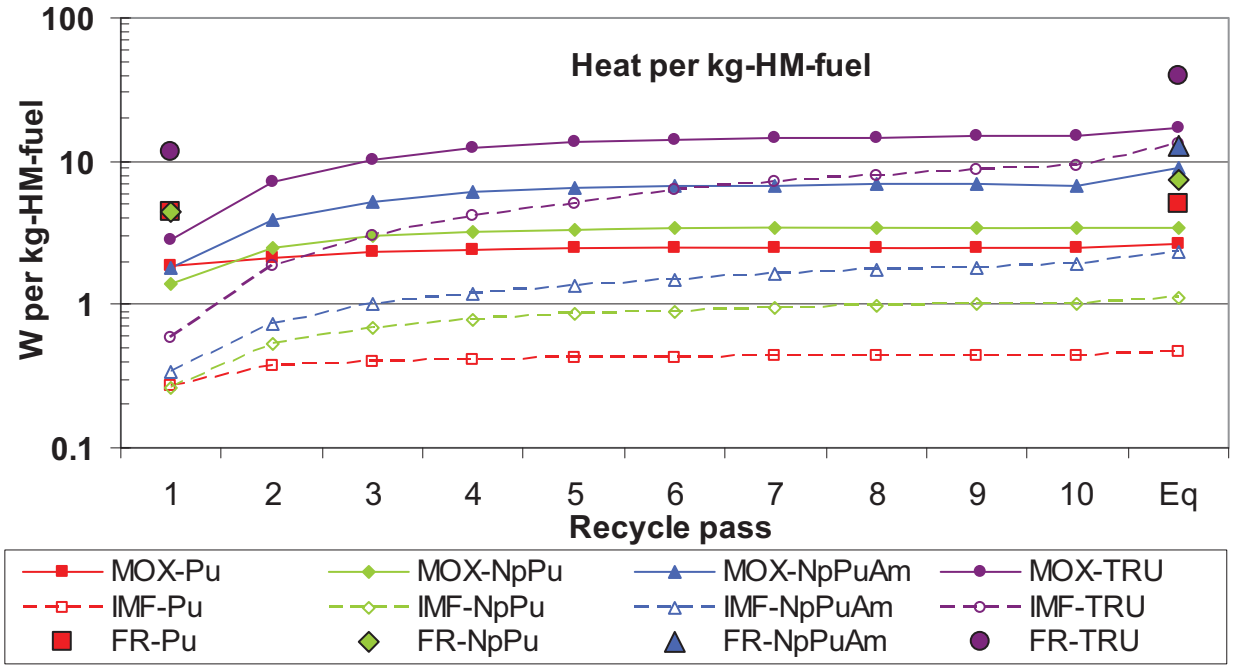

Figure 2-30. Fresh fuel decay heat power as function of the number of recycles and MA partitioning strategy, per mass of heavy metal (FR-oxide at CR=0.50, MOX-UE, heterogeneous-IMF)

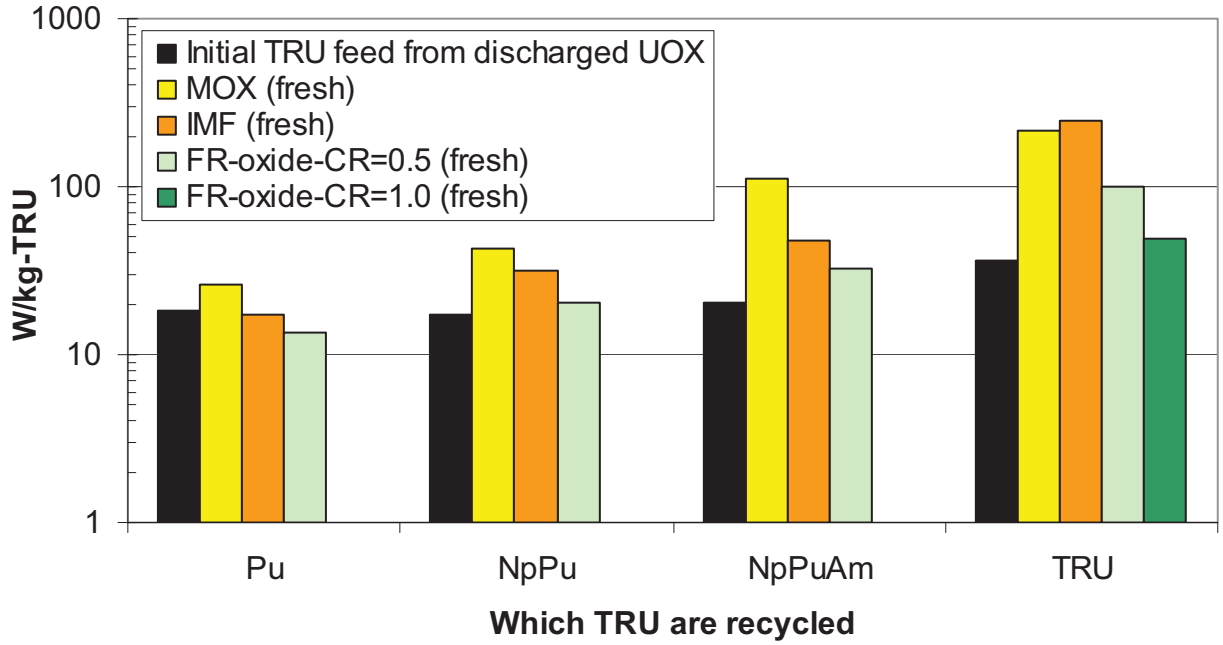

Figure 2-31. Equilibrium recycle fresh fuel decay heat powers as a function of MA partitioning strategy, per mass of TRU

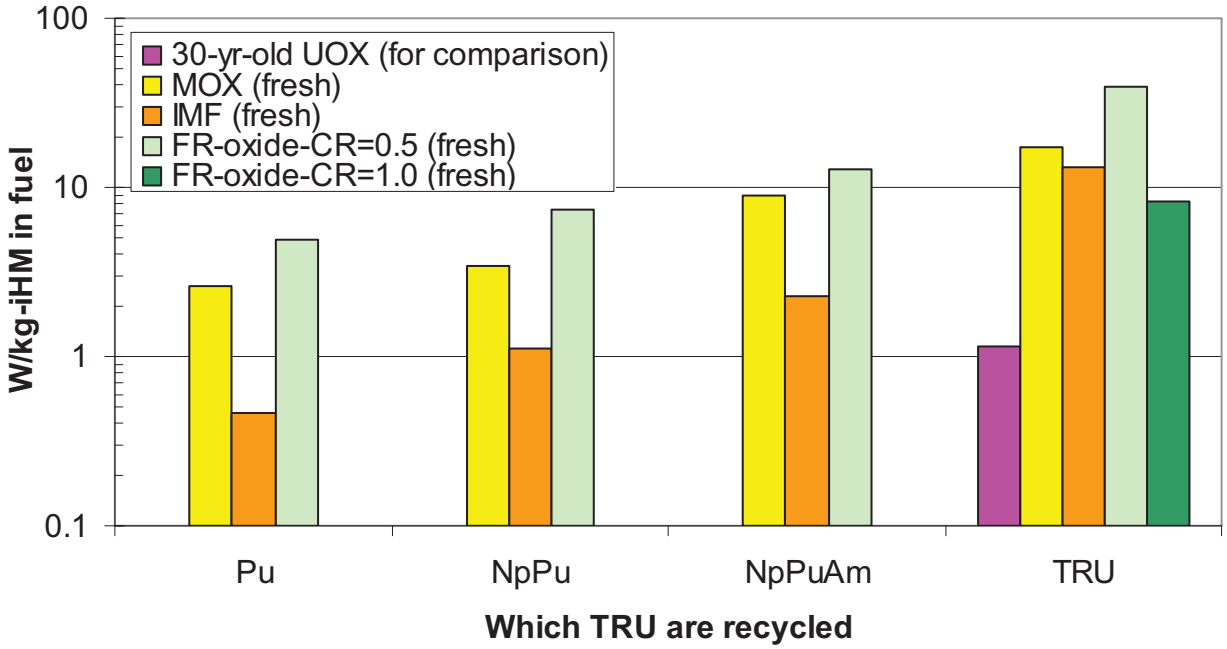

Figure 2-32. Equilibrium recycle fresh fuel decay heat powers as a function of MA partitioning strategy, per mass of heavy metal

A point of comparison is that material at 450 W/kg may be considered "self protecting" to some degree, as follows. The IAEA denotes Pu mixtures with 80% Pu-238 as self-protecting because of heat generation [16]. This works out to about 450 W/kg-Pu. Figure 2-29 and Figure 2-31 (both "per kg-

TRU") show that none of the cases reach 450 W/kg-Pu but the all-TRU cases come close. When one considers diluting the TRU with U, Figure 2-30 and Figure 2-32 (both "per kg-HM"), the mixtures are further from 450 W/kg. Of course, it is also possible to take the TRU mixtures and subsequently separate the high heat MA from lower heat Pu, in which the Pu would not be generating such heat.

2.4.3 Gamma Emission Energy

The gamma emission comparison is very similar to the heat comparison. Figure 2-33 and Figure 2-34 show the evolution of gamma emission upon multiple recycles, for the four recycle strategies (Pu, PuNp, PuNpAm, all-TRU), and the three reactor-fuel concepts being compared.

Figure 2-35 and Figure 2-36 show the gamma emission at equilibrium. Figure 2-35 (per kg TRU) shows the initial TRU feed from discharged UOX for comparison so that one can see how recycling has changed gamma emission from its starting point - a modest impact. Figure 2-36 (per kg HM) shows gamma emission normalized to mass of heavy metal, for which a comparison with used UOX is possible. Used UOX emits about 1.2 W/kg-HM at 5 years after discharge, dropping to 0.3 W/kg-HM at 30 years and 0.06 W/kg-HM at 100 years. Fresh recycled fuel is below such numbers.

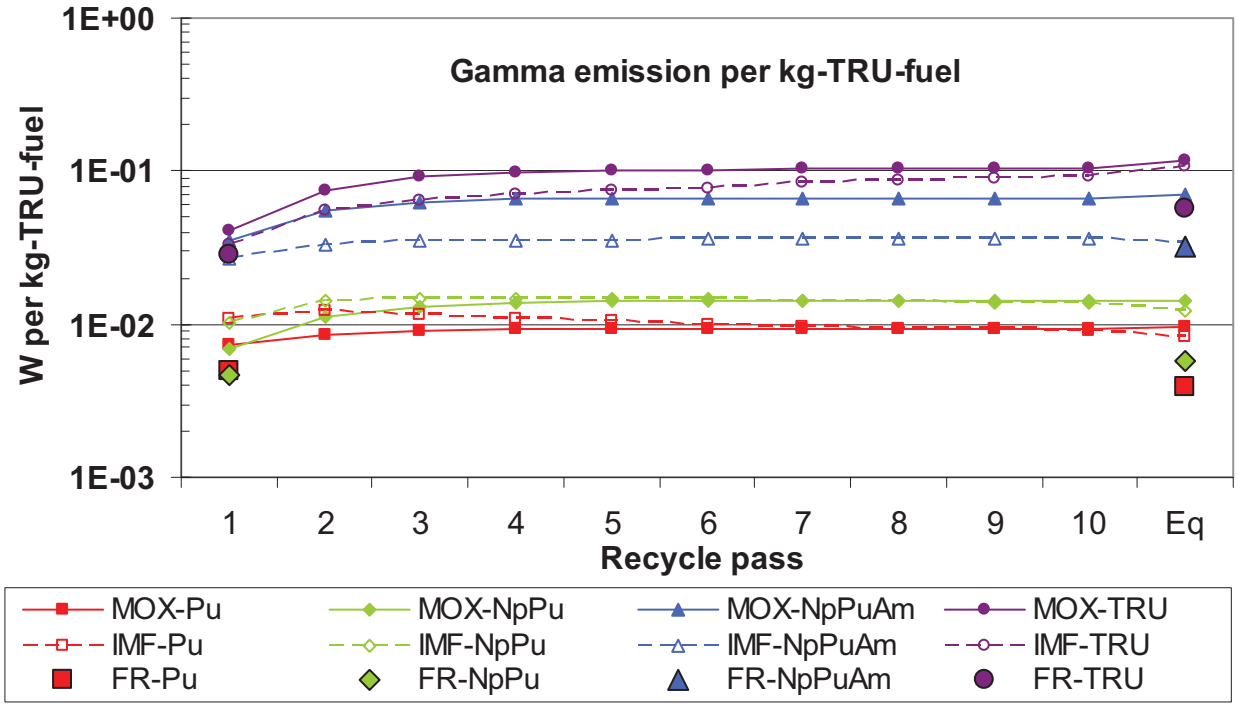

Figure 2-33. Fresh fuel gamma emission as function of the number of recycles and MA partitioning strategy, per mass of TRU (FR-oxide at CR=0.50, MOX-UE, heterogeneous-IMF)

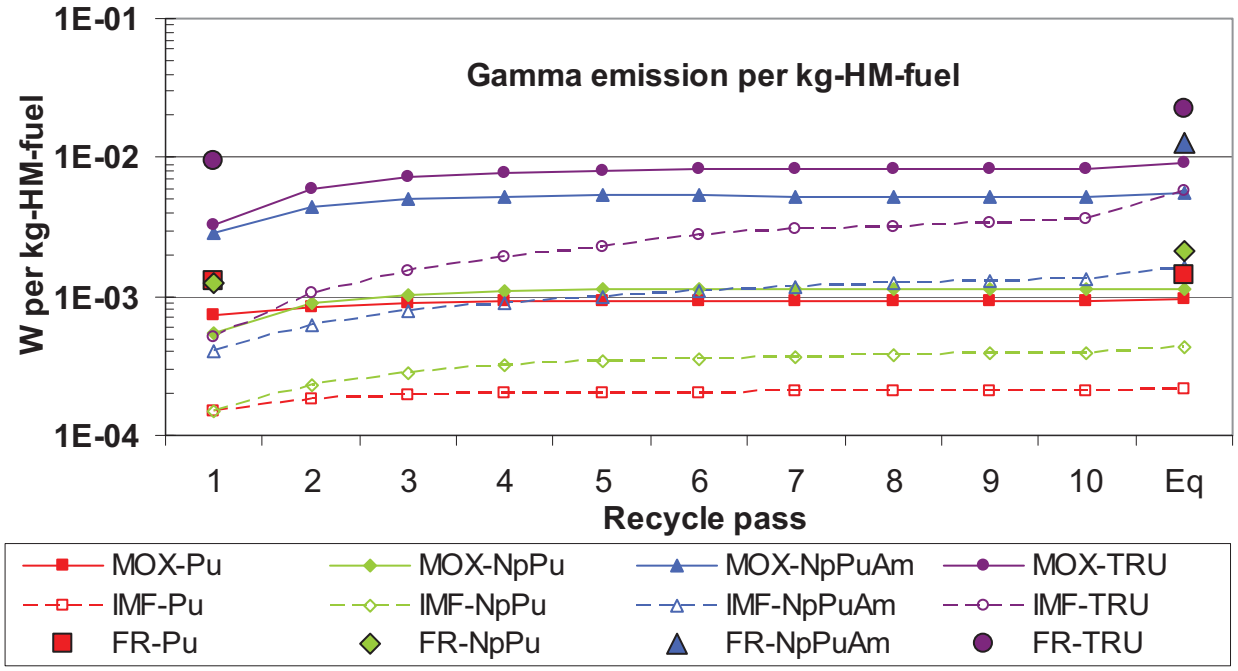

Figure 2-34. Fresh fuel gamma emission as function of the number of recycles and MA partitioning strategy, per mass of heavy metal (FR-oxide at CR=0.50, MOX-UE, heterogeneous-IMF)

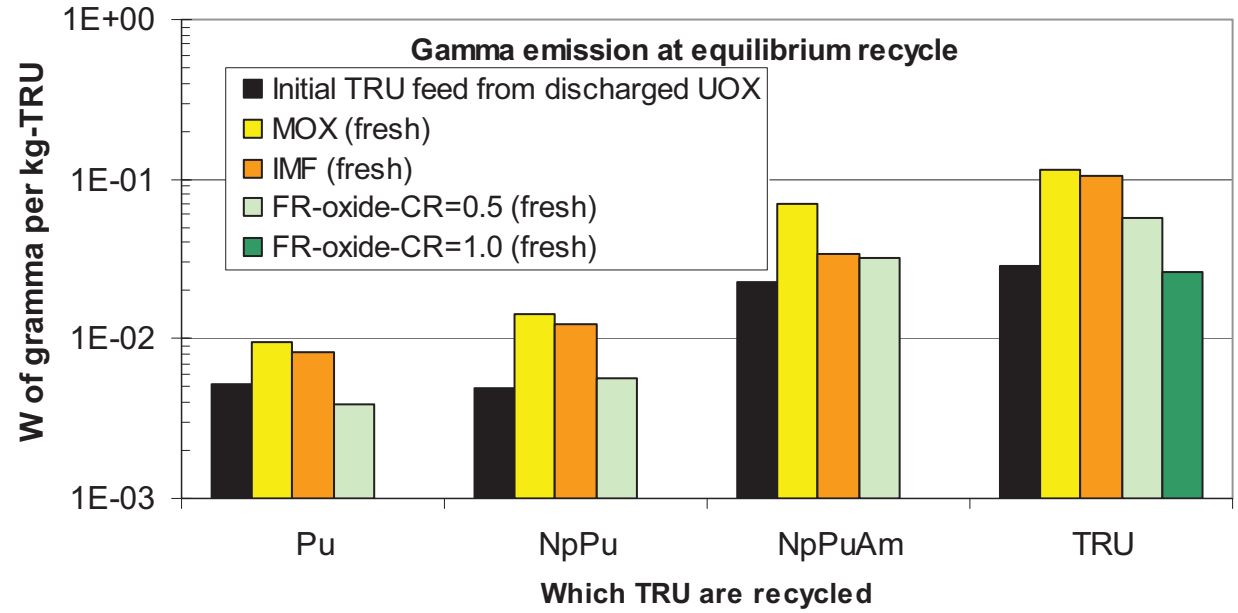

Figure 2-35. Equilibrium recycle fresh fuel gamma emission as a function of MA partitioning strategy, per mass of TRU

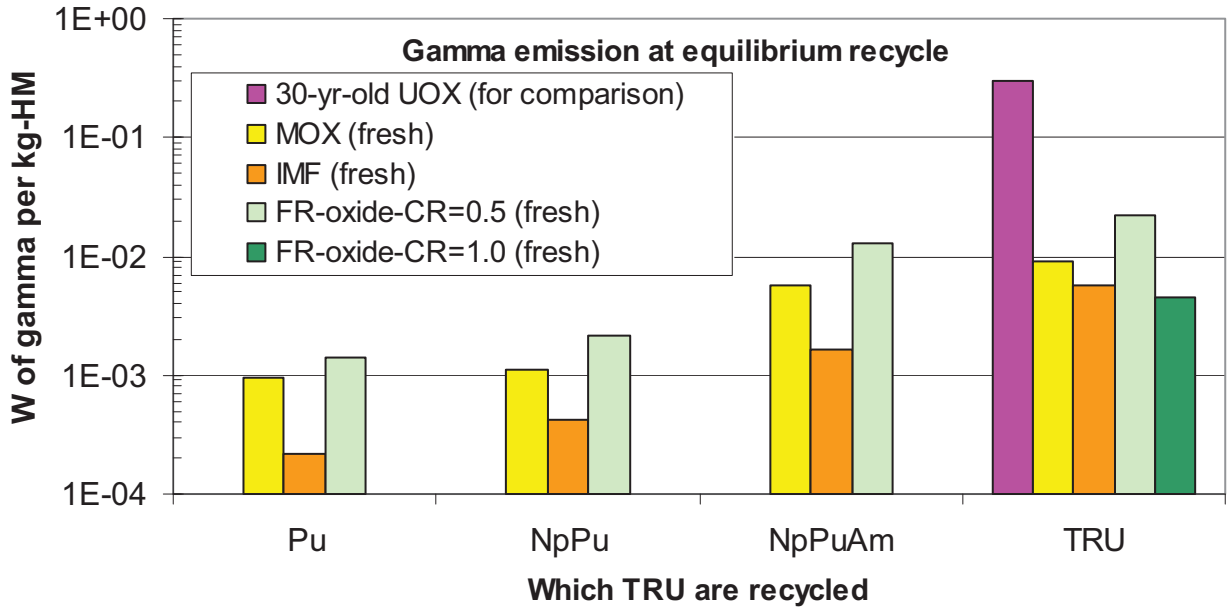

Figure 2-36. Equilibrium recycle fresh fuel gamma emission as a function of MA partitioning strategy, per mass of heavy metal

2.4.4 Spontaneous Fission Neutron Emission

Figure 2-37 and Figure 2-38 show the evolution of neutron emission upon multiple recycles, for the four recycle strategies (Pu, PuNp, PuNpAm, all-TRU), and the three reactor-fuel concepts being compared. Figure 2-39 and Figure 2-40 show the neutron emission at equilibrium. Use of fast reactors, rather than LWRs mitigates some of the neutron penalty of recycling Cm-Bk-Cf but not by multiple orders of magnitude. Given that recycle-by-recycle data is absent it is difficult to discern the relevance of contrasting equilibrium scenarios between thermal and fast neutron spectrum systems. The following plots are indicative of the fission-to-absorption ratio differences between thermal and fast reactors. Fast reactors have generally higher fission-to-absorption ratios than thermal reactors. Hence, fast reactors are more adept at transmuting by fission as opposed to neutron capture the higher mass actinides, Cm-Bk-Cf. Thus, the buildup of the primary spontaneous fission neutron emitters is less in fast reactors than it is in thermal reactors[g]. Nevertheless, the effect of global reaction rate (i.e., gross transmutation/s) is also relevant as it reflects the transient buildup of the Cm-244 and Cf-252 evolution as a function of calendar time over multiple recycles[h].

[g] The neutron source contribution of alpha,n reactions is also important, at least for the first few recycles until the contribution of spontaneous fission emitting dominates as the Cm-244 and Cf-252 concentration saturates at the fuel cycle equilibrium. Alpha,n contributions is discussed in detail in the contributing report by G. Youinou as well as the data contributed by D. Hawn given in Chapter 6 [1].

[h] This issue of T&P dynamic response is discussed in detail in the Chapter 3.

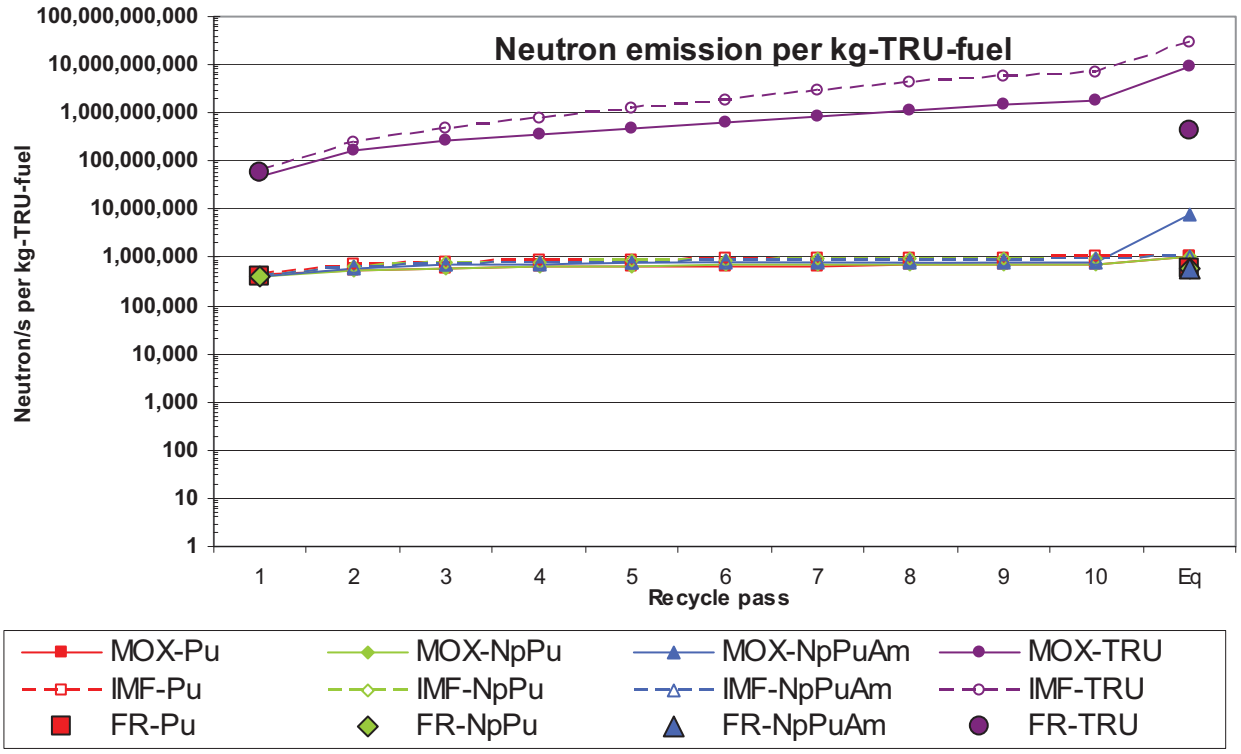

Figure 2-37. Fresh fuel neutron emission as function of the number of recycles and MA partitioning strategy, per mass of TRU (FR-oxide at CR=0.50, MOX-UE, heterogeneous-IMF), (alpha,n) reactions not included

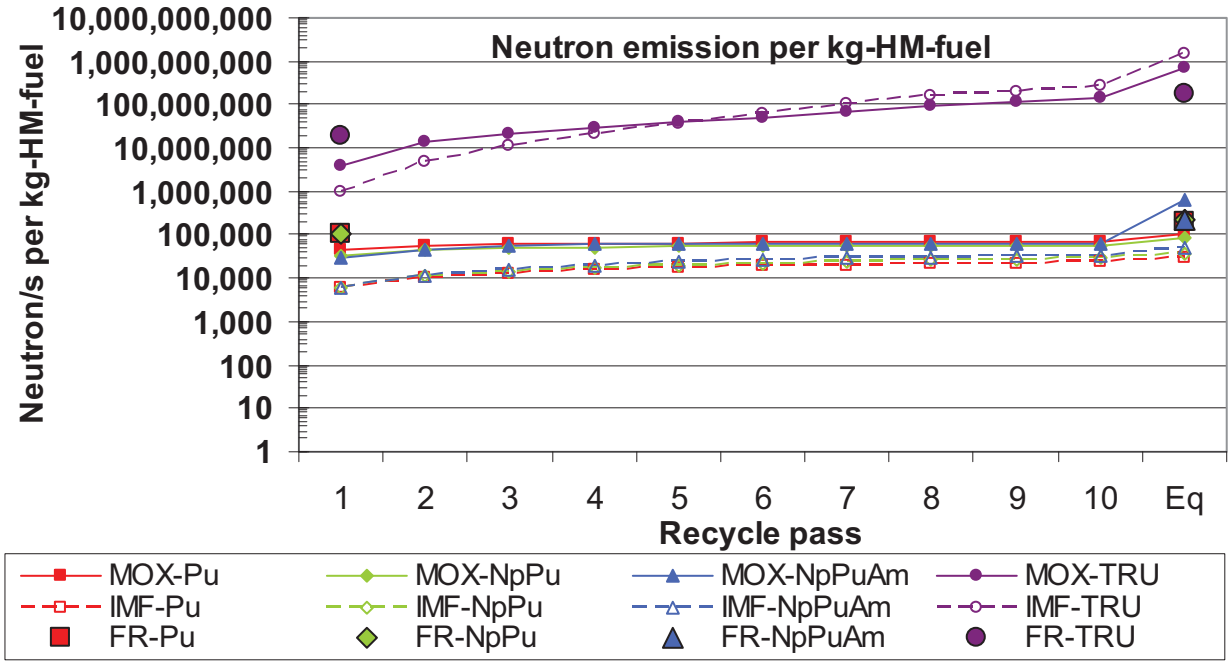

Figure 2-38. Fresh fuel neutron emission as function of the number of recycles and MA partitioning strategy, per mass of heavy metal (FR-oxide at CR=0.50, MOX-UE, heterogeneous-IMF), (alpha,n) reactions not included

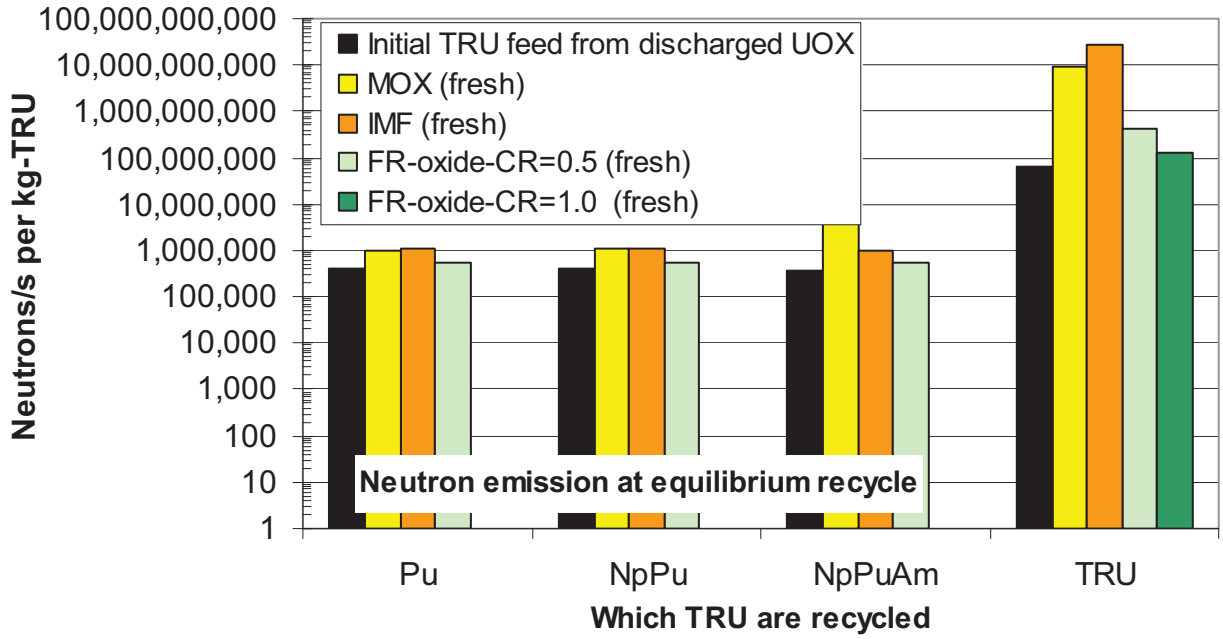

Figure 2-39. Equilibrium recycle fresh fuel neutron emission as a function of MA partitioning strategy, per mass of TRU, (alpha,n) reactions not included

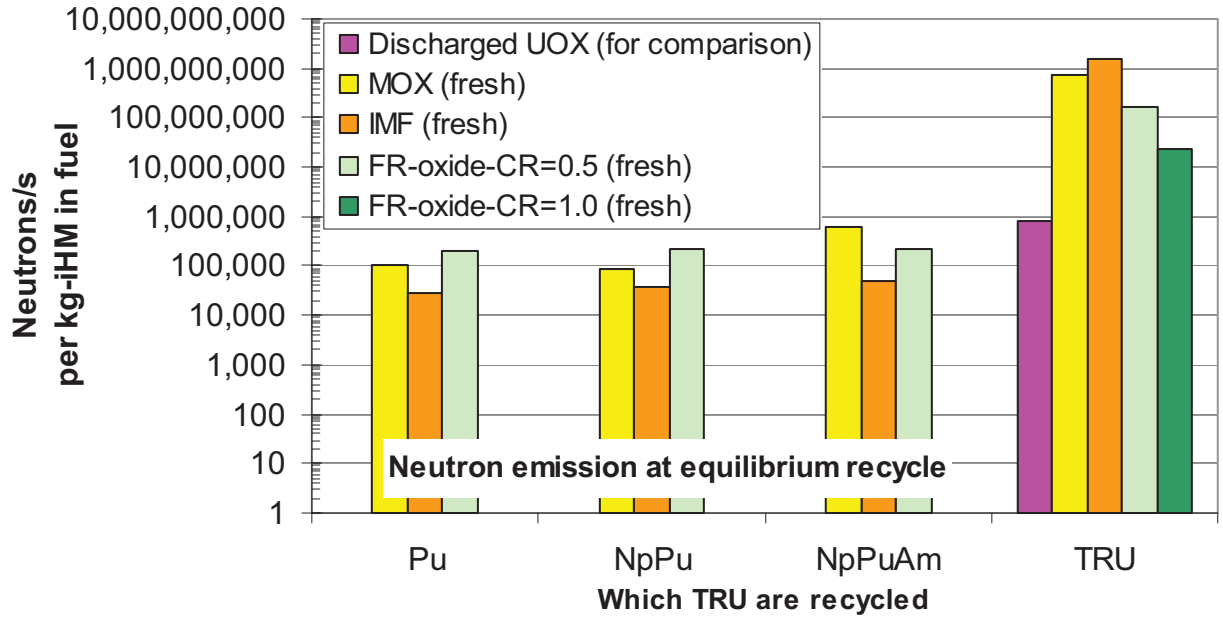

Figure 2-40. Equilibrium recycle fresh fuel neutron emission as a function of MA partitioning strategy, per mass of heavy metal, (alpha,n) reactions not included

2.5 Gateway Isotopes

The following discussion is a summary of neutron physics that offers a likely explanation for increasing higher mass actinide and hence radiologic source intensities with decreasing conversion ratio in fast burner reactors. This discussion is also a useful prelude to the following Chapter on transmutation dynamics which is partly dictated by the control of isotopes that possess a gateway property for breeding higher mass actinide chains.

Transuranic isotopes are formed by neutron capture (i.e.: without fission) in U-238 resulting in a transmutation into Pu-239. From Pu-239, further neutron absorptions, not resulting in fission, lead to transmutation of increasingly heavier isotopes. Coupled with subsequent decay, transmutation of key *gateway isotopes* (e.g., Pu-241, Pu-242, Am-243) results in formation of trans-plutonium (i.e., AmCmBkCf). Gateway isotopes have a central importance in a given transmutation chain such that its partitioning during recycle results in greatly reduced buildup of its transmutation daughters in the fuel cycle. An example of this is the capture transmutation of Am-243 into Cm-244. In a thermal reactor, the fission-per-absorption ratio is virtually zero for these gateway isotopes. In a SFR, this ratio ranges from 10% to 20% depending on the hardness of the fast energy spectrum (Figure 2-41). Therefore even in a fast spectrum, nearly all neutron interactions with this isotope result in production of Cm-244. This isotope comprises approximately 1/3rd of all americium in SNF (~50 GW day/tonne, 5 years cooled). Therefore it should be expected that for SFRs, Cm-244 buildup will be in step with the SNF americium contribution to the fuel composition, just as it is for thermal transmutation fuels such as heterogeneous-IMF or MOX-UE. This general statement will be quantified in the following discussion comparing fast burner reactors of varying conversion ratio with MOX-UE and heterogeneous-IMF.

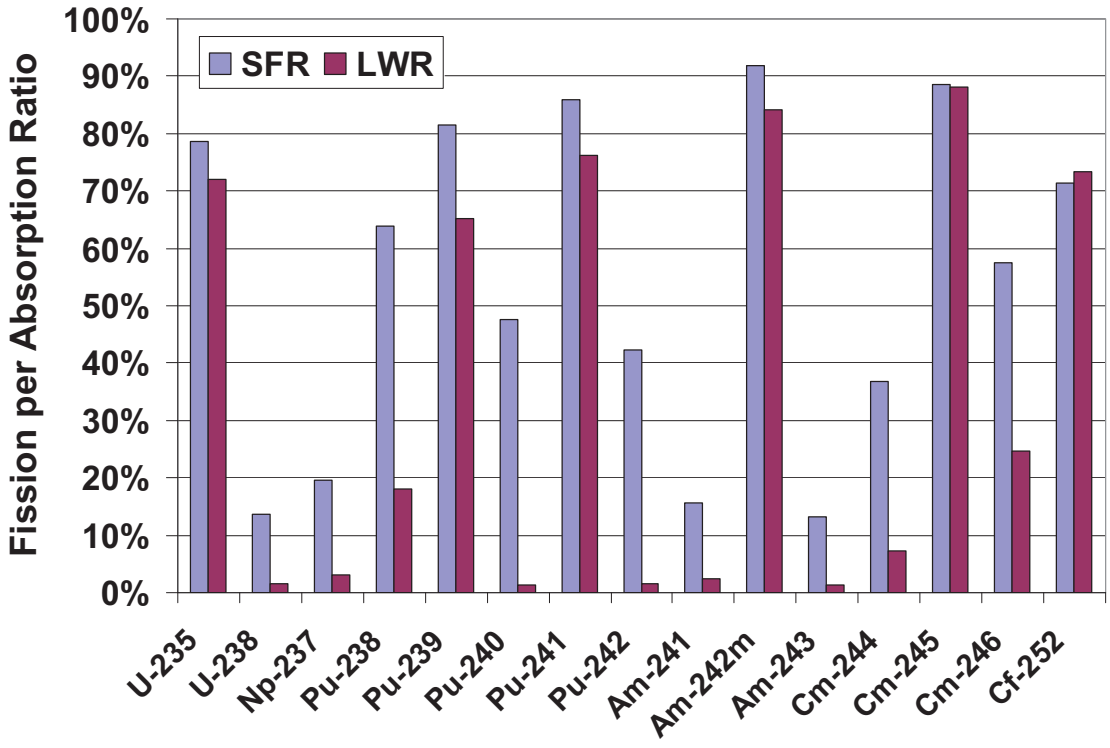

Figure 2-41. Fission-per-absorption ratios for fast reactor compared with light water reactor

2.5.1 Trans-Plutonium Generation (Am – Cf) and LWR Grade Pu Burning

A SFR in a purely plutonium breeding mode does not exhibit a large amount of trans-plutonium creation, due to the fact that these gateway isotopes are not allowed to form in the first place due to a high probability for fission relative to neutron capture[i]. In a fast burner reactor, however, these isotopes are produced by thermal reactors and then externally introduced to the SFR via SNF recycle. In a thermal reactor spectrum, the probability of fission per neutron capture is less than fast spectra (Figure 2-41). This allows Pu-241 to be formed by successive neutron capture starting from Pu-239 (Figure 2-42). Long cooling times, typical of much of the LWR commercial industry, has allowed this Pu-241 to decay into Am-241, allowing for a gateway into creation of trans-plutonium actinides. Further neutron absorptions, not leading to fission, transmute Pu-241 into the gateway Pu-242. Pu-242 is not fissile and exhibits transmutes into Am-243 which in turn is a gateway into Cm-244. Cm-244 is the first transmutation parent in a series of fissile and non-fissile curium and californium isotopes ultimately terminating in Cf-252. Thus, Cm-244 is a gateway for the ultimate buildup of Cf-252.

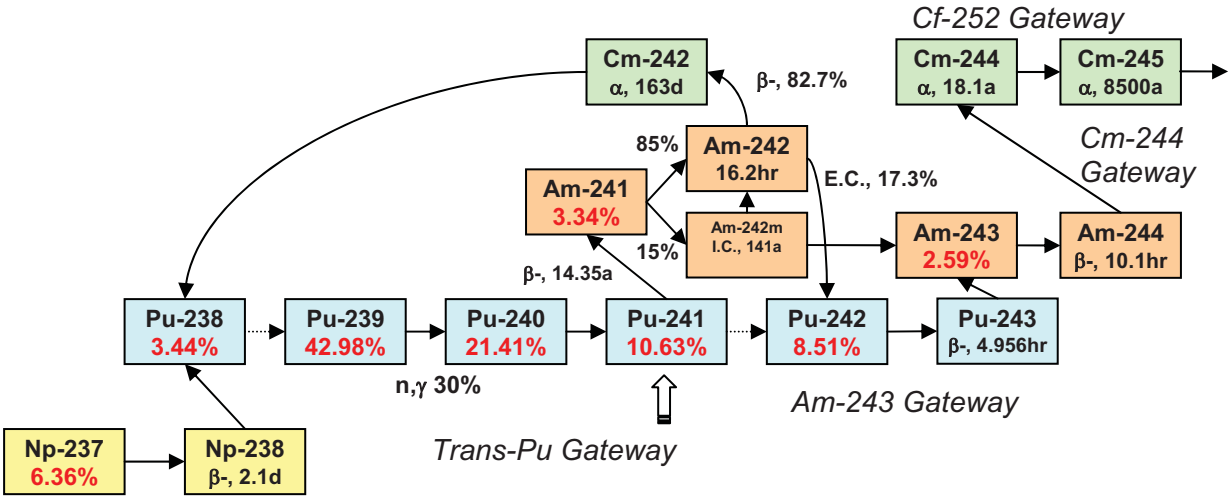

Figure 2-42. Transuranic transmutation chains. Red percentages are the concentrations in SNF TRU

These long-lived americium isotopes, Am-241 and Am-243, are not fissile, but rather exhibit a sharp energy threshold that must be overcome for fission to occur. Even in the SFR's fast spectrum, much of the neutron flux lies below this fission threshold energy. Cm-244 also has a fission threshold and is readily transmuted into Cm-245. Isotopes exhibiting this fission threshold property include fertile U-238, the problem minor actinides Np-237, Am-241, Cm-244 and the gateway isotopes, Pu-242, Am-243. These isotopes have an even neutron number, which gives them longer half lives compared to the odd-neutron isotopes of their respective elements. This explains why there are no long lived fissile neptunium or americium isotopes, because there are no long-lived isotopes with odd proton number (MAs) with odd neutron numbered (fissile). The even neutron number parity also tends to cause these isotopes to have a threshold for fission on the order of 1 MeV (Figure 2-43) [17].

The fast spectrum provides some neutrons at energies above this fission threshold, thus the higher mass actinide accumulation rate is slower for fast than for thermal spectra. It is this capacity to fission any

[i] Note that trans-plutonium and trans-americium are not typically standard in current nomenclature but are used in this report to reduce the use of long acronyms or phrases.

actinide to some extent, that retards the accumulation of higher mass actinides in the traditional breeder SFR. In a breeder SFR, the transmutation precursors to these elements, Pu-241, Pu-242 and Am-243, were sufficiently destroyed by fission as they were created. Therefore for breeders, isotopes heavier than Pu-241 never accumulate in the SFR's fuel cycle to an appreciable amount. For burner SFRs, because the LWR grade (thermal reactor) plutonium is introduced every recycle, the higher mass actinides build to a much higher equilibrium concentration in the fuel cycle. However, because of the higher fission-to-absorption ratios, this equilibrium concentration is qualitatively less than multi-recycling in a thermal spectrum as will be seen in the next chapter on transmutation dynamic feedback.

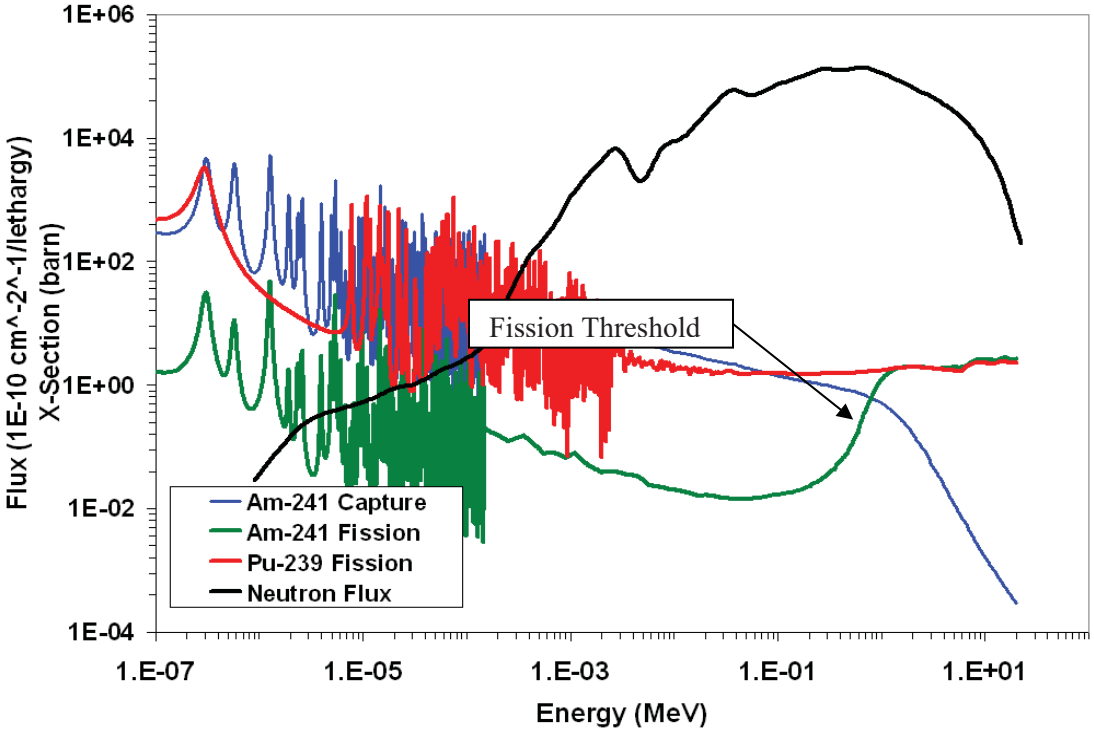

Figure 2-43. Cross Section Comparison of fissile and fertile transuranics

2.5.2 Trans-Americium Generation (Cm – Cf) and Americium Burning

The neutron capture cross-section exhibits an opposite trend to that of fission for even neutron numbered actinides near the fission threshold. Therefore, the neutron capture cross-section generally drops off rapidly below the fission threshold (Figure 2-43). Moderation decreases neutron energies, increasing the reaction rates experienced in the moderated. In particular, the neutron capture cross-sections of the long-lived MAs, Am-241, 243 and Cm-244 are two orders of magnitude greater just below 1 MeV than just above 1 MeV (Figure 2-43). Reduction of neutron energies to just below 1 MeV or lower, gives an immediate jump in transmutation efficiency of the initially loaded even neutron numbered actinides. Further moderation will increase transmutation rates and efficiencies due to the 1/E nature of neutron capture cross-sections in the thermal-epithermal range.

2.5.2.1 Curium Generation

Enhanced americium transmutation, however, comes at the expense of an increase in Cm-244 generation rate. Am-243 is the fertile source of Cm-244 breeding (Figure 2-42). Therefore, as americium isotopes are depleted relatively exponentially, Cm-244 builds up until the rate of transmutation from Am-243 is matched by the rate of Cm-244 transmutation into Cm-245. This Cm-244 buildup and burn-down

requires a significantly longer irradiation than for burning out americium isotopes, because it is the transmutation product for a large fraction of the original americium mass. Though not of great importance to repository performance due to its much shorter half-life, compared to Am-241, it is Cm-244 that poses an engineering problem for interim storage prior to geologic disposal or for further multi-recycling.

2.5.2.2 Californium Generation

Subsequent transmutation of Cm-244, not resulting in fission, ultimately leads to generation of Cf-252. Both Cm-244 and Cf-252 have a primary decay mode by alpha emission. However, their secondary decay mode is by spontaneous fission. Cm-244 has a spontaneous fission yield of 1.3E-4%, whereas Cf-252 is much higher at 3.09% [18]. The large spontaneous fission yield of Cf-252 causes this isotope to have a significant and often dominating contribution to neutron dose for scenario studies of both thermal and fast reactors depending on the amount of spent fuel cooling allowed prior to recycling.

3. Fast Parametric Sensitivity Analysis Methods for Option Studies

For most uranium and plutonium isotopes, the fuel composition as a function of recycle number does not change greatly after approximately 10 reactor-passes. After this many recycles, the uranium and plutonium fuel vectors are considered to be in a state of dynamic equilibrium. This equilibrium occurs when the destruction in isotope mass, due to depletion and decay, is balanced every recycling with externally supplied enriched U and reprocessed SNF. Here the term externally is used to mean the external input on the closed recycle loop of this dynamic system (Figure 3-1).

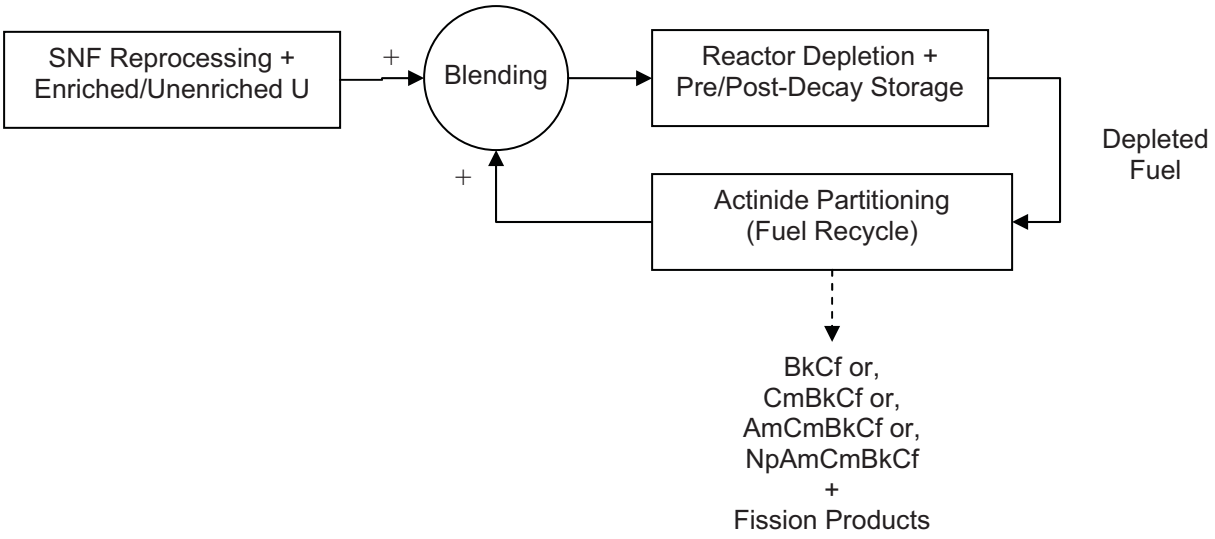

Figure 3-1. Block diagram representation of the multi-reprocessing dynamic system

Here the reactor and decay storage of fresh and spent fuel serves as a transfer function that modifies the fuel vector as a function of time. Fuel recycling provides varying degrees of actinide partitioning feedback. The SNF reprocessing and/or enriched uranium supply is the external forcing function of the system, as it adds the fissile material which drives depletion. Blending is represented here as a summing junction. With respect to transuranic isotopes, recycle acts as negative feedback or discriminator as it removes actinide isotope mass from the system. It can also be neutral feedback if all transuranics are reprocessed (i.e., PuNpAmCmBkCf). Since Pu isotopes are never removed, the feedback is always plutonium neutral. Therefore, the plutonium elemental, as well as isotopic, composition equilibrates much more quickly than MAs that may be preferentially removed during reprocessing. Additionally, MA production occurs by transmutation of mainly plutonium isotopes (with the exception of Np-237 which is produced by successive neutron captures starting with U-235). Therefore, the buildup of gateway Pu isotopes must first occur before the buildup and eventual equilibrium of MAs can occur. The equilibrium of these MA isotopes can not take place until many recycle passes beyond that of the approximate 10 needed for plutonium equilibrium. This chapter describes the software methodology and some analysis modeling the feedback loop depicted in Figure 3-1.

3.1 The MRTAU Code

Multi-Reactor Transmutation Analysis Utility (MRTAU) is a generic depletion/decay algorithm with features for modeling transmutation and element/isotope feed and removal streams over multiple recycles. This software is written in the Fortran-90 computer language. MRTAU is a further enhancement of a previous depletion tool developed for calculating transmutation helium and fission gas generation [19].

The motivation for creating MRTAU was to simulate sustained multi-recycle of MOX-UE to the point of Cf-252 equilibration (equilibrium cycle) for the MOX-UE study authored by G. Youinou [1]. Youinou's study performed detailed lattice-physics calculations using the SCALE5.1 TRITON module for the first 10 recycle passes of MOX-UE (See Chapter 2). This is sufficient recycle passes to achieve equilibration of most actinides except for the higher mass actinides (Cm-Cf). Using, TRITON for the further recycle passes to achieve equilibrium of these isotopes was considered to be too computationally expensive. Thus physics calculations up to 10 recycle passes were performed using TRITON to achieve uranium and plutonium equilibrium. The burnup dependent cross-section data from the 10^{th} recycle was then extracted from the SCALE5.1 *ft33f001* binary file into ASCI format using the SCALE5.1 XSECLIST post-processing module [20]. These cross-sections were then used by MRTAU for an additional 50 recycle-passes to reach equilibrium of all isotopes, including Cf-252. This equilibrium is assumed to have been achieved once the fresh fuel isotopics does not change from one recycle to the next.

MRTAU uses the exponential matrix method for estimating the depletion or pure-decay of isotopes over discrete *time-steps* [21]. The depletion code currently tracks isotopes between U-234 and Cf-252. The number of time-steps used is arbitrarily set by the user. The code input format is formatted in such a way that the *recycle-period*, the time from reprocessing in recycle N to time of reprocessing in recycle N+1, is arbitrarily set by the user. A detailed description of the exponential matrix method is given in Appendix A.

An additional feature allows closure of the loop in Figure 3-1 by defining the number of *recycle-loops* that the depletion problem of one recycle-period is to be iterated. At completion of each recycle-loop iteration, the code takes the composition from the last time-step of the recycle-period and then performs a blending calculation using user specified external supply streams. The blended composition then becomes the starting point of the first time-step of the recycle-period in the next recycle-loop iteration. This blending calculation has a provision for a makeup fertile species of isotopes and a makeup fissile species for reconstituting the fuel back to its original total mass and user specified enrichment.

The recycle period is divided into arbitrary *burnup-steps*. Each burnup-step specifies an exact 1-group cross-section set and flux, power level (including zero power for pure decay) and separation efficiency (used to define losses from the system within the burnup-step). Burnup-steps represent changes in the transmutation physics during a recycle period. Time-steps represent the discretization of time in the depletion/decay solution and are a finer resolution than burnup-steps. The information contained in the burnup-step is assigned or mapped to all time-steps within the time interval of the given burnup-step (Figure 3-2). As the depletion algorithm marches from time-step to time-step, old physics data is swapped out for that of each new burn-step sharing the same place time as the new time-step. This mapping strategy allows the depletion algorithm to march seamlessly from beginning to end of the recycle-period irrespective to the changing physics conditions.

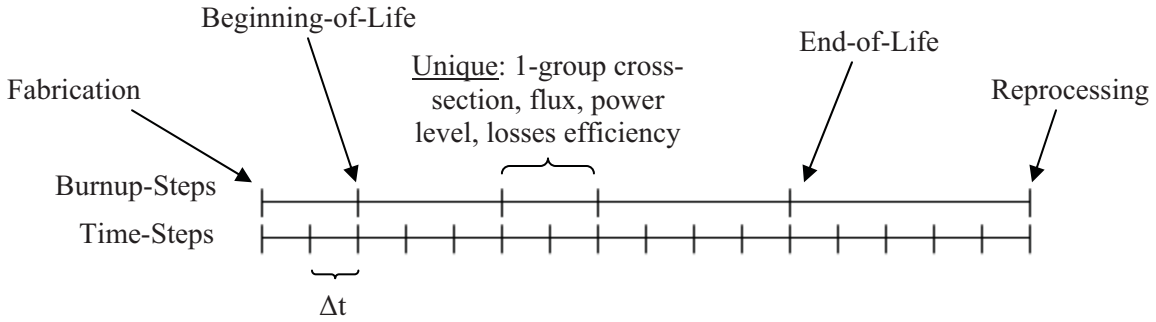

Figure 3-2. Schematic of a single recycle-period showing the mapping of burn-steps onto time-steps

This ultimate flexibility by the user facilitates simulation of any arbitrary combination of decay and irradiation modes of operation, e.g., changes in core power level, changes in material losses from the fuel cycle, burnup depended cross-section data, etc. The code is currently designed to flag the burnup-step corresponding to post-fabrication decay time, end-of-life of the fuel in the reactor, and duration in the cooling pond.

A cautionary note is given. Just as with other standalone depletion codes, the quality of the depletion data produced is only as reliable as the input cross-section data. Therefore, MRTAU is not a replacement for detailed core physics data generation but is rather a user of such data in order to explore the fuel cycle design envelope that is less known. Often times rigorous cross-section generation and collapsing for every recycle is computationally and manpower expensive. Because cross-section data does not vary greatly once the fissile isotopes have equilibrated, MRTAU is also useful in carrying out the repetition to equilibrium using the first few detailed flux and cross-section calculations that were performed to get to fissile isotope equilibrium.

3.2 Sensitivity of Cross-Section to Scenario Study

The uncertainty of MRTAU results is dependent on the suitability of the 1-group cross-section and flux data being used to represent the actual depletion system being simulated. Aside from data uncertainties in the original measured cross-section data, representivity of 1-group data is dictated by: (1) the similarity between the MRTAU scenario and the original reactor system studied during 1-group data generation and (2) the sensitivity of the 1-group data to isotopic evolution after subsequent recycling, beyond that considered in the original physics study. Collapsed cross-section data is sensitive to the neutron flux spectrum, which in turn is dependent by the spatial and energy self-shielding effect that the fuel and structural material isotopes have on that spectrum. In thermal reactors, i.e., LWRs, it is common that the spectrum will evolve as the fuel's fissile isotopes are being depleted. Cross-section data for this behavior is known as *burnup-dependent*, because the 1-group cross-section values evolve as self-shielding changes with changes in fuel composition due to burnup.

Isotopic evolution as a result of multi-recycle also affects the neutron spectrum. From one recycle to the next, end-of-life isotopics are reconstituted to the prescribed fresh-fuel transuranic enrichment. Therefore, it should be expected that the fresh-fuel spectrum of the next recycle is more representative of the end-of-life spectrum of the previous recycle. This is the idealized example. In reality, out-of-core effects of decay storage, MA partitioning, and blending with external fuel feeds will also affect the general spectrum and burnup dependency. Under a given set of conditions, the isotopes most controlling of self-shielding and burnup-dependency will equilibrate after successive recycles. However, until this dynamic equilibrium is reached, the self-shielding and burnup dependency will change as a function of the recycling number. Figure 3-3 shows the differences in Pu-239 and Am-243 cross-sections for the 1st and 10th recycling of Pu-only MOX-UE.

The addition of MAs for any particular transmutation scenario study also affects the spectrum because they compete for the same neutrons as the uranium and plutonium isotopes. Not only do MAs generally perturb the neutron spectrum, but the level of perturbation will change as these isotopes are depleted from the fuel. Thus the buildup and burn-down of MAs during irradiation will also dictate the burnup decencies. Figure 3-4 and Figure 3-5 shows the burnup-dependent cross-sections of Pu-239 and Am-243, respectively, for different MA partitioning scenarios involving MOX-UE.

As can be seen from the plots there is approximately 6% maximum error between any given Pu-239 capture cross section. This holds true for both dependency on recycle number and actinide partitioning scenario. The Pu-239 fission cross-section error is in the range of 4-5% for both recycle number and actinide partitioning scenario sensitivities. The error on Am-243 capture cross-section is much more, with a maximum of 30% between partitioning scenarios with americium and cases without americium.

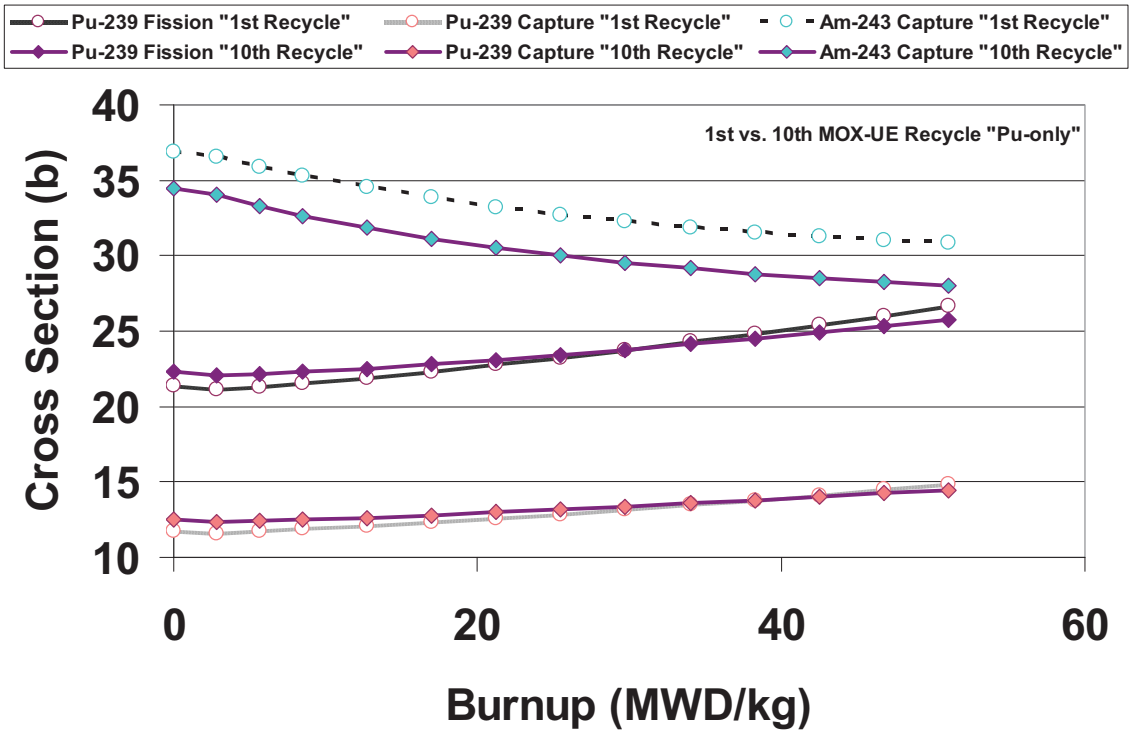

Figure 3-3. MOX-UE Pu-239 and Am-243 cross-section dependency for 1st and 10th recycle

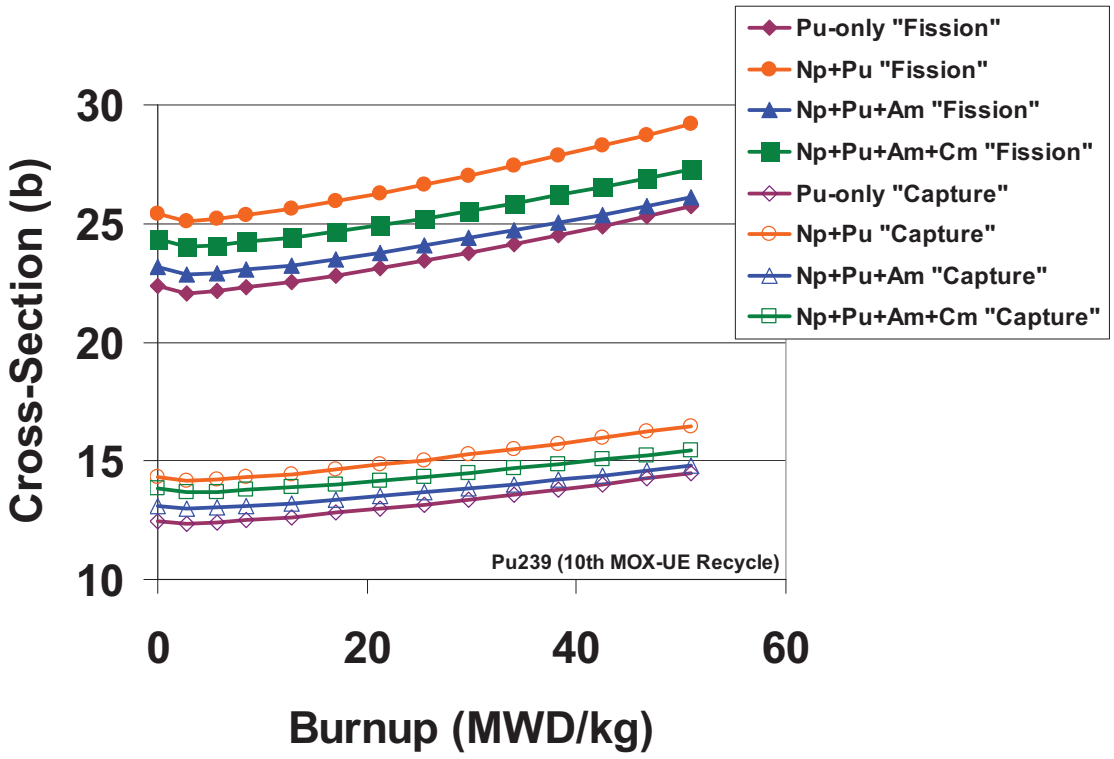

Figure 3-4. MOX-UE Pu-239 cross-section dependency per partitioning scenario

The maximum Am-243 capture cross-section error based on recycling number is approximately 7%. Am-243, as well as most other MA isotopes, can be highly absorbing in the thermal spectrum, thus giving a significant self-shielding effect when present in the fuel in high enough concentrations. Thus, the inclusion of MA (particularly americium) in the fuel gives a strong self-shielding penalty on the neutron capture cross-section worth of the MAs, themselves.

Given the burnup dependency trends in the LWR cross-sections, MRTAU calculations for LWR fuels will likely require burnup-dependent cross-section data from a higher fidelity physics calculation. From observing the MOX-UE cross-section trends, a few guidelines for selecting the most suitable burnup-dependent data set can be made. First, there is less cross-section agreement error from recycle-to-recycle then there is for different actinide partitioning scenarios. Second, the concentration of MAs in the LWR fuel should be observed and matched to the MRTAU predicted MA concentrations whenever possible.

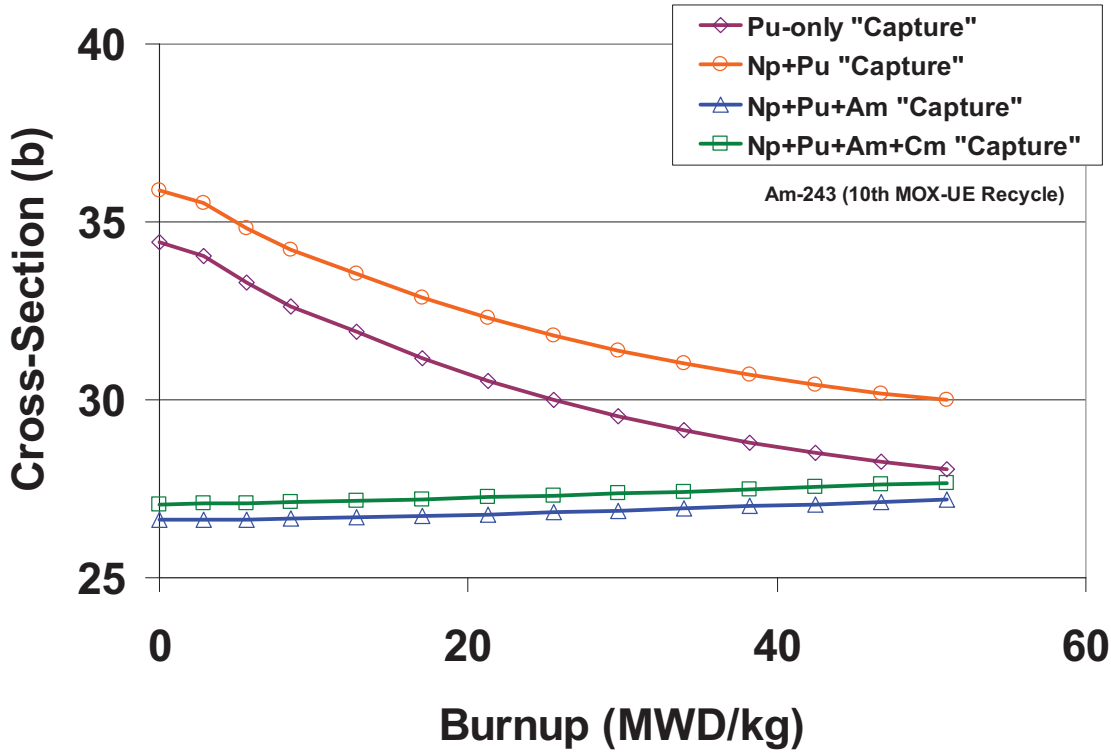

Figure 3-5. MOX-UE Am-243 cross-section dependency per partitioning scenario

The effect of MA self-shielding can also be seen in fast reactor cross-sections. Figure 3-6 and Figure 3-7 shows the capture and fission cross-sections, respectively, for U-234 through Cf-252 in an oxide fueled SFR with a CR=0.5. Note that burnup-dependent cross-sections are not common in SFR calculations because the degree of burnup related spectral shift is much less pronounced than with LWRs. Notice that the main differences in cross-section occur for MA isotopes. The largest error in both capture and fission cross-sections among all isotopes was approximately 30%. The highest error occurs in the curium and higher mass actinide isotopes for both capture and fission cross-sections. The error in most uranium and plutonium isotopes among different partitioning scenarios was only a few percent.

This trend in agreement error between various scenario studies generally holds true when comparing SFRs of different conversion ratios and also for metal fuel. Therefore, use of generic cross-section data in the MRTAU code to analyze multi-recycle dynamics should yield low calculation error for uranium and plutonium isotopes but high calculation error in the higher mass actinides.

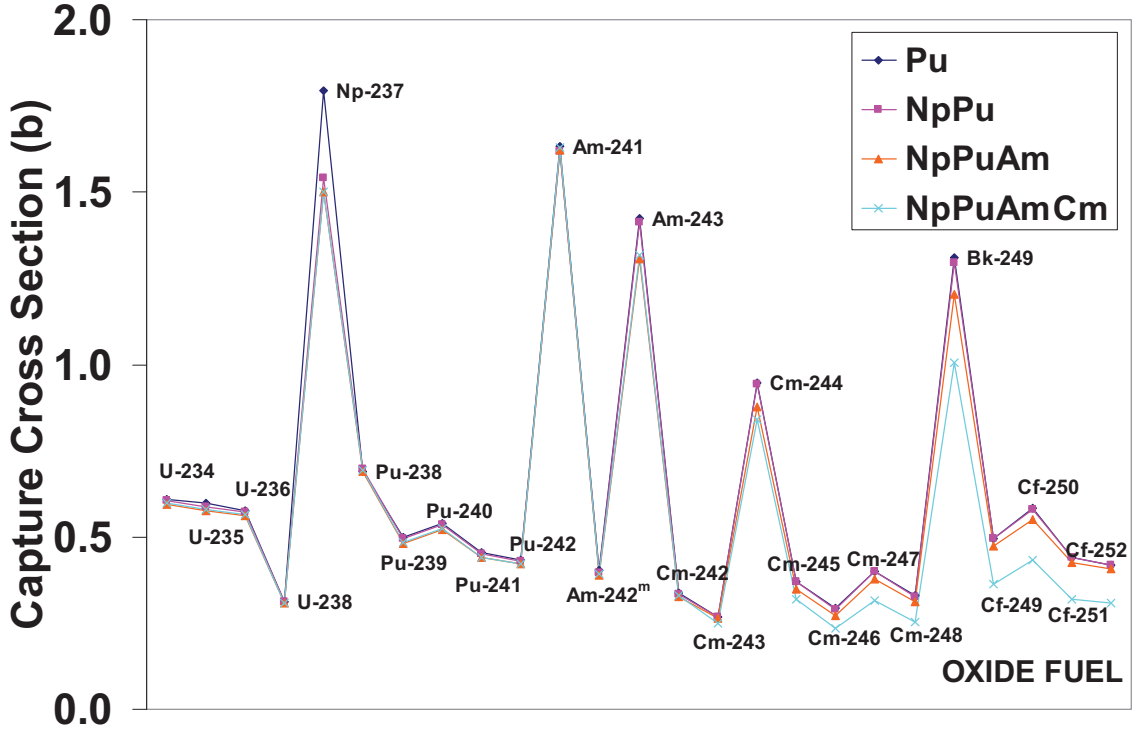

Figure 3-6. Oxide fueled SFR CR=0.5 capture cross-section per partitioning scenario

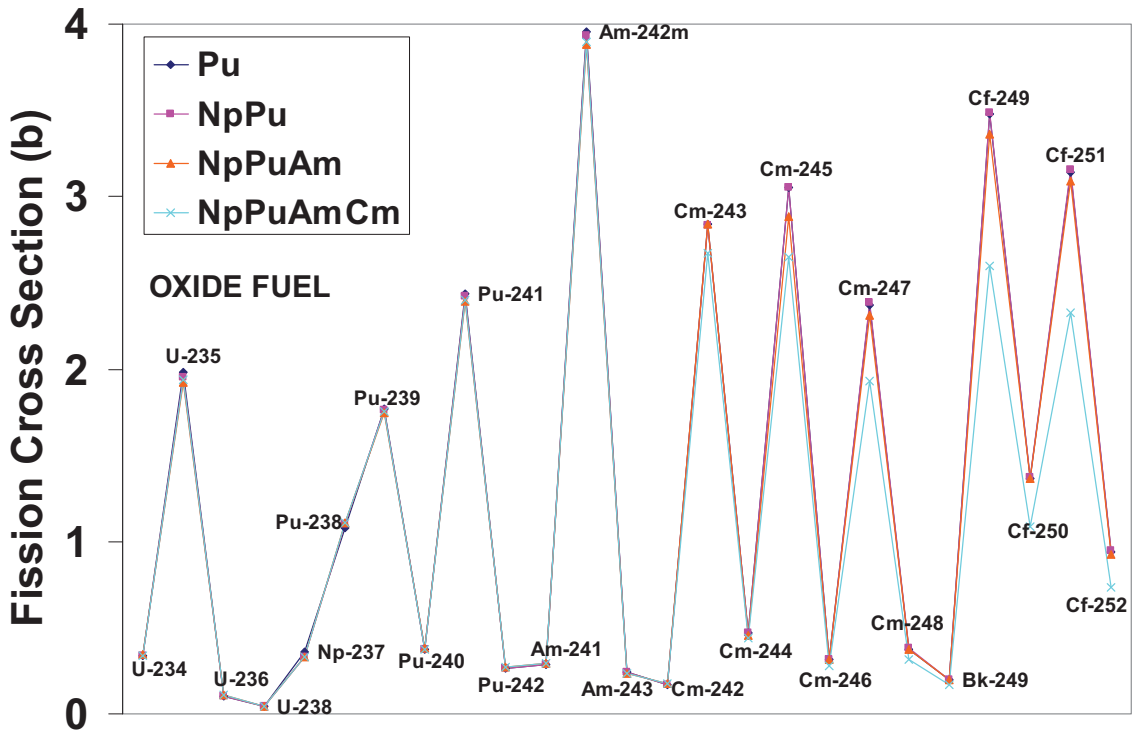

Figure 3-7. Oxide fueled SFR CR=0.5 fission cross-section per partitioning scenario

For both thermal and fast neutron spectrum systems, cross-section agreement errors when put into the MRTAU recycle feedback loop will propagate with each successive recycle. This propagated error will require quantification for future studies. However, the level of error propagation in the MRTAU calculation will depend on the relevance of high error isotopes to specific transmutation chains of interest (e.g., gateway isotopes).

3.3 Dynamic Response and Isotopic Evolution

Just as with any mechanical feedback system, fuel cycle feedback is a function of *gain* and *frequency*. The inverse of the recycle-period is the frequency of recycling per calendar time. In dynamic feedback loops, the gain is the transfer function that converts input signal into output signal. Feedback is the conversion of output signal into input signal and can have its own secondary gain. These gains can be amplifying, dampening or discriminating. Fission, capture and radioactive decay are all three forms of transmutation that changes the concentration of an isotope; decreasing its own concentration while contributing to the buildup of another. Therefore, these transmutation processes are the gain associated with each individual isotope. Much emphasis is usually placed on the flux and cross-section processes of gain in typical static equilibrium fuel cycle analysis. In such fuel cycle analysis, decay gain or decay storage of spent fuel is usually arbitrarily set in the scenario based on assumptions of fission product cooling time requirements. These assumptions are typically based on historical evidence or engineering judgment. Most actinide isotopes are typically too long lived to have a strong sensitivity to decay gain. However, several isotopes have relatively short half-lives on the same order as the recycle-period. These isotopes of interest include Pu-241, Cm-242, Cm-244, Cf-252. As will be shown, changing the decay storage time can dramatically change both the equilibrium concentration and the amount of time it takes to achieve equilibrium for these isotopes (i.e., transient response time).

MRTAU was used to analyze the dynamic evolution of TRU recycling scenarios of MOX-UE and SFRs. For the MOX-UE cases, burnup dependent cross-section data for the 10th MOX-UE recycling of the Youinou study was used [1]. For the SFR cases, burnup independent cross-section data from a past INL study on oxide and metallic SFRs with CR=0.5, authored by Ferrer et al. al., was used [22]. For both MOX-UE and SFR cases, a sensitivity study was performed by keeping all irradiation conditions constant while varying the decay storage time. In addition, both oxide and metallic fast reactor fuels were considered. For a more accurate analysis of dynamic feedback, capturing changes in cross-section data as a function of recycle number, the TRITON calculations (MOX-UE) and REBUS (SFR) calculations would have to be completely redone. Given the previous discussion on cross-section agreement error between different scenario studies, selection of these cross-section data sets to represent scenarios with different cooling times is deemed acceptable for this sensitivity analysis.

Table 3-1 gives the irradiation and cooling times used for each MRTAU case. Each MRTAU case was started with an initial transuranic composition in the first recycle corresponding to PWR SNF with a burnup of 50 GW-day/tonne and a cooling time of 5 years (Table 3-2). This SNF TRU isotopic vector also defined the composition of the external makeup feed composition.

Table 3-1. Scenario descriptive parameters used as MRTAU input

	MOX-UE		SFR (CR=0.5)		
Cross-section and Flux Data	MOX		M	M	O
Post-Fabrication Time (years)	1	1	0.4	2	2
Irradiation (Full-Power-Years)	4.1	4.1	3.7	3.7	3.7
Spent Fuel Cooling Time	5	10	0.8	10	10
TRU enrichment (%)	8	8	33	33	33
U enrichment (%)	6.5	6.5	0.2	0.2	0.2

Note: M=metal, O=oxide SFR (CR=0.5) 1-group burnup independent; MOX data was burnup dependent

Table 3-2. Transuranic vector used for both initial (1st-recycle) and external makeup feed composition

	w/o
Np-237	5.36%
Pu-238	2.63%
Pu-239	48.18%
Pu-240	21.58%
Pu-241	10.37%
Pu-242	6.11%
Am-241	3.32%
Am-242m	0.01%
Am-243	1.70%
Cm-243	0.01%
Cm-244	0.65%
Cm-245	0.06%
Cm-246	0.01%

Figure 3-8 shows the dynamic evolution of Pu-239 for the scenarios described in Table 3-1 over the course of repeated post-fabrication storage, irradiation, spent fuel cooling, actinide partitioning and blending. Notice that for both MOX-UE and SFRs the concentration of Pu-239 in fresh fuel (i.e., beginning of irradiation) drops off with successive recycle. This is due to the fact that both cases consume more fissile isotopes then they create. Therefore from a fissile isotope standpoint, the transuranic vector rapidly degrades with successive recycle. This denatured equilibrium happens fairly quickly after only a few recycle iterations.

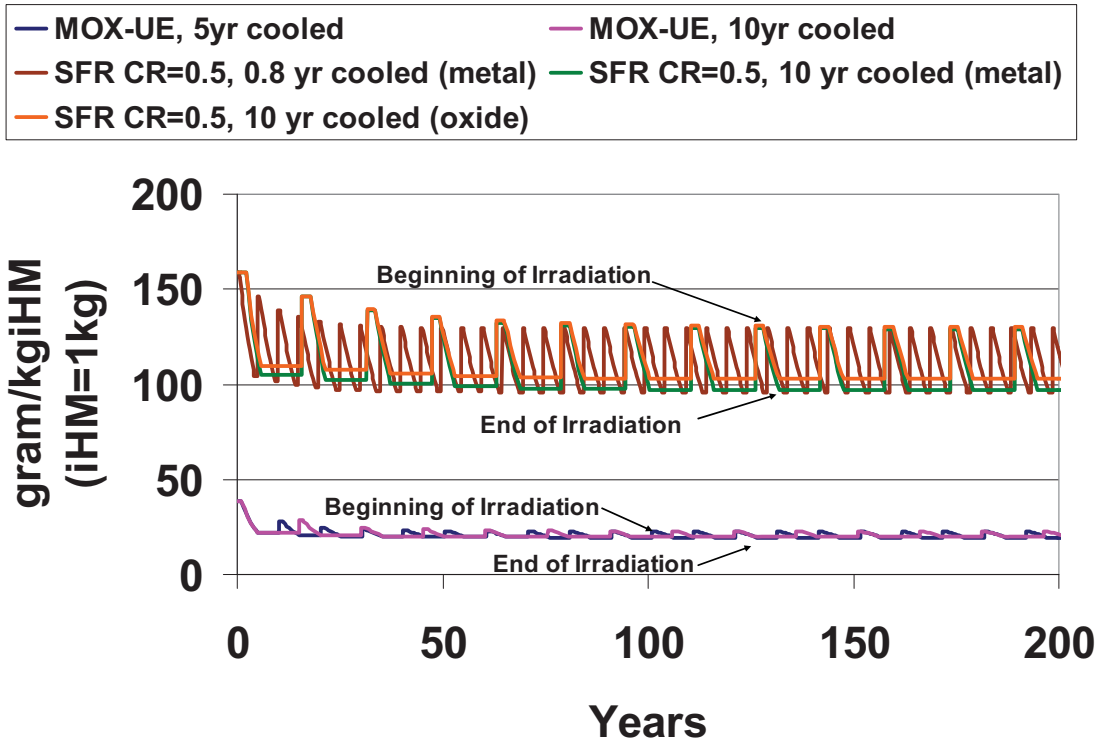

Figure 3-8. Pu-239 isotopic evolution during successive fuel recycles per heavy metal

Figure 3-9 shows the dynamic evolution of Pu-241 per successive recycle. It is interesting to note that reduction of the Pu-241 concentration in the fresh fuel with successive recycles is even more pronounced for fast reactors than for thermal reactors. In both MOX-UE and SFR scenarios, the Pu-241 is first being bred (increasing concentration during irradiation) from capture reactions of Pu-240. After irradiation the amount of Pu-241 breeding is negated by decay transmutation into Am-241. This trend is true even of the very short cooling time (0.8 year) scenario, except that the spent fuel content in this case equilibrates to a higher concentration than the longer cooling time scenarios (10 year). Coincidently, the Pu-241 concentrations after spent fuel cooling are not nearly as dissimilar as the fresh fuel between the MOX-UE and SFR scenarios. This is noteworthy because the transuranic enrichment between MOX-UE and the SFR is greater than a factor of three.

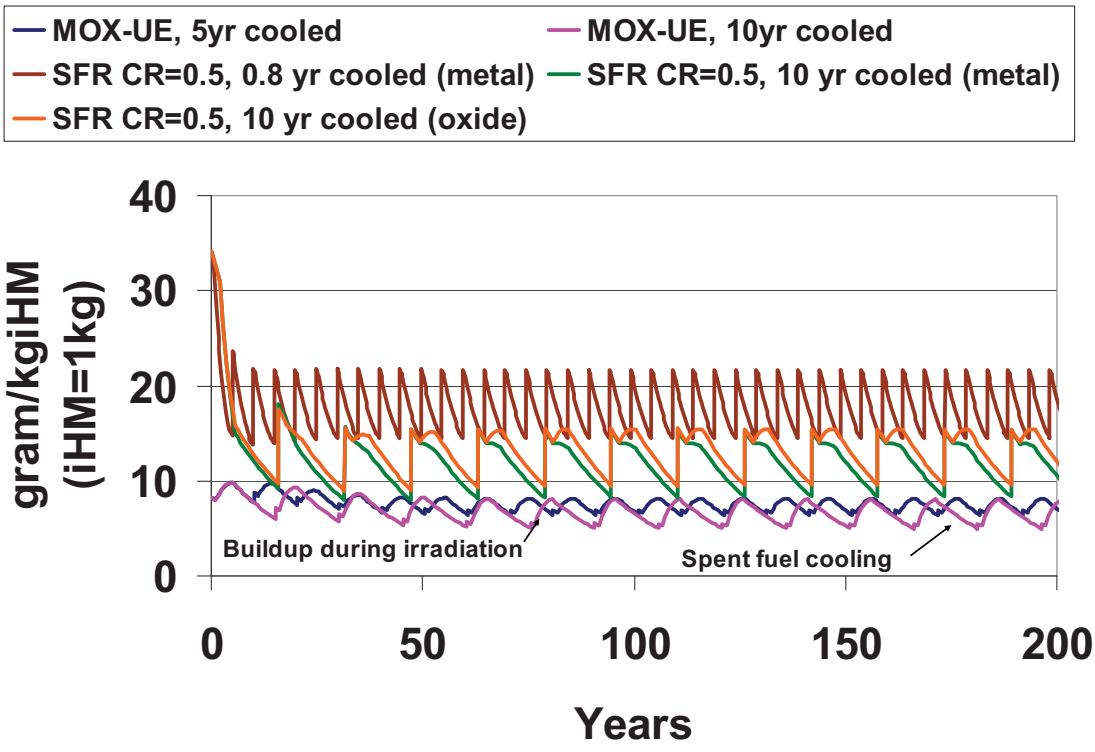

Figure 3-9. Pu-241 isotopic evolution during successive fuel recycles per heavy metal

Figure 3-10 shows the dynamic evolution of Am-241 per successive recycle. For both MOX-UE and SFR scenarios, the Am-241 concentration is being burned down during irradiation and then increases noticeably during both spent fuel cooling and post-fabrication storage. The sharp step-function between spent fuel cooling and post-fabrication storage is the additional Am-241 from SNF being blended into the fuel composition.

Figure 3-11 shows the dynamic evolution of Cm-244 per successive recycle. The concentration of Cm-244 for both MOX-UE and SFR scenarios with 10 year cooling was very similar, despite being of two completely different neutron energy spectrums. This is somewhat counter-intuitive considering that fast reactors have a much higher fission-per-absorption ratio than thermal spectrum reactors. However, it is the reaction rate stemming from the transmutation precursor, Am-243, that is the generation source of Cm-244. Thus, the buildup of Cm-244 is partly fixed to the concentration of Am-243 in the fuel.

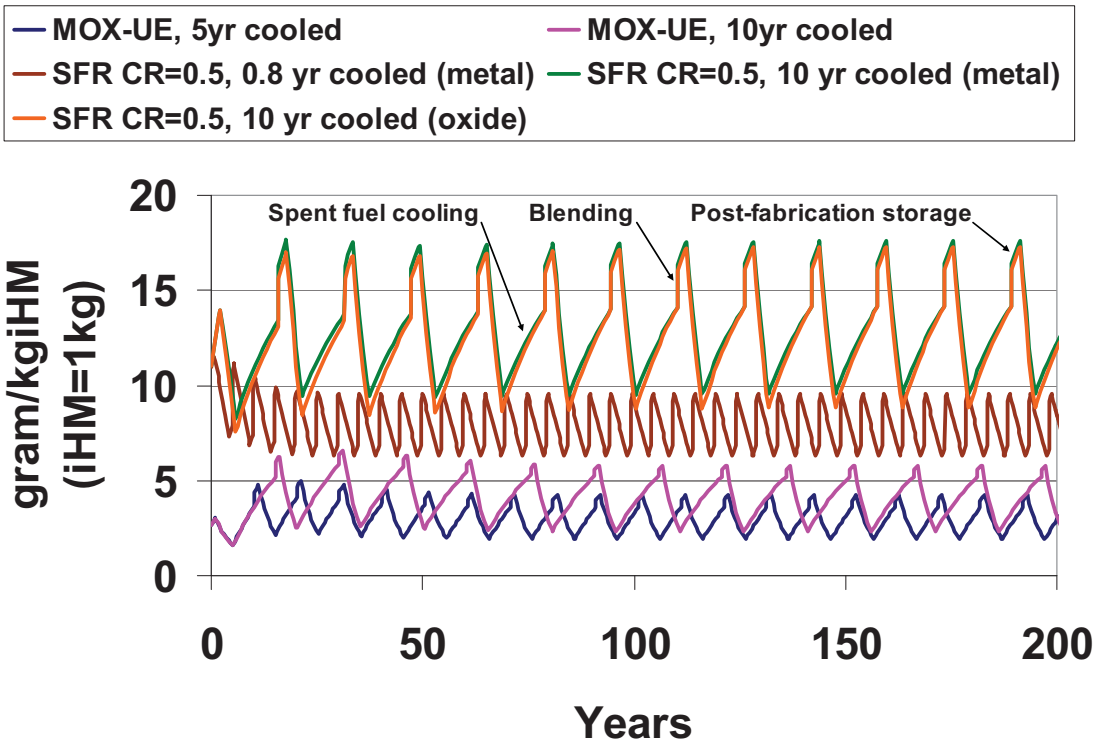

Figure 3-10. Am-241 isotopic evolution during successive fuel recycles per heavy metal

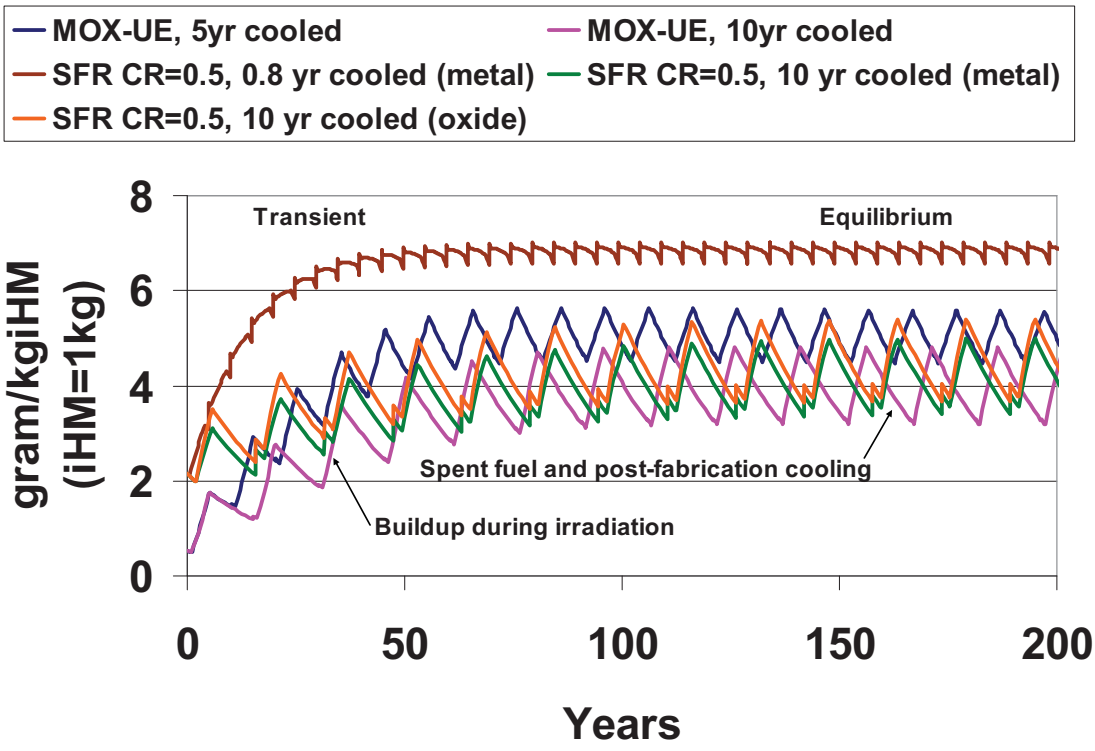

Figure 3-11. Cm-244 isotopic evolution during successive fuel recycles per heavy metal

The other driver in Cm-244 buildup is the cross-section multiplied by flux magnitude. This value for Am-243 is roughly the same between MOX-UE (~7E-9 s^{-1}) and SFR (~4E-9 s^{-1}), which can be verified by comparing the slopes of the buildup portion of the curves in Figure 3-11. The slightly greater transmutation rate and irradiation time of MOX-UE (4.1 years) as opposed to SFR (3.7) dictates that the transient in Cm-244 accumulation from one recycle-to the next will be greater for MOX-UE then for SFR. This is evidenced by the fact that the Cm-244 concentration in MOX-UE at time zero is much less than for that of SFR but builds to equilibrium faster and to almost the same equilibrium concentration as that of the SFR scenarios.

The other controlling physics effect on the transient time as well as the equilibrium concentration is the out-of-core decay time. The concentration of Cm-244 was highest for cases with the shortest cooling time. This was the SFR case with 0.8 years cooling time followed by the MOX-UE case with 5 years cooling time. These cases reach a higher equilibrium concentration as well as endure a shorter transient time to reach this equilibrium. This can be explained by the fact that less time is allowed for Cm-244 to decay away before the next irradiation, thus more Cm-244 is carried over per recycle iteration than if longer cooling times are used.

A similar trend can be observed for Cf-252 but to a greater degree. Figure 3-12 shows the dynamic evolution of Cf-252 per successive recycle. There is a four order of magnitude difference between the MOX-UE and the SFR Cf-252 concentrations. This is principally due to the greater fission-to-absorption ratio attributed to fast spectrum physics. It is also interesting to note that due to the short half-life of Cf-252 (2.6 years) short cooling times give an order of magnitude higher fresh-fuel concentration in fresh SFR fuel than if longer cooling times are used.

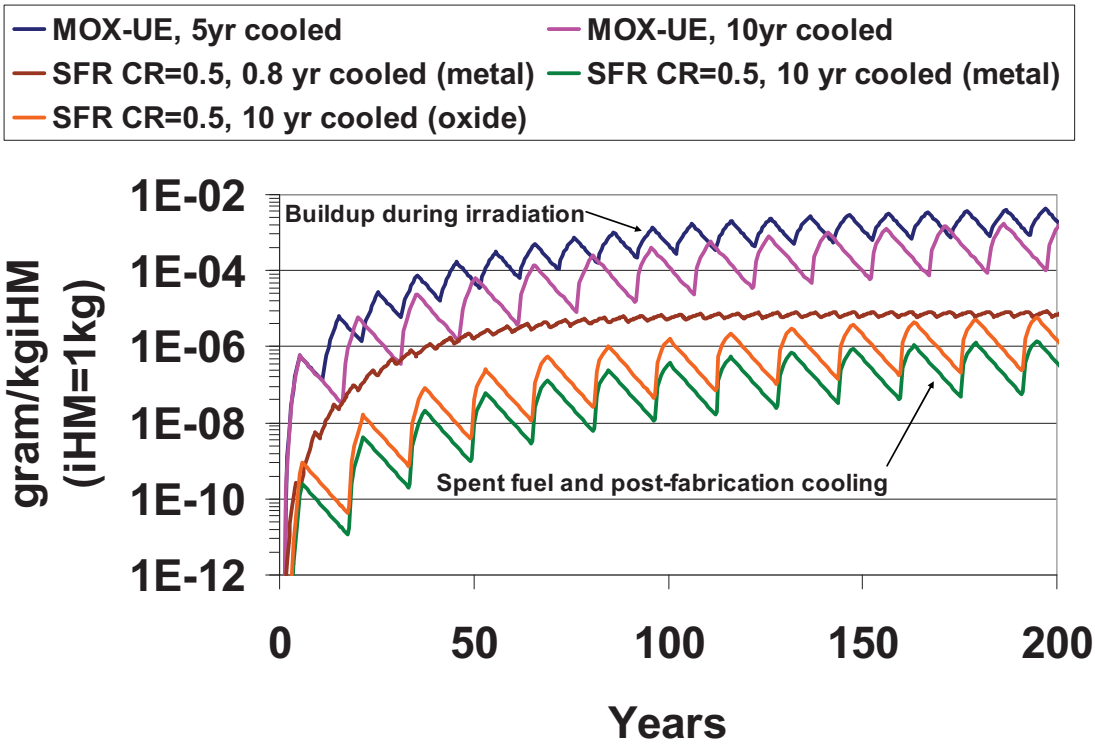

Figure 3-12. Cf-252 isotopic evolution during successive fuel recycles per heavy metal

Finally, it is important to note that for the first ~50 years of recycling (4-5 recycle-loops) the buildup of Cm-244 and Cf-252 is still transient and far below the equilibrium concentration. Convergence to

equilibrium of these isotopes, which are most limiting in terms of radiologic source terms, does not occur until at least a century of operating the fuel cycle. Unless the same fuel recycle facility is used for the entire century, the equilibrium radiologic source terms become relevant only for the second and N-th of a kind fuel recycle facilities.

3.4 Isotope Concentrations per Assembly

The quantification of radiologic source terms, alpha, gamma and neutron emission, is relevant to determining the level of radiation protection for protecting exposure to radiation workers handling fresh and spent fuel assemblies. To put these radiation source terms into the proper context for comparison among MOX-UE and SFR scenarios, it is valuable to convert the *per HM* isotope concentrations of the previous sections into concentrations *per fuel assembly*. Table 3-3 gives the fuel assembly dimensions and material densities used to calculate the mass of each fuel assembly type.

Table 3-3. Assembly mass calculation for converting per HM to per assembly isotope concentrations

	MOX-UE [1]	SFR CR=0.5 [22]	
Fuel Type	Oxide	Metal	Oxide
Geometric Dimensions			
Pin (Clad) Outer Diameter (cm)	0.95	0.62	0.66
Cladding Inner Diameter (cm)	0.83	0.50	0.53
Pellet/Slug Diameter (cm)	0.82	0.43	0.49
Active Fuel Length (cm)	365.76	101.60	137.16
Fuel Pins per Assembly	264	324	271
TRU Enrichment (v/o)	8.00%	33.40%	38.40%
Zr-metal Concentration (v/o)		20.00%	
Material Densities (g/cm^3) [23]			
UOX	10.97		10.97
TRU-O2	11.5		11.5
TRU -metal		19.7	
U - metal		19.1	
Zr-metal		6.5	
Aggregate Theoretical Density (g/cm^3)	11.01	16.90	11.17
Percent TD (%)	95.00%	100.00%	89.40%
Actual Density (g/cm^3)	10.46	16.90	9.99
Assembly Masses			
Pellet/Slug Mass per Assembly (kg)	5.33E+02	8.06E+01	8.36E+01
HM Mass per Assembly (kg)	4.70E+02	6.45E+01	7.37E+01

Notice that MOX-UE assembly is much more massive than that of the two SFR assemblies[j]. Therefore, it is expected that the disparity between MOX-UE and SFR isotope concentrations per heavy metal will be increased proportionally to the difference in masses per assembly. Thus, even though the equilibrium Cm-244 concentration per heavy metal is approximately comparable, the MOX-UE assembly will have much more Cm-244 per assembly.

[j] This is primarily because the active fuel length of a MOX-UE assembly is at least three times the length of a SFR fuel assembly despite the fact that the total length of assembly including gas plenums and reflectors is approximately the same.

The concentration per assembly of this alpha emitting isotope, along with Am-241 and Pu-238 to a lesser degree, dominates the decay heat generated per fresh assembly. The decay heat per assembly dictates the complexity of heat dissipation and limitations in both on-site fuel assembly transfer equipment and off-site transportation casks. These complexities become a controlling factor on the maximum number of assemblies that can be feasibly loaded per transportation cask. Figure 3-13 shows the dynamic evolution of Cm-244 per fuel assembly.

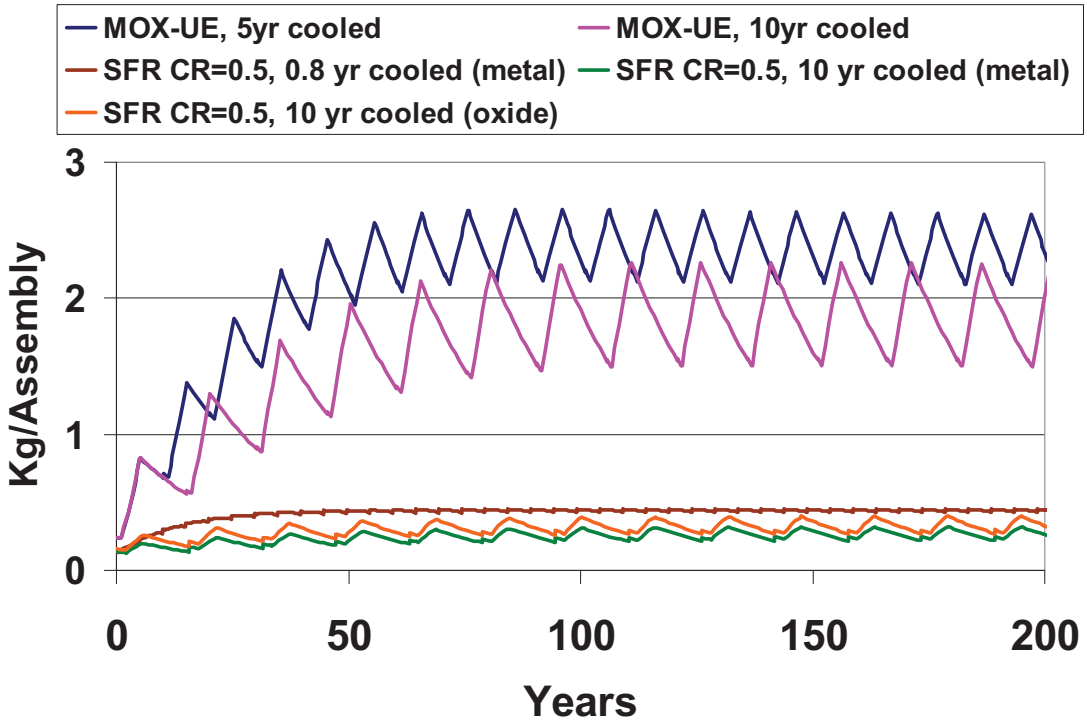

Figure 3-13. Isotopic evolution of the Cm-244 concentration per fuel assembly, MOX: 470 kg/assembly, Metal SFR: 65 kg/assembly, Oxide SFR: 74 kg/assembly

Both Cm-244 and Cf-252 have a primary decay mode by alpha emission. However, their secondary decay mode is by spontaneous fission. Cm-244 has a spontaneous fission yield of 1.3E-4%, whereas Cf-252 is much higher at 3.09%. However, the Cm-244 concentration per HM is many orders of magnitude greater than that of Cf-252 in both MOX-UE and SFR scenarios. Hence, the neutron contribution by the two can be approximately equal. Nevertheless, due to the short 2.6 year half-life of Cf-252, only a few years of post-reactor decay time, such as in a spent fuel cooling pond is sensible to allow for the Cf-252 to decay away. Allowing Cf-252 to decay can significantly reduce spontaneous fission neutron emission in spent and recycled fuel.

Figure 3-14 shows the dynamic evolution of Cf-252 per fuel assembly. Due to the large difference in magnitudes in the per HM Cf-252 concentrations, difference in assembly mass has little impact on the differences between the MOX-UE and SFR Cf-252 assembly concentrations. As observed with previous equilibrium scenario studies, the neutron source intensity associated with the Cf-252 fresh-fuel concentration will always be higher for MOX-UE than it is for SFR scenarios. This is due to the differences in fission-to-absorption ratios of curium and californium isotopes (Cm-244 and higher) between thermal and fast energy neutron spectra. Since the Cm-244 transient and equilibrium concentrations for MOX-UE and SFR are of the same order of magnitude (Figure 3-11, Figure 3-13), the much larger Cf-252 concentration of MOX-UE irrespective of cooling time must be dominated by the higher capture reaction rate relative to fission.

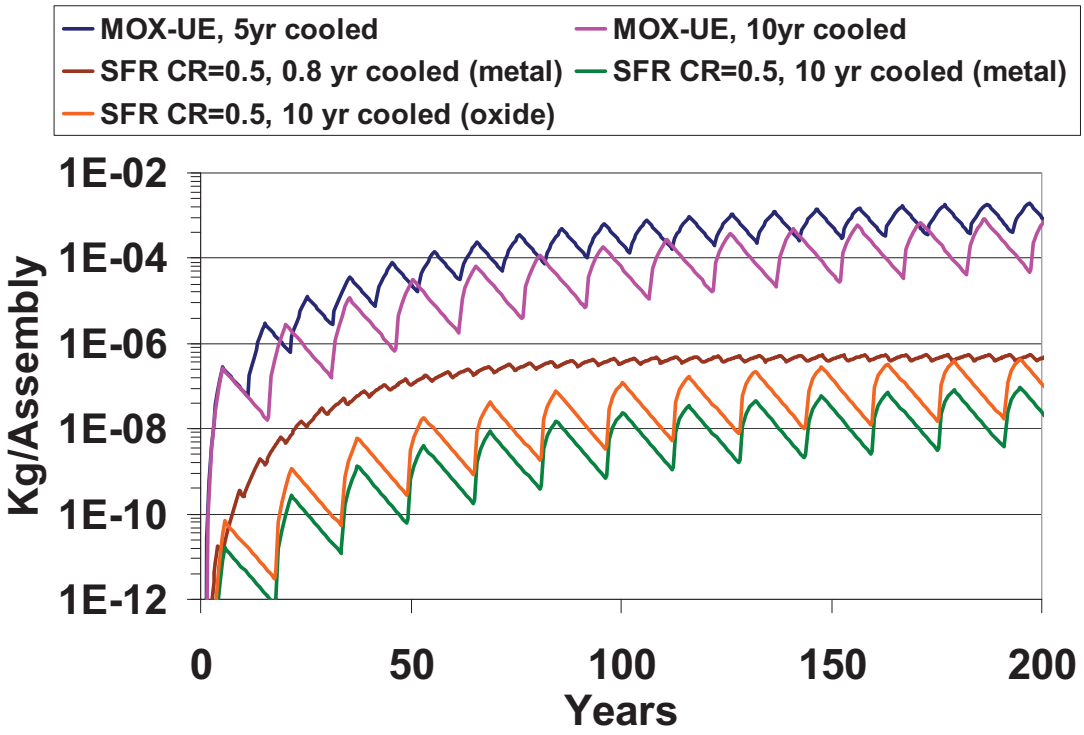

Figure 3-14. Isotopic evolution of the Cf-252 concentration per fuel assembly, MOX: 470 kg/assembly, Metal SFR: 65 kg/assembly, Oxide SFR: 74 kg/assembly

3.5 Impact of Actinide Partitioning Scenario on SFR Buildups

Given the transmutation affinity to breed Cm-244 through Cf-252, even in a fast spectrum an effort was made to quantify the change in higher mass actinide breeding if elemental partitioning were performed to remove gateway isotopes. Figure 3-15 through Figure 3-18 shows the effect of actinide partitioning out CmBkCf and AmCmBkCf for metal and oxide fuel. Both recycling schemes assumed the exact same decay times. Metal and oxide 1-group flux and cross-section data were used for the metal and oxide cases, respectively. Core average fuel enrichment, and irradiation duration representative for metal and oxide SFR with a CR=0.5 years was used [24]. Also, grouped transuranic reprocessing was assumed for spent metallic fast reactor fuel to represent the current understanding of electrochemical reprocessing. Elemental separation of spent oxide fast reactor fuel was assumed possible. Finally, elemental separation of the SNF providing the external supply of TRU to the SFR was assumed possible for both metal and oxide cases.

It is important to note the effect of aqueous reprocessing of spent SFR fuel. In all of the metal cases, the retained curium and californium after every recycle, due to the grouped element reprocessing, equilibrates to an asymptotic value after ~100 years for Cm-244 and 200 years for Cf-252. Because, the oxide cases allow for partitioning of the TRU elements, the curium and californium are zeroed out for the PuNp and PuNpAm cases and therefore do not appear in fuel fabrication. It is interesting to note that even though the curium and californium are set to zero every recycling, the peak concentration at the end of irradiation, still exhibits an equilibration trend. This is due to the fact that transmutation precursors still exist in the element that is left in the fuel. For the PuNp scenario, this precursor is Pu-242. For the PuNpAm scenario, this precursor is Pu-242 and Am-243. This explains the equilibration trend of Cm-244 and to a lesser extent, Cf-252, even when these isotopes are being removed every recycle.

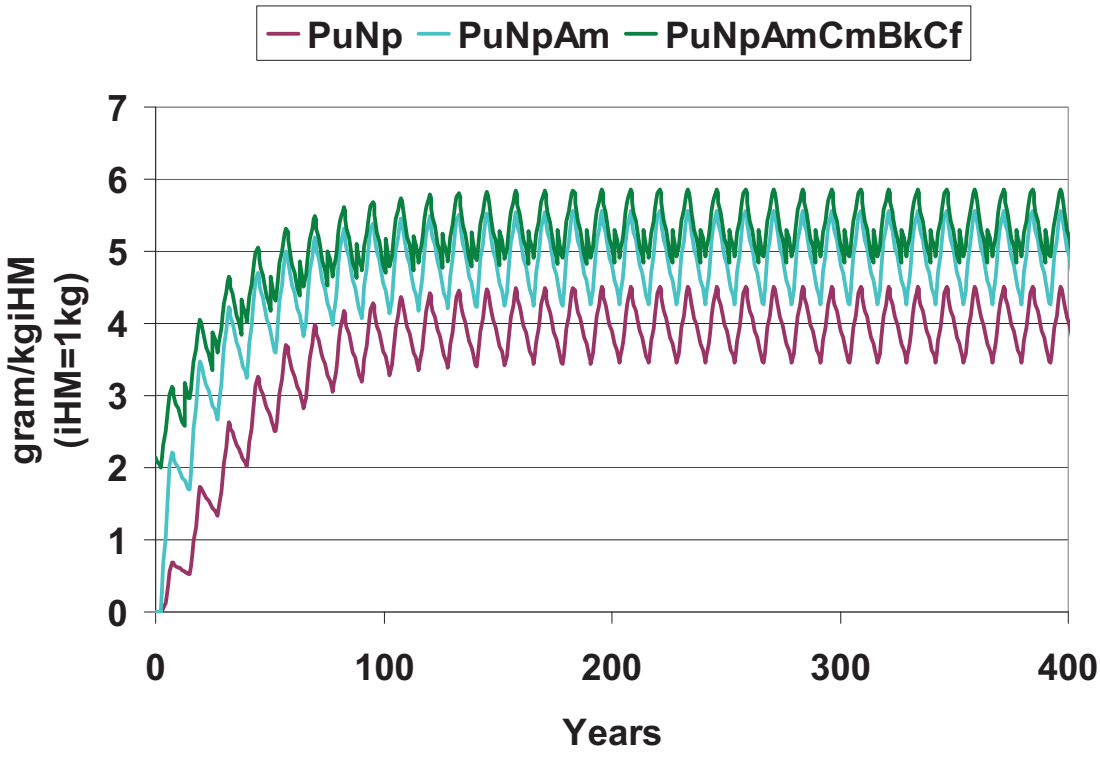

Figure 3-15. Cm-244 buildup in SFR CR=0.5 with metal fuel and electrochemical reprocessing

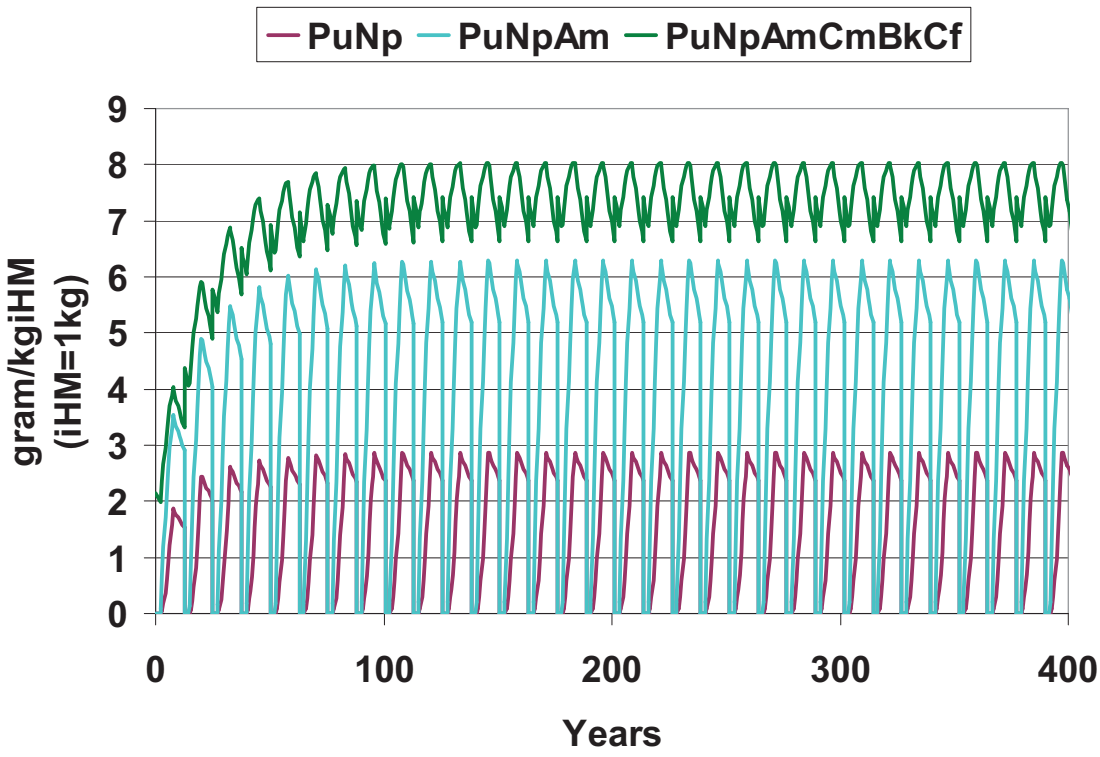

Figure 3-16. Cm-244 buildup in SFR CR=0.5 with oxide fuel and aqueous reprocessing

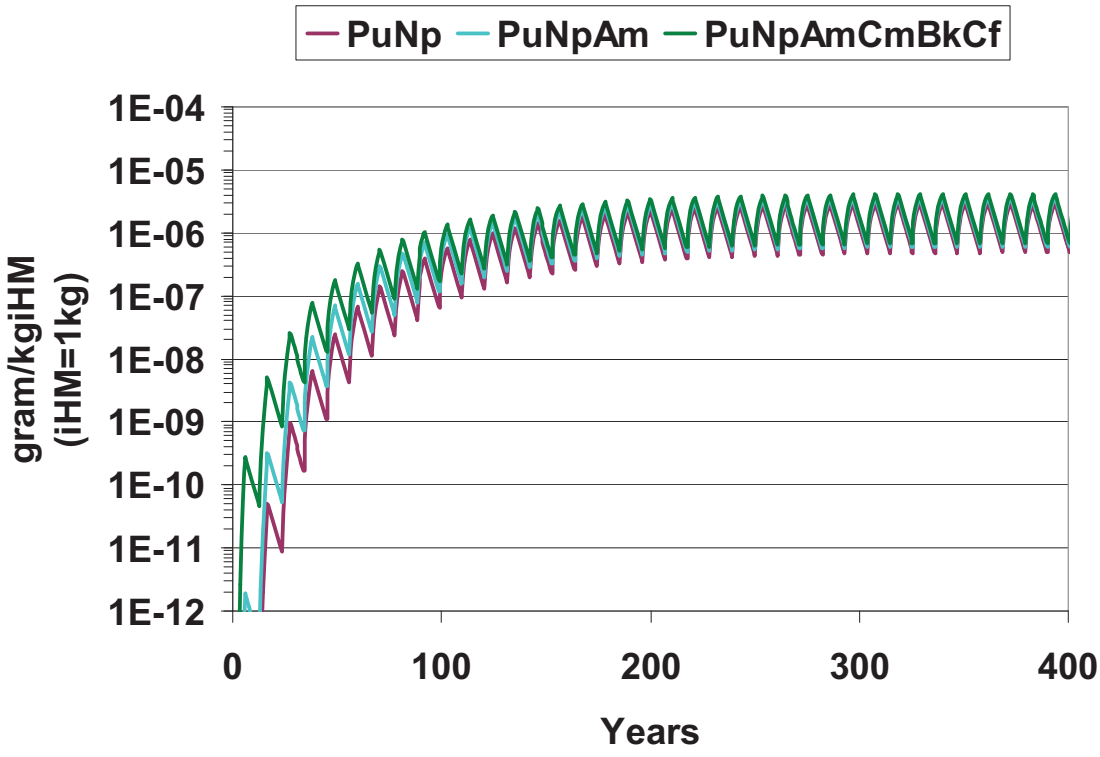

Figure 3-17. Cf-252 buildup in SFR CR=0.5 with metal fuel and electrochemical reprocessing

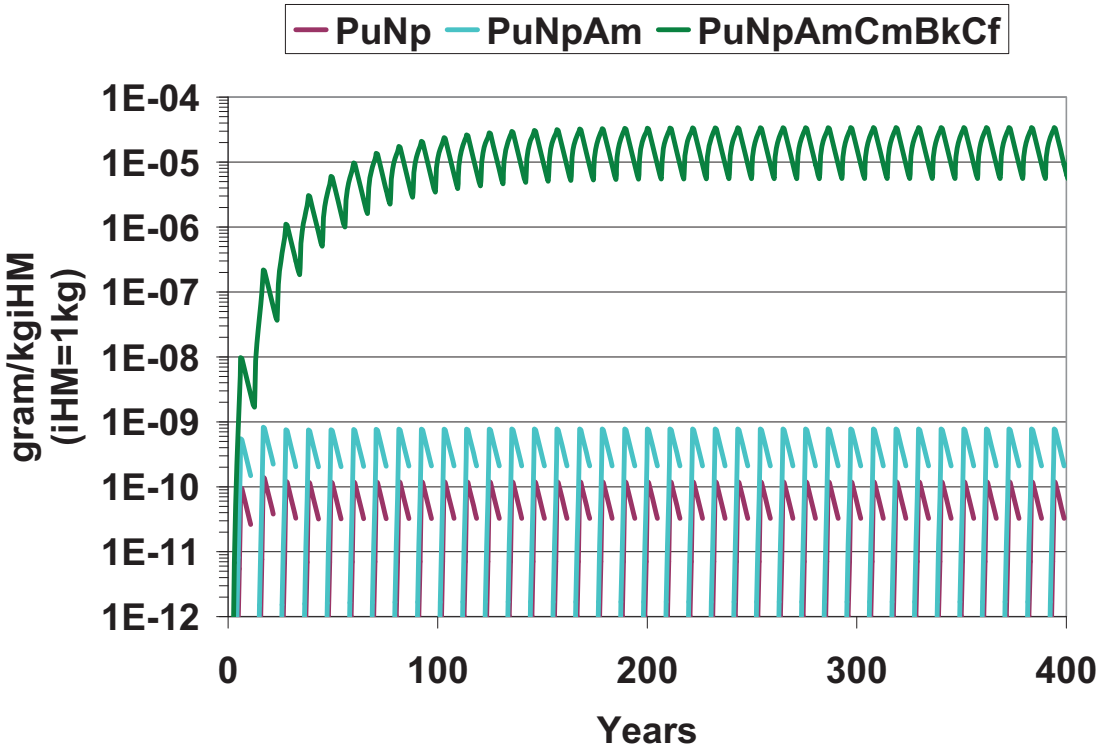

Figure 3-18. Cf-252 buildup in SFR CR=0.5 with oxide fuel and aqueous reprocessing

Note that when Am-243 is present (i.e., PuNpAm scenario), the Cm-244 and Cf-252 builds to a higher equilibrium value then when only Pu-242 is present (i.e., PuNp scenario). The curium and californium buildups, prior to recycling, do not pose any credible issue to fuel fabrication operations for the PuNp or PuNpAm partitioning scenarios. However, these buildups will dictate the quantity of curium and californium waste volumes generated by separating these elements from the fuel stream. The volume of the waste forms needed for dealing with these wastes could be large as they would have to deal with the high decay heat power density as well as gamma and neutron fields. Also, the alpha decay of Cm-244 produces a helium nucleus, thus resulting in an internal source of inert gas pressure [25].

3.6 Time to Reach Equilibrium

Not every isotope equilibrates rapidly in the fuel cycle. Some isotopes can take years to decades to equilibrate depending on the transmutation and partitioning strategy as well as the cooling time. This can be seen by visual inspection of plots in the previous sections. However, this visual inspection is a cumbersome process for distinguishing the transient from the equilibrium behavior of the isotopic evolution. Therefore, a standard methodology was devised for quantifying the transient or equilibration time required before the fuel cycle could be considered in equilibrium for the more interesting isotopes, Np-237, Pu-241, Am-241, Cm-244 and Cf-252. As a demonstration, this methodology is applied to equilibration of isotopes in the fuel cycle at times just after blending occurs.

3.6.1 Method of Calculation

To evaluate a standardized equilibrium magnitude and evolution time, only concentrations at the point of blending with external supply is plotted in a spreadsheet. This exemplifies the relevant impact of isotopic evolution to radiological workers. Using this plot, the asymptotic minimum or maximum is determined. This minimum or maximum is established by running the MRTAU calculation to very long times until there is no discernable change in isotope concentrations just after blending from recycle to recycle within a given tolerance. This concentration then is considered the equilibrium or asymptotic concentration. Then the time required for the evolving concentration to reach 95% of this asymptotic value is calculated. This time to reach 95% of the evaluated equilibrium concentration is designated as t_{95}. Similarly, the number of recycles to react 95 % of the evaluated equilibrium concentration is designated as R_{95}. The asymptotic equilibrium concentration is designated as I_{∞}. Figure 3-19 shows an example of the t_{95} and I_{∞} determination for Cm-244.

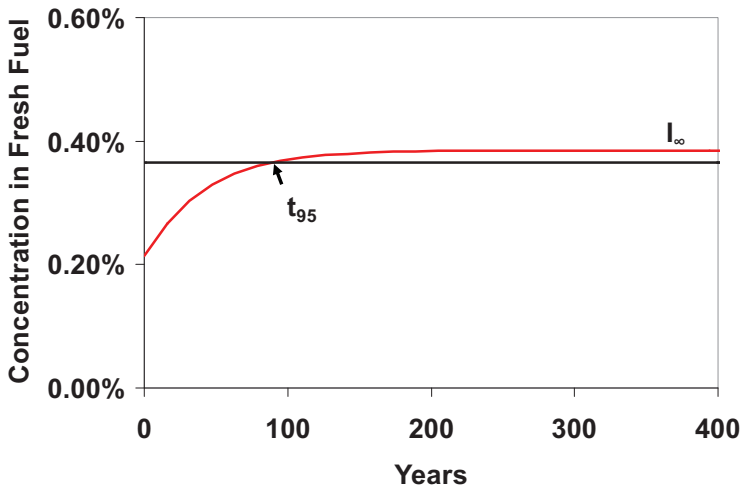

Figure 3-19. Equilibration time determination for Cm-244 concentration in fresh fuel (SFR CR=0.5 with a 10 year cooling time)

3.6.2 Equilibration Time (t_{95})

For isotopes that decrease with increasing decay time (e.g., Cm-244 and Cf-252), a shorter cooling time means less decay before the next recycle iteration. Therefore, the rate of isotope buildup per recycle is greater. Because of the greater buildup rate per recycle, there is a general trend for more recycles required in order to achieve equilibrium. Because of the greater buildup rate in combination with more recycles required to achieve equilibrium, the actual equilibrium concentration (I_∞) is also greater. This behavior is exemplified for Cm-244 and Cf-252 in Figure 3-20 and Figure 3-21, respectively. In general, a faster rate of buildup results in a longer equilibration time. This can be seen by comparing the number of recycles required to equilibrate between MOX-UE and the SFR cases. It takes ~7 recycles to equilibrate Cm-244 in both the MOX-UE and SFR scenarios with the exception of the very short 0.8 year cooling time which takes ~9 recycles. It takes ~33 recycles to equilibrate Cf-252 in both MOX-UE scenarios. It takes ~27 recycles to equilibrate Cf-252 in both SFR scenarios.

Figure 3-22 and Figure 2-23 shows that the actual time to equilibration due to using a longer cooling time is actually longer. The longer equilibration time as a result of longer cooling times is primarily due to the fact that each recycle pass take more time. The most pronounced example of this trend is the Cf-252 equilibration time. The charts also reveal an interesting fuel cycle dynamic between globally parent and daughter actinides. Since MA production occurs by transmutation of mainly Pu isotopes, this element needs to build up before heavier elements can show appreciable buildup as a result. That is the reason why further MA has to wait many recycles after Pu reaches equilibrium to reach their own one. Thus, equilibration times become longer for increasingly higher mass actinides.

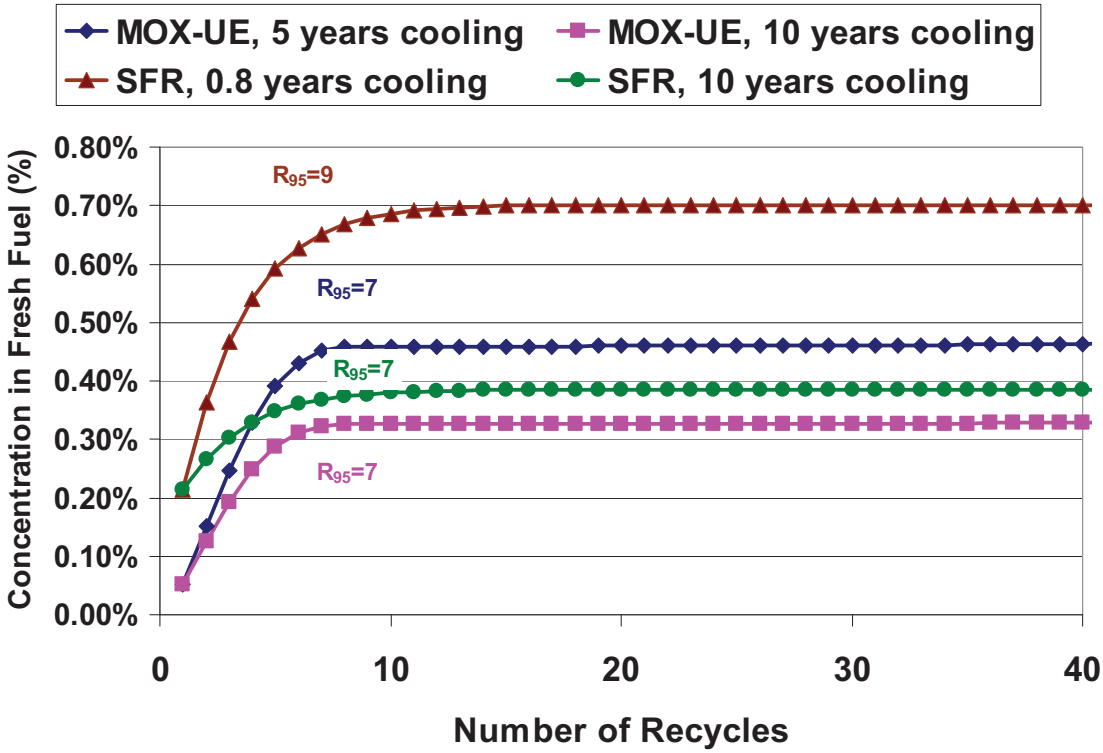

Figure 3-20. Buildup of Cm-244 concentration in fresh fuel as a function of recycles

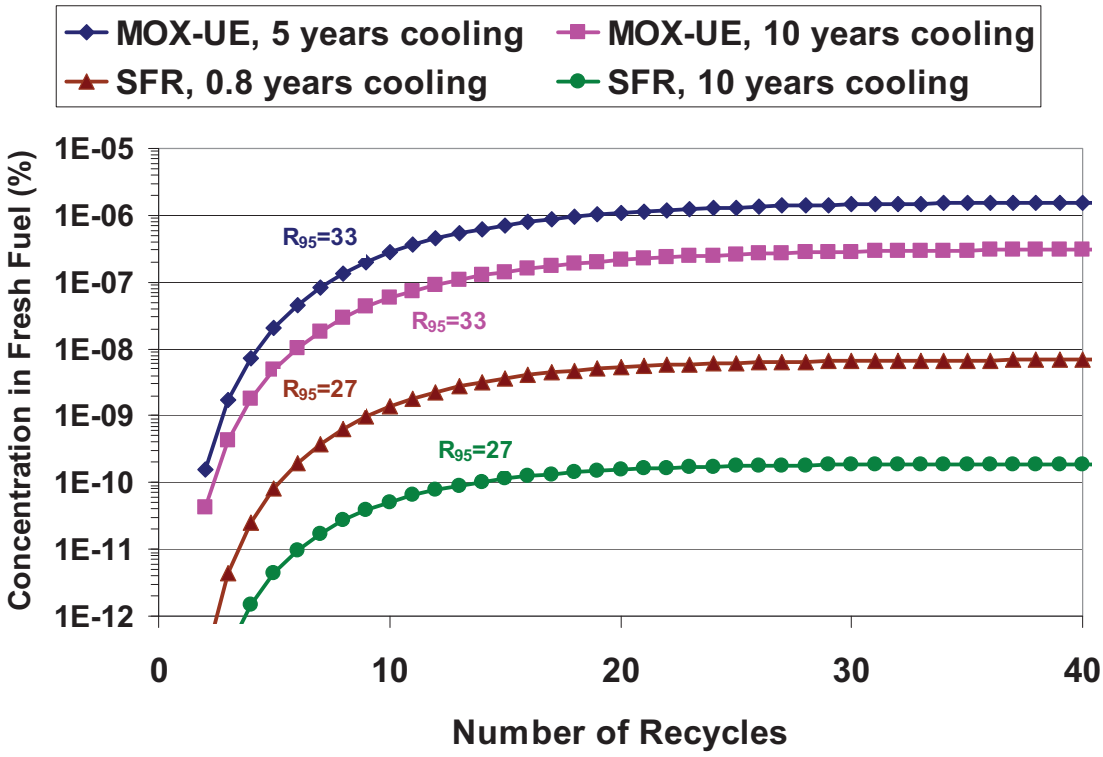

Figure 3-21. Buildup of Cf-252 concentration in fresh fuel as a function of recycles

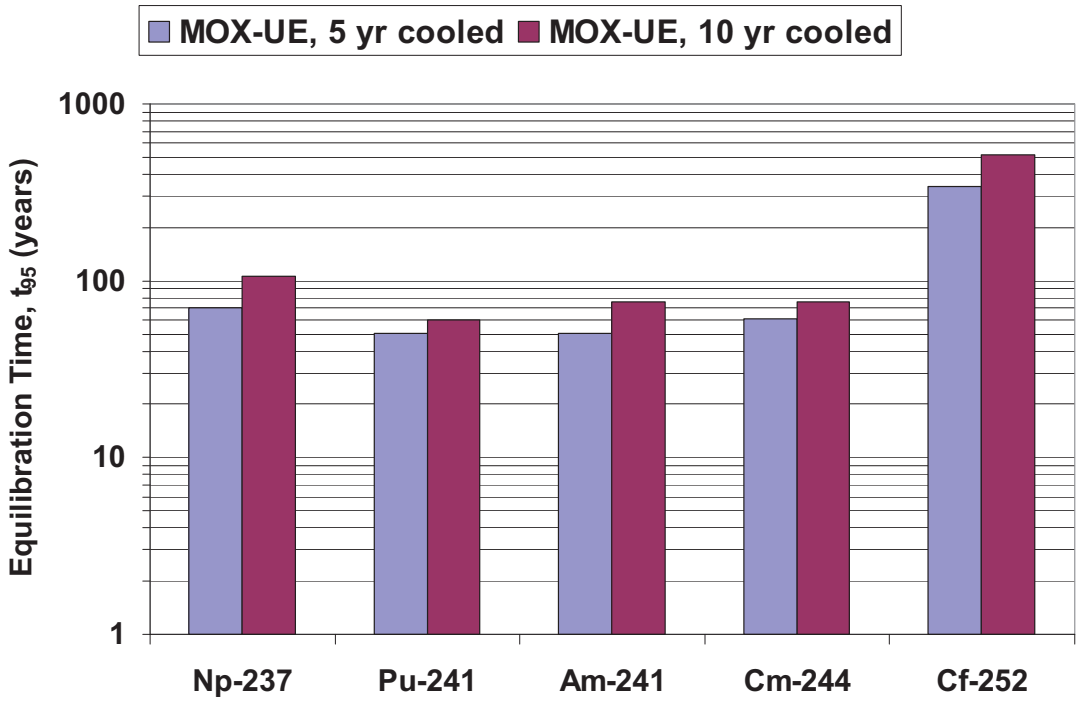

Figure 3-22. Equilibration time (t_{95}) of isotope concentrations in fresh fuel for all-TRU recycling in MOX-UE of two different cooling times

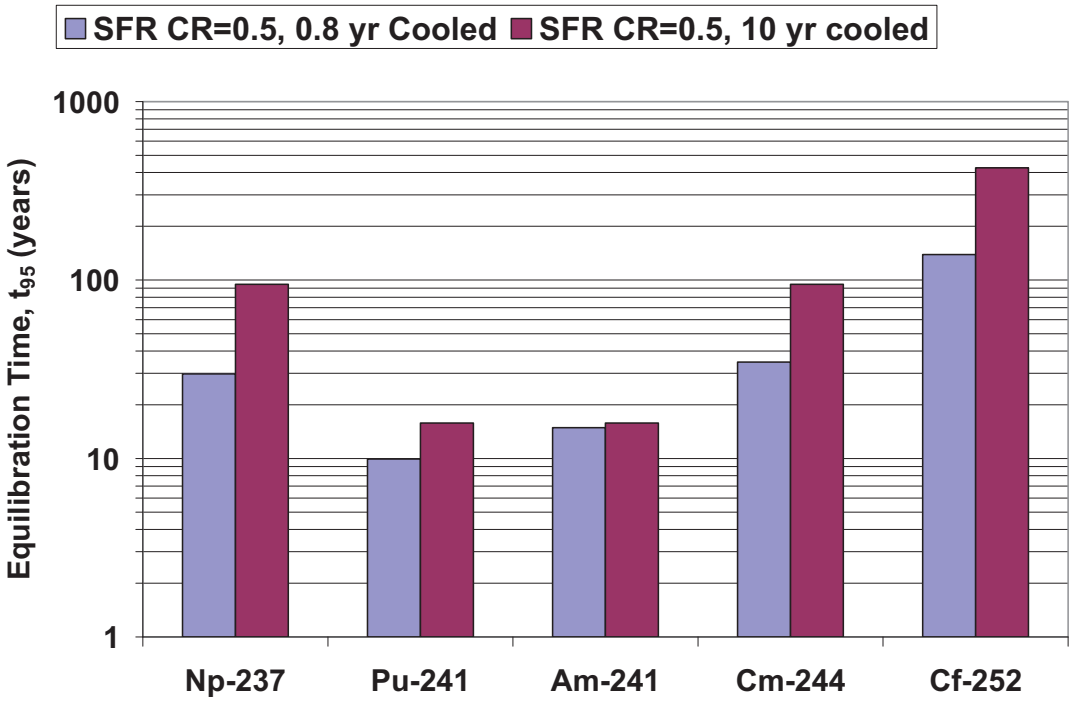

Figure 3-23. Equilibration time (t_{95}) of isotope concentrations in fresh fuel for all-TRU recycling in SFR of two different cooling times

3.7 Radiologic Source Term Evolution of Fresh Assemblies

Combing the different buildup rates and resulting equilibration trends for the radiologic source term controlling isotopes gives the overall growth of radiation fields that should be expected during fuel fabrication and handling over the course of operating the fuel cycle. The three radiologic source terms considered are alpha decay heat, gamma energy and spontaneous neutron source intensity. Alpha, neutron reactions are also contributing radiologic source terms, though not considered in this Chapter. For a detailed study of alpha,n contrasted with spontaneous fission neutron source intensity, see Chapter 6. A summary of the short isotope list considered in calculating the radiologic source terms in this section is given in Table 3-4. Again, for a more comprehensive analysis of radiation source terms by isotope, the reader is referred to Chapter 6.

Table 3-4. Alpha, gamma and spontaneous fission mass specific emission source intensities [26,27]

	Alpha Heat (kW/kg)	Gamma Energy (kW/kg)	Spontaneous Fission (n/s/kg)
Np-237	2.15E-05	1.41E-07	1.39E-01
Pu-241	3.19E-03	2.32E-06	4.94E+01
Am-241	1.14E-01	4.95E-04	1.24E+03
Cm-244	2.83E+00	7.32E-04	1.11E+10
Cf-252	3.84E+01	1.26E+00	2.30E+15

Note that different isotopes are more controlling for one specific radiation type then another. The combination of each isotope contribution to the aggregate radiologic source term evolves with time as shown throughout this chapter. Figure 3-24, Figure 3-25 and Figure 3-26 shows the evolution of alpha, gamma and spontaneous fission sources over time.

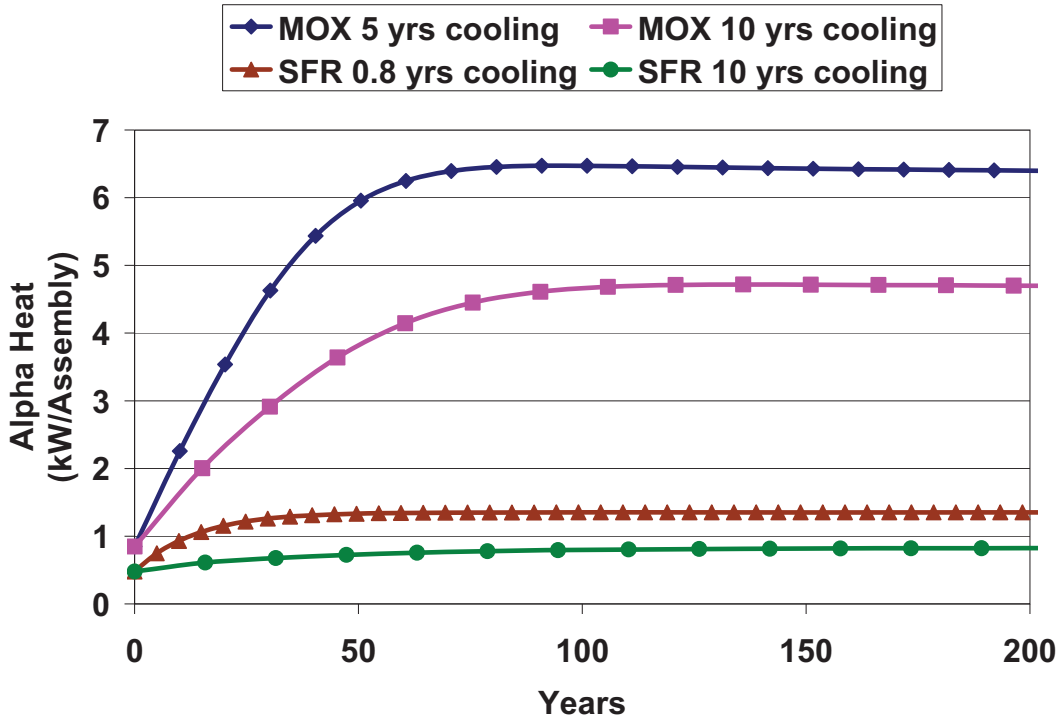

Figure 3-24. Alpha decay heat power per assembly of fresh fuel as a function of time, MOX: 470 kg/assembly, Metal SFR: 65 kg/assembly, Oxide SFR: 74 kg/assembly

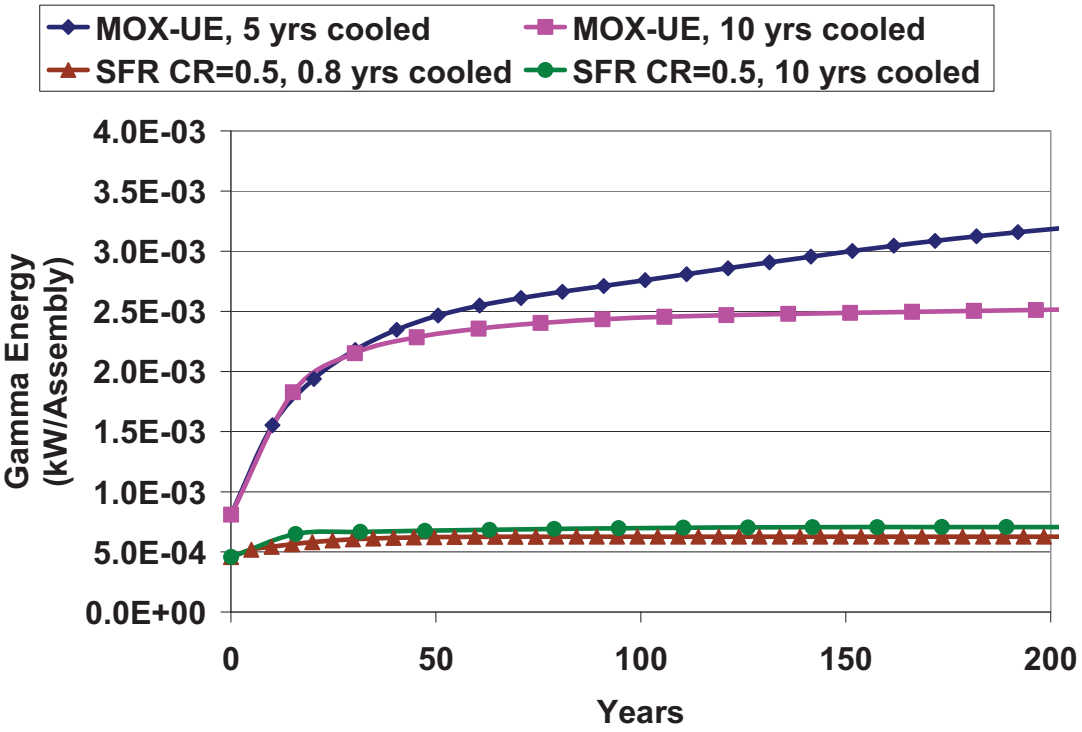

Figure 3-25. Gamma emission decay energy per assembly of fresh fuel as a function of time, MOX: 470 kg/assembly, Metal SFR: 65 kg/assembly, Oxide SFR: 74 kg/assembly

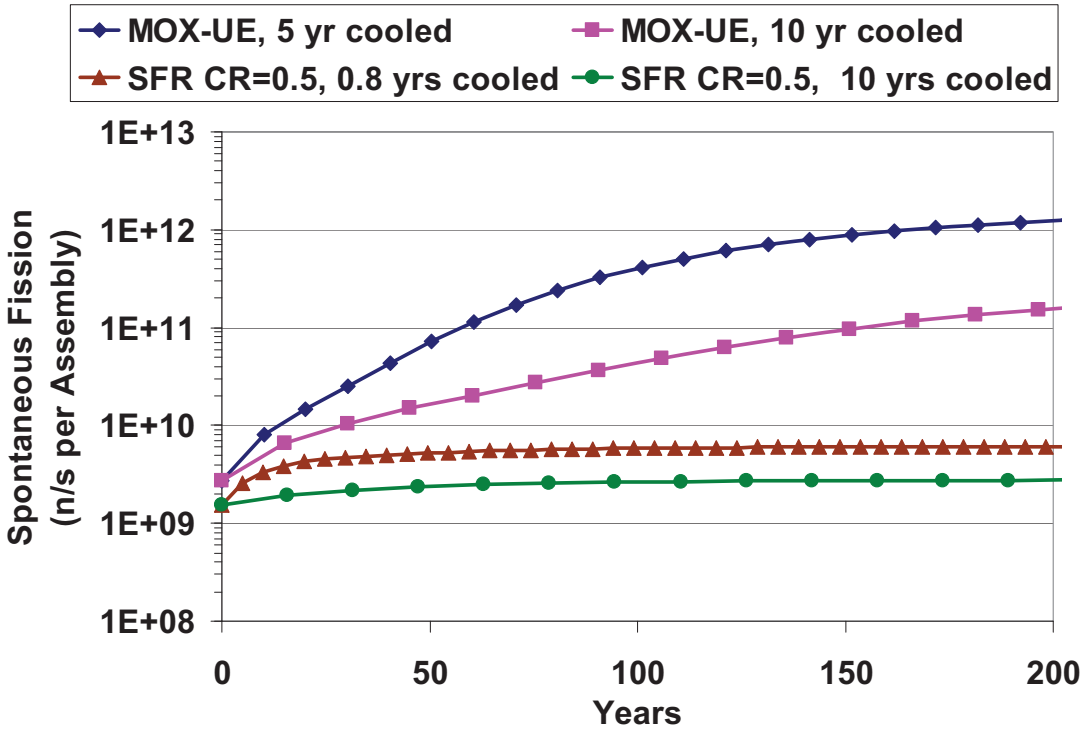

Figure 3-26. Spontaneous fission neutron emission per assembly of fresh fuel as a function of time, MOX: 470 kg/assembly, Metal SFR: 65 kg/assembly, Oxide SFR: 74 kg/assembly

In general all source terms were higher for the MOX-UE scenarios. This is partly because of the greater HM mass of a MOX than an SFR assembly. It is also due to the transmutation performance differences between the two reactor systems. Just as it was discussed in previous sections, the ability to breed higher mass actinides is greater in MOX-UE than it is for SFR. However, the more interesting trend is the transient behavior of the spontaneous fission neutron source in the first 50-75 years. In this time range, Cm-244 is just barely starting to equilibrate (Figure 3-22, Figure 3-23). The Cf-252 neutron contribution is still growing. This is why the MOX-UE equilibrium neutron dose is so much greater than that of the first 50-75 years. However, because of the slow Cf-252 growth, the first century MOX-UE neutron sources term is still only a factor of 10 as opposed to hundreds or thousands away from that of SFR.

4. Fuel Value

One of the motivations for recycling used nuclear fuel is to capture the value of the recycled material in new fuel. This chapter explains methodologies for assessing fuel value and applies them to two issues - the positive value of minor actinides in the "Minor Actinide" study [28] and the negative value of impurities in the "Losses" study [29]. This chapter starts with underlying physics methodologies and progresses to those applications. We anticipate future applications such as the general issue of dynamic simulations of the fuel cycle in which the composition of available isotopes will be continually varying and never exactly match any fixed input composition recipe. A specific example of dynamic perturbations is the loss of fuel reactivity as transuranic material is stored for an increased period of time.

In all of these application areas, there are so many relevant reactor conditions that it is not practical to perform detailed reactor physics calculations for each set of conditions. Instead, we have developed methods to adjust the input and output fuel composition ("recipes") of previous detailed calculations according to the perturbation in question. Results from previous calculations are assembled in the AFCI Transmutation Library, which is described elsewhere [14].

The output fuel adjustment method was described in section 3.

The core will be just critical at the end of cycle, which will be a weighted average of the fuel in the reactor at that time. The fuel will consist of fuel that has been in the core for an integer numbers of cycles up to the limit for that fuel. The weighted average of this fuel will have a k-effective of exactly 1.0 at the end of cycle, which is what was predicted in the detailed reactor physics calculations. However, fuel perturbations will change the end of cycle k-effective. In order to ensure that it remains exactly 1.0, the perturbation must be compensated for via modifications to the fuel lifetime, fuel enrichment, or fuel design, or a combination of them. Using properly averaged cross sections, k-effective can be written in the simple form.

To ensure criticality for a system, compensatory perturbations must be made, which change the average neutron production ($\overline{\nu\sigma_f^{fis}} N_{fis} + \overline{\nu\sigma_f^{fer}} N_{fer}$), the neutron absorption ($\overline{\sigma_a^{fis}} N_{fis} + \overline{\sigma_a^{fer}} N_{fer} + \overline{\sigma_a^{other}} N_{other}$), or the non-leakage probability (P_{NL}), and any changes will likely change all of these terms. For a given perturbation that reduces the end of cycle k-effective (opposite changes for increases). There are three changes that can be used to compensate for the reduced k-effective; 1) reduce burnup, 2) increase enrichment, and 3) modify fuel design.

Reducing the average discharge burnup (i.e., shorter cycle length) will have the primary effect of increasing the number densities of the heavy metal isotopes and reducing the fission product inventory. However, the fuel will not be irradiated to the irradiation damage limit in this approach.

Increasing the enrichment (ratio of more reactive fissile elements to less reactive fertile elements) will have the primary effect of increasing average reactivity of the fuel. Changing the fuel enrichment will change the conversion ratio and breeding ratio of the fuel, which may result in inconsistent comparisons. Additionally, increasing the fissile density will change the flux level and may result in the fuel residence time being different from what was assumed in the calculations.

The third way is to modify the fuel design. Specifically, the fuel volume fraction can be increased. This has the primary effect of increasing the heavy metal density, reducing the discharge burnup, and reducing the non-leakage probability. Again, the fuel will likely not have reached the irradiation damage limit without addition modifications to optimize the design.

In order to maintain conversion ratio, fuel near the irradiation damage limit, and any other constraints, it is likely that a combination of changes will be the optimum approach to compensate for perturbations in the feed composition compared to that of which was assumed in the original reactor physics calculations. In order to avoid a large number of complex analyses, simplified approximations have been developed in order to give first-order estimates of the significance of the perturbations by estimating the necessary adjustments to the input vector and the resulting output vector.

The input adjustment methods start with the observation that the criticality/reactivity of the available mix of isotopes will be higher or lower than the initial initialed input composition. To ensure proper performance of a fuel made with recycled materials, one must then adjust the U to TRU ratio accordingly. (The case where only Pu is recycled is simply a subset of the full TRU case.) In FY2009, we have developed and used three methods, as follows:

1. Constant reactivity worth - adjust composition so that the "reactivity worth" of the adjusted composition matches that of the initial composition. Developed by S. Yee and summarized below.[29]

2. Constant k-effective - adjust composition so that k_{eff} of the adjusted composition matches that of the initial composition. Developed by S. Piet and explained below.

3. Differential reactivity impact - Developed by E. Hoffman and summarized below.[5]

The first two methods use 1-group cross sections for fission, neutron capture, and neutron multiplication. They differ in how those 1-group cross sections are combined. We have applied these methods to the Minor Actinide study as they work reasonably well when only the uranium and transuranic composition varies from an initial composition. It is relatively easy to obtain 1-group cross sections, so we are assembling a library of such parameters for many reactor conditions. At present, neither method provides data on the impact of composition change associated with non-fissionable impurity elements. Future work would expand the methods with 1-group capture cross sections and compare with the results of the differential reactivity method for assessing impurities.

The third method uses differential reactivity impact coefficients calculated for three reactor conditions - fast reactor with metal fuel and transuranic conversion ratio 0.50, fast reactor with oxide fuel and transuranic conversion ratio 0.50, and LWR with MOX-Pu fuel. This method was used in support of the Losses study because it provides a way to assess all isotopes (fissionable and non-fissionable). As it is labor intensive to generate these coefficients it is relatively less usable for examining the impact of minor changes in a range of uranium and transuranic compositions.

All methods are approximations and do not replace detailed reactor physics calculations.

4.1 Methods

This subsection describes the three methods, with relatively more emphasis on the constant k-effective method because the other two methods are described in more detail elsewhere [6,29]. All of these methods are related to estimating the new enrichment in order for the reactor to remain critical while allowing the conversion ratio to float from the original value and not considering the effects on fuel lifetime. As with all first-order perturbation methods, the larger the perturbation, the more important the second order effects become. These methods allow for a near instantaneous first-order perturbation estimate of the impact on the system. As long as this impact is small, the results should be adequate. If any large differences are identified, the validity of these first-order approaches should be confirmed by appropriate reactor physics calculations. This is the most effective method for identifying system drivers, but the magnitude of the impact of these drivers is no more than a first-order estimate.

4.1.1 Terminology and Definitions

Start with defining the following four types of compositions.

Initial composition = The input/output composition recipes corresponding to the case being simulated e.g., uranium oxide at 51 GW-day/tonne-HM burnup (UOX-51) or metal fast reactor fuel for TRU conversation ratio=0.50 based on 5-year old feed from UOX-51.

Available composition = The input composition available in the simulation in a given time step.

Adjusted composition = The input/output composition resulting from the winery adjustment methods described below. During the time period that the adjusted composition is in force, it is used in the simulation as a replacement to the initial composition. Initially, the plan is for the input and output compositions to be adjusted every 5 years, in conjunction with changes to the initial recipes.

Real composition = An actual set of input/output recipes corresponding to an adjusted composition. For example, to test the methods, consider an initial composition with TRU conversion ratio = 0.50. Then, using these methods, estimate the recipe for ratio = 0.75 and then compare with the actual input/output recipes for 0.75.

Basically, the objective is to adjust the "available composition" so that the "adjusted composition" has the same k-effective or reactivity worth as an "initial composition" that was calculated by standard reactor physics methods. The adjustment accounts for changes in uranium and/or transuranic isotope mix in the "available composition" relative to the "initial composition" by modifying the U/TRU ratio so that the reactivity worth or k-effective of the "adjusted composition" matches the "initial composition."

We can test the methods by comparing the "adjusted composition" to a "real composition" that was done for the isotopic mix in question but not used in the adjustment process.

Define the following parameters:

k_∞ is the criticality ratio for an infinite lattice

k_{eff} is the effective criticality ratio

v is the average number of neutrons per fission

$\sigma_{n,fission}$ is the 1-group fission cross section for a composition

$\sigma_{n,\gamma}$ is the 1-group neutron capture cross section (sometimes called σ_c)for a composition

$\sigma_{n,2n}$ is the 1-group neutron multiplication (n,2n) cross section for a composition

m_i is the mass fraction of each isotope (among U isotopes or among TRU isotopes as appropriate)

M_U is the fraction of uranium in the fuel composition

M_{TRU} is the fraction of transuranic elements in the fuel composition

ρ is the reactivity of an isotope

P is the non-leakage fraction so that $k_{eff} = P k_\infty = 1$ at criticality

Q_p is the capture by non-fuel elements within fuel pellets such as fission products

Q_c is the capture by non-fuel core materials such as cladding, assembly structure

We define the mass fractions such that …

$$M_U + M_{TRU} = 1 \qquad \text{Eqn 4-1}$$

$$\sum_{U\ isotopes} m_U = 1 \qquad \text{Eqn 4-2}$$

$$\sum_{TRU\ isotopes} m_{TRU} = 1 \qquad \text{Eqn 4-3}$$

The approximation of k_∞ for 1-group cross sections is as follows:

$$k_\infty = \frac{\nu\,\sigma_{n,fission}}{(\sigma_{n,fission} + \sigma_{n,\gamma})} \qquad \text{Eqn 4-4}$$

4.1.2 Method 1 - Reactivity Worth

Shannon Yee [29] defines the excess reactivity or Reactivity Worth Value (RWV) of an isotope ρ_i as

$$\rho_i = P\,k_{\infty,i} - 1 \qquad \text{Yee eqn 3.19}$$

Then, demanding that the excess reactivity summing over isotopes is zero, he derives

$$\sum_{U\ isotopes} \frac{\rho_U\, m_U}{M_U^{Target}} M_U^{Adjusted} + \sum_{TRU\ isotopes} \frac{\rho_{TRU}\, m_{TRU}}{M_{TRU}^{Target}} M_{TRU}^{Adjusted} = 0 \qquad \text{Yee eqn 3.29}$$

For the case where we are considering the initial composition, Yee obtains the simpler equation

$$\sum_{U\ isotopes} \rho_U\ m_U + \sum_{TRU\ isotopes} \rho_{TRU}\, m_{TRU} = 0 \qquad \text{Yee eqn 3.31}$$

The non-leakage parameter P is embedded in this equation; Yee estimates it via the following equation and holds P constant from the original initial composition to the adjusted recipe.

$$P = \frac{2}{\sum_{U\ isotopes} k_{\infty,U}\, m_U + \sum_{TRU\ isotopes} k_{\infty,TRU}\, m_{TRU}} \qquad \text{Yee eqn 3.33}$$

Implicitly, Yee's method sets non-fuel capture parameters (Q) to zero.

$$Q_c = Q_p = 0 \qquad \text{Eqn 4-5}$$

This method calculates P using Yee equation 3.33. Note what happens when Yee equation 3.33 is substituted into Yee equation 3.31. That is, Yee equation 3.3 solves equation 3.31 for P.

$$\frac{2\left[\sum_{U\ isotopes} k_{\infty,U}\, m_U + \sum_{TRU\ TRU} k_{\infty,TRU}\, m_{TRU}\right]}{\sum_{U\ isotopes} k_{\infty,U}\, m_U + \sum_{TRU\ isotopes} k_{\infty,TRU}\, m_{TRU}} - \sum_{U\ isotopes} m_U - \sum_{TRU\ isotopes} m_{TRU} = 2 - 1 - 1 = 0 \qquad \text{Eqn 4-6}$$

The adjusted composition among uranium isotopes and among TRU isotopes, respectively, is the available composition.

$$m_{adjusted} = m_{available} \qquad \text{Eqn 4-7}$$

We then use the value for P, set capture terms Q to zero, use ν, $\sigma_{n,fission}$, $\sigma_{n,\gamma}$, for the initial composition to calculate k_∞, use M_U^{Target}, use M_{TRU}^{Target}, and use $m_{adjusted,}$ to solve Yee equation 3.29 for the adjusted values $M_U^{Adjusted}$ and $M_{TRU}^{Adjusted}$.

$$M_{TRU}^{Adjusted} = \frac{-\sum_{U\ isotopes}(P k_{\infty,U} - 1) m_U \Big/ M_U^{Target}}{\left\{\sum_{TRU\ isotopes}(P k_{\infty,TRU} - 1) m_{TRU} \Big/ M_{TRU}^{Target}\right\} - \left\{\sum_{U\ isotopes}(P k_{\infty,U} - 1) m_U \Big/ M_U^{Target}\right\}} \qquad \text{Eqn 4-8}$$

$$M_U^{Adjusted} = 1 - M_{TRU}^{Adjusted} = \frac{\sum_{TRU\ isotopes}(P k_{\infty,TRU} - 1) m_{TRU} \Big/ M_{TRU}^{Target}}{\left\{\sum_{TRU\ isotopes}(P k_{\infty,TRU} - 1) m_{TRU} \Big/ M_{TRU}^{Target}\right\} - \left\{\sum_{U\ isotopes}(P k_{\infty,U} - 1) m_U \Big/ M_U^{Target}\right\}} \qquad \text{Eqn 4-9}$$

These two expressions can alternatively be expressed as

$$M_{TRU}^{Adjusted} = \frac{-M_{TRU}^{Target}\sum_{U\ isotopes}(P k_{\infty,U} - 1) m_U}{M_U^{Target}\sum_{TRU\ isotopes}(P k_{\infty,TRU} - 1) m_{TRU} - M_{TRU}^{Target}\sum_{U\ isotopes}(P k_{\infty,U} - 1) m_U} \qquad \text{Eqn 4-10}$$

$$M_U^{Adjusted} = \frac{M_U^{Target}\sum_{TRU\ isotopes}(P k_{\infty,TRU} - 1) m_{TRU}}{M_U^{Target}\sum_{TRU\ isotopes}(P k_{\infty,TRU} - 1) m_{TRU} - M_{TRU}^{Target}\sum_{U\ isotopes}(P k_{\infty,U} - 1) m_U} \qquad \text{Eqn 4-11}$$

The two expressions have the same denominator. The summation of these two expressions equals one, as it should. Plugging them into Yee equation 3.29 yields zero, as it should, as follows:

$$\sum_{U\ isotopes}\frac{\rho m}{M_U^{Target}}\left\{\frac{M_U^{Target}\sum_{TRU\ isotopes}\rho m}{M_U^{Target}\sum_{TRU\ isotopes}\rho m - M_{TRU}^{Target}\sum_{U\ isotopes}\rho m}\right\} + \sum\frac{\rho m}{M_{TRU}^{Target}}\left\{\frac{-M_{TRU}^{Target}\sum_{U\ isotopes}(P k_\infty - 1) m}{M_U^{Target}\sum_{TRU\ isotopes}\rho m - M_{TRU}^{Target}\sum_{U\ isotopes}\rho m}\right\}$$

$$= \left\{\frac{\sum_{U\ isotopes}\rho m \sum_{TRU\ isotopes}\rho m}{M_U^{Target}\sum_{TRU\ isotopes}\rho m - M_{TRU}^{Target}\sum_{U\ isotopes}\rho m}\right\} + \left\{\frac{-\sum_{TRU\ isotopes}\rho m \sum_{U\ isotopes}\rho m}{M_U^{Target}\sum_{TRU\ isotopes}\rho m - M_{TRU}^{Target}\sum_{U\ isotopes}\rho m}\right\} = 0 \qquad \text{Eqn 4-12}$$

In summary, method 1 contains these steps:

- Calculate $P_{Initial}$ using Yee equation 3.33, then assume $P_{adjusted} = P_{Initial}$.

- Ignore non-fuel capture (Q).
- Set $m_{adjusted} = m_{available}$.
- Calculate the adjusted M_U and M_{TRU} using equations 4-10 and 4-11.

4.1.3 Method 2 - Constant k-effective

The basic requirement is that the input composition provides adequate criticality, k_∞, and is adjusted as close to the available composition of isotopes as possible. The criticality check makes the rate of fuel fabrication more accurate than use of unadjusted initial input recipes. The adjustment to the available composition reduces the difference between what is available and the recipe used in the calculation (versus initial - available), which reduces the fictitious accumulation of some isotopes in the simulation.

The basic equation for the input adjustment is as follows.[k]

$$k_\infty = \frac{\sum_{isotopes} \nu \sigma_{n,fission}\, m \Phi t}{\sum_{isotopes} (\sigma_{n,fission} + \sigma_{n,\gamma})\, m \Phi t + Q \Phi t} = \frac{\sum_{isotopes} \nu \sigma_{n,fission}\, m}{\sum_{isotopes} (\sigma_{n,fission} + \sigma_{n,\gamma})\, m + Q} \qquad \text{Eqn 4-13}$$

At present, the only physical adjustment available as isotopic mix in available material changes would be adjustment of the ratio of TRU to U. Yet, for future applications in which it may be valuable to differentiate Q between capture within fuel pellets (such as fission products) versus outside of pellets (fuel cladding, fuel assemblies, etc.). The idea is that fission products and other poisons may vary among cases but for a given reactor and fuel concept, the non-pellet materials (hence non-pellet capture) would always be kept constant.

So, we restate equation 4-13 as follows,

$$k_\infty = \frac{\sum_{U\ isotopes} \nu \sigma_{n,fission}\, m_U\, M_U + \sum_{TRU\ isotopes} \nu \sigma_{n,fission}\, m_{TRU}\, M_{TRU}}{\sum_{U\ isotopes} (\sigma_{n,fission} + \sigma_{n,\gamma})\, m_U\, M_U + \sum_{TRU\ isotopes} (\sigma_{n,fission} + \sigma_{n,\gamma})\, m_{TRU}\, M_{TRU} + Q_p + Q_c} \qquad \text{Eqn 4-14}$$

And, we also require

$$k_{eff} = P k_\infty = 1 \qquad \text{Eqn 4-15}$$

And therefore, we obtain

[k] We considered adding (n,2n) to the denominator but found it made less than 1% impact for relevant isotopes, hence insignificant to the total sum.

$$k_{eff} = P\frac{\sum_{U\ isotopes} \nu\sigma_{n,fission}\, m_U\, M_U + \sum_{TRU\ isotopes} \nu\sigma_{n,fission}\, m_{TRU}\, M_{TRU}}{\sum_{U\ isotopes}(\sigma_{n,fission}+\sigma_{n,\gamma})\, m_U\, M_U + \sum_{TRU\ isotopes}(\sigma_{n,fission}+\sigma_{n,\gamma})\, m_{TRU}\, M_{TRU} + Q_p + Q_c} = 1$$

Eqn 4-16

For each initial recipe, use isotope-specific parameters ν, $\sigma_{n,fission}$, $\sigma_{n,\gamma}$, and $m_{initial}$, and $M_{initial}$. The basic idea is require that Q, P, k_∞, and k_{eff} are determined using the initial composition and then kept constant. So as the composition changes from the original initial fixed recipe to what is actually available, equation 4-16 is solved to find the new M_U and M_{TRU}.

There is one exception and one complication involved.

The exception is that although Q_c is kept constant, we may wish in the future to allow Q_p to vary as fission products are assumed to in the separation process to contaminate recycled fuel material.

The complication is that equation 4-16 has three unknowns when applied to the original initial recipe, namely P, Q_c, and Q_p. So, there must be two more equations or assumptions so that the set of three equations can be solved, thereby identifying the values of the three unknowns. Then, equation 4-16 can be re-applied as the composition of available isotopes varies. There are four approaches considered to allow determination of these three unknowns. For now, all four approaches assume $Q_p = 0$, so only one more constraint must be added to solve equation 4-16 for the original initial composition.

a. Assume specific values for P, which is the same as assuming values for k_∞.
b. Calculate P from Shannon Yee's method.
c. Assume Q_c is zero, which is effectively interpreting equation 4-13 to apply to only fuel isotopes so that all losses (leakage and non-fuel capture) are accounted for in the P term, which is kept constant.
d. Iterate with the output composition so that an appropriate value of k_∞ at end of cycle is matched. We have not attempted this.

4.1.3.1 Method 2, variation 2a, assume values of k∞

The user must specify the appropriate value of k_∞ at beginning of cycle. This allows calculation (either in spreadsheet or in VISION itself) of P, which remains fixed for that initial composition for this simulation. For now, default values are suggested as follows

k_∞ = 1.2 for thermal reactor and k_{eff}=1, hence P = 0.8333 Eqn 4-17

k_∞ = 1.4 for fast reactors and k_{eff}=1, hence P = 0.7149

Use of equation 4-16 with the values for the initial composition allows estimation of Q_c from the original fixed initial composition.

$$Q_c = P\left[\sum_{U\ isotopes} \nu\sigma_{n,fission}\, m_U\, M_U + \sum_{TRU\ isotopes} \nu\sigma_{n,fission}\, m_{TRU}\, M_{TRU}\right] - \left[\sum_{U\ isotopes}(\sigma_{n,fission}+\sigma_{n,\gamma})\, m_U\, M_U + \sum_{TRU\ isotopes}(\sigma_{n,fission}+\sigma_{n,\gamma})\, m_{TRU}\, M_{TRU}\right]$$

Eqn 4-18

Armed with values for P, Q_p, and Q_c, one can then adjust M_U and M_{TRU} as the isotopic mix of available material changes, see below.

4.1.3.2 Method 2, variation 2b, calculate P using Yee's method

Once P is calculating using Yee equation 3.33, one proceeds using equation 4-18 to find Q_c. Armed with values for P, Q_p, and Q_c, one can then adjust M_U and M_{TRU} as the isotopic mix of available material changes, see below.

4.1.3.3 Method 2, variation 2c, assume Q is zero

This effectively means that all losses are accounted for in the P term. This is comparable to Shannon Yee's method. Then we can solve for P for the initial composition by rearranging equation 4-16.

$$P = \frac{\sum_{U\ isotopes} (\sigma_{n,fission} + \sigma_{n,\gamma}) m_U M_U + \sum_{TRU\ isotopes} (\sigma_{n,fission} + \sigma_{n,\gamma}) m_{TRU} M_{TRU}}{\sum_{U\ isotopes} \nu \sigma_{n,fission} m_U M_U + \sum_{TRU\ isotopes} \nu \sigma_{n,fission} m_{TRU} M_{TRU}} \qquad \text{Eqn 4-19}$$

Note that equation 4-19 (method 2) places the same role as Yee equation 3.33 does for method 1. Note the similarities and differences when Yee equation 3.33 is rearranged as follows:

$$P = \frac{2}{\sum_{U\ isotopes} \frac{\nu \sigma_{n,fission}}{\sigma_{n,fission} + \sigma_{n,\gamma}} m_U + \sum_{TRU\ isotopes} \frac{\nu \sigma_{n,fission}}{\sigma_{n,fission} + \sigma_{n,\gamma}} m_{TRU}} \qquad \text{Yee eqn 3.33}$$

Both expressions (equation 4-19 and Yee equation 3.33) use values for ν, $\sigma_{n,fission}$, $\sigma_{n,\gamma}$, m_U, and m_{TRU}. Equation 4-19 additionally uses M_U and M_{TRU}. The parameter ν can be considered to have units of neutrons/fission. The parameters $\sigma_{n,fission}$ and $\sigma_{n,\gamma}$, can be considered to have units of barns-fission and barns-capture, respectively. Thus, both expressions have units of barns/barns-neutrons or neutrons^{-1}, or equivalently stated as loss per neutron.

Using equation 4-19 for method 2c, one has a value for P and both Qs are zero. Armed with values for P, Q_p, and Q_c, one can then adjust M_U and M_{TRU} as the isotopic mix of available material changes, see below.

4.1.3.4 Method 2, variation 2d, iterate with output composition (not implemented)

Iterate with the output composition so that an appropriate value of k_∞ at end of cycle is matched. The simplest way to implement this is to calculate P with the initial output composition. Then, use of initial input composition allows estimation of k_∞ at beginning of cycle. The approach then mirrors the other methods.

One variation would be to allow for a change in burnup (total neutron fluence, cycle length) as would be appropriate if FR conversion ratio was changing. The major change in fuel composition as FR conversion ratio change is the U/TRU mixture, as U content increases the allowable burnup (hence fluence, hence cycle length) increases. This variation is possible because the output adjustment method depends on fluence (φt).

4.1.3.5 Method 2, after solving for initial unknowns

Having solved equation 4-16 for the initial recipe, one can then estimate adjusted compositions (U versus TRU) as the isotopic mix of available material varies from the original initial composition. As with method 1, the adjusted composition among uranium isotopes and among TRU isotopes, respectively, is the available composition.

$$m_{adjusted} = m_{available} \qquad \text{Eqn 4-7}$$

This means that no TRU isotopes will be "left over", the recipe for the input TRU isotopes is adjusted so that they match the available composition.

Given equations 4-1, 4-2, 4-3, and 4-7, and the values of P, Q_c, Q_p, ν, $\sigma_{n,fission}$, $\sigma_{n,\gamma}$, from the initial composition using either method 1 or method 2 and $m_{adjusted,}$ is then possible to solve equation 4-16 for the adjusted composition. That is, one calculates $M_{adjusted}$ for U and for TRU. The two equations 4-1 and 4-16 have two unknowns ($M_{uranium}$ and M_{TRU}); they are solved as follows:

$$M_{TRU} = \frac{\sum_{U\ isotopes}(\sigma_{n,fission}+\sigma_{n,\gamma})m_U - P\sum_{U\ isotopes}\nu\sigma_{n,fission}m_U + Q_p + Q_c}{P\left\{\sum_{TRU\ isotopes}\nu\sigma_{n,fission}m_{TRU} - \sum_{U\ isotopes}\nu\sigma_{n,fission}m_U\right\} + \left\{\sum_{U\ isotopes}(\sigma_{n,fission}+\sigma_{n,\gamma})m - \sum_{TRU\ isotopes}(\sigma_{n,fission}+\sigma_{n,\gamma})m\right\}} \qquad \text{Eqn 4-20}$$

$$M_U = \frac{-\sum_{TRU\ isotopes}(\sigma_{n,fission}+\sigma_{n,\gamma})m_{TRU} + P\sum_{TRJ\ isotopes}\nu\sigma_{n,fission}m_{TRU} - Q_p - Q_c}{P\left\{\sum_{TRU\ isotopes}\nu\sigma_{n,fission}m_{TRU} - \sum_{U\ isotopes}\nu\sigma_{n,fission}m_U\right\} + \left\{\sum_{U\ isotopes}(\sigma_{n,fission}+\sigma_{n,\gamma})m - \sum_{TRU\ isotopes}(\sigma_{n,fission}+\sigma_{n,\gamma})m\right\}} \qquad \text{Eqn 4-21}$$

As a check, note that $M_{TRU} + M_U$ equals 1.

As a second check, consider what is required for M_{TRU} to be zero.

$$M_{TRU} = 0 = \sum_{U\ isotopes}(\sigma_{n,fission}+\sigma_{n,\gamma})m_U - P\sum_{U\ isotopes}\nu\sigma_{n,fission}m_U + Q_p + Q_c \qquad \text{Eqn 4-22}$$

Or, re-arranging ….

$$\sum_{U\ isotopes}(\sigma_{n,fission}+\sigma_{n,\gamma})m_U + Q_P + Q_C = P\sum_{U\ isotopes}\nu\sigma_{n,fission}m_U \qquad \text{Eqn 4-23}$$

Or using equation 4-15, we find new equation 4-24 that says if the U isotopes can provide adequate criticality to overcome P and Q terms, TRU isotopes are not required.

$$1 = P\frac{\sum_{U\ isotopes}\nu\sigma_{n,fission}m_U}{\sum_{U\ isotopes}(\sigma_{n,fission}+\sigma_{n,\gamma})m_U + Q_p + Q_C} = Pk_\infty \qquad \text{Eqn 4-24}$$

As a third check, consider what is required for M_U to be zero.

$$0 = -\sum_{TRU\ isotopes}(\sigma_{n,fission}+\sigma_{n,\gamma})m_{TRU} + P\sum_{TRJ\ isotopes}\nu\sigma_{n,fission}m_{TRU} - Q_p - Q_c \qquad \text{Eqn 4-25}$$

And, again, using equation 4-15, we find new equation 4-26 that says if the TRU isotopes can provide adequate criticality to overcome P and Q terms, U isotopes are not required.

$$1 = P\frac{\sum_{TRU\ isotopes} \nu\sigma_{n,fission}\, m_{TRU}}{\sum_{TRU\ isotopes}(\sigma_{n,fission}+\sigma_{n,\gamma})\, m_{TRU} + Q_p + Q_C} = P\,k_\infty \qquad \text{Eqn 4-26}$$

If M_U and M_{TRU} are balanced for some composition, then adding additional neutron capture Q, to compensate, the M_{TRU} must be increased from the previous balance point by

$$\Delta M_{TRU} = \frac{Q}{P\left\{\sum_{TRU\ isotopes} \nu\sigma_{n,fission}\, m_{TRU} - \sum_{U\ isotopes} \nu\sigma_{n,fission}\, m_U\right\} + \left\{\sum_{U\ isotopes}(\sigma_{n,fission}+\sigma_{n,\gamma})m - \sum_{TRU\ isotopes}(\sigma_{n,fission}+\sigma_{n,\gamma})m\right\}} \qquad \text{Eqn 4-27}$$

So, as capture (Q) increases or non-leakage P decreases, M_{TRU} must increase, assuming that the neutrons provided by TRU exceed those from U (the P term in the denominator is positive) and the neutrons captured by U exceed those from TRU (the second term in the denominator is positive. This means that if the TRU isotopes are driving the fuel, increasing Q or increasing leakage requires more TRU.

If the denominator terms are negative (indicating the fuel is driven by U instead of TRU), then increasing capture or non-leakage means M_{TRU} must decrease, i.e., M_U must increase.

Equations 4-20 and 4-21 can be restated in terms of k_∞ instead of P since $k_\infty P = 1$.

$$M_{TRU} = \frac{k_\infty \sum_{U\ isotopes}(\sigma_{n,fission}+\sigma_{n,\gamma})\, m_U - \sum_{U\ isotopes} \nu\sigma_{n,fission}\, m_U + k_\infty Q_p + k_\infty Q_c}{\left\{\sum_{TRU\ isotopes} \nu\sigma_{n,fission}\, m_{TRU} - \sum_{U\ isotopes} \nu\sigma_{n,fission}\, m_U\right\} + k_\infty\left\{\sum_{U\ isotopes}(\sigma_{n,fission}+\sigma_{n,\gamma})m - \sum_{TRU\ isotopes}(\sigma_{n,fission}+\sigma_{n,\gamma})m\right\}} \qquad \text{Eqn 4-28}$$

and

$$M_U = \frac{-k_\infty \sum_{TRU\ isotopes}(\sigma_{n,fission}+\sigma_{n,\gamma})\, m_{TRU} + \sum_{TRJ\ isotopes} \nu\sigma_{n,fission}\, m_{TRU} - k_\infty Q_p - k_\infty Q_c}{\left\{\sum_{TRU\ isotopes} \nu\sigma_{n,fission}\, m_{TRU} - \sum_{U\ isotopes} \nu\sigma_{n,fission}\, m_U\right\} + k_\infty\left\{\sum_{U\ isotopes}(\sigma_{n,fission}+\sigma_{n,\gamma})m - \sum_{TRU\ isotopes}(\sigma_{n,fission}+\sigma_{n,\gamma})m\right\}} \qquad \text{Eqn 4-29}$$

As a final cross check, substituting these expressions into equation 4-14, after multiplying the denominator and numerator of equation 4-14 by the denominator of equations 4-28 and 4-29, we obtain a complex expression as follows:

Numerator =

$$\left\{\sum_{U\ isotopes} \nu\sigma_{n,fission}\, m_U\right\}\left\{-k_\infty \sum_{TRU\ isotopes}(\sigma_{n,fission}+\sigma_{n,\gamma})\, m_{TRU} + \sum_{TRJ\ isotopes} \nu\sigma_{n,fission}\, m_{TRU} - k_\infty Q_p - k_\infty Q_c\right\} +$$

$$\left\{\sum_{TRU\ isotopes} \nu\sigma_{n,fission}\, m_{TRU}\right\}\left\{k_\infty \sum_{U\ isotopes}(\sigma_{n,fission}+\sigma_{n,\gamma})\, m_U - \sum_{U\ isotopes} \nu\sigma_{n,fission}\, m_U + k_\infty Q_p + k_\infty Q_c\right\}$$

This simplifies to the following expression for the numerator:

$$k_\infty \left\{ \sum_{TRU\ isotopes} \nu \sigma_{n,fission}\, m_{TRU} \right\} \left\{ \sum_{U\ isotopes} (\sigma_{n,fission} + \sigma_{n,\gamma})\, m_U + Q_p + Q_c \right\} -$$
$$k_\infty \left\{ \sum_{U\ isotopes} \nu \sigma_{n,fission}\, m_U \right\} \left\{ \sum_{TRU\ isotopes} (\sigma_{n,fission} + \sigma_{n,\gamma})\, m_{TRU} + Q_p + Q_c \right\}$$

Denominator =

$$\left\{ \sum_{U\ isotopes} (\sigma_{n,fission} + \sigma_{n,\gamma})\, m_U \right\} \left\{ -k_\infty \sum_{TRU\ isotopes} (\sigma_{n,fission} + \sigma_{n,\gamma})\, m_{TRU} + \sum_{TRJ\ isotopes} \nu \sigma_{n,fission}\, m_{TRU} - k_\infty Q_p - k_\infty Q_c \right\} +$$
$$\left\{ \sum_{TRU\ isotopes} (\sigma_{n,fission} + \sigma_{n,\gamma})\, m_{TRU} \right\} \left\{ k_\infty \sum_{U\ isotopes} (\sigma_{n,fission} + \sigma_{n,\gamma})\, m_U - \sum_{U\ isotopes} \nu \sigma_{n,fission}\, m_U + k_\infty Q_p + k_\infty Q_c \right\}$$
$$+ \{Q_p + Q_c\} \left\{ \left\{ \sum_{TRU\ isotopes} \nu \sigma_{n,fission}\, m_{TRU} - \sum_{U\ isotopes} \nu \sigma_{n,fission}\, m_U \right\} + k_\infty \left\{ \sum_{U\ isotopes} (\sigma_{n,fission} + \sigma_{n,\gamma}) m - \sum_{TRU\ isotopes} (\sigma_{n,fission} + \sigma_{n,\gamma}) m \right\} \right\}$$

This simplifies to the following expression for the denominator:

$$\left\{ \sum_{U\ isotopes} (\sigma_{n,fission} + \sigma_{n,\gamma})\, m_U \right\} \left\{ \sum_{TRJ\ isotopes} \nu \sigma_{n,fission}\, m_{TRU} \right\} -$$
$$\left\{ \sum_{TRU\ isotopes} (\sigma_{n,fission} + \sigma_{n,\gamma})\, m_{TRU} \right\} \left\{ \sum_{U\ isotopes} \nu \sigma_{n,fission}\, m_U \right\}$$
$$+ \{Q_p + Q\} \left\{ \sum_{TRU\ isotopes} \nu \sigma_{n,fission}\, m_{TRU} - \sum_{U\ isotopes} \nu \sigma_{n,fission}\, m_U \right\}$$

Re-arranging gives a somewhat simplified expression for the denominator:

$$\left\{ \sum_{U\ isotopes} (\sigma_{n,fission} + \sigma_{n,\gamma})\, m_U + Q_p + Q_c \right\} \left\{ \sum_{TRJ\ isotopes} \nu \sigma_{n,fission}\, m_{TRU} \right\} -$$
$$\left\{ \sum_{TRU\ isotopes} (\sigma_{n,fission} + \sigma_{n,\gamma})\, m_{TRU} + Q_p + Q_c \right\} \left\{ \sum_{U\ isotopes} \nu \sigma_{n,fission}\, m_U \right\}$$

The simplified numerator over the denominator is merely k_∞ as it should be.

In summary, method 2 contains these steps:

- Calculate P, Q_c using variations a, b, or c above.

  Variation a - assume values for P, solve for Q_c using equation 4-18.

  Variation b - calculate P from Yee equation 3.33, solve for Q_c using equation 4-18.

  Variation c - assume Q_c=0, calculate P from equation 4-19.

- Ignore non-fuel capture in the pellet (Q_p)
- Set $m_{adjusted} = m_{available}$
- Calculate the adjusted M_U and M_{TRU} using equations 4-20 and 4-21.

In comparison, method 1 contains these steps

- Calculate $P_{Initial}$ using Yee equation 3.33, instead of equation 4-19 in method 2c.
- Ignore non-fuel capture (Q_c and Q_p are zero).
- Set $m_{adjusted} = m_{available}$
- Calculate the adjusted M_U and M_{TRU} using equations 4-10 and 4-11.

Method 2 is more grounded in the textbook definition of k_∞. If one can obtain the non-leakage parameter P by guessing it (method 2a) or by using Yee's expression for P (method 2b), it is possible to derive an expression (equation 4-27) that tells us how much the TRU fraction fuel has to be increased if one adds non-fuel neutron capture material to a fuel mixture previously in balance. Method 2c sets the non-fuel neutron capture to zero, this is analogous to Yee's method in that all the non-fuel material (leakage and capture) is accounted for in the P term. Thus, there is a key difference in the P values.

- Method 1 and Method 2c, P must account for all non-fuel leakage and capture, there is no separate non-fuel capture term, Q.
- Method 2a and 2b, non-fuel capture, Q, is not zero, P only accounts for non-fuel leakage.

4.1.4 Method 3 - Reactivity Differential Impact

As noted above, the third method was used for different assessments. The differential reactivity impact was calculated by adding to a known "pure" composition (no impurities, only U and TRU elements) a small concentration of each isotope sufficient to produce a significant perturbation - 100 micrograms per gram of initial transuranic material. This was done for 300 individual isotopes for metal fuel and oxide fuel fast reactor with transuranic conversion ratio of 0.5. The result is a set of 300 values in units of percent milli-rho per micrograms per gram of initial TRU, or percent milli-rho per ppm of each isotope in question.

This method differs from the other two because it includes both neutron absorption (as do the other methods) and displacement of fuel isotopes (unlike the other methods), lowering the density of fuel. This method must therefore be used with caution as it is not appropriate to apply the coefficients to intended non-fuel elements such as cladding. Furthermore, depending on the fuel type and reactor design., it could be easy to compensate for lower density by increasing the mass of fuel slightly.

For each isotope of interest, a small amount (100 micrograms) of the isotope was added to the nominal fuel mix in units of micrograms per gram (i.e. ppm). The change in reactivity was noted in detailed physics calculations. The results are reported in units of percent milli-rho per microgram of impurity per gram of fuel. This method is described in more detail elsewhere [6].

The elements Se to Yb can arise from either fission products or natural sources. The other elements below Pb are presumably from natural sources. So, in looking at the overall reactivity penalty, Hoffman considered for each element which had the higher reactivity penalty - fission product isotopic mix or natural isotopic mix - and used whichever gave the higher reactivity penalty.

4.2 Testing and Calibration

4.2.1 Methods 1 and 2

Methods 1 and 2 were tested for the cases described in Table 4-1. Recipes and cross sections from cases in the AFCI Transmutation Library. None of the cases in the AFCI Transmutation Library provide cross sections for all relevant isotopes, so missing isotopes' cross sections were taken from the MOX-Pu or LMFBR cross section data in the ORIGEN 2.2 library.

Table 4-1. Description of Cases for Testing 1-Group Methods

	Case Name	Initial Recipe	Available Material	Source of Cross sections	Real Recipe to use to compare quality of approximation
1	Estimate MOX-NU-Pu from MOX-RU-Pu (ANL xsec)	MOX-RU-Pu	NU plus Pu from UOX-51 (age 5 yr)	ANL MOX-Pu + ORIGEN MOX	MOX-NU-Pu
2	Estimate MOX-RU-Pu from MOX-NU-Pu (origen xs)	MOX-NU-Pu	RU and Pu from UOX-51 (age 5+2 yr)	ORIGEN MOX	MOX-RU-Pu
3	Estimate MOX-PuNp from MOX-RU-Pu (ANL xsec)	MOX-RU-Pu	NU, Np, Pu from UOX-51 (age 5 years)	ANL MOX-Pu + ORIGEN MOX	MOX-PuNp
4	Estimate MOX-PuNpAm from MOX-RU-Pu (ANL xsec)	MOX-RU-Pu	NU, Np, Pu, Am from UOX-51 (age 5 years)	ANL MOX-Pu + ORIGEN MOX	MOX-PuNpAm
5	Estimate MOX-PuNpAm from MOX-PuNp (origen xsec)	MOX-PuNp	NU, Np, Pu, Am from UOX-51 (age 5 years)	ORIGEN MOX	MOX-PuNpAm
6	Estimate MOX-TRU from MOX-RU-Pu (ANL xsec)	MOX-RU-Pu	RU, TRU from UOX-51 (age 5 years)	ANL MOX-Pu + ORIGEN MOX	NONE
7	Estimate MOX-PuNp from MOX-PuNpAm (origen xsec)	MOX-PuNpAm	MOX-PuNpAm recipe, delete Am	ORIGEN MOX	MOX-PuNp
8	Estimate MOX-PuNp from MOX-PuNpAm (SY data, origen xsec)	MOX-PuNpAm	MOX-PuNpAm recipe, delete Am	ORIGEN MOX	MOX-PuNp
9	Estimate MOX-PuNp from MOX-PuNpAm (older data set from Library, origen data	MOX-PuNpAm	MOX-PuNpAm recipe, delete Am	ORIGEN MOX	MOX-PuNp
10	Estimate FR with 30-yr feed from FR=0.50 (origen xsec)	CR=0.50 with UOX-50 feed ANL	UOX-33 output, aged 30 years	ORIGEN LMFBR	CR=50 with UOX-33/30-yr feed (ANL)

11	Estimate FR with 30-yr feed from FR=0.50 (INL xsec)	CR=0.50 with UOX-50 feed INL	UOX-33 output, aged 30 years	INL CR=0.50 + ORIGEN LMFBR	CR=50 with UOX-33/30-yr feed (INL)
12	Estimate FR with 30-yr feed from FR=0.50 (SY data, origen xsec)	CR=0.50 with UOX-50 feed ANL	UOX-33/30-yr feed from older calc (SY)	ORIGEN LMFBR	CR=50 with UOX-33/30-yr feed (ANL)
13	Estimate FR with 30-yr feed from FR=0.50 (older data set from Library, origen data	CR=0.50 with UOX-50 feed ANL	UOX-33/30-yr feed from an older calc in the library	ORIGEN LMFBR	CR=50 with UOX-33/30-yr feed (ANL)
14	Estimate 1-tier FR (PWR=2) from ANL (PWR=5) ANL xsec	CR=0.50 equilibrium ANL (PWR=5)	U, TRU from UOX-51 (aged 2)+self (ANL)	ANL CR=0.50 + ORIGEN LMFBR	1-tier FR (PWR=2)
15	Estimate 1-tier FR (PWR=2) from INL (PWR=10) INL xsec	CR=0.50 equilibrium INL (PWR=10)	U, TRU from UOX-51 (aged 2)+self (INL)	INL CR=0.50 + ORIGEN LMFBR	1-tier FR (PWR=2)
16	Estimate 1-tier FR (PWR=10) from ANL (PWR=5) ANL xsec	CR=0.50 equilibrium ANL (PWR=5)	U, TRU from UOX-51 (aged 10)+self (ANL)	ANL CR=0.50 + ORIGEN LMFBR	1-tier FR (PWR=10)
17	Estimate 1-tier FR (PWR=20) from ANL (PWR=5) ANL xsec	CR=0.50 equilibrium ANL (PWR=5)	U, TRU from UOX-51 (aged 20)+self (ANL)	ANL CR=0.50 + ORIGEN LMFBR	1-tier FR (PWR=20)
18	Estimate 1-tier FR (PWR=20) from INL (PWR=10) INL xsec	CR=0.50 equilibrium INL (PWR=10)	U, TRU from UOX-51 (aged 20)+self (INL)	INL CR=0.50 + ORIGEN LMFBR	1-tier FR (PWR=20)
19	Estimate 1-tier FR (PWR=50) from ANL (PWR=5) ANL xsec	CR=0.50 equilibrium ANL (PWR=5)	U, TRU from UOX-51 (aged 50)+self (ANL)	ANL CR=0.50 + ORIGEN LMFBR	1-tier FR (PWR=50)
20	Estimate 1-tier FR (PWR=50) from INL (PWR=10) INL xsec	CR=0.50 equilibrium INL (PWR=10)	U, TRU from UOX-51 (aged 50)+self (INL)	INL CR=0.50 + ORIGEN LMFBR	1-tier FR (PWR=50)

ANL = Argonne National Laboratory
INL = Idaho National Laboratory
FR = Fast reactor
CR = transuranic conversion ratio
PWR = pressurized water reactor, the number PWR=XX refers the number of years of aging after LWR discharge before insertion of recycled material into the next reactor.
UOX = uranium oxide fuel, the number UOX-XX refers to the burnup of the UOX in GWth-day/tonne-iHM.
ORIGEN LMFBR = Liquid metal fast breeder reactor, a case in ORIGEN 2.2's data library.
ORIGEN MOX = U-Pu mixed oxide, a case in ORIGEN 2.2's data library.

EU = enriched uranium
NU = natural uranium
RU = recovered uranium (hence significant content of neutron absorber U-236)
SY = data that S. Yee used in his thesis [29] to confirm the present calculational tool replicated his results.
xsec = cross section

Table 4-2 provides the estimations for required percent transuranic material in fresh fuel and the "real" composition. Table 4-3 expresses the results as a percent error in the TRU result. As an example, consider case 1, estimate MOX-NU-Pu (NU=natural uranium) from the MOX-RU-Pu (RU=recovered uranium). Table 4-4 shows that the estimated results range from 9.3% (method 2c) to 10.2% (methods 1 and 2b); the "real" result was 9.8%. Table 4-3 shows that these results have an error of 4% (methods 1 and 2b), -3% (method 2a), and -6% (method 2c).

Table 4-2. Percent Transuranic Material Estimated for the Test Cases

	Case Name	Method 1	Method 2a	Method 2b	Method 2c	Real
1	Estimate MOX-NU-Pu from MOX-RU-Pu (ANL xsec)	10.2%	9.5%	10.2%	9.3%	9.8%
2	Estimate MOX-RU-Pu from MOX-NU-Pu (origen xs)	9.8%	9.9%	9.8%	10.2%	10.7 %
3	Estimate MOX-PuNp from MOX-RU-Pu (ANL xsec)	11.5%	11.3%	11.1%	11.3%	13.1 %
4	Estimate MOX-PuNpAm from MOX-RU-Pu (ANL xsec)	13.1%	15.4%	12.5%	16.6%	17.4 %
5	Estimate MOX-PuNpAm from MOX-PuNp (origen xsec)	14.8%	17.1%	14.5%	28.6%	17.4 %
6	Estimate MOX-TRU from MOX-RU-Pu (ANL xsec)	13.3%	16.0%	12.7%	17.5%	TBD
7	Estimate MOX-PuNp from MOX-PuNpAm (origen xsec)	15.6%	13.1%	15.8%	9.8%	13.1 %
8	Estimate MOX-PuNp from MOX-PuNpAm (YS data, origen xsec)	15.6%	13.1%	15.8%	9.8%	13.1 %
9	Estimate MOX-PuNp from MOX-PuNpAm (old data, origen xsec)	15.6%	13.1%	15.8%	9.8%	13.1 %
10	Estimate FR with 30-yr feed from FR=0.50 (origen xsec)	31.5%	34.2%	33.0%	35.1%	30.9 %
11	Estimate FR with 30-yr feed from FR=0.50 (INL xsec)	31.8%	31.1%	30.5%	31.8%	32.5 %
12	Estimate FR with 30-yr feed from FR=0.50 (YS data, origen xsec)	31.5%	33.4%	32.6%	34.3%	30.9 %
13	Estimate FR with 30-yr feed from FR=0.50 (old data, xsec)	31.7%	33.8%	33.1%	34.6%	30.9 %
14	Estimate 1-tier FR (PWR=2) from ANL (PWR=5) ANL xsec	32.9%	32.7%	32.7%	32.7%	32.3 %
15	Estimate 1-tier FR (PWR=2) from INL (PWR=10) INL xsec	32.6%	32.3%	32.3%	32.3%	32.3 %
16	Estimate 1-tier FR (PWR=10) from ANL (PWR=5) ANL xsec	33.0%	32.8%	32.8%	32.9%	32.9 %

17	Estimate 1-tier FR (PWR=20) from ANL (PWR=5) ANL xsec	33.1%	33.0%	32.9%	33.1%	33.5 %
18	Estimate 1-tier FR (PWR=20) from INL (PWR=10) INL xsec	32.8%	32.6%	32.5%	32.6%	33.5 %
19	Estimate 1-tier FR (PWR=50) from ANL (PWR=5) ANL xsec	33.2%	33.2%	33.1%	33.3%	34.0 %
20	Estimate 1-tier FR (PWR=50) from INL (PWR=10) INL xsec	32.8%	32.8%	32.7%	32.8%	34.0 %

Table 4-3. Percent Error in Calculated Transuranic Content in Fresh Fuel

	Case Name	Method 1	Method 2a	Method 2b	Method 2c
1	Estimate MOX-NU-Pu from MOX-RU-Pu (ANL xsec)	4%	-3%	4%	-6%
2	Estimate MOX-RU-Pu from MOX-NU-Pu (origen xs)	-9%	-7%	-9%	-5%
3	Estimate MOX-PuNp from MOX-RU-Pu (ANL xsec)	-12%	-14%	-15%	-14%
4	Estimate MOX-PuNpAm from MOX-RU-Pu (ANL xsec)	-25%	-12%	-28%	-5%
5	Estimate MOX-PuNpAm from MOX-PuNp (origen xsec)	-15%	-2%	-17%	64%
6	Estimate MOX-TRU from MOX-RU-Pu (ANL xsec)	NA	NA	NA	NA
7	Estimate MOX-PuNp from MOX-PuNpAm (origen xsec)	19%	0%	20%	-25%
8	Estimate MOX-PuNp from MOX-PuNpAm (YS data, origen xsec)	19%	0%	20%	-25%
9	Estimate MOX-PuNp from MOX-PuNpAm (old data, origen xsec)	19%	0%	20%	-25%
10	Estimate FR with 30-yr feed from FR=0.50 (origen xsec)	2%	11%	7%	14%
11	Estimate FR with 30-yr feed from FR=0.50 (INL xsec)	-2%	-4%	-6%	-2%
12	Estimate FR with 30-yr feed from FR=0.50 (YS data, origen xsec)	2%	8%	6%	11%
13	Estimate FR with 30-yr feed from FR=0.50 (old data, xsec)	3%	10%	7%	12%
14	Estimate 1-tier FR (PWR=2) from ANL (PWR=5) ANL xsec	2%	1%	1%	1%
15	Estimate 1-tier FR (PWR=2) from INL (PWR=10) INL xsec	1%	0%	0%	0%
16	Estimate 1-tier FR (PWR=10) from ANL (PWR=5) ANL xsec	0%	0%	0%	0%
17	Estimate 1-tier FR (PWR=20) from ANL (PWR=5) ANL xsec	-1%	-1%	-2%	-1%
18	Estimate 1-tier FR (PWR=20) from INL (PWR=10) INL xsec	-2%	-3%	-3%	-3%
19	Estimate 1-tier FR (PWR=50) from ANL (PWR=5) ANL xsec	-3%	-3%	-3%	-2%
20	Estimate 1-tier FR (PWR=50) from INL (PWR=10) INL xsec	-4%	-4%	-4%	-4%
	Average of thermal reactor cases (absolute values)	15%	5%	17%	21%
	Average of fast reactor cases (absolute values)	2%	4%	4%	5%

Cases 1-9 are LWR with MOX fuel; cases 10-20 are fast burner reactor cases. The fast reactor cases have significantly lower errors, presumably because the variation in cross sections among specific reactor conditions in fast reactors is markedly lower than in thermal reactors. This is exemplified in Section 3.2.

Analysis of these results led to adoption of method 2a for thermal reactors and method 1 for fast reactors. The average absolute value of error for method 2a was 5% with a high of -14%. The average absolute value of error for method 1 was 2% with a high of -4%.

To put these results into perspective, consider an instance in which there are two "real" calculations. Cases 10 and 11 are both estimating the recipe for FR CR=0.50 with 30-year old feed from UOX-33. In this instance, we have two FR detailed calculations with that feed material; with a difference of 1.7% (30.9% in an ANL calculation, case 10, and 32.5% in an INL calculation, case 11). Said another way, the fast reactor results are in the same range as the variation in some of the detailed physics calculations.

The LWR results are less trustworthy, as had been expected, because thermal reactor neutron spectra (and hence 1-group cross sections) are more sensitive to the details of the case and the change of composition during irradiation.

4.2.2 Method 3

This method does not need testing in the same sense as the other two methods as it is the result of detailed physics calculations, isotope by isotope.

It is important to note how different this method is from the others and the underlying assumption about the importance of displacement of fuel atoms. The largest coefficients are for the light elements, which actually have low neutron absorption. As Hoffman notes, the high coefficients are due to having more atoms per microgram for the light elements, i.e., one gram of a light element has far more atoms than a gram of fuel.

Hoffman did check for the impact of linearly adding the product of impurity levels times the reactivity coefficients. Table 4-4 shows that the combined effect of all postulated impurities is under predicted by the sum of the individual isotopes, about 15% low for metal fuel and 25% low for oxide fuel, but only about 1-2% for the LWR MOX-Pu case. "Without detailed analysis, the reason is unclear, but it seems likely that softening of the neutron spectrum will enhance parasitic absorption by heavier impurity isotopes. Whatever the case, the results are somewhat non-linear so results should not be extrapolated too far, but are certainly sufficiently accurate for the preliminary nature of the impurity studies.

Table 4-4. Estimated Maximum Reactivity Penalty for Impurities in Fast Reactors with Transuranic Conversion Ratio of 0.5 and in LWR with MOX-Pu [6]

	Metal fuel fast reactor		Oxide fuel fast reactor		LWR with MOX-Pu	
Units of percent milli-rho per microgram of impurity per g-fuel	Beginning of cycle	End of cycle	Beginning of cycle	End of cycle	Beginning of cycle	End of cycle
Estimated by linear addition of impurity times coefficient	-450	-471	-285	-299	-472	-442
Calculated for entire set of impurity isotopes	-527	-550	-380	-399	-476	-451

4.3 Application to Value of Minor Actinides

The Minor Actinide study is documented elsewhere [28]. The objective was to assess the advantages and disadvantages of recycling the minor actinides (MA) - Np, Am, Cm, Bk, Cf - from the first U.S. UOX separation plant rather than disposing of the MA from that plant as waste. The key underlying assumption was that the first UOX separation plant provides two products, recovered U and Pu and additional recovered U, based on existing or nearly existing technology. (The U-Pu product is envisioned to make MOX; as shown below, most of the uranium recovered from UOX is not required to make MOX and so there is a separate RU stream.) Since existing technology does not recover the MA elements, scenario 1 was defined in which the MA from UOX separation is sent to waste. Two additional scenarios were defined in which MA are recycled (in fast reactors) rather than sent to waste. Scenario 2 involves MOX followed by fast reactors, as does Scenario 1; but unlike Scenario 1, Scenario 2 retains the MA for eventual use in fast reactors. Like Scenario 2, Scenario 3 recycles the MA; but unlike Scenario 2, Scenario 3 skips the MOX recycle step.

This subsection explains the fuel value calculation done for the Minor Actinide study. This involved using fuel isotopic mixtures ("recipes") previously developed by the transmutation analysis group within Systems Analysis. The isotopic mixtures of the recovered materials did not exactly match recipes in the fuels library [14] so the 1-group methods explained above were used to evaluate the impact of the isotopic differences. This method used one-group cross section data for thermal and fast spectrums for each heavy metal isotope to estimate the fissile probability of each isotope coupled with the neutron yield of each isotope, producing an estimate of the difference in "octane" (reactivity worth) between the isotopic mix of the recipe Pu or TRU and the actual Pu or TRU. This difference was used to calculate the ratio of Pu or TRU to U in the MOX and FR fuels (the TRU enrichment) necessary to achieve the same burnup, and therefore the same thermal energy yield per tonne of fuel. (Note that since the composition of the recovered U is fixed, the U-235 level is a constant. Therefore, any enrichment adjustments occur only through changes in the TRU to U ratio.)

4.3.1 Scenario Definition

Figure 4-1 illustrates the three scenarios considered in the Minor Actinide study, as interpreted for purposes of analyzing fuel value. The differences among the scenarios are shown in red text or red lines. They have the following common characteristics:

- Scenarios start with LWR UOX fuel with 51 GWth-day/tonne-iHM burnup
- UOX cools for 5 years before separation at 800 tonnes-UOX/year, which is the nominalization for flow rates among the three cases.
- Fast reactors (CR=0.50) recycle material from thermal reactors; however, which material and how long it has cooled varies.
- Because MOX fuel spends about 5 years in the reactor, all cases have the same time lag between UOX discharge and the first fast reactor recycle (35 years).[1]

[1] Because all TRU are recycled from UOX separation in case 3, the specific timing of UOX separation between UOX discharge and insertion into the fast reactor does not matter as long as the total time between UOX discharge and FR insertion is kept constant, i.e., 30+5, 35+0, 0+35 give the same result as pictured here (5+30).

- 2 years between fast reactor discharge and insertion into fast reactor.
- Modeling of fast reactors by two discrete recycle passes, followed by an equilibrium recycle pass in which no net TRU material is lost, i.e., the equilibrium recycle is modeled as TRU in (from second recycle pass) and only fission products and electricity out.

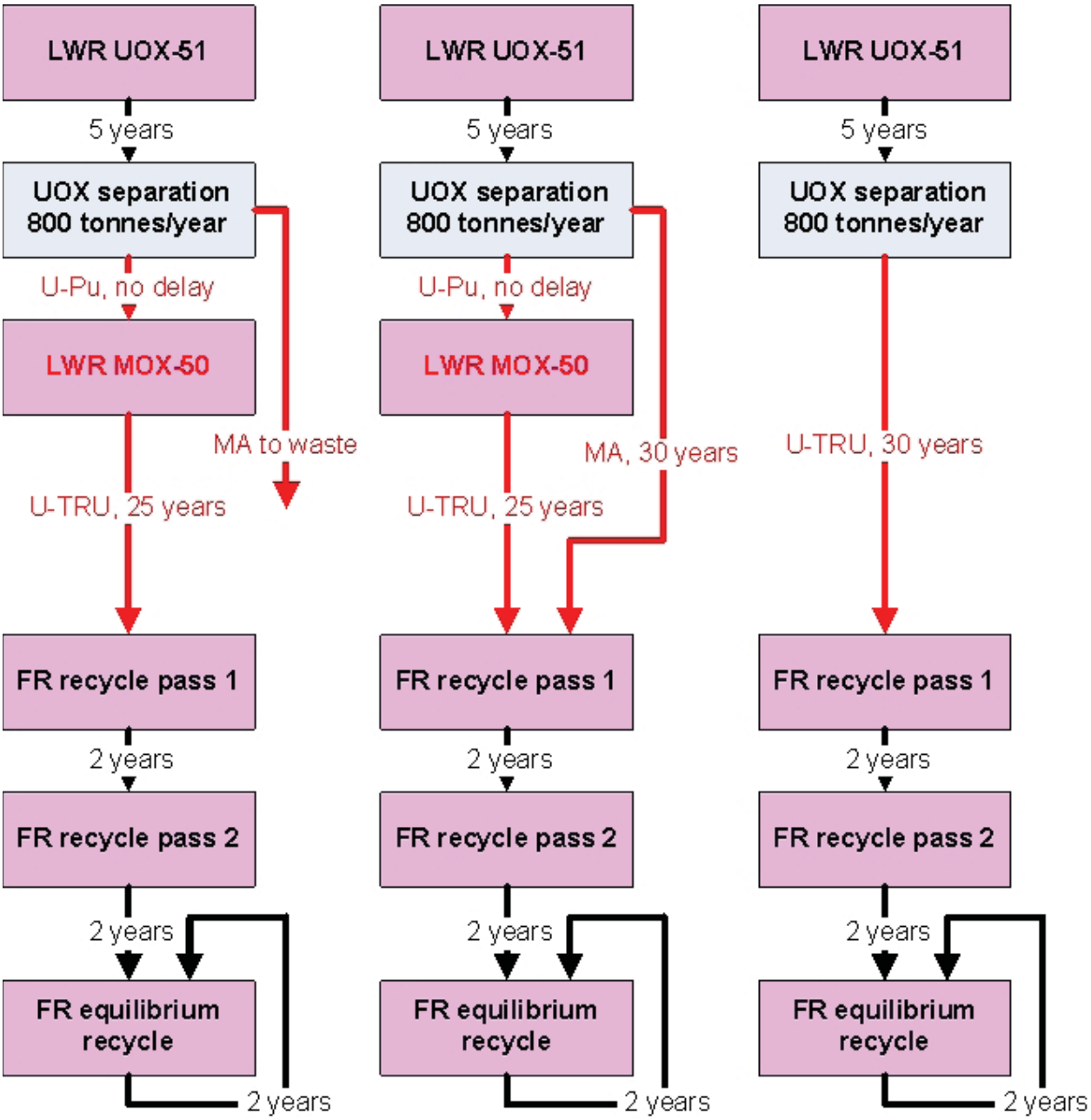

Figure 4-1. Illustration of the minor actinide scenarios

Scenarios 1 and 2 differ in that minor actinides (MA) from UOX separation are discarded in Scenario 1 and recycled in fast reactors in Scenario 2. Scenario 3 differs from either Scenario 1 or Scenario 2 in that the MOX-Pu step is eliminated. Scenarios 2 and 3 create only fission products as waste.

Four factors alter the isotopic mixes among the scenarios.

- Recycling MA rather than sending to waste in Scenarios 2 and 3 increases MA content in fast reactors.
- Including one MOX-Pu in Scenarios 1 and 2 increases the MA content in fast reactors because much of the Pu fissions in the MOX step.
- The time lags in the defined scenarios do not exactly match cases in the Transmutation Library.
- To gain deeper insights, the fast reactor portion of the analysis was modeled as first recycle, second recycle, and equilibrium recycle. The Transmutation Library presently only includes first recycle and equilibrium recycle compositions.

With one exception, all the isotopic changes apply to fast reactor compositions, for which the 1-group perturbation methods were shown in section 4.2 to work particularly well. The one exception is that the closest MOX-RU-Pu recipe in the Transmutation Library uses 5 years cooling from UOX discharge to UOX separation and 2 years cooling from UOX separation to MOX insertion whereas the Minor Actinide study specifications do not include the 2 year cooling from UOX separation to MOX insertion. Thus, the MOX-RU-Pu recipe in the Minor Actinide study lacks 2 years of Am-241 in-growth from Pu-241 and thus lacks both the neutron absorption by Am-241 and the loss of fuel value by decay of Pu-241.

4.3.2 How Tools Were Used for this Application

The fuel yield calculated from recovered TRU depends on a number of factors. The most important factor is the target burnup for the fuel. As burnup increases, enrichment requirements also increase to support the higher cumulative irradiation. However, increasing burnup also directly increases the amount of thermal energy produced, and therefore the electricity generated.

Another important factor is the irradiation spectrum of the reactor. The cross section of an isotope determines the likelihood of a heavy metal atom interacting with a neutron. Cross sections are larger in thermal reactors, which is why they have lower fuel enrichment needs. However, the spectrum also determines what type of interaction occurs; the primary interactions are fission and neutron capture. The TRU isotopes are more likely to fission in a fast spectrum. The evolution of fertile isotopes to fissile isotopes is also spectrum-dependent.

A third factor is the design TRU conversion ratio of the reactor core – the ratio of TRU created to TRU destroyed during irradiation. The GNEP approach was to use a low conversion ratio in the fast reactor to minimize the number of fast reactors needed to utilize the TRU generated in thermal reactors, and the analyses here assume a CR = 0.5. At higher conversion ratios, the reactors have a smaller net consumption per pass of the TRU material, requiring more fast reactors to utilize all of the available TRU. (At conversion ratios of 1.0 or higher, the TRU generated by thermal reactors would be utilized solely for startup of new fast reactors).

To facilitate fuel yield comparisons, the same MOX burnup was used for Scenarios 1 and 2 and the same FR burnup and conversion ratio for all scenarios. Constant capacity factors of 90% for the thermal reactor and 82% for the fast reactor then determined the annual fuel discharge per year per continuous gig watt of thermal energy produced. Thermal efficiencies of 34% for the thermal reactor and 38% for the fast reactor were used to determine the amount of electricity produced.

The electricity generated in the UOX, MOX and FR passes were calculated to generate a fuel value improvement factor for each scenario. The UOX pass at the designed annual fuel flow, burnup, capacity factor and thermal efficiency yields an average continuous level of electricity generation of 38 GWe. Additional electricity generated from the MOX and FR fuel fabricated from the recycled materials provides the improvement factor.

The isotopic flow into the UOX separation plant is the same in all three Scenarios.

4.3.2.1 MOX-RU-Pu adjustment

Table 4-5 shows the flows from the UOX separation plant. At the time of UOX separation in Scenarios 1 and 2, there is 10.37 tonnes-TRU/year - 9.30 Pu and 1.07 MA. To simplify calculations (one decay of isotopes for 35 years instead of one for 5 years and a second one for 30 years), we did the UOX separation for Scenario 3 just before FR fabrication at which time the 10.37 tonnes is 8.45 Pu, 1.88 MA, and 0.04 U (PU-238 decay into U234). Note how much more RU is used in MOX than the FR. MOX is 9-11% TRU and FR fuel at this conversion ratio is 29-36% TRU.

Table 4-5. UOX Separation Mass Flows

	Scenario 1 (discard MA from UOX, use MOX-Pu)	Scenario 2 (keep all MA, use MOX-Pu)	Scenario 3 (keep all MA, no MOX)
RU from separation plant to recycle (tonnes/year)	85.81	85.81	19.90
RU from separation plant to storage (tonnes/year)	661.71	661.71	727.66
Subtotal - all RU	747.52	747.52	747.56
TRU from separation plant to recycle (tonnes/year)			10.33
Pu from separation plant to recycle (tonnes/year)	9.30	9.30	
MA from separation plant to waste (tonnes/year)	1.07		
MA from separation plant to recycle (tonnes/year)		1.07	
Subtotal - all TRU	10.37	10.37	10.33
FP from separation plant to waste (tonnes/year)	42.11	42.11	42.11
Total mass from LWR-UOX separation plant	800.00	800.00	800.00

The Transmutation Library case closest to the MOX recipe requried for Scenarios 1 and 2 is MOX-RU-Pu with 7 years total decay (5 before separation and 2 after). The required TRU content in the MOX is 10.62%, which includes some Am-241 from Pu-241 decay after UOX separation. The 1-group perturbation method obtained a required TRU content for Scenarios 1 and 2 of 9.78%. This determined the flow requiredments of 85.81 tonnes-RU/year to match 9.30 tonnes-Pu/year, making 95.11 tonnes-MOX/year.

The fuel composition was then depleted using the MRTAU code (no recycle iteration performed) was then used with the associated isotopics (5 years decay of UOX-51) and 9.78% TRU to obtain the output composition from MOX irradiation. Table 4-6 shows the flows from the MOX separation plant.

Table 4-6. MOX Separation Mass Flows

	Scenario 1 (discard MA from UOX, use MOX-Pu)	Scenario 2 (keep all MA, use MOX-Pu)	Scenario 3 (keep all MA, no MOX)
RU from separation plant to recycle (tonnes/year)	69.13	70.12	
RU from separation plant to storage (tonnes/year)	13.43	12.44	
Subtotal - all RU	82.56	82.56	
Pu from separation plant to recycle (tonnes/year)	6.41	6.41	
MA from separation plant to recycle (tonnes/year)	1.26	1.26	
Subtotal - all TRU	7.68	7.68	

FP from separation plant to waste (tonnes/year)	4.87	4.87	
Total mass from LWR-UOX separation plant	95.11	95.11	

4.3.2.2 1st fast reactor recycle pass adjustment

Table 4-7 shows the mass flow into FR recycle pass 1. As with MOX, the first step is to ignore the RU and consider the total flow of TRU and its isotopics. The isotopics account for radioactive decay. As an example, in Scenario 2, 3.65% of the MA feed from UOX separation, which bypassed the MOX step, has decayed from MA into Pu.

Table 4-7. Mass Flow into First Fast Reactor Recycle Pass

	Scenario 1 (discard MA from UOX, use MOX-Pu)	Scenario 2 (keep all MA, use MOX-Pu)	Scenario 3 (keep all MA, no MOX)
RU from UOX separation (tonnes/year)			19.90
RU from MOX separation (tonnes/year)	13.43	12.44	
RU total input(tonnes/year)	13.43	12.44	19.90
Pu from UOX separation (tonnes/year)	0.00	0.04	8.45
Pu from MOX separation (tonnes/year)	6.41	6.41	0.00
Pu total (tonnes/year)	6.41	6.45	8.45
MA from UOX separation (tonnes/year)	0.00	1.03	1.88
MA from MOX separation (tonnes/year)	1.26	1.26	0.00
MA total (tonnes/year)	1.26	2.29	1.88
TRU total (tonnes/year)	7.68	8.75	10.32
Total feed (tonnes/year)	21.11	21.18	30.22

The isotopic composition of these mass flows differ. The percent of Pu in the TRU is 83.6% (Scenario 1), 74.1% (Scenario 2), and 81.8% (Scenario 3). The highest Pu content is Scenario 1 in which the MA from UOX separation (but not the MA from MOX separation) were discarded. The lowest Pu content is Scenario 2 in which not only have the MA been retained but significant Pu was consumed as MOX.

The initial compositions for fast reactor recycle pass 1 for Scenarios 1 and 2 was the nominal recipe for UOX to MOX-Pu to FR-pass 1 for CR=0.50. Its TRU is 82.1% Pu, lower than 83.6% (Scenario 1) because Scenario 1 discards the MA from UOX, higher than 74.1% because of the additional years of decay here (30 years) versus 5+2 years for the original recipe.

The initial composition for Scenario 3 was the nominal recipe for UOX to FR-pass 1 for CR=0.50. Its TRU is 89.8% Pu, higher than Scenario 3 because of the greater decay in Scenario 3.

The 1-group method provides the required TRU/RU ratio, which then fed into the RU portion of the mass flows. When the Pu content in the scenarios was higher than the original recipe, less TRU (more RU) was in the adjusted recipe and vice versa. Table 4-8 shows the output from the first fast reactor recycle pass. These are calculated from the total input mass flow (Table 4-7) times the output recipe mass fractions calculated by MRTAU associated with the input isotopics. Of course, the total TRU flow from the fast reactor (Table 4-8) is less than the TRU flow into the fast reactor (Table 4-7).

Table 4-8. Mass Flows from First Fast Reactor Recycle Pass

	Scenario 1 (discard MA from UOX, use MOX-Pu)	Scenario 2 (keep all MA, use MOX-Pu)	Scenario 3 (keep all MA, no MOX)
RU from fast reactor recycle pass 1	11.91	11.10	17.73
TRU from fast reactor recycle pass 1	6.24	7.14	8.20
Fission products (waste) from recycle pass 1	2.95	2.95	4.29
Total mass (tonnes/year)	21.11	21.18	30.22

4.3.2.3 2nd fast reactor recycle pass adjustment

Table 4-9 shows the mass flow into fast reactor recycle pass 2. The TRU flow is, of course, directly from the output of pass 1. The TRU/RU ratio is set by the 1-group perturbation method. The starting point for perturbation of recipes in all three scenarios is the same as for the first fast reactor recycle pass because there are not second pass recipes in the Transmutation Library. It turned out that the required TRU fraction differed little from the first recycle pass. Note that the RU flow into reactor pass 2 is slightly different than the RU flow from pass 1; this differences send mass to or from RU storage.

Table 4-9. Mass Flow into Second Fast Reactor Recycle Pass

	Scenario 1 (discard MA from UOX, use MOX-Pu)	Scenario 2 (keep all MA, use MOX-Pu)	Scenario 3 (keep all MA, no MOX)
U	11.23	11.18	16.28
TRU from fast reactor recycle pass 1	6.24	7.14	8.20
Total flow into fast reactor recycle pass 2	17.47	18.32	24.48

Table 4-10 shows the mass flow from the second fast reactor recycle pass, produced by multiplying the output mass fractions from MRTAU calculations times the mass into the reactors. Comparison with Table 4-9 shows that there is net reduction in the TRU flow.

Table 4-10. Mass Flows from Second Fast Reactor Recycle Pass

	Scenario 1 (discard MA from UOX, use MOX-Pu)	Scenario 2 (keep all MA, use MOX-Pu)	Scenario 3 (keep all MA, no MOX)
RU from fast reactor recycle pass 2	9.93	9.95	14.48
TRU from fast reactor recycle pass 2	5.10	5.83	6.52
Fission products (waste) from recycle pass 2	2.44	2.55	3.48
Total mass (tonnes/year)	17.47	18.32	24.48

4.3.2.4 Equilibrium fast reactor recycle pass adjustment

The TRU isotopic mix from the second fast reactor recycle pass was put into the 1-group perturbation method with the "initial recipe" being the equilibrium analogs of the startup recycle cases used earlier. Table 4-11 shows how the TRU fraction in fresh fuel evolved in the three scenarios.

Table 4-11. Evolution of TRU Fraction in Fast Reactor Fuel for MA Scenarios

	Scenario 1 (discard MA from UOX, use MOX-Pu)	Scenario 2 (keep all MA, use MOX-Pu)	Scenario 3 (keep all MA, no MOX)
Initial recipe for 1st recycle pass from Transmutation Library	0.359	0.359	0.294
Fast reactor recycle pass 1, calculated here	0.364	0.413	0.342
Fast reactor recycle pass 2, calculated here	0.357	0.390	0.335
Fast reactor equilibrium recycle, calculated here	0.353	0.372	0.341
Initial recipe for equilibrium recycle pass from Transmutation Library	0.359	0.359	0.333

In Scenario 1, there is little adjustment from the 'initial recipes" to the adjusted ones used in this analysis and little evolution from 1st to equilibrium recycle. Basically, the higher aging of the feed into fast reactors (lower fuel value), relative to the UOX-MOX-FR recipe in the Transmutation Library and the discard of minor actinides (higher fuel value per mass) compensate.

Scenario 2 requires more adjustment from the "initial recipes", all of the adjusted recipes require significantly more TRU than the initial recipes because of the higher aging of the feed into the fast reactors. Unlike scenario 2, there is no compensation from discarding MA isotopes. The adjustment relative to the initial recipes decreases from the first to equilibrium recycle as the "coupling" to the initial feed decreases.

Scenario 3 also requires more adjustment from the "initial recipes," and again all of the adjusted recipes require more TRU than the initial recipes.

Table 4-12 show the mass flows for the fast reactor equilibrium recycle. The input and output compositions are determined as for the scenario steps above. The effective total mass flow per recycle pass is given by the TRU flow from the second recycle pass divided by the input TRU mass fraction, e.g. for Scenario 1, the TRU flow from the second recycle pass is 5.10 tonnes/year divided by a TRU mass fraction of 0.359 gives a mass flow of 14.45 tonnes/year. The mass flow times the net mass fraction (input-output) gives us the mass flow change per recycle pass. That result is divided into the TRU mass flow from the second recycle pass to estimate the effective number of recycle passes at the equilibrium composition, e.g., 5.10 tonnes-TRU divided by 0.913 tonnes-TRU/recycle pass gives 5.591 recycle passes.

Table 4-12. Mass Flows for Equilibrium Recycle

	Scenario 1 (discard MA from UOX, use MOX-Pu)	Scenario 2 (keep all MA, use MOX-Pu)	Scenario 3 (keep all MA, no MOX)
	0.647	0.628	0.659
Input composition (U/TRU), sum = 1.00	0.353	0.372	0.341
Mass flow for each recycle pass, tonnes/year	14.45	15.67	19.09
	0.571	0.557	0.607
	0.290	0.304	0.250
Output composition (U/TRU/FP), sum = 1.000	0.139	0.139	0.143
	-0.076	-0.071	-0.051
	-0.063	-0.068	-0.092
Net change each pass (U/TRU/FP), sum = 0.000	0.139	0.139	0.143
Net change each pass, TRU consumption	0.913	1.064	1.754
Effective number of recycles	5.591	5.481	3.717
	-6.126	-6.104	-3.635
Net mass flow from all recycle passes (U/TRU/FP), tonnes/year	-5.103	-5.829	-6.519
	11.229	11.933	10.154

4.3.3 Results

Table 4-13 shows that recycling the 1.07 tonnes/year of minor actinides from UOX separation saves 16.7 tonnes-UOX/year. That much enriched UOX contains 0.7 tonnes-fissile, so recycling 1.07 tonnes-MA/year saves 0.7 tonnes-fissile-U-235/year. Scenario 3 requires more uranium resources than either of the MOX scenarios. All scenarios have substantial uranium improvement versus once through.

Table 4-13. UOX-51 Savings from Minor Actinide Recycle

	Scenario 1 (discard MA from UOX, use MOX-Pu)	Scenario 2 (keep all MA, use MOX-Pu)	Scenario 3 (keep all MA, no MOX)
Amount of UOX-51 required if all electricity were produced by once through (tonnes-UOX/year)	1226	1243	1163
Tonnes of UOX-51 saved versus once through	426	443	373
Delta tonnes-UOX-51 saved versus Scenario 1, i.e., the value of recycling 1.07 tonnes-MA/year		16.7	-62.7
Uranium improvement factor relative to once through	1.53	1.55	1.45

Table 4-14 shows the electricity produced in each step of the scenarios; the data are also graphed in Figure 4-2. Remember that the scenarios are defined so that each fast reactor recycle would occur at the same point in time so it is appropriate to graph them with each analogous step in each scenario occurring at the same time. The MOX scenarios get more energy earlier than the non-MOX Scenario 3, Scenario 2 is 10% higher than Scenario 3 after the MOX step. In the sense of time value of money, that is an advantage. That advantage persists but declines to 5-6% through the equilibrium recycle, i.e., at all points in time, the MOX cases have produced more electricity than the non-MOX cases.

Table 4-14. Electricity Produced in Minor Actinide Scenarios

	Scenario 1 (discard MA from UOX, use MOX-Pu)	Scenario 2 (keep all MA, use MOX-Pu)	Scenario 3 (keep all MA, no MOX)
LWR UOX (GWe-FPY/year)	38.0	38.0	38.0
LWR MOX (GWe-FPY/year)	4.4	4.4	*No MOX*
FR recycle 1 (GWe-FPY/year)	2.8	2.8	4.1
FR recycle 2 (GWe-FPY/year)	2.3	2.4	3.4
FR equilibrium recycle (GWe-FPY/year)	10.7	11.4	9.7
Total electricity produced	58.2	59.0	55.2

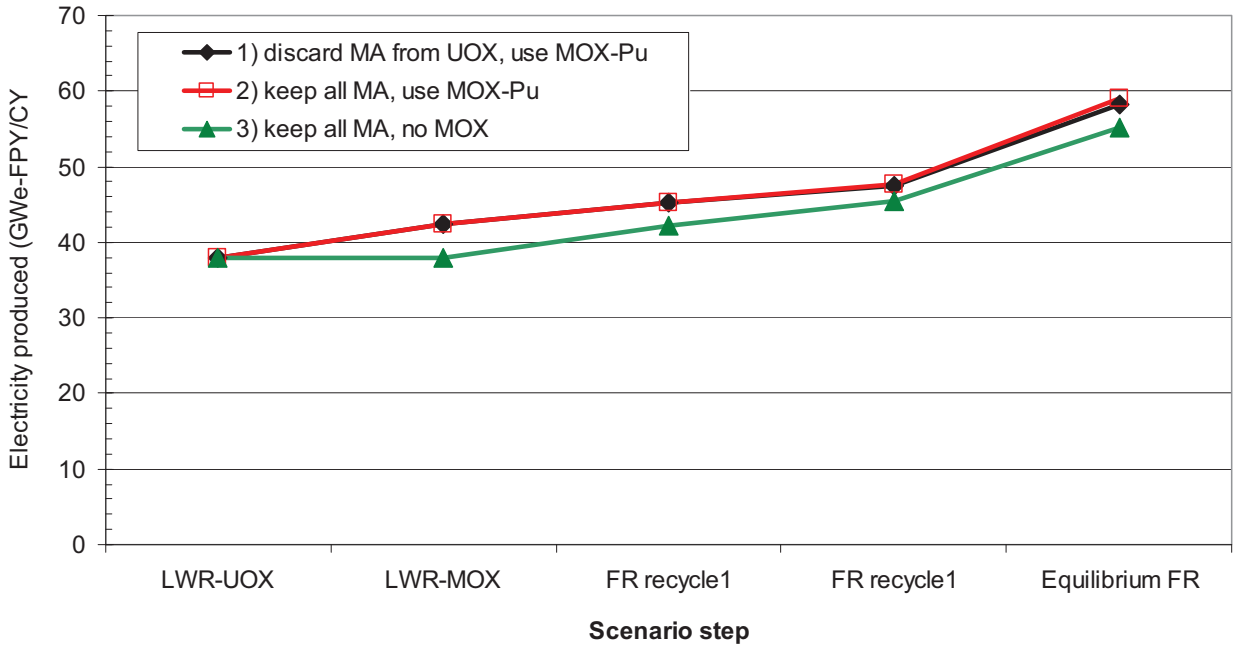

Figure 4-2. Electricity produced in minor actinide scenarios as function of scenario step

Figure 4-3 shows the distribution of electricity produced from LWR-UOX, LWR-MOX, and FR. As in traditional static analyses, use of MOX slightly reduces the fraction of FR contributing to total electricity production.

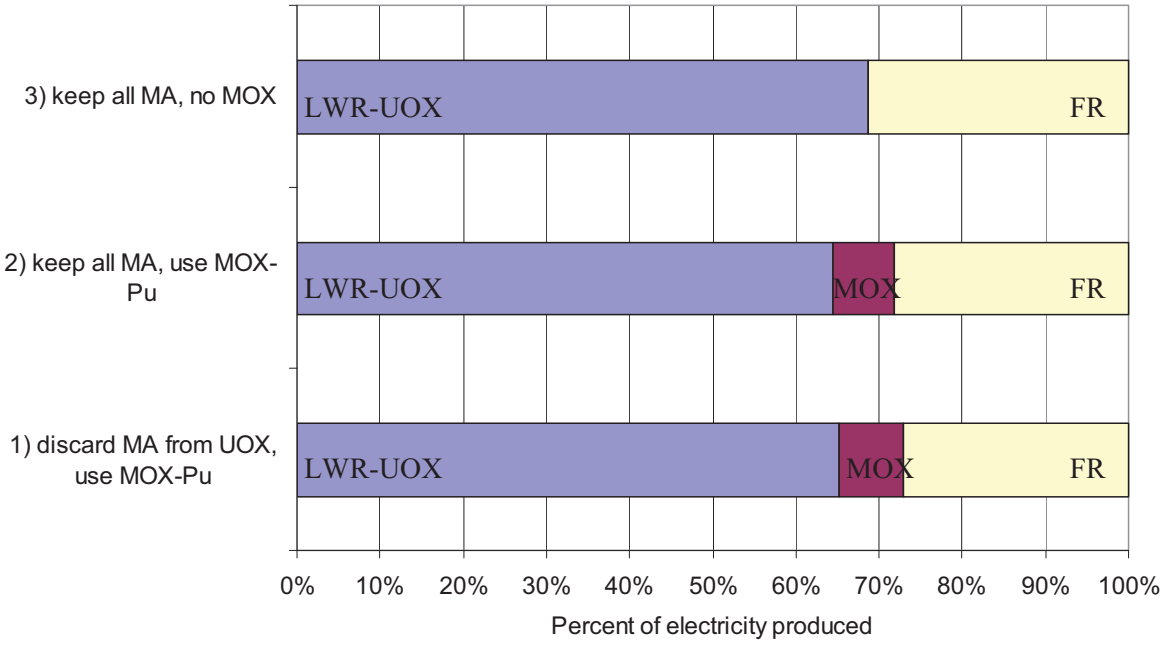

Figure 4-3. Fraction of electricity produced by LWR-UOX, LWR-MOX, and fast reactors in minor actinide scenarios

Table 4-15 provides the uranium balance for the scenarios. Table 4-16 shows the waste production. If one adds the total RU into storage from Table 4-15 plus the total waste from Table 4-16 for each scenario, the result is 800 tonnes/year as it should be. In all scenarios, the waste is 1.09 tonnes-fission-products/GWe-FPY. Addition of the MA from UOX separation in Scenario 1 raises its waste production to 1.11 tonnes-FP-MA/GWe-FPY.

Table 4-15. Uranium Balance in Minor Actinide Scenarios

	Scenario 1 (discard MA from UOX)	Scenario 2 (keep all MA, use MOX-Pu)	Scenario 3 (keep all MA, no MOX)
RU into storage from UOX separation (tonnes-RU/year)	661.71	661.71	727.66
RU into storage from MOX separation(tonnes-RU/year)	69.13	70.12	0.00
RU from storage to make FR-pass-1 fuel (tonnes-RU/year)	Zero (accounted for in the mass balance of UOX and MOX separation		
RU into storage after making FR-pass-2 fuel (tonnes-RU/year)	0.68	-0.09	1.46
RU into storage after making FR-pass-EQ fuel (tonnes-RU/year)	3.80	3.84	10.84
Total RU into storage (tonnes-RU/year)	735.32	735.59	739.97

Table 4-16. Waste Produced in Minor Actinide Scenarios

	Scenario 1 (discard MA from UOX)	Scenario 2 (keep all MA, use MOX-Pu)	Scenario 3 (keep all MA, no MOX)
Waste from UOX separation (tonnes-iHM/year)	43.18	42.11	42.11
Waste from MOX separation(tonnes-iHM/year)	4.87	4.87	0.00
Waste from FR recycle 1 separation (tonnes-iHM/year)	2.95	2.95	4.29
Waste from FR recycle 2 separation (tonnes-iHM/year)	2.44	2.55	3.48
Waste from FR recycle 2 separation (tonnes-iHM/year)	11.23	11.93	10.15
Total waste (tonnes-iHM/year) - all fission products except for 1.07 tonnes-MA/year from UOX separation in Scenario 1.	64.68	64.41	60.03

Table 4-17 shows the separation flow. The MOX scenarios produce more electricity but they also require more flow through separations. The separation flow per electricity produced is 17.4, 17.3, 16.8 tonnes-iHM/GWe-FPY for the three scenarios. Scenarios 1 and 2 (with MOX) require more separation flow per electricity because the fuel burnup is lower, 50-51 for the LWR fuels and 127-132 for the FR fuels in this study. So, the MOX scenarios require 3-4 more separation flow per unit of electricity produced. Note that the hypothetical impurity limits were lowered by the Fuels Campaign during the course of this study so that the values in Table 4-17 are overestimates compared with their current limits.

Table 4-17. Separation Flow in Minor Actinide Scenarios

	Scenario 1 (discard MA from UOX)	Scenario 2 (keep all MA, use MOX-Pu)	Scenario 3 (keep all MA, no MOX)
UOX separation (tonnes-iHM/year)	800	800	800
MOX separation(tonnes-iHM/year)	95	95	0
FR recycle 1 separation (tonnes-iHM/year)	21	21	30
FR recycle 2 separation (tonnes-iHM/year)	17	18	24
FR recycle 2 separation (tonnes-iHM/year)	81	86	71
Total (tonnes-iHM/year)	1014	1021	926

4.3.4 Discussion

In support of the Minor Actinide study, the fuel value of minor actinide recovery from UOX separation was assessed via three scenarios: 1) discard MA from UOX, use MOX-Pu, 2) keep all MA, use MOX-Pu, 3) keep all MA, no MOX. Each scenario is taken through to equilibrium fast reactor recycle until all transuranics are consumed, except for the discard of MA from UOX separation in Scenario 1. Recycling 1.07 tonnes of MA per year saves 16.7 tonnes-UOX/year or 0.7 tonnes-U-235/year. The MOX scenarios produce more 5-7% more electricity and the advantage is front loaded in time because the MOX recycle starts before the FR recycle. However, the higher FR fuel burnup means that the MOX scenarios require 3-4% more separation flow per electricity produced. The FR disadvantage arises because it is operating at a transuranic conversion ratio of 0.5, whereas MOX is 0.70-0.75. Thus, in this instance the UOX-MOX-FR scenarios 1 and 2 have the fast reactor benefit of consuming all the transuranics plus slightly higher transuranic conversion ratio due to one MOX recycle. Thus, the MOX-FR comparison is specific to these cases and would disappear and reverse at higher fast reactor conversion ratios.

The fuel value improvement factor is the ratio of total electricity to electricity from UOX, and indicates how much additional electricity was generated from the recycle passes (45% to 55%, depending on the scenario). The UOX equivalent values show the amount of UOX which would be needed to generate the same electricity, indicating the amount saved in the MOX and FR recycle passes.

Several factors drive the differences observed in the fuel value calculations. The most obvious difference is the electricity from MOX in the first two scenarios. The MOX pass consumes some of the TRU such that less electricity is produced in the first FR pass versus Scenario 3. However, the MOX pass also generates some additional TRU such that when all the recycle electricity is summed Scenario 3 has the lowest fuel value improvement factor. This result is primarily due to the CR used for the fast reactor, which, at 0.5, is lower than the estimated CR of LWR-MOX (~0.7-0.75). Basically, more net TRU consumption occurs in the first recycle pass for Scenario 3 and with all subsequent passes for all scenarios at the same 0.5 CR, Scenario 3 never can catch up.

A second important difference is the TRU that goes into FR fuel for the first two scenarios has been significantly depleted in the "high octane" isotopes of Pu-239 and Pu-241, resulting in higher enrichment requirements for the FR fuel. These isotopes constitute 50% of the Pu for these scenarios versus 61% for Scenario 3. The higher ratio for Scenario 3 results in lower TRU enrichments and higher initial fuel yield (see Table 3-1), but also more of the TRU being consumed each pass.

The difference between the first two scenarios is not apparent in the initial FR passes because Scenario 2 has more TRU mass, but the isotopes are of average lower fuel value and therefore the enrichment is higher. The net result is similar fuel yield in the initial FR passes. However, as the isotopic mix moves toward equilibrium the compositional difference (and the enrichment differences) between the two scenarios decrease. During the equilibrium cycles, the additional mass from the retained MA in Scenario 2 result in larger fuel yields (shown by the average electricity produced per pass), giving Scenario 2 a slight advantage in overall fuel value.

4.4 Application to Negative Value of Impurities

We examined the impact of impurities using method 3 and by simply multiplying cross sections times the impurity level. The former accounts for neutron absorption and fuel atom displacement; the latter accounts for only neutron absorption. Data Tables are given in Appendix B.

Hoffman notes there are three ways to compensate for the impact of impurities [6].

1. Reduce fuel residence time,
2. Increase the number of fuel atoms, i.e., increase volume or density of fuel, and
3. Increase TRU enrichment and thus slightly decrease the TRU conversion ratio.

4.4.1 Using Method 3

4.4.1.1 Fast reactors

For the metal-fuel fast reactor case, Hoffman considered several ways to bound the impact of hypothetical impurities as estimated using method 3 (differential reactivity).

He found the most relevant approach would be to account for impurities by increasing the heavy metal fuel mass (kg/cycle) by 0.87%.

Alternative methods would have higher impact. These fast reactor cases have a low change in reactivity with burnup and higher end of cycle burnup than LWRs. So, the same impurity level would have more impact on cycle length if that were the chosen method of compensating for impurities. Hoffman

estimated the bounding value at about 14% reduction in cycle length, hence average discharge burnup. Hoffman's results suggest that increased fuel mass (modification of the fuel design) would be the most optimum approach of compensating for the impurities, followed by increased enrichment, and cycle length reduction would be excessively penalizing.

4.4.1.2 LWRs

The same differential reactivity assessment was performed by Hoffman for MOX-Pu. As noted in previous Table 4-4, the reactivity penalty in units of percent milli-rho per microgram of impurity per gram of fuel mass is about the same as in the fast reactor cases.

To compensate for the impurities by increasing the Pu loading would require 4% increase in Pu, compared with 0.87% increasing in heavy metal for the metal-fuel fast reactor.

To compensate by cycle length reduction, the impact would be about 8.6% decrease in burnup, less than the corresponding impact in the CR=0.50 fast reactor cases. Hoffman's results suggest that increased enrichment is preferred to reductions in cycle length reduction. Modification of the fuel geometry was not considered, even though this is probably the most efficient method of compensation in the fast reactor.

4.4.2 Looking Deeper into Impurities

We looked deeper into the impurities using a combination of fission product yield, cross sections, and differential reactivity coefficients for several reasons. First, is the production of fission products sufficient to require their removal to meet the current Fuel Campaign limits? If so, how much of the fission products must be removed in order to meet the limits for the next batch of fresh fuel? What elements dominate neutron capture? What elements dominate differential reactivity? Does it matter if natural sources or fission product source dominate elements?

Figure 4-4 and Figure 4-5 shows the fraction of total fission products in the output fuel from metal and oxide fueled fast reactors at transuranic conversion ratio of 0.50 and LWR with MOX-Pu fuel. (One plot is log, the other plot is linear.) The two fast reactor curves are almost identical, as they would be expected to be. The MOX curve varies slightly from the fast reactor curves because the fission yield curves of various fissionable isotopes varies slightly. To the degree that the curves diverge, it is important to assess the fission product mixes of different fuel/reactor combinations instead of simply using a generic set of fission products.

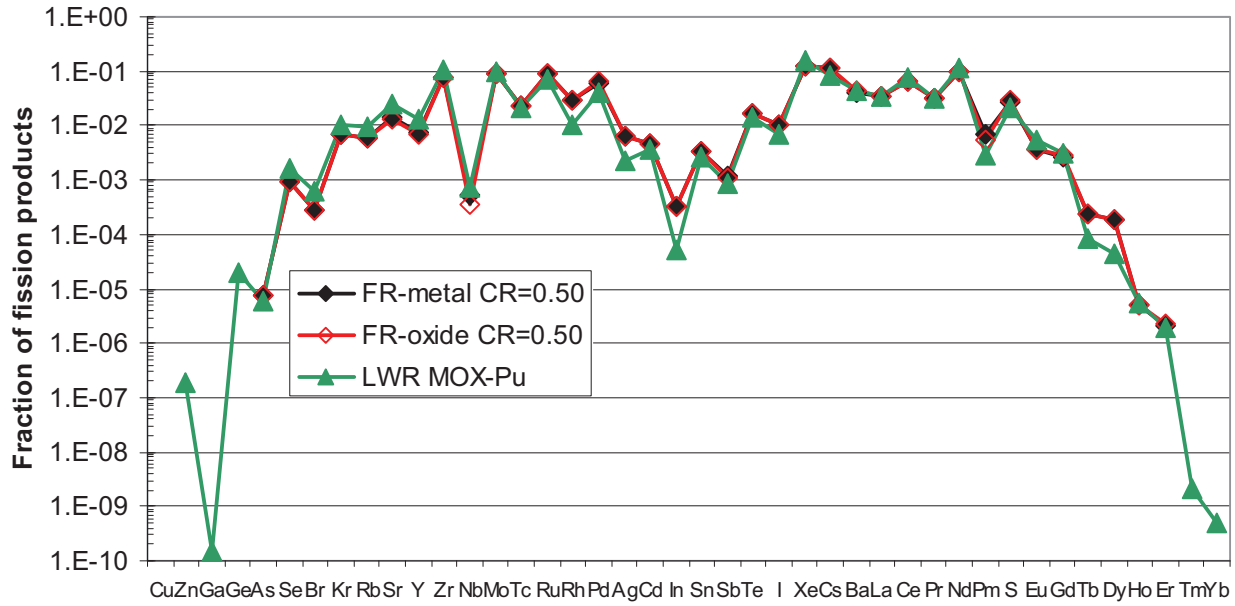

Figure 4-4. Fraction of fission products by chemical element (log plot)

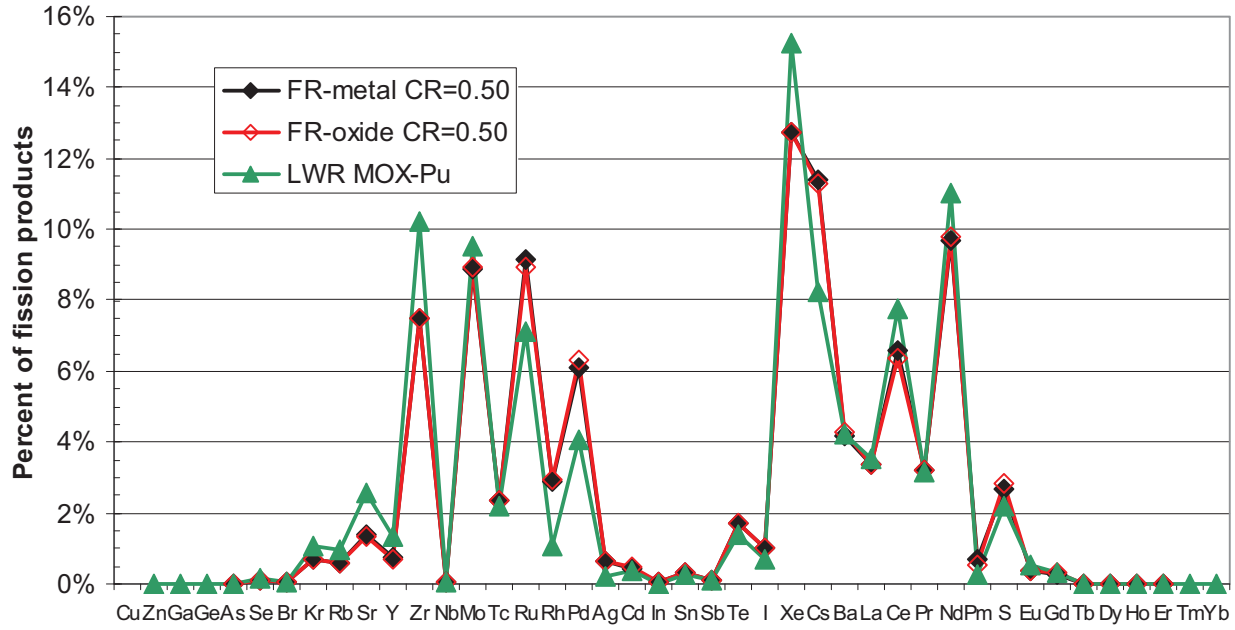

Figure 4-5. Fraction of fission products by chemical element (linear plot)

The Fuels Campaign has evolving limits on many, but not all, of the elements from H to Th. Many of their limits are for a group of elements, e.g., a limit on the total lanthanides. To perform an exploratory assessment, we made three modifications to their current limits. First, limits for a group of elements were allocated equally among the elements in the group. Second, hypothetical values were used for unlimited elements by analogy to elements that were limited. Third, we used the oxide limits for MOX-Pu to perform an exploratory assessment of that case as well. Finally, the units of the limits had to be changed. The Fuels Campaign specifies elemental limits on the incoming transuranic feedstock, as they make the

assumption that incoming uranium is far more pure. Reactor physics calculations use the density of materials in fuel (ppm of isotope in total heavy metal). Based on the fuel compositions for the three cases, we used enrichments of 31% TRU (FR metal), 35% (FR oxide), and 10% (MOX-Pu). This procedure gave us a set of hypothetical limits for all elements except noble gases.

With one final assumption, it is then possible to examine to what degree fission products have to be removed from recycled material to meet the impurity limits of the next recycle. The assumption is that all the impurities not removed re-appear in the new fuel without net dilution or concentration. This means that if an impurity is X percent of discharged fuel, and is not chemically removed, it is X percent of the new fuel. This would appear to be a good assumption for the fast reactor fuels that are repeatedly recycled; the U vs. TRU composition changes little each recycle. This assumption is probably wrong by an order of magnitude for MOX-Pu if impurities tend to be in Pu versus U, because there is about an order of magnitude concentration increase from used UOX to MOX-Pu. That is, used UOX is about 1% Pu, but fresh MOX-Pu is about 10% Pu. So, if impurities flow with Pu rather than U, then there is a factor of 10 increase in the impurity level in going from UOX to MOX. For example, consider an impurity at X ppm in used UOX. Its concentration in the Pu stream is 100X ppm (=X/0.01). The Pu is diluted 10:1 by uranium so that its concentration in the new fuel is 10X ppm. For simplicity, we ignore this issue and simply assume no net concentration or dilution.

Figure 4-6 shows the result of dividing the assumed tolerable chemical limit by the concentration produced via fission products. (There is no calculated value for noble gases Kr and Xe.) A number greater than one means that all the fission products could pass into new fuel without any separation, assuming there were no other sources of those elements. A number less than one means that only that fraction of fission products can be tolerated in the new fuel. That is, 1 minus that fraction is the minimum tolerable separation fraction of that element.

As an example, consider Europium (Eu). It is 469 ppm in used FR-metal fuel from fission. The calculation path for the limit in the proper units starts with the current specification of 2500 ppm for all the lanthanides in the TRU feedstream. There are 15 lanthanide elements (including yttrium), so the limit assigned to Eu is 2500/15 = 167 ppm. This fuel is 31% TRU, so dilution by presumably pure uranium brings Eu down to 52 ppm-Eu in fuel. Since 469 ppm-Eu is produced and only 52 ppm-Eu is tolerated, the tolerable fraction of fission-source Eu in recycled material is 0.11, i.e., at least 89% of the Eu must be removed. Using this procedure, the required removal fraction varies for the lanthanides varies from 99.6% (Nd) to zero (Tb, Dy, Ho, Er). A rebalancing of the assumed allocation of the 2500 ppm-lanthanide limit would tell us what average lanthanide removal fraction would be required. A crude estimate is 93%, naturally less restrictive than the worst case (Nd) and more than Eu.

Of course, this procedure only addresses one recycle. Lanthanide isotopes that absorb a neutron during re-irradiation only turn into another lanthanide element, so irradiation does not change the numbers. So, an equilibrium will be established during repeated recycle with the net production of lanthanides by fission balanced by net removal of lanthanides during recycling.

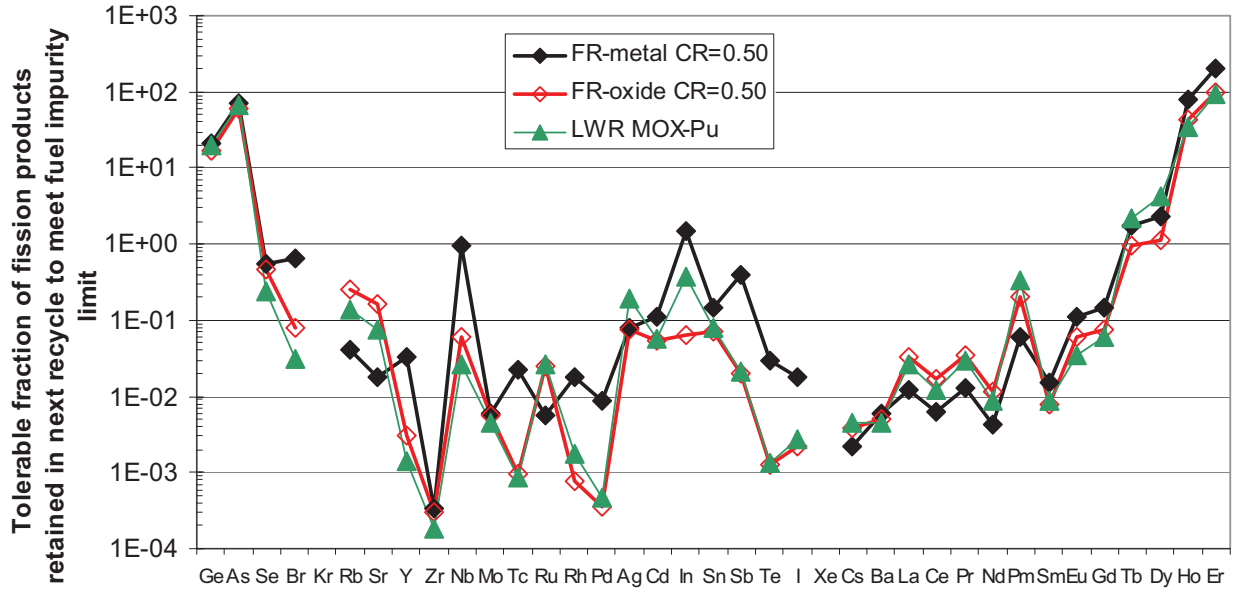

Figure 4-6. Fraction of fission products that can be kept in the next recycle, assuming initially pure material before the preceding irradiation, probably overestimates MOX-Pu tolerance by an order of magnitude

We now turn to neutron absorption. Figure 4-7 shows the contribution of different sets of elements to the total neutron absorption (mass fraction times neutron capture cross section) and to the total differential reactivity - assuming each element's isotopes match natural abundances. The lanthanides dominate parasitic neutron capture, followed by the transition metals Nb to Te, and the transition metals Hf to Pb. Note that the Fuels Campaign does not generally have limits for the Hf-Pb set of transition metals, yet they do contribute significantly to total neutron capture, with the assumed values used here.

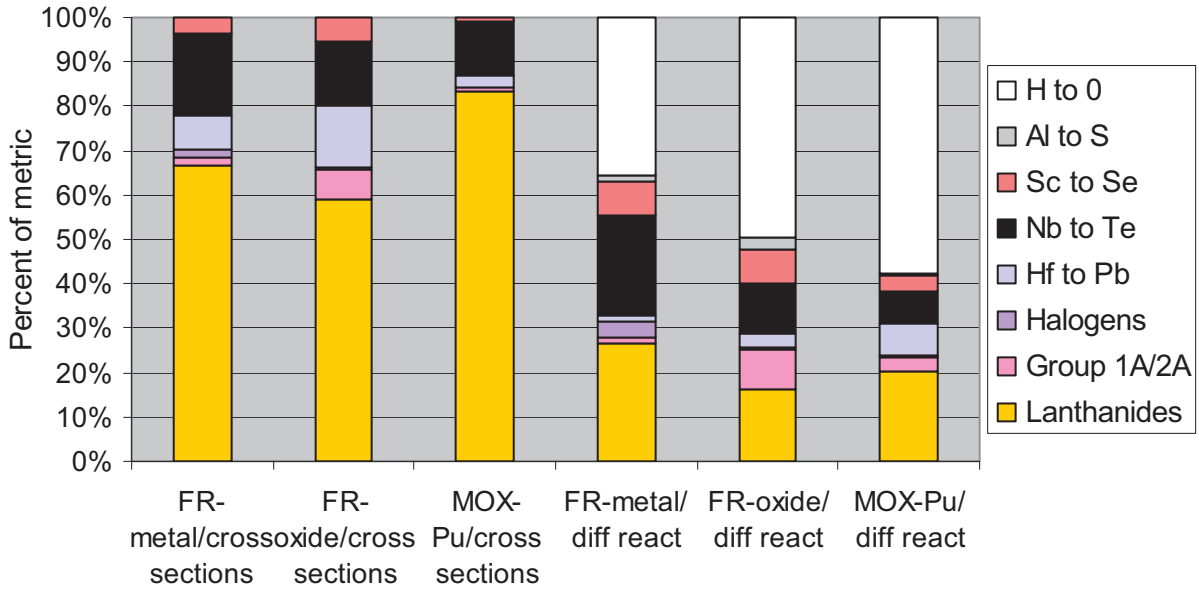

Figure 4-7. Percent weighted cross sections or percent of differential reactivity, assuming all elements have natural isotopic abundances

The relative contribution to differential reactivity is fundamentally different. As Hoffman points out,[6] the light elements (H to O here) dominate differential reactivity. Few of these have large neutron capture cross sections; the primary impact is fuel atom displacement. Depending on fuel and reactor design, that may or may not be a significant issue. The next important group is the lanthanides, followed by the Nb to Te transition metals.

The previous analysis assumed natural isotopic abundances for all elements. We repeated the analysis using for each element, whichever is worse - fission or natural. Figure 4-8 shows the result in the same format as Figure 4-7. The relative importance of the lanthanides and Nb to Te transition metals, which are all produced as fission products, increases. Recall that the total mass of these elements has not increased; each element is kept to the same limit. However, the isotopic mixes of the elements have changed. The neutron capture has increased by factors of 1.75 (FR-metal), 199 (FR-oxide), and 1.50 (MOX-Pu) relative to assuming natural isotopic abundances. The differential reactivity has increased factors of 1.62 (FR-metal), 1.50 (FR-oxide), and 1.56 (MOX-Pu). The transition from natural-worse to fission-worse occurs with the elements Sr, Y, and Zr; that is, below Sr natural abundance is worse; above Zr fission abundance is worse. For those three elements, it depends on which of the reactor/fuel cases and which metric (neutron capture or differential reactivity). At the other end of the fission product regime, the transition from fission-worse to natural-worse occurs with the elements Sm, Eu, Gd, Tb, and Dy. An extreme case of natural abundance having higher neutron capture is Gd. For MOX-Pu, natural Gd has about 100 times higher neutron capture than fission product Gd. Gd-155, Gd-157, Gd-161 each have thermal neutron capture cross sections over 1000 barns; their natural isotopic abundances are 14.8%, 15.65%, and 21.88%. The fraction of these isotopes to total Gd in discharged MOX-Pu is 0.13%, 0.10%, and <0.01%, two orders of magnitude lower than natural Gd. Their capture cross sections are so high they "burn out" during irradiation.

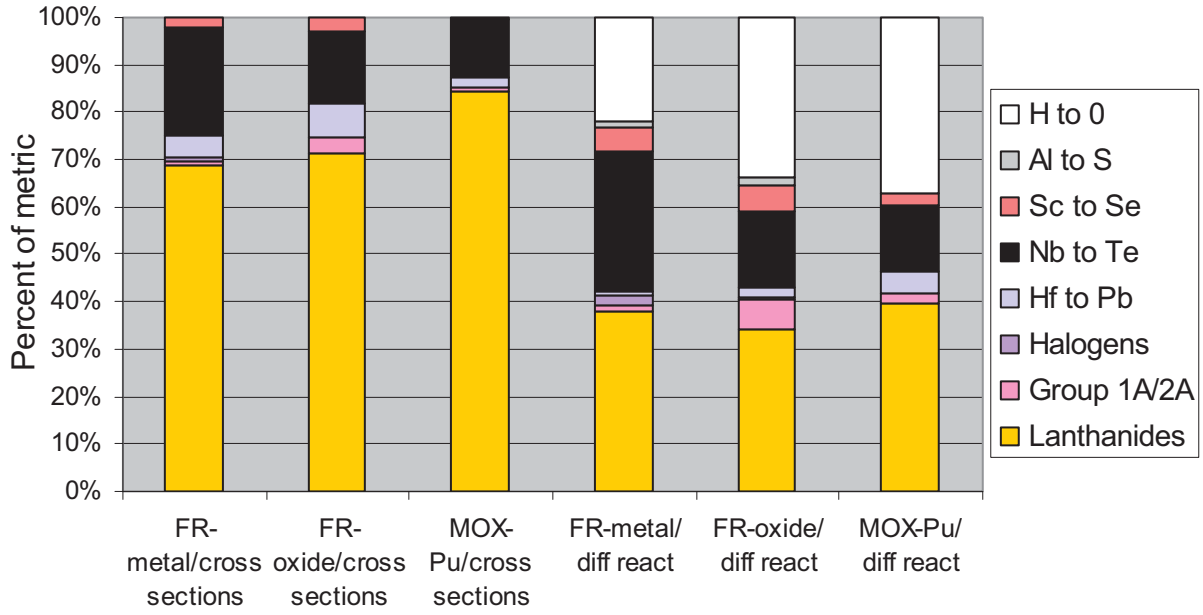

Figure 4-8. Percent weighted cross sections or percent of differential reactivity, assuming the worse of natural or fission product isotopic abundances

5. Reactor Void Reactivity and Isotope Evolution

5.1 Multi-Recycle MOX-UE Coolant Void Reactivity

Many options exist for recycling used LWR fuel with the ultimate goal of closing the nuclear fuel cycle. In the fuel cycle depicted in Figure 5-1, enriched uranium is used as feed material to fabricate UOX fuel which is then burned in LWRs. The used fuel is then reprocessed according to one of the five listed reprocessing schemes. The transuranic elements listed in each reprocessing scheme are homogenously combined with additional enriched uranium to produce MOX-UE fuel that is also burned in LWRs. The used MOX-UE fuel is also reprocessed according to the same scheme as the UOX fuel. During each recycle, transuranics and fission products not indicated in the reprocessing scheme are sent to a repository.

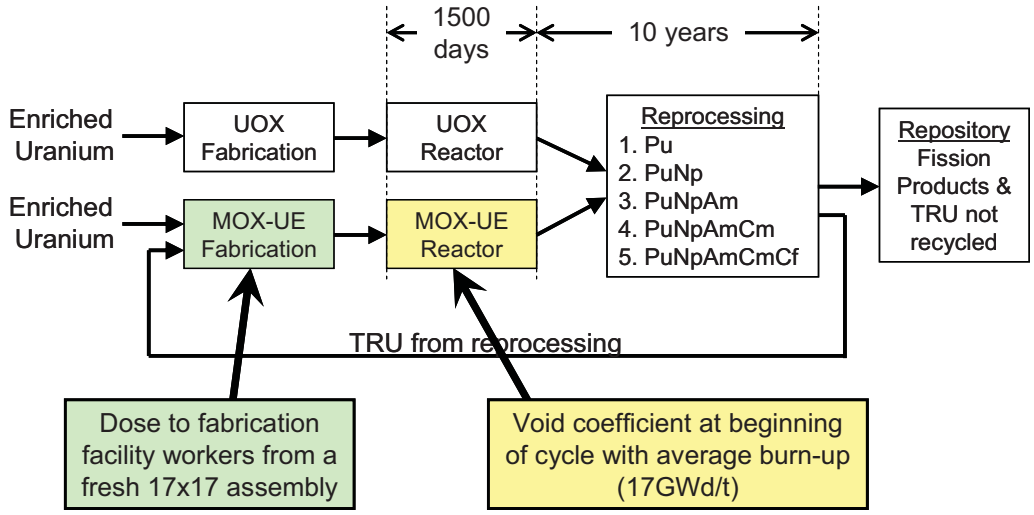

Figure 5-1. Block diagram of conceptualized MOX-UE fuel cycle

The isotopic composition of the new MOX-UE fuel evolves as a function of the fuel burnup, the cooling time prior to reprocessing, delay between reprocessing and beginning of irradiation, and the number times the material is recycled. The calculations in this project assumed a burnup of 51 GW-day/tonne, a cooling time of ten years, and one year between reprocessing and beginning of irradiation. As an example,

Figure 5-2 shows the isotopic evolution of the primary isotopes in the Pu-only reprocessing scheme for the first, second, third, fourth, fifth, tenth, and sixtieth recycling [1]. The isotopic evolution in the fresh fuel impacts the radiation dose to workers at the fuel fabrication facility and also affects the void coefficient of reactivity of reactors loaded with this fuel. In this section, the five actinide partitioning schemes were analyzed at the first, tenth, and sixtieth recycle to evaluate the impact of the isotopic evolution on the void coefficient of reactivity for LWRs loaded with this fuel[m].

[m] In the next chapter, the computer models of these MOX-UE assemblies are reused in a calculation of absorbed dose to humans at varying distance from the fuel.

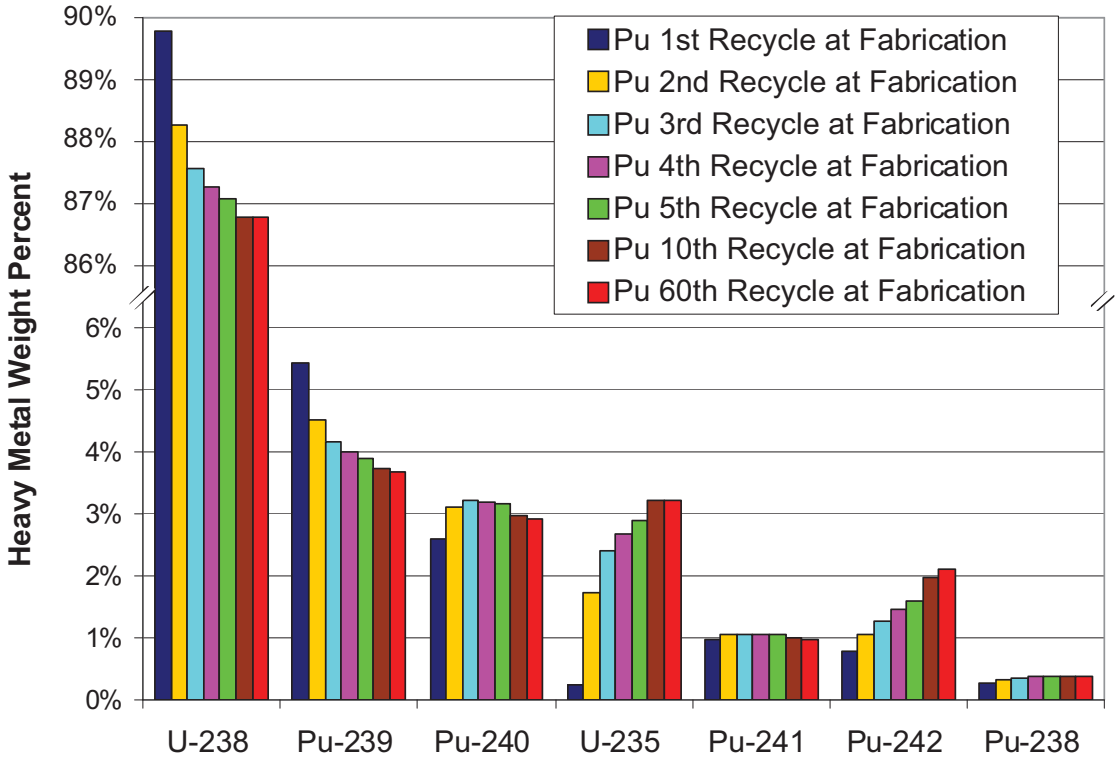

Figure 5-2. Isotopic evolution in the Pu-only actinide partitioning scenario

5.1.1 Method of Calculation

Calculations were performed to determine void coefficient of reactivity of reactors fueled with MOX-UE fuel reprocessed according to the five schemes considered during this internship. Four specific cases were analyzed: Pu-only 1st recycle, Pu-only 10th recycle, PuNpAm 1st recycle and PuNpAm 10th recycle. Time constraints did not permit additional cases to be analyzed. In all of these cases the void coefficients were determined for an average core burnup at beginning of cycle. At the beginning of each cycle one-third of the core would contain fresh fuel, one-third of the core would contain fuel burned at 500 full power days, and one-third of the core would contain fuel burned to 1000 full power days. Thus, the average burnup at beginning of cycle in this three batch scheme would correspond to an irradiation of 500 days. Therefore, the isotopic composition of fuel burned to 500 full power days was used in the void coefficient calculations. In an effort to model the worst-case scenario, the fission product neutron poisons were removed from the fuel composition. Before the void coefficients could be calculated, the boron concentration at the beginning of cycle had to be determined for each of the four cases.

Several software packages were used during this internship. MCNP5 version 1.51 was used for radiation transport when performing dose and k-inf calculations. MCNP is a general purpose Monte Carlo N–Particle (MCNP) code that can be used for neutron, photon, electron, or coupled neutron/photon/electron transport [31]. MCNP simulates particle transport using the Monte Carlo method in arbitrary geometry, continuous energy, and continuous angle. MCNP is used by this section to calculate the critical eigenvalue of the fuel assembly for the assembly void calculations. OrigenArp from the Scale 6 package was used to determine source terms as inputs for the dose calculations [20,32]. Origen is a multi-purpose depletion/decay code that is often used to calculate radiologic source terms (alpha, gamma, neutron) projections.

A single 17x17 pressurized water reactor (PWR) fuel assembly was modeled in MCNP. A top view of this geometry is shown in Figure 5-3. By applying reflected boundary conditions to this single assembly geometry, the k-inf representative of a complete core, without neutron leakage, is calculated. It was assumed that the fuel pellets had swelled to the inside dimension of the fuel cladding and the fuel density was appropriately decreased to account for this smearing. The helium that normally fills the gap between the fuel and the clad was not included in this model. Important geometry parameters of the MOX-UE MCNP model are given in Table 5-1.

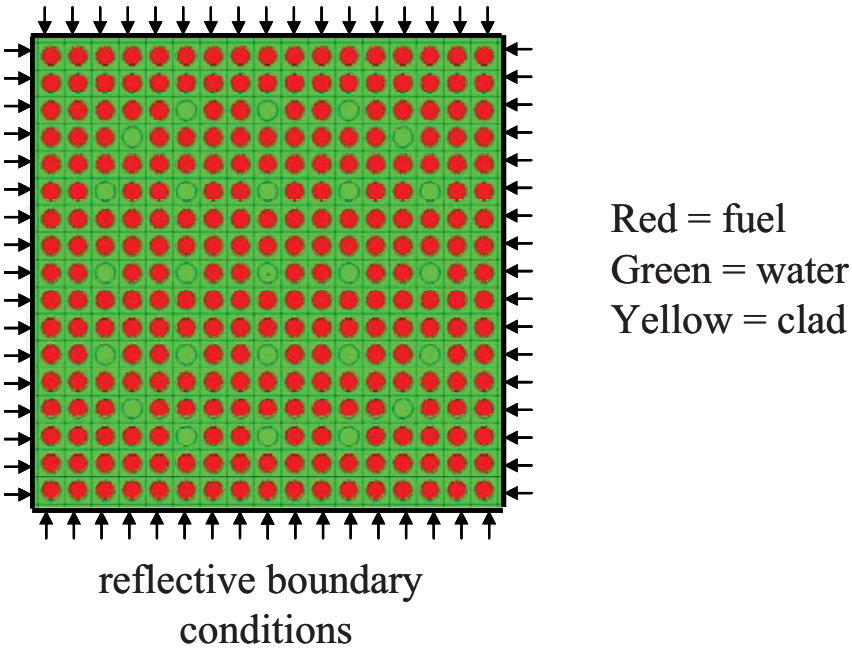

Figure 5-3. Top view of 17x17 PWR MOX-UE assembly with smeared fuel pellets

Table 5-1. MOX-UE MCNP model parameters

Description	Value
Fuel burnup (Full Power Days)	500
Water Pressure (MPa)	15.5
Water Temperature (K)	550
Nominal Water Density (g/cm^3)	0.77
Fuel Temperature (K)	900
Fuel density (smeared) (g/cm^3)	10.0
Clad material	Zircaloy 4
Cladding density (g/cm^3)	6.55
Cladding temperature (K)	600
Assembly Type	17 x 17 PWR
Fuel pins	264
Control rod guide tubes	24
Instrumentation tubes	1
Cladding inner radius (cm)	0.418
Cladding outer radius (cm)	0.475
Pin pitch (cm)	1.26
Active fuel height (cm)	365.76
Control rod guide tube inner radius (cm)	0.438
Control rod guide tube outer radius (cm)	0.485

Binary *ft71f001* data files containing every isotopic composition as a function of burnup generated by and saved from the Youinou TRITON calculations were post-processed using the SCALE5.1 OPUS module [33]. The isotopic composition included the top five hundred isotopes by mass for each case. Of these five hundred isotopes, neutron cross sections evaluated at the appropriate temperature were available for around 238 isotopes, depending on the case. These included isotopes accounted for more than 99.999% of the total isotopes by mass or by number of atoms, again depending on the case. In each of the four cases, the masses of certain isotopes were zeroed and added to other isotopes either to eliminate a neutron poison or to move a short lived isotope with substantial mass without cross section data to the appropriate daughter isotope, if cross section data was available for the daughter. A summary of these changes is shown in Table 5-2. In all other cases where cross section data was not available, the isotopes were not included on the MCNP material card, effectively setting their masses to zero.

Table 5-2. Summary of mass lumping assumptions

Ba-235^{m} mass added to Ba-135
Ba-137^{m} mass added to Ba-137
Kr-83^{m} mass added to Kr-83
Kr-85^{m} mass distributed to Kr-85 (21.4%) and Rb-85 (78.6%)
Cs-134^{m} mass added to Cs-134
Cs-135^{m} mass added to Cs-135
Xe-135 mass added to Cs-135
Xe-135^{m} mass added to Cs-135
I-135 mass added to Cs-135
Te-135 mass added to Cs-135
I-136^{m} mass added to Xe-136
Te-129 mass added to I-129
Te-129^{m} mass added to I-129

5.1.2 Boron Concentration

Boron is used as a soluble poison to control reactivity in PWRs. Before determining the void coefficient of reactivity, the boron concentration at the beginning of cycle had to be determined for each of the four cases. According to the Youinou report, the target k-inf for these calculations was 1.04335 to account for the neutron leakages that would be expected for a full core representative model. The boron concentration was varied over eight steps from a value of 800 PPM (by mass) to a value of 2200 PPM. During these calculations it was estimated that the concentration of naturally enriched boron (20% B-10, 80% B-11) necessary to achieve the desired k-inf for the Pu 1st recycle case was greater than 2500 PPM. According to Youinou, the boron concentration should not be greater than 2500 PPM to avoid crystallization. Because of this, a boron enrichment of 25% B-10 and 75% B-11 was used in all four cases. Using this enrichment and the eight boron concentrations, boron worth curves were generated for each of the four scenarios. The exact boron concentration to achieve the desired 1.04335 k-eff was interpolated from these worth curves (Table 5-3). The boron worth curves for the different scenarios are given in Figure 5-4.

Table 5-3. Estimated Boron Concentration for K-inf = 1.04335

Partitioning Scenario	Boron concentration
Pu-only (1st Recycle)	1877
Pu-only (10th Recycle)	1740
PuNpAm (1st Recycle)	1543
PuNpAm (10th Recycle)	1216

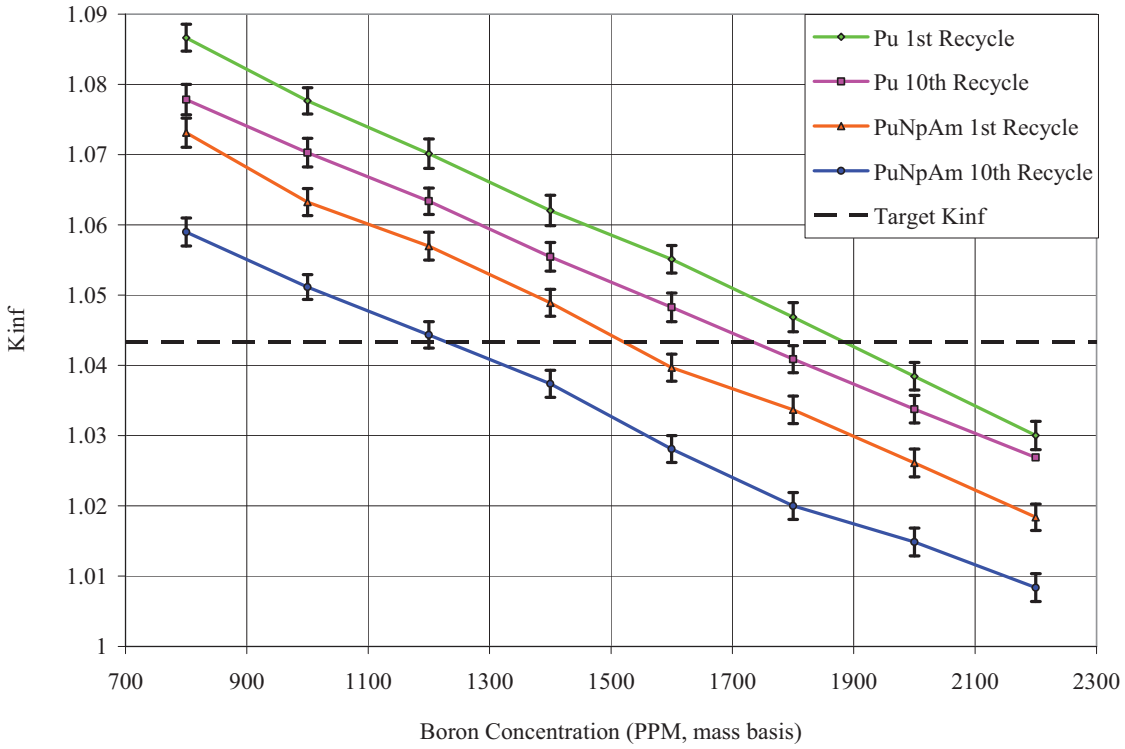

Figure 5-4. K-inf as a function of beginning-of-cycle boron concentration in the water coolant for Pu-only and PuNpAm MOX-UE Fuel (Boron is enriched: 25% B-10, 75% B-11)

5.1.3 Incremental Voiding of the MOX-UE Fuel Assembly

These calculated beginning of cycle boron concentrations were then used in the coolant water isotopic compositions in the coolant density calculations. For each actinide partitioning scenario, the boron concentration in these decks was kept constant and the borated water density was incrementally reduced starting from all-water to completely voided coolant. The nominal water density was 0.76971g/cm3 and the following percentages of the nominal density were used: 100%, 90%, 80%, 70%, 60%, 50%, 40%, 30%, 20%, 10%, 8%, 6% 4%, 2%, 1% and 0%. Figure 5-5 shows the results of these calculations. The k-inf of three of the four cases stays below 1.04, but the PuNpAm 10th recycle case reaches a k-inf of 1.074 as the core is voided. The original recipe for this reprocessing option limited the recycled transuranic content of the fresh fuel to 8%. The PuNpAm 10th recycle result shown in Figure 5-5 indicates that limiting the transuranic content to 8% was not quite conservative enough for this particular recycling scheme.

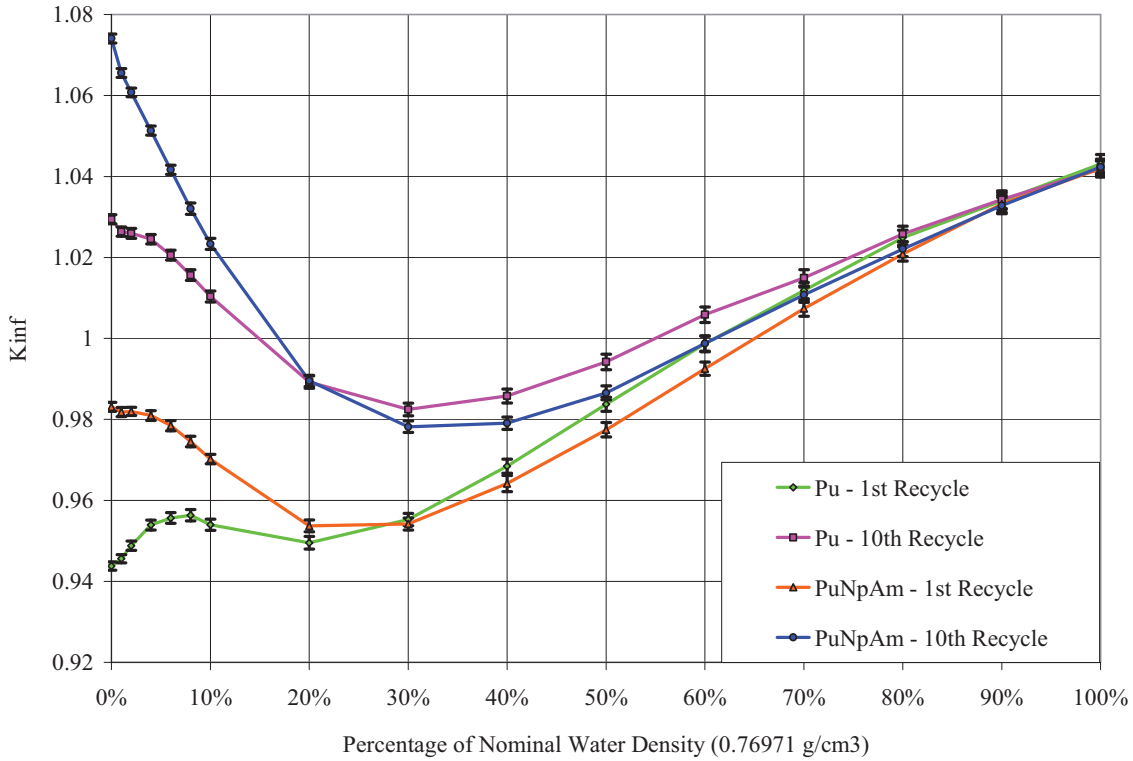

Figure 5-5. K-inf as a function of water density for Pu-only and PuNpAm MOX-UE fuel

5.2 Multi-Recycle SFR Coolant Void Reactivity

An effort was made to investigate the topic of sodium void and resulting reactivity perturbation. This investigation was made to gauge the sensitivity of the SFR void reactivity to the MA concentration in the fuel and isotopic evolution over multiple recycles. This initial investigation and the rudimentary method developed for creating bounding cases is intended for sensitivity of void reactivity. Though robust physics codes are used, this work is not proposed as a replacement for detailed reactor safety analysis.

Most SFR designs have a positive sodium density coefficient. The positive reactivity feedback is a direct consequence of neutron energy spectrum hardening resulting from the loss of the slight neutron down-scattering and capture provided by the sodium coolant. When the spectrum hardens, the lack of down scattering causes the number of neutrons above the fission threshold of fertile isotopes (U-238 and MAs) to increase. An increase in above-threshold fissions and poor parasitic absorption in the fuel causes an increase in the neutron multiplication contribution of these fertile isotopes.

The loss of sodium also influences the amount of neutron leakage from the core which increases as the down-scattering from sodium atoms decreases. The resulting effect of the spectrum hardening on core reactivity is dominated by the spatial dependence of this neutron leakage [34]. This spatial dependence is important for evaluating the void reactivity.

5.2.1 Method of Calculation

Calculations were performed to determine reactivity change with respect to sodium density of a fast burner core with oxide fuel and a nominal conversion ratio of CR=0.75. Core design data for the Advanced Burner Reactor designed by Hoffman et. al., were used as the basis of constructing an MCNP computer modelization of Hoffman's design [4,31]. A general description of geometry parameters used is

given in Table 5-4. For more detailed information on this design the interested reader is referred to Hoffman's report.

Table 5-4. SFR MCNP model parameters

Description	Value
Conversion Ratio	0.75
Fuel Type	Oxide
Inner Core Enrichment (%)	21
Middle Core Enrichment (%)	27
Outer Core Enrichment (%)	32
Fuel pins per assembly	271
Height of core (cm)	137
Height of plenum (cm)	171
Overall pin length (cm)	422
Pin Diameter (cm)	0.8
Pin Pitch to Diameter Ratio	1.1
Fuel Pins per Assembly	271

It should be noted that in Hoffman's work, an elaborate full core 3-dimensional depletion, tracking the depletion of individual batches of fuel with respect to their r-z location within the core. In this work, such a detailed analysis was not as important as the fundamental deliverable was sensitivity in void performances to changes in sodium density globally, locally or uniformly across the core. The sodium densities were performed in a radial-only fashion. No attention was given to axial changes in sodium density. Therefore, it is expected that the axial burnup dependency of the fuel will have a secondary effect on the results of this sensitivity analysis.

The aim of this study was to use recycle-by-recycle isotopic data produced by MRTAU to approximate the average fuel composition of a fast reactor operating with fuel characteristic of an arbitrary N^{th} recycle. In this section the N^{th} recycles chosen for comparison was the 1^{st} and 10^{th} recycles of the oxide SFR (CR=0.75) design by Hoffman. A methodology was devised for the depletion data for the irradiation phase of any given MRTAU recycle pass. This averaging process involved integrating over time the concentration evolution of each isotope, I(t), and then dividing this integrand by the time elapsed over the irradiation. The physical meaning of this new averaged concentration is the equivalent to saying that no change in the isotope occurred during depletion but the integrated area under the averaged flat slope depletion curve is the same as under the actual depletion curve (Figure 5-6).

$$\bar{I} = \frac{A}{t_{EOL} - t_{BOL}} = \frac{\int_{t_{BOL}}^{t_{EOL}} I(t)dt}{t_{EOL} - t_{BOL}} \qquad \text{Eqn 5-1}$$

This averaging method was done merely to approximate the average fuel composition operating in an arbitrary recycling in the future assuming the core was fully fueled by material from that particular N^{th} recycle. Since this method is completely numerical, it does not respect the fuel reactivity at any specified point in an actual depletion. However, in order to compare the sodium void effects in an unbiased manner, it was felt that it would be more accurate to start with the same approximate critical spectrum and flux distribution in the core. Therefore, the concentration of fission product isotopes was arbitrarily adjusted to bring the core reactivity to near k-eff=1. An approximate 48 fission product isotope vector representing the most reactive isotopes in their equilibrium concentrations during irradiation was used to specify the give the fission product isotopic concentration in the fuel. Note that for this work, k-eff=1 is

desired instead of k-eff=1.04 because the physics model represents the whole core and not a single assembly as in the MOX-UE study in the above section.

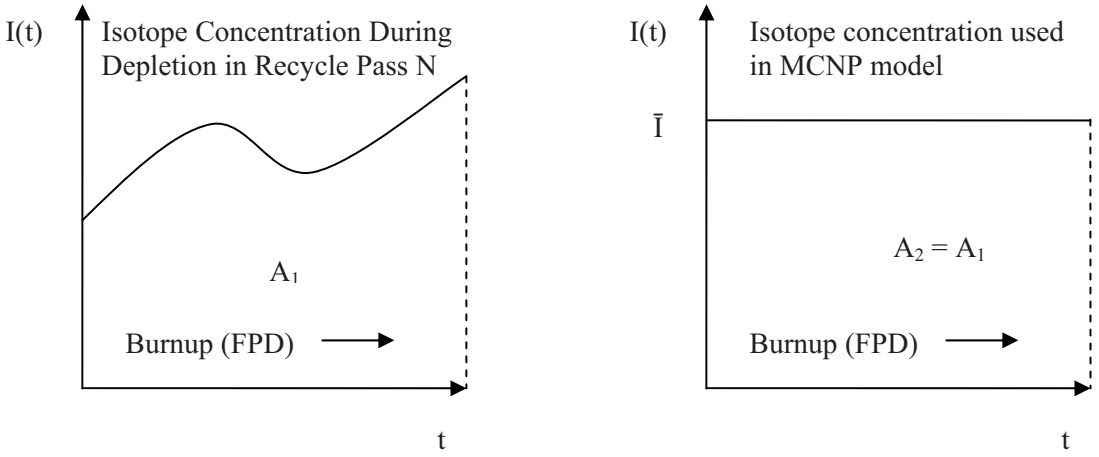

Figure 5-6. Representation of averaging process for converting MRTAU depletion data into time independent concentrations for use in the MCNP SFR model

MCNP5 version 1.51 was used for performing k-eff calculations in this section. Figure 5-7 shows the initial full core MCNP model with no fuel pin geometries defined. Figure 5-8 shows the MCNP model used in the sodium worth calculations. This MCNP model represents a $1/12^{th}$ core symmetric slice of the Hoffman core design was created. This model has all fuel pins represented. The physics of the full core model is represented by the $1/12^{th}$ model by way of reflective boundary conditions on the leading edges. Vacuum boundary conditions were used on the outer arch bounding the reflector region.

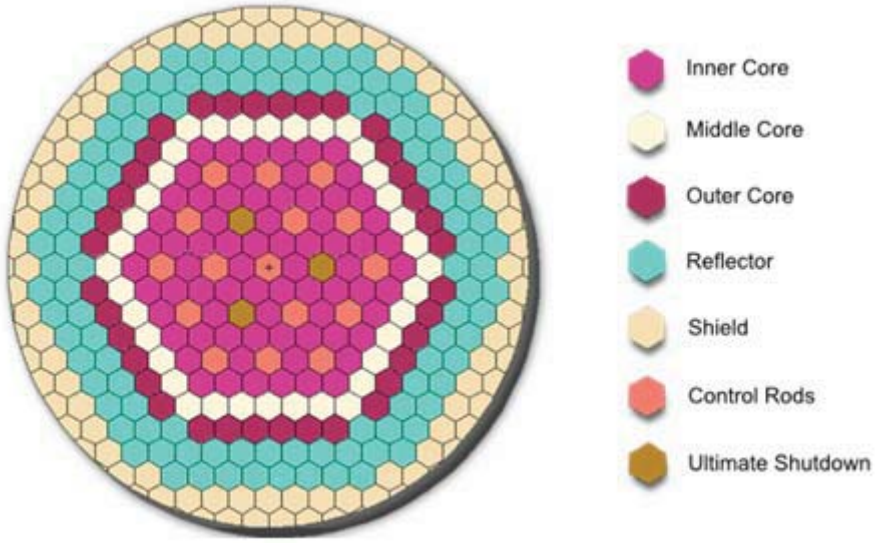

Figure 5-7. Full core MCNP model of an oxide fueled fast burner reactor with CR=0.75 (Fuel pins and coolant, etc. smeared within each assembly)

The purpose of reducing the model size to a $1/12^{th}$ representation was to save computational time while accommodated the added dimensionality of full pin detail. The interest in having a full pin detail model was to look at the power-peaking relationships between neighboring enrichment zones and ultimately

between fuel and a radial target region. Modelization of this radial target region was added, but results were not completed this year.

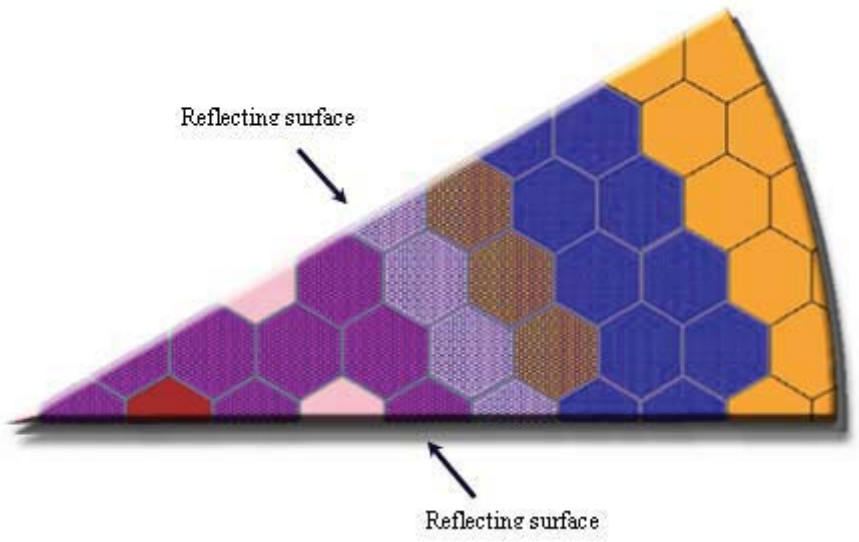

Figure 5-8. One-twelfth MCNP model of an oxide fueled SFR with CR=0.75 (all fuel pins modeled)

It should be noted that reactivity in this section presented in units of dollars ($\$=\rho/\beta_{eff}$). Where β_{eff} is the effective delayed neutron fraction. For lack of a more detailed calculation capability, the β_{eff} was assumed to be equal to 0.003.

A comprehensive set of calculations for different conversion ratios in addition to partitioning scenario and MA to Pu ratio would be valuable in gaining a comprehensive understanding of the sodium worth sensitivities to these parameters. Note that it has been postulated in the literature that SFRs are not suitable to burn MA-only TRU in a uranium free (i.e., CR=0) fuel and core design [35]. A comprehensive set of scenario studies using the MRTAU-to-MCNP method could readily ascertain the magnitude of sensitivities to these "what-if" questions. This approach could then provide guidance to what kind of in-depth physics and safety analysis is necessary.

5.2.2 Sodium Density Reactivity Worth

For a change in sodium density, leakage is increased evenly across the entire core geometry. Hypothetical scenarios where the bulk density in the sodium pool could decrease are Loss-of-Heat-Sink and Loss-of-Primary-Pump capability [36].

The sodium density was incrementally reduced starting from all-sodium to completely voided coolant. Figure 5-9 shows the sodium density worth curve for the oxide fueled fast burner reactor (CR=0.5) using fuel isotopic compositions characteristic of 1st and 10th recycle. The isotopic composition of the 1st recycle is characteristic of SNF TRU blended with depleted uranium (i.e., the very first startup core). The 10th recycle isotopic composition is characterized by multi-recycle feedback with a virtually equilibrated transuranic vector.

There is very little difference between the two sodium density worth curves. However, this result is representative of a relatively high conversion ratio so the effect of MA positive feedback may not be dominating. Further calculations over a range of conversion ratio using the MRTAU-to-MCNP method are necessary to fully capture the effects of MA concentration on the sodium density reactivity.

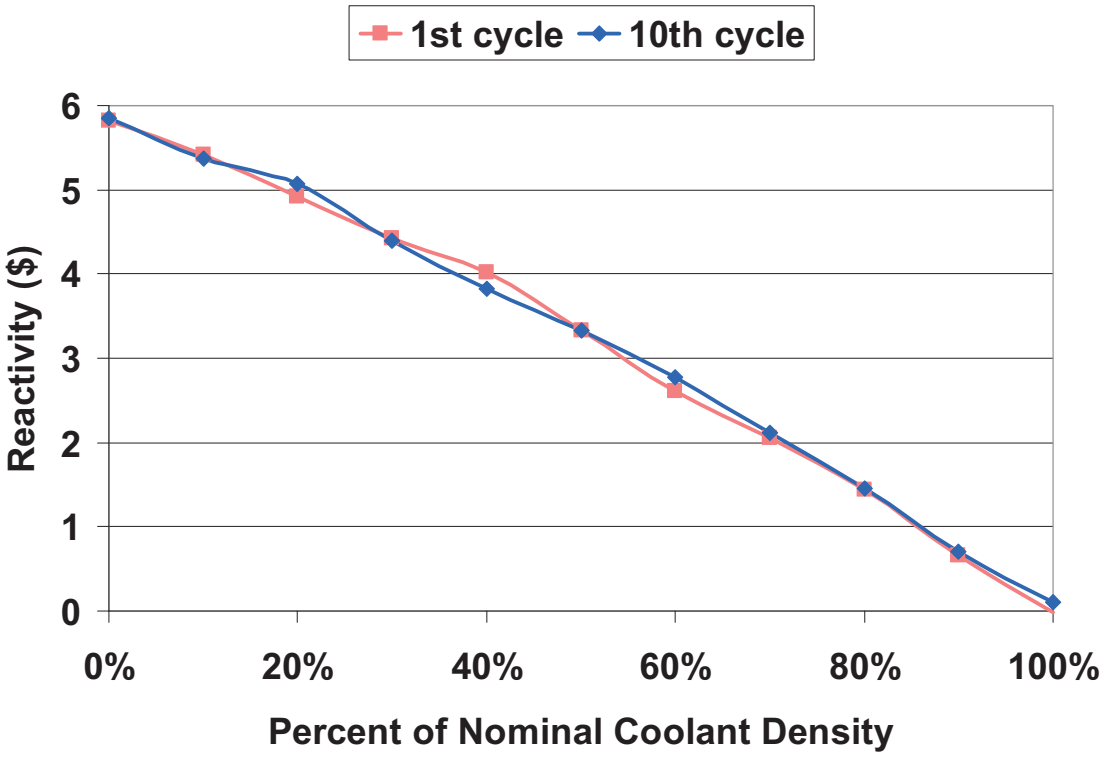

Figure 5-9. Sodium density worth curve of oxide-SFR (CR=0.5) for 1st and 10th recycling all-TRU

5.2.3 Local Void Coefficient

Since SFR use ducted assemblies, there is potential to have bubbles or voiding in an individual assembly. This *local* void, if near the active core periphery, can cause reactivity to decrease by allowing leakage to increase. If placed away from the periphery, the localized leakage is not enough to offset the increase in multiplication from spectrum hardening, thus causing core reactivity to increase.

The sodium density in the incrementally increasing rows of fuel was voided one ring at a time. Figure 5-10 shows the reactivity worth of each voided ring. It is interesting to note that even though there are no reflector regions near assemblies in the inner core, this region does not have the highest void worth per assembly. A likely explanation for this is the fact that the inner core is not the highest enrichment zone. The outer row of fuel (row 8) is the highest enrichment zone. Also, the high number of control assembly locations may be allowing for some streaming effect which would allow neutrons from a neighboring voided fuel assembly to escape or leak thus mitigating positive reactivity.

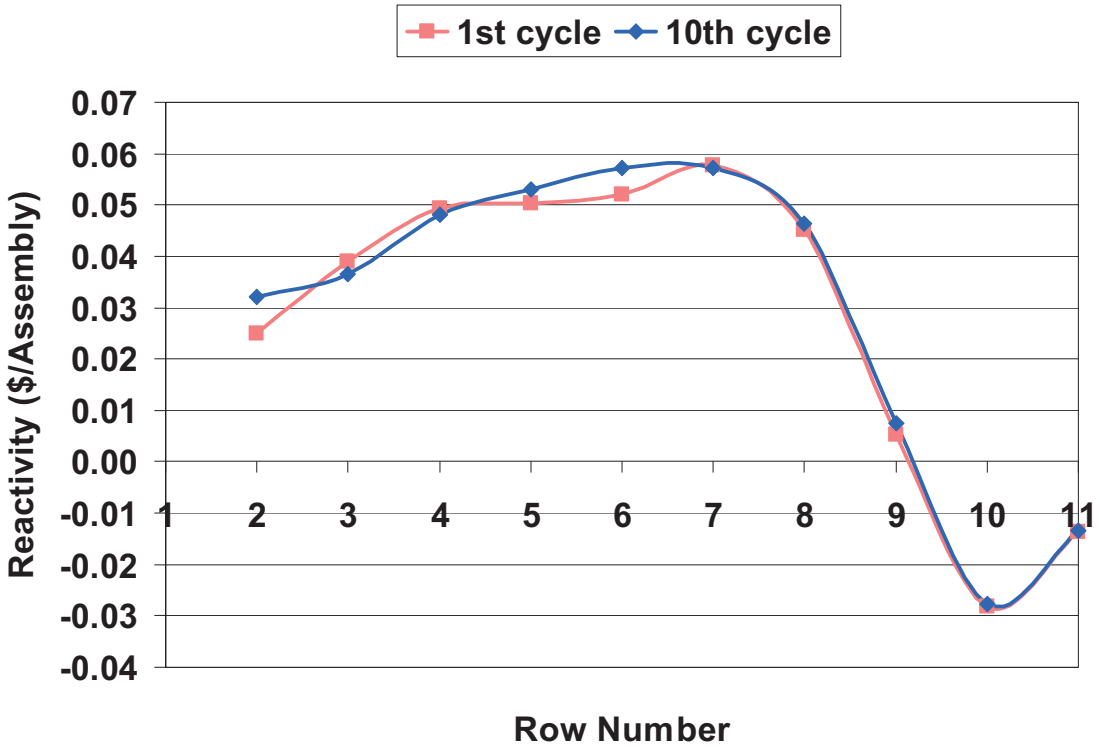

Figure 5-10. Local inserted void worth curve for oxide-SFR (CR=0.75) for 1st and 10th recycling all-TRU (Note: reactivity values represent a single voided row normalized to number of assemblies in that row)

5.2.4 Global Void Coefficient

A very large instantaneous displacement of sodium in the core could give a large instantaneous insertion of positive reactivity. It should be noted that with a pool type design and a relatively compact core size, a scenario where such an insertion could occur is difficult to imagine with any credible probability. The reactivity effect is due to a *globally* voided portion of the core. Depending on the size and shape of a hypothetical global void, the core could incur the highest positive feedback without any attribute of leakage feedbacks. In this study, the amount of positive reactivity feedback from voids of incrementally increasing size was determined by voiding all sodium in the given row number plus all rows it encompasses. As shown in Figure 5-11, the positive reactivity steadily increases for global voids of increasing radius, starting at the center, until the outermost row of fuel is voided where reactivity goes down to the increased opportunity for leakage at the core periphery. As with the local void, the reactivity worth of the voided inner core is much less than that of the outer core.

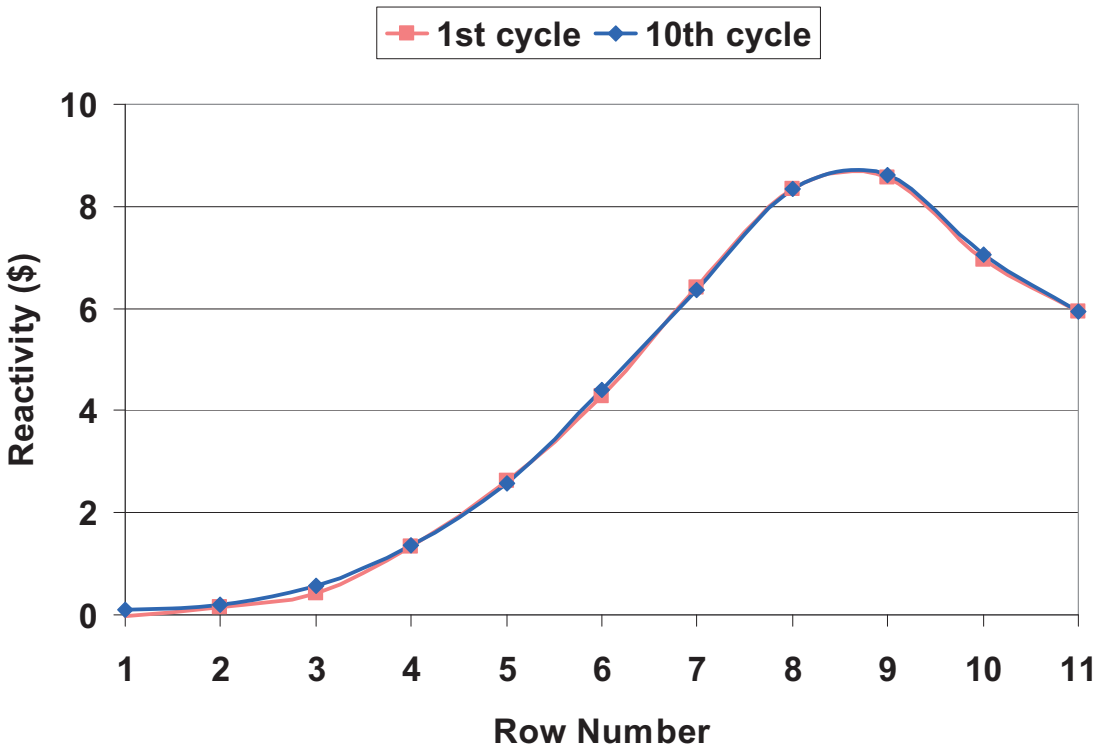

Figure 5-11. Global inserted void worth curve for oxide-SFR (CR=0.75) for 1st and 10th recycling all-TRU (Note: reactivity values represent all rows up to and including row number)

6. Dose Issues and Isotope Evolution

The dose rates to fuel fabrication workers from fresh MOX-UE assemblies for the five actinide partitioning schemes described in Section 5.1 at the 1st, 10th and 60th recycles were calculated using MCNP [31,37]. In the context of this report, the term 'dose rate' refers to the dose equivalent rate calculated in milli-Rem per hour. A 30 cm diameter International Commission on Radiation Units and Measurements (ICRU) sphere was used to represent the human target [38]. The dose rate to this sphere was calculated at four distances between the surface of the assembly and the surface of the ICRU sphere: 0 cm, 50 cm, 100 cm, and 300 cm. The dose rate contributions from spontaneous fission neutrons, (alpha, n) neutrons, and gamma rays were evaluated separately. Finally, the dose was calculated in two ways. First, dose rates were calculated using the complete material composition of the fuel resulting in an isotope aggregate dose rate from each assembly. Second, the dose rates from specific isotopes were calculated to generate a database of dose rate per isotope per kilogram from a generic fresh MOX-UE assembly. The aggregate isotope calculation provides the most accurate dose rate estimates because all isotopes in the fresh fuel composition are used to generate a single radiation source energy spectrum explicitly applicable to a single scenario study (i.e., fresh MOX-UE composition). However, the isotope-by-isotope calculations allow the dose rate to be calculated in support of future studies for any arbitrary fuel recipes corresponding to a characteristic MOX-UE fuel. The dose calculation methodologies described in this chapter can also be used for SFR fuels. In addition, these methods could be further used to study other fuel handling case studies, such as dose and radiation damage to hot-cell electronics. These topics could be the subject of future research efforts.

6.1 Geometry and Materials

The geometry of the MOX-UE fuel assembly in MCNP was nearly identical to the geometry used in the boron concentration and void coefficient calculations in Chapter 5. The density and diameter of the fuel pellets was changed to reflect the fact that the fuel assemblies were fresh and not burned. The gap between the fuel pellet and the cladding was modeled as void (i.e., vacuum)[n]. All of the water in the model was voided. The reflective boundary conditions were set to non-reflective (i.e., vacuum). All of the material temperatures were set to 300K. Also, the critical eigenvalue (i.e., k-eff) search algorithm of MCNP was turned off and the code was used in a purely *source driven mode*. A summary of the MCNP model parameters used for the dose calculations is shown in Table 6-1.

Table 6-1. Dose calculation MCNP model parameters[o]

Description	Value
Assembly type	17x17 PWR
Fuel burnup	Fresh Fuel
Water parameters	N/A
Fuel temperature (K)	300
Fuel density (not smeared) (g/cm^3)	10.4
Fuel pellet outside diameter (cm)	0.819
Phantom sphere diameter (cm)	30
Phantom positions (assembly surface to phantom surface) (cm)	0, 50, 100, 300

[n] From a radiation transport standpoint, vacuum is representative of air or other gaseous atmosphere

[o] For a more detailed description of the MCNP geometry, see Section 5.1

In addition to the changes to the assembly, four 30 cm diameter ICRU sphere phantoms were added to the model to act as targets. These spheres were centered vertically with the fuel assembly and were positioned with four distances between the assembly surface and the phantom surface, as shown in Figure 6-1 and Figure 6-2. Also, each ICRU distance was modeled independently and not in the same calculation as depicted in the Figures. Thus, each dose calculation consists of one sphere and one assembly, only.

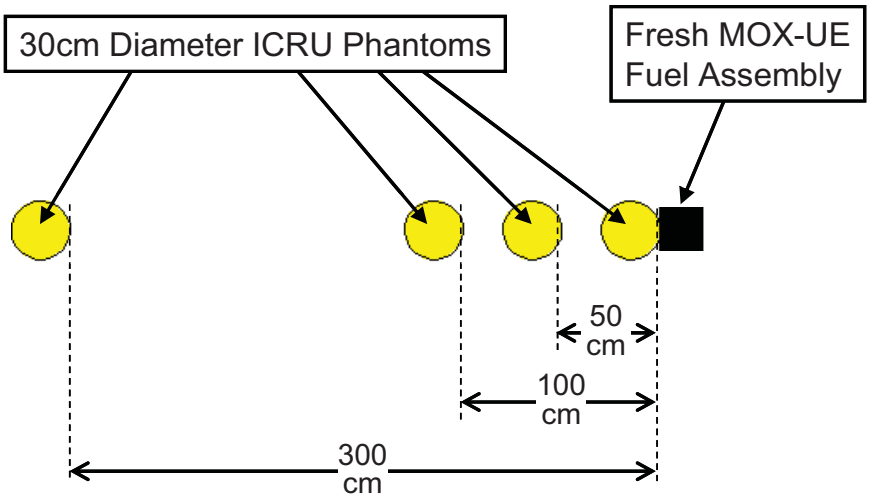

Figure 6-1. Top view of phantom locations for MCNP dose calculations

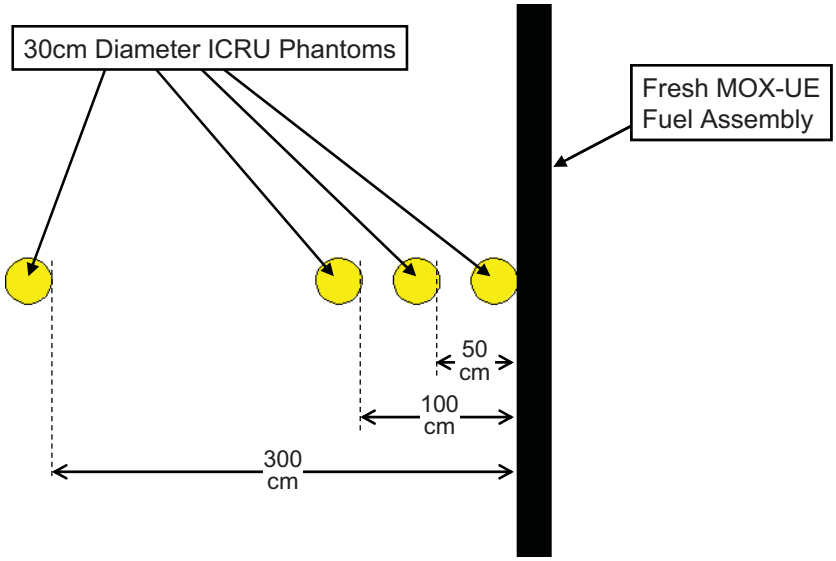

Figure 6-2. Side view of phantom locations for MCNP dose calculations

For the aggregate isotope cases, the fuel material composition was changed for each calculation based on the reprocessing scheme and the number of recycles. The fuel compositions were taken from the report by Youinou and were compiled in a spreadsheet that was used to calculate atom fractions and generate MCNP material card inputs. In this calculation, the fuel density was assumed to be 10.4 g/cm3 and it was assumed that all of the transuranic isotopes form dioxides. This assumption is important for generating alpha,n reaction neutron source terms. Finally, neutron cross section data did not exist for Am-242 ground state and this isotope was excluded from the MCNP material cards for neutron dose rate calculations. The mass of this isotope was included in the total mass of Americium used in the photon dose rate calculations.

The material specification for the isotope by isotope calculations was handled differently because the isotope specific dose rates were calculated for a generic MOX-UE 17x17 PWR assembly. The material composition for the PuNp 1st recycle was chose, somewhat arbitrarily, as the material composition for all of the isotope specific dose rate calculations. The material compositions from the Pu-only scenario were not used because the mass percent of transuranic material in the Pu cases was 10% while it was 8% for all of the other recycling schemes. It is unlikely that this would make a significant impact on the dose results.

6.1.1 Phantom Definition

The phantom used in these dose calculations was a 30 cm diameter sphere filled with material simulating the composition of an adult human. The phantom did not include specific internal structure as is typically used for medical physics phantoms when the dose to a specific internal organ needs to be determined. The homogenous phantom used in these calculations is commonly used for radiation shielding calculations and should provide a more conservative result. The elemental composition was specified according to an ICRU standard and the isotopic composition was determined using the natural isotopic abundance of the particular elements [38]. The elemental composition of the sphere is shown in Table 6-2.

Table 6-2. ICRU Phantom composition [38]

Element	Mass Fraction (%)
Hydrogen	10.1
Carbon	11.1
Nitrogen	2.6
Oxygen	76.2

6.1.2 Source Spectra and Activity Calculations

The dose contribution from spontaneous fission neutrons, (alpha, n) neutrons, and gamma rays were calculated separately. Because of this, three source terms needed to be generated for each recycling case for each reprocessing scenario. Origen-Arp was used to generate the source terms used for these calculations [20,32,33]. For the aggregate isotope source terms, the fuel composition at fabrication from Youinou's report was entered into Origen-Arp. In addition, the appropriate mass of oxygen was also entered into the Origen-Arp composition. The 44 group ENDF5 energy binning structure was used to discretize the gamma and neutron source term energies. This is done automatically by SCALE. In the Origen-Arp output files, the spontaneous fission neutron activity, the (alpha, n) neutron activity, and the gamma activity are all tabulated separately. This data was copied into spreadsheets that were used to normalize the activity to a basis of 1 metric ton of heavy metal and then calculate a histogram for each source term. These histograms were then formatted so that they could be easily copied and pasted into an MCNP source definition card.

The Origen-Arp decay feature was used to produce a source term based on the entered material composition as a function of decay time during the time allotted for fuel fabrication. The decay times were set to 0 days, 1 month, 2 months, 3 months, 6 months, and 1 year. It is important to distinguish the differences in radiologic source spectrum between beginning and the end of the time allotted for fuel fabrication. As with the Youinou study, the fabrication stage was assumed to be one year. In this year, the isotopic composition of the reprocessed material changes as does the source term which is depicted in Figure 6-3 and Figure 6-4.

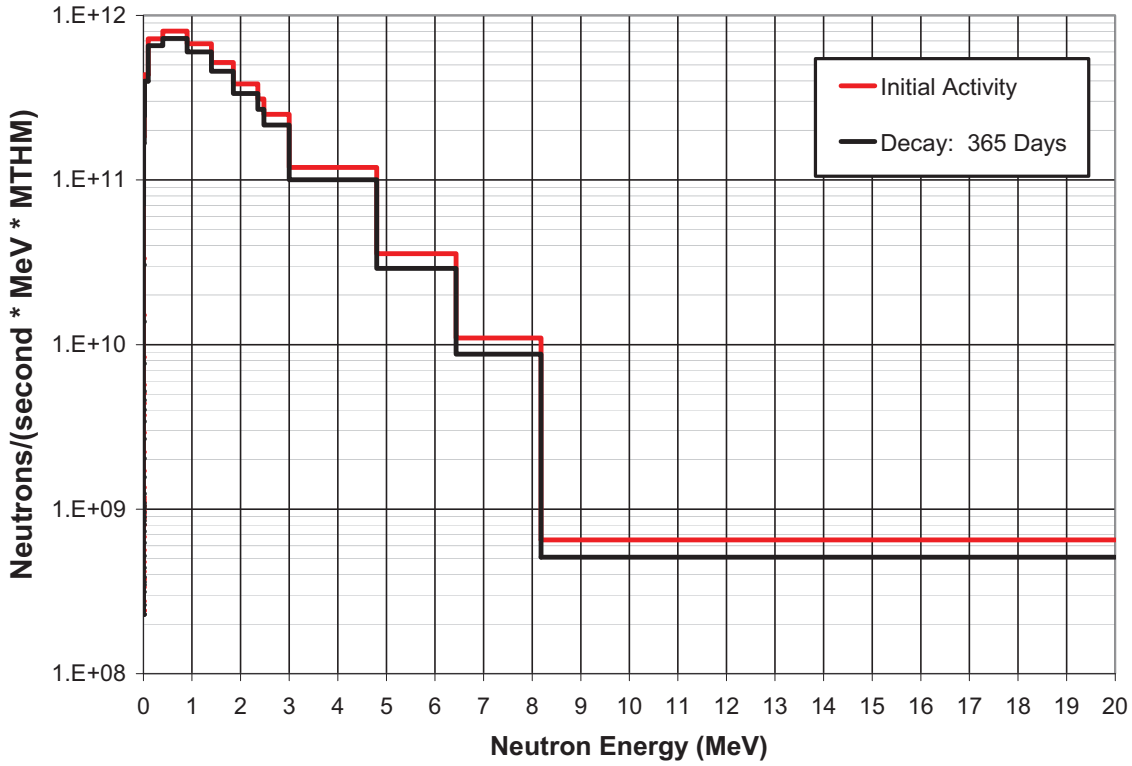

Figure 6-3. Aggregate spontaneous fission neutron activity for the PuNpAmCmBkCf 60th recycle

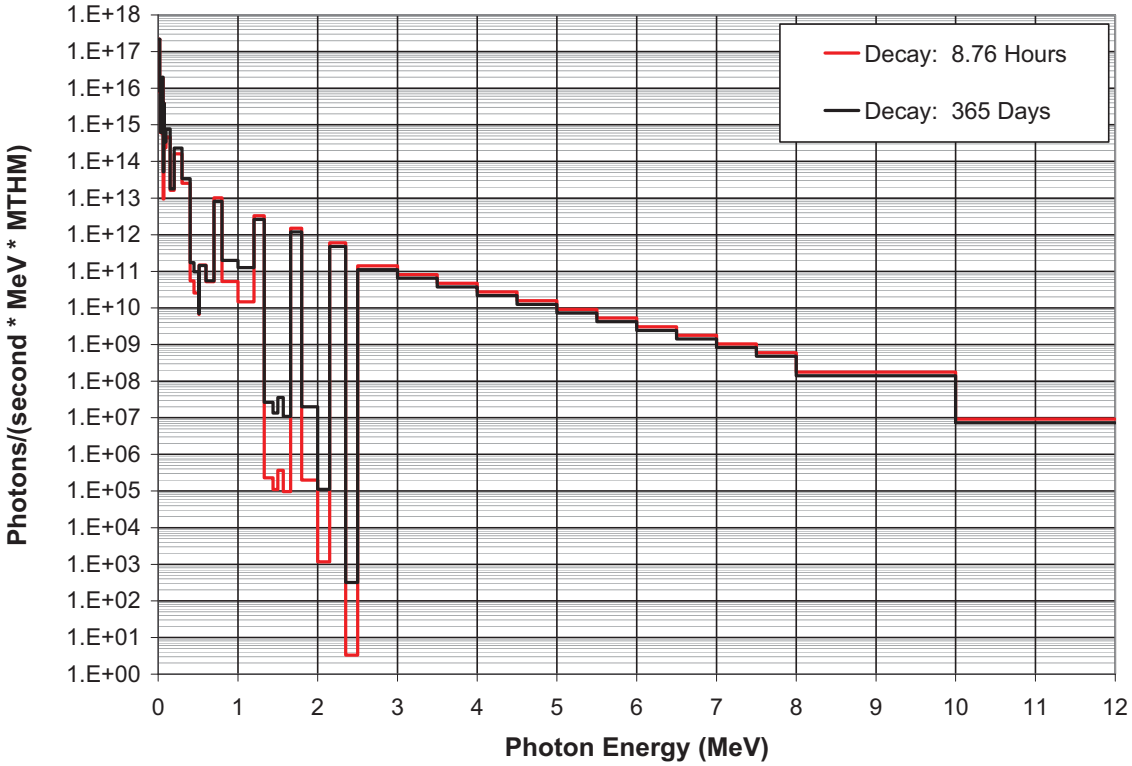

Figure 6-4. Aggregate gamma activity for the PuNpAmCmBkCf 60th recycle

The isotope specific source terms were generated in a similar way. Instead of entering the entire fuel composition, only one kilogram of one isotope was entered. For the alpha,n calculations it was assumed that the interaction medium for the emitted alpha particles would be a sea of UOX as opposed to a continuous medium of the particular alpha emitter in its oxide form. This is a standard feature offered by Origen-Arp and seems to be the more appropriate approximation of the actual MOX-UE composition, which is mostly comprised of UOX.

6.1.3 Source Geometry Modelization

The gamma rays and neutrons isotropically originate in the fuel material. Because the fuel is fresh, the zirconium clad is not radioactive and therefore is not modeled as a source. The fuel material and the cladding offer significant self shielding that should be considered in the model. The simplest way to model this source term would be to define a rectangular prism that contains the fuel assembly and allow particles to be randomly started from within that volume. This method, however, would allow particles to originate from the air gaps between fuel pins and would not take full credit for the self shielding caused by the fuel and clad. The source definition used in all of the MCNP dose rate calculations only allowed particles to originate in the fuel material.

6.1.4 Dose Tally Modelization

Two different MCNP tallies were used with multiplier cards to determine the dose in the phantom. The *track-length-estimate-of-cell-flux* (F4) tally was used to determine the flux by summing the particle track lengths in the phantom volume resulting in an output with the units: particles per cm^2 per source particle[p]. The *track-length-estimate-of-cell-energy-deposition* (F6) tally was used to sum the energy deposition of particles as they passed through the volume resulting in an output with the units: MeV per gram per source particle. The results of the F4 and F6 tallies were binned into energy group structures based on the energy structure of the factors used to convert from the respective tally units into Rem per source particle. Converting from the F4 and F6 tally units into dose was accomplished by multiplying the tally results by factors that account for the biological damage created in a human as a function of particle type and particle energy. These conversion factors are difficult to quantify because of the difficulties associated with assessing the biological damage created by radiation in human tissue. Because of this, several ‘standards’ exist that list similar, but slightly different, factors for converting flux into dose. In addition, the F6 tally calculates energy deposition according to ‘heating factors’ that are a function of material type, particle type, and particle energy. The F6 energy deposition results can be converted into Rad, or joules per 100 kg, which can then be multiplied by quality factors resulting in units of Rem[q]. Like the flux to dose conversion factors, the quality factors are also a function of the particle type and particle energy and different ‘standards’ for quality factors exist[r].

---

[p] F4 and F6 are MCNP software specific nomenclatures

[q] A Rad is a unit of absorbed dose which is the energy imparted to a mass by ionizing radiation. A Rem is a measure of the dose-equivalent which is a multiplication product of absorbed dose with a tissue specific weighting factor known as a *quality factor*, thus taking into effect the damage that an absorbed dose has on a given tissue.

[r] In the above discussion, the F6 tally quantifies absorbed dose and requires a simple unit conversion to convert MCNP data into common units used in radiation protection. The F4 tally quantifies pure particle flux, only. Thus conversion factors for the F4 tallies also factor in the expected absorbed dose in human tissue in addition to the dose-equivalent conversion (10CFR20 Subpart A).

For the neutron dose calculations, the conversion factors prescribed in the Title 10 Code of Federal Regulations, 10CFR20 Subpart A were used [39]. The conversion factors included in 10CFR20 were adopted from ANSI/ANS–6.1.1–1977, which differ slightly from more recently revised standards, such as the ICRP-21 standard. Regardless, because these are the factors used by the Nuclear Regulatory Commission (NRC), they were used in these calculations. The neutron flux-to-dose and quality factor conversion factors used in these calculations are shown in Table 6-3.

Table 6-3. Neutron flux-to-dose conversion factors from 10CFR20 Subpart A [39]

Neutron Energy (MeV)	Quality Factor (Rem per Rad)	Fluence per Unit Dose Equivalent (Rem per $^{1}n/cm^{2}$)
2.50E-08	2	1.02E-09
1.00E-07	2	1.02E-09
1.00E-06	2	1.23E-09
1.00E-05	2	1.23E-09
1.00E-04	2	1.19E-09
1.00E-03	2	1.02E-09
1.00E-02	2.5	9.90E-10
1.00E-01	7.5	5.88E-09
5.00E-01	11	2.56E-08
1	11	3.70E-08
2.5	9	3.45E-08
5	8	4.35E-08
7	7	4.17E-08
10	6.5	4.17E-08
14	7.5	5.88E-08
20	8	6.25E-08

The gamma dose calculations were completed in a similar way to the neutron dose calculations. Photon flux-to-dose conversion factors are not included in the Code of Federal Regulations. 10CFR20 Subpart A does specify the quality factor (Rad to Rem) for all gamma doses is one. Photon flux-to-dose conversion factors were specified in ANSI/ANS–6.1.1–1977 and these factors were used in the gamma dose calculations. The gamma flux-to-dose and quality factor conversion factors used in these calculations are shown in Table 6-4.

Table 6-4. Photon flux-to-dose conversion factors from 10CFR20 Subpart A [39]

Photon Energy (MeV)	Quality Factor (Rem per Rad)	Fluence per Unit Dose Equivalent (Rem per γ/cm^{2})
0.01	1	1.10E-09
0.03	1	1.62E-10
0.05	1	8.06E-11
0.07	1	7.17E-11
0.1	1	7.86E-11
0.15	1	1.05E-10
0.2	1	1.39E-10
0.25	1	1.75E-10
0.3	1	2.11E-10
0.35	1	2.44E-10
0.4	1	2.74E-10
0.45	1	3.00E-10
0.5	1	3.25E-10

Table 6-4 (cont.). Photon flux-to-dose conversion factors from 10CFR20 Subpart A [39]

Photon Energy (MeV)	Quality Factor (Rem per Rad)	Fluence per Unit Dose Equivalent (Rem per γ/cm^2)
0.55	1	3.53E-10
0.6	1	3.78E-10
0.65	1	4.00E-10
0.7	1	4.22E-10
0.8	1	4.67E-10
1	1	5.50E-10
1.4	1	6.97E-10
1.8	1	8.31E-10
2.2	1	9.50E-10
2.6	1	1.06E-09
2.8	1	1.11E-09
3.25	1	1.23E-09
3.75	1	1.34E-09
4.25	1	1.45E-09
4.75	1	1.56E-09
5	1	1.61E-09
5.25	1	1.67E-09
5.75	1	1.77E-09
6.25	1	1.87E-09
6.75	1	1.98E-09
7.5	1	2.13E-09
9	1	2.44E-09
11	1	2.86E-09
13	1	3.28E-09
15	1	3.69E-09

Figure 6-5 shows a dose rates calculated using F4 and F6 tallies for the Pu-only 1st recycle case. The dose rates from neutrons were consistently higher using the results of the F6 tally. The dose rates from photons were consistently higher using the results of the F4 tally. Because the cause of the difference between these tallies was not resolved, to maintain conservatism the higher dose rate was always used. It is possible that the difference stems from different assumptions in phantom modelization (e.g., phantom diameter, hydrogen density, etc.) of that used in the ANSI/ANS standard and the one that was used in this work.

6.2 Aggregate Dose Calculations for Actinide Partitioning Scenarios

The isotope aggregate (alpha, n) neutron, spontaneous fission neutron, and gamma dose rates from the Pu-only, PuNp, PuNpAm, PuNpAmCm, and PuNpAmCmBkCf reprocessing scenarios were calculated for the 1st, 10th and 60th recycle at 0 cm, 50 cm, 100 cm, and 300 cm. These calculations required 180 MCNP runs. The dose to the phantom was determined using an F4 and an F6 tally, both with multiplier cards to convert from flux to dose-equivalent and absorbed-dose to dose-equivalent, respectively. The resulting dose determined by MCNP, in Rem per source particle, for the two tallies were consistently less than a factor of two different. An effort was made to rectify the difference, but it was eventually decided that the values were similar enough and to be conservative, the higher of the two values would be used.

6.2.1 Dose Attributed by Spontaneous Fission

Figure 6-6 shows the dose rate evolution from spontaneous fission neutrons for the five reprocessing scenarios at a position 50 cm from the assembly surface. Recycling Curium and Californium has a huge impact on the spontaneous fission source term. Note, the composition of the PuNpAmCm material and the PuNpAmCmBkCf material at the first recycle is identical, explaining the identical spontaneous fission, (alpha, n) and gamma dose rates from these two cases[s].

6.2.2 Dose Attributed by (Alpha,n) Reactions

Figure 6-7 shows the dose rate evolution from (alpha, n) neutrons for the five reprocessing schemes at a position 50 cm from the assembly surface. The recycle of Californium does not add significantly to the (alpha, n) neutron dose between the PuNpAmCm and PuNpAmCmBkCf cases, as is shown.

6.2.3 Dose Attributed by Gamma Emission

Figure 6-8 shows the dose rate evolution from gamma rays for the five reprocessing schemes at a position 50 cm from the assembly surface. The additional recycle of neptunium does not appreciably add to the gamma dose between the Pu and the PuNp reprocessing schemes.

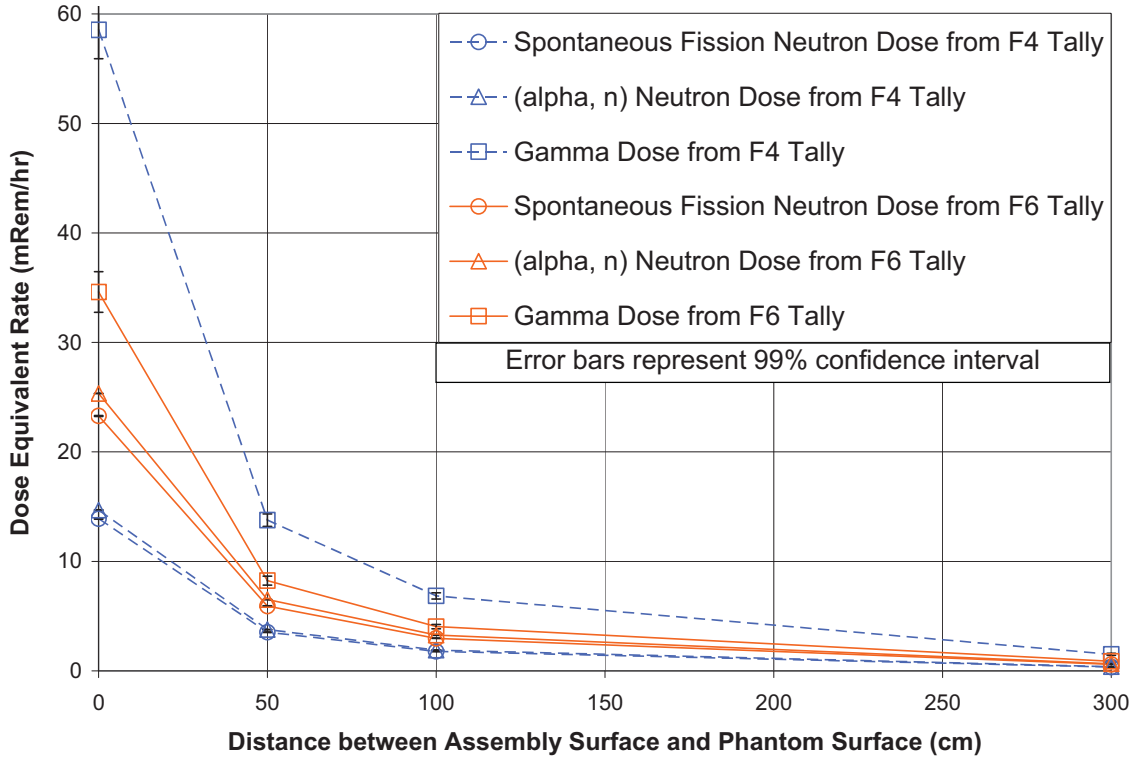

Figure 6-5. F4 and F6 tally comparison for dose rate components of Pu-only 1st recycle

[s] It should be noted that the decrease in dose rate between the Pu and PuNp cases is caused by the reduction in weight percent of recycled transuranics from 10% to 8%.

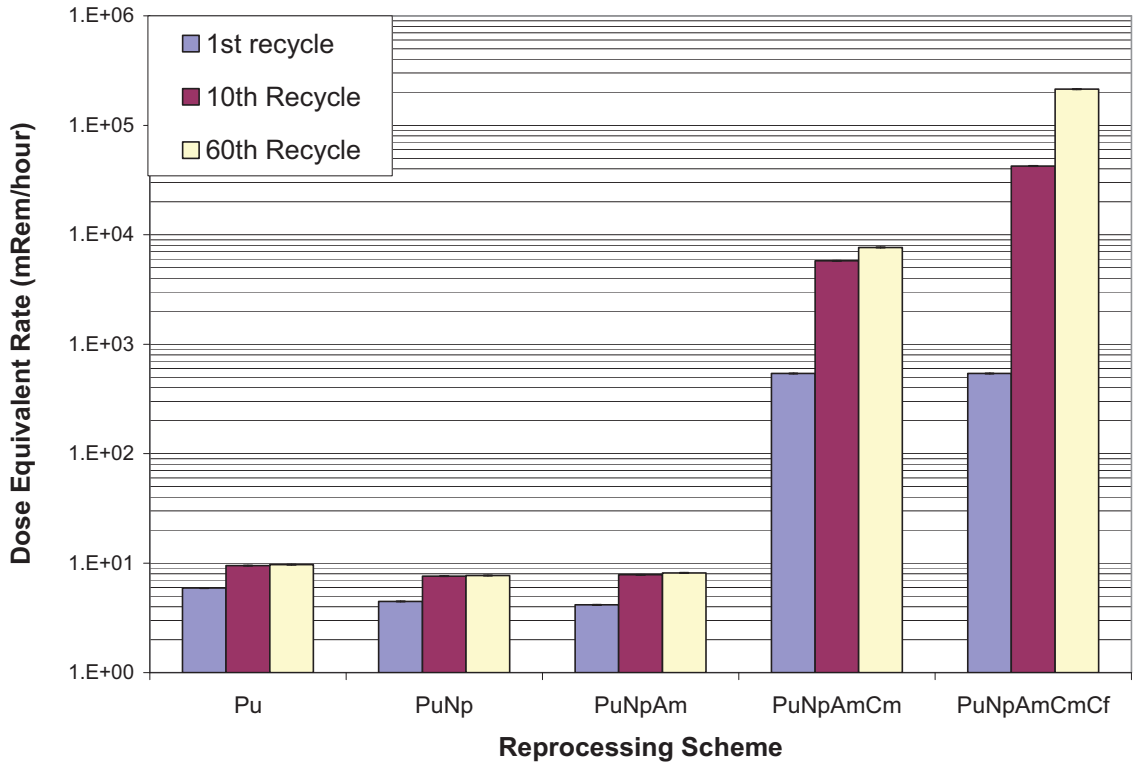

Figure 6-6. Dose rate from spontaneous fission neutrons, 50 cm from the assembly surface

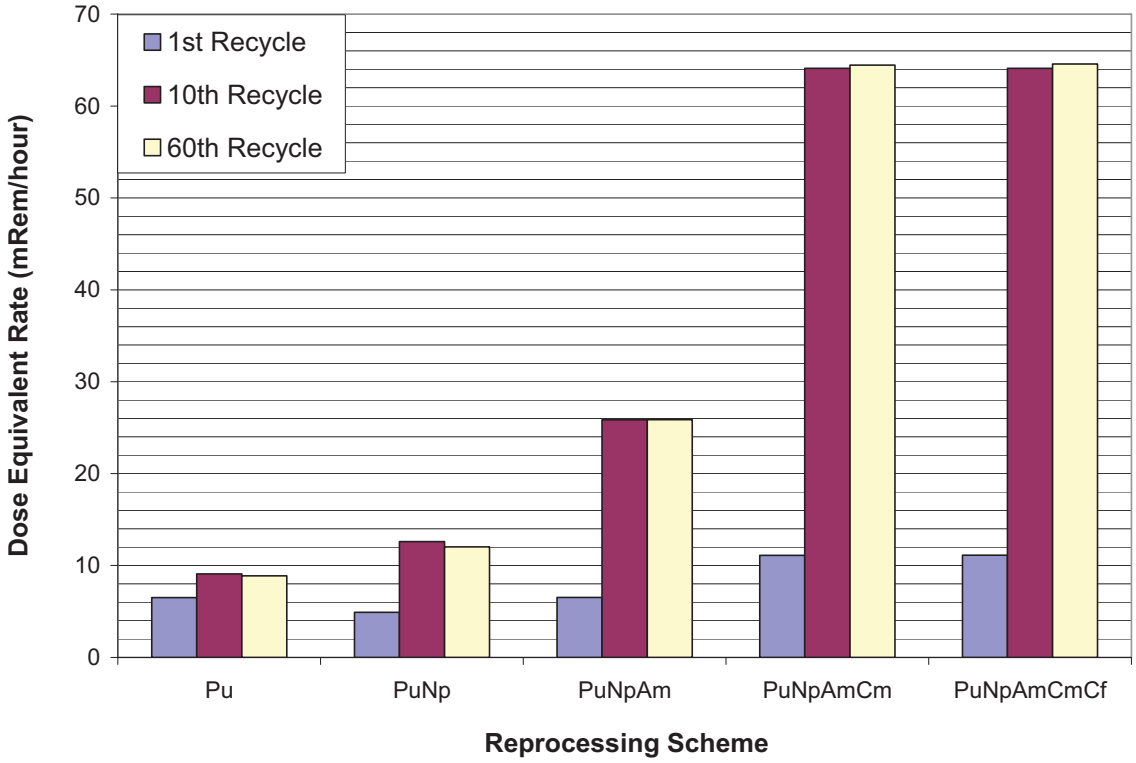

Figure 6-7. Dose rate from neutrons produced by alpha,n reactions, 50 cm from the assembly surface

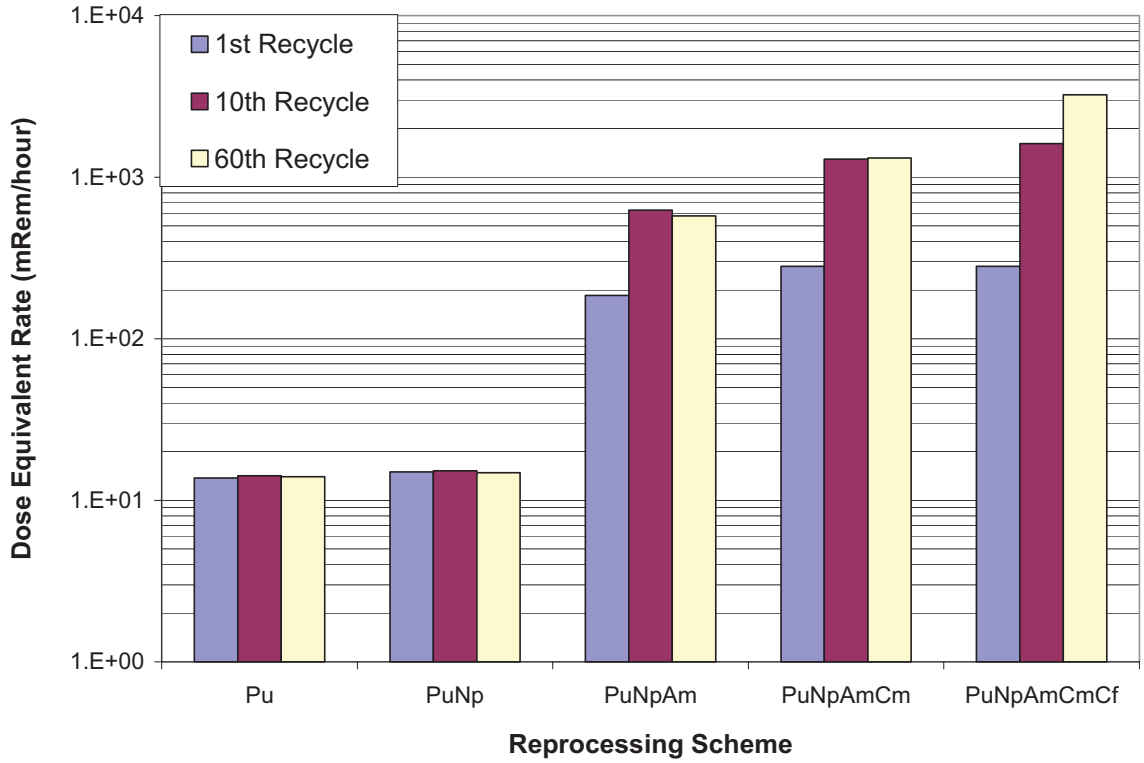

Figure 6-8. Dose rate from gamma emission, 50 cm from the assembly surface

6.2.4 Combined Dose Contributions

Figure 6-9 shows the total dose rate for each of the five reprocessing schemes at the 1st, 10th, and 60th recycle at a position 50 cm away from the fuel assembly. The dose rates increase predictably as additional transuranic elements are included in the recycle stream. The dose rates also increase predictably as the material in each scheme is recycled more times. Figure 6-10 shows the total dose rates from the five reprocessing schemes at the 1st and 60th recycle at four positions from the fuel assembly. The dose rates decrease predictably with increasing distance from the fuel assembly. The dose rate from a fresh uranium dioxide fuel assembly is also shown on this Figure.

It should be noted that the NRC 10CFR20.1201 regulation limits "The licensee shall control the occupational dose to individual adults, except for planned special exposures under § 20.1206, to the following dose limits. [39]".

- "An annual limit, which is the more limiting of-
- The total effective dose equivalent being equal to 5 Rems; or
- The sum of the deep-dose equivalent and the committed dose equivalent to any individual organ or tissue other than the lens of the eye being equal to 50 Rems.
- A lens dose equivalent of 15 Rems (0.15 Sv), and
- A shallow-dose equivalent of 50 rem (0.5 Sv) to the skin of the whole body or to the skin of any extremity."

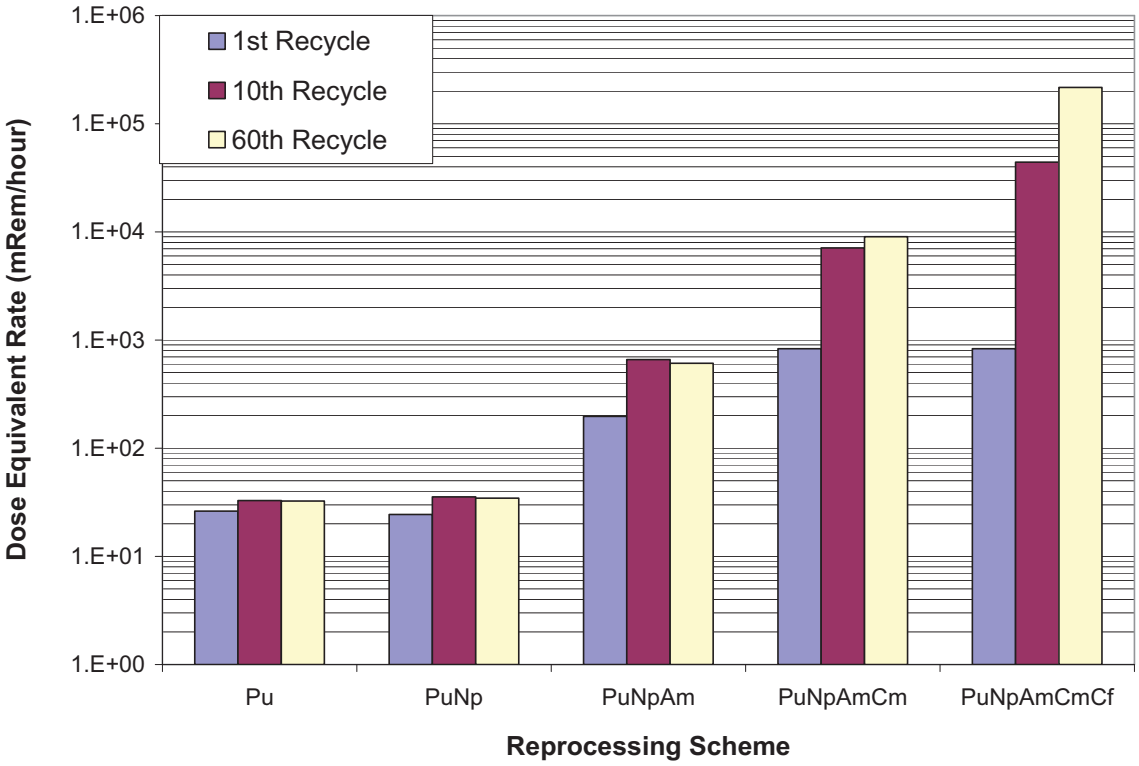

Figure 6-9. Total dose rate, 50 cm from the assembly

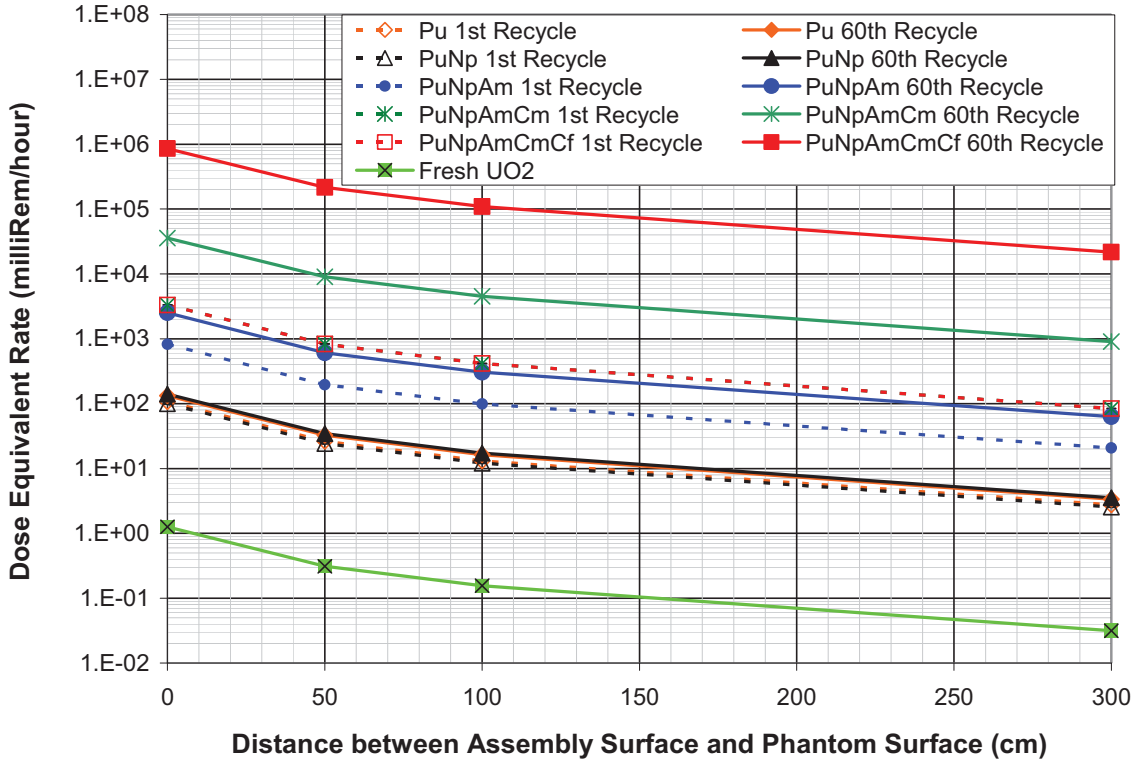

Figure 6-10. Total dose rates as a function of distance from the surface

These *annual* dose limits are comparable to the *hourly* dose rates for PuNpAm and PuNpAmCm recycling. Therefore, the window of opportunity to perform fuel fabrication maintenance operations inside of a glove-box environment dealing with these fuel types is arguably less forgiving than for Pu-only or PuNp MOX-UE. Figure 6-11 compares the individual dose contributor evolution from the five reprocessing scenarios for the 1st and 60th recycle at a distance of 50 cm from the fuel assembly. The gamma dose component was the largest contributor for the Pu-only, PuNp, and PuNpAm cases. The addition of curium and californium in the recycling schemes caused the spontaneous fission neutron dose contribution to become the largest contributor.

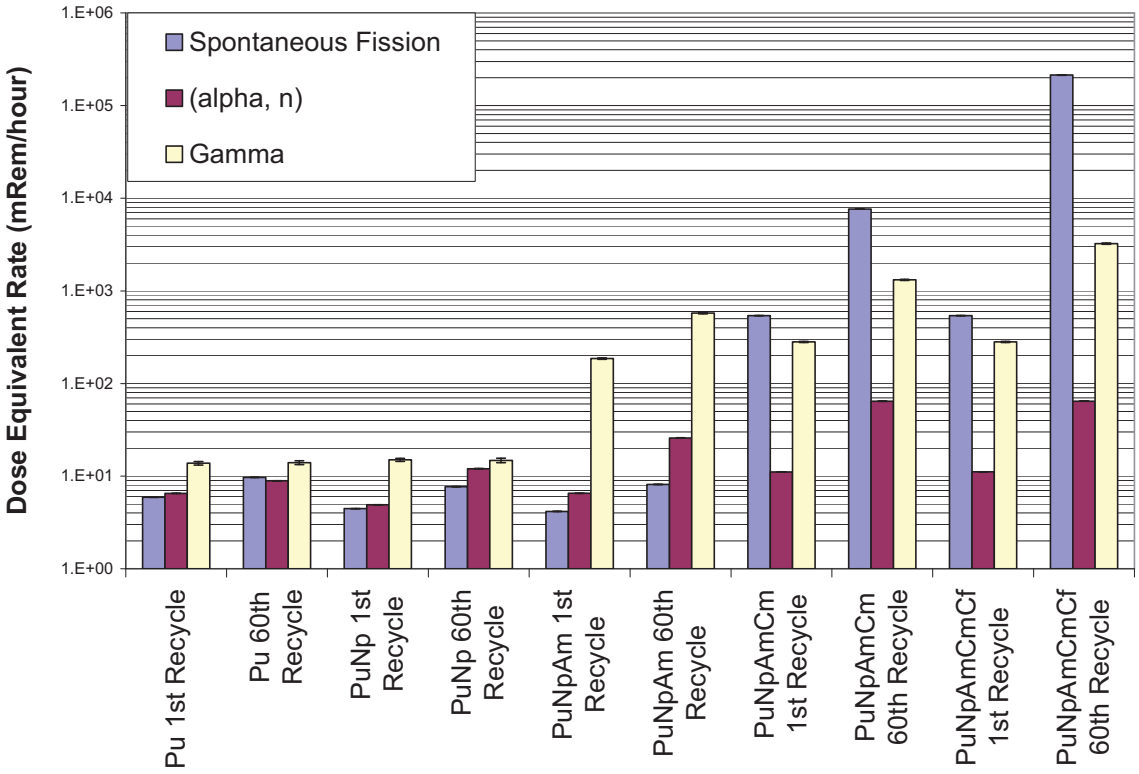

Figure 6-11. Dose rate contribution evolution, 50cm from the assembly

6.3 Dose Calculations Broken Down by Isotope

The isotope specific spontaneous fission neutron, (alpha, n) neutron, and gamma dose contributions were determined for the most contributing isotopes in the fresh fuel using both specific activity and emitted energy as criteria for the ranking. The MCNP geometry and phantom locations for these cases were exactly the same as the configuration for the aggregate isotope dose calculations. Unlike the aggregate isotope calculations, there was not a need to change the fuel material specification with each run. The fuel material for the isotope specific cases was set to the material composition of the PuNp 1st recycle case.

The (alpha, n) neutron, spontaneous fission neutron, and gamma source terms were calculated for all 37 isotopes using Origen-Arp. The activities of the (alpha, n) neutron and spontaneous fission neutron producing isotopes were ranked from top to bottom without regard to the energy of the emitted radiation. The activities of the photon producing isotopes were ranked from top to bottom by looking at the activity of the photons greater than 3 MeV. This criterion was used because of the self-shielding that significantly attenuates lower energy photons. Table 6-5 gives the results of the isotope ranking.

Table 6-5. Ranking by specific activity of isotopes contributing to each source type (showing only those isotopes for which dose calculations were performed)

	Spontaneous Fission	Alpha, n	Gamma Emission
1	Cf-252	Cm-242	Cf-252
2	Cf-250	Th-228	Cf-250
3	Cm-250	Cf-252	Cm-250
4	Cm-248	Cf-250	Cm-248
5	Cm-242	Cm-244	Cm-242
6	Cm-244	Cm-243	Cm-244
7	Cm-246	U-232	Cm-246
8	Pu-238	Pu-238	Th-228
9	Pu-242	Cf-249	Pu-238
10	Pu-244	Am-241	Cf-249
11	Pu-240	Cf-251	Pu-244
12	Cf-249	Ac-227	Pu-242
13		Ra-226	U-232
14		Cm-246	Pu-240
15		Pu-240	Cm-243
16		Am-243	Am-242M
17		Cm-245	Am-241
18		Th-229	Cf-251
19		Pu-239	Ra-226
20		Am-242M	Ac-227
21		Pa-231	Am-243
22		Th-230	Th-229
23		U-233	Cm-245
24		U-234	Pu-239
25			Pa-231
26			Th-230
27			U-233
28			U-234
29			Am-242
30			Pu-241
31			Np-237
32			U-238
33			U-236
34			Cm-247
35			U-235
36			Th-232
37			Ra-228

6.3.1 Tabulation Tools

A spreadsheet calculation tool was created that conveniently combines the dose rate from all of the isotope specific contributions shown in Table 6-5. The user input to the calculator is the mass of each of the 37 isotopes, in kilograms. The calculator automatically calculates the (alpha, n) neutron, spontaneous fission neutron, and gamma dose rate and 99% confidence interval for each isotope at four distances from the fuel assembly. In addition, the calculator sums the (alpha, n) neutron, spontaneous fission neutron, and gamma dose rates and confidence intervals from all of the isotopes at each distance from the assembly. Finally, the calculator sums a total dose rate and confidence interval from the three particle types at each distance.

6.3.2 Spontaneous Fission Tabulation Comparison with Aggregate Calculation

The dose rate from spontaneous fission neutrons calculated with the aggregate isotope method was compared to the dose rate calculated by summing the individual contributions of the specific isotopes. The result of this comparison is shown in Table 6-6. In this comparison, it was assumed that the aggregate isotope calculation provided the most accurate dose rate and the specific isotope combination was compared to this result. Using the top twelve spontaneous fission neutron contributors accounts for 99% of the aggregate dose rate.

6.3.3 Alpha,n Tabulation Comparison with Aggregate Calculation

The dose rate from (alpha, n) neutrons calculated with the aggregate isotope method was compared to the dose rate calculated by summing the individual contributions of the specific isotopes. The result of this comparison is shown in Table 6-7. In this comparison, it was assumed that the aggregate isotope calculation provided the most accurate dose rate and the specific isotope combination was compared to this result. Using the top twelve (alpha, n) neutron contributors only accounted for 90% of the aggregate dose rate, so an additional twelve contributors were analyzed and added to the analysis. With the top twenty-four contributors, around 98% of the aggregate dose rate is accounted.

6.3.4 Gamma Tabulation Comparison with Aggregate Calculation

The dose rate from photons calculated with the aggregate isotope method was compared to the dose rate calculated by summing the individual contributions of the specific isotopes. The result of this comparison is shown in Table 6-8. In this comparison, it was assumed that the aggregate isotope calculation provided the most accurate dose rate and the specific isotope combination was compared to this result. Using all 37 of the gamma emitters does not sufficiently reproduce the dose rates determined with the aggregate isotope calculations. There are a couple possibilities for this discrepancy. First, there could be an error in the spreadsheet, which is considered at this point unlikely. Second, and more likely, the aggregate isotope gamma dose rate was calculated with the fuel composition after one year of decay. This was done to give a more conservative dose estimation, since gamma activity in the fresh assembly increases with time due to buildup of decay daughters to the initial actinides (Figure 6-4). The fuel composition used in these tabulated dose contribution calculations was immediately after reprocessing with no decay. Using the fuel composition listed in Youinou's report improves the results, but many gamma emitting daughter products are not tracked in this composition. It is likely that a more complete list of specific isotope gamma emitters is needed to improve the dose rate calculated by summing contributions.

6.3.5 Total Dose Tabulation Comparison with Aggregate Calculation

The dose rate from all neutron and photon sources calculated with the aggregate isotope method was compared to the dose rate calculated by summing the individual contributions of the specific isotopes. The result of this comparison is shown in Table 6-9. Due to the poor representivity of the gamma ray source spectrum at beginning of the fabrication time to match that at the end of the fabrication time, the agreement with the aggregate method is poor for scenarios dominated by gamma emission. These are the Pu-only, PuNp, and PuNpAm cases. The agreement becomes much better when the neutron fields become the dominating radiation sources as with the PuNpAmCm and PuNpAmCmBkCf cases. This disagreement between the tabulation method and the aggregate calculation does not necessarily mean that the method of tabulation is incorrect. It purely means that the tabulation method with the currently available isotope listing is not sufficient to represent fuel handling at any reasonable length of time beyond the exact moment of blending. To consider dose to radiation workers that may be handling fuel weeks to months after the initial moment of blending, many more decay daughters of the initial actinides must be considered. An example of this may be the loading or emptying of transportation casks.

Table 6-6. Spontaneous fission neutron contribution at 50 cm, comparison of a 12 isotope tabulation with aggregate equivalent calculation (mRem/hour)

	Aggregate	3 Sigma	Tabulation	3 Sigma	Percent of Aggregate
Pu-only 1st Recycle	5.922	0.023	5.887	0.015	99.41%
Pu-only 10th Recycle	9.470	0.037	9.374	0.023	98.99%
Pu-only 60th Recycle	9.690	0.038	9.607	0.024	99.15%
PuNp 1st Recycle	4.463	0.017	4.462	0.011	99.97%
PuNp 10th Recycle	7.591	0.030	7.571	0.017	99.74%
PuNp 60th Recycle	7.689	0.030	7.668	0.018	99.73%
PuNpAm 1st Recycle	4.156	0.016	4.143	0.011	99.71%
PuNpAm 10th Recycle	7.817	0.030	7.734	0.018	98.95%
PuNpAm 60th Recycle	8.142	0.032	8.061	0.018	99.01%
PuNpAmCm 1st Recycle	539.920	2.106	538.723	2.063	99.78%
PuNpAmCm 10th Recycle	5770.305	22.504	5722.176	18.225	99.17%
PuNpAmCm 60th Recycle	7652.280	29.844	7592.561	20.172	99.22%
PuNpAmCmBkCf 1st Recycle	539.920	2.106	538.723	2.063	99.78%
PuNpAmCmBkCf 10th Recycle	42428.969	165.473	42077.796	102.216	99.17%
PuNpAmCmBkCf 60th Recycle	213552.611	832.855	211964.366	563.761	99.26%

Table 6-7. alpha,n neutron contribution at 50 cm, comparison of a 24 isotope tabulation with the aggregate equivalent calculation (mRem/hour)

	Aggregate	3 Sigma	Tabulation	3 Sigma	Percent of Aggregate
Pu-only 1st Recycle	6.515	0.023	6.512	0.020	99.96%
Pu-only 10th Recycle	9.079	0.033	8.970	0.029	98.80%
Pu-only 60th Recycle	8.891	0.032	8.657	0.028	97.37%
PuNp 1st Recycle	4.908	0.018	4.948	0.015	100.82%
PuNp 10th Recycle	12.606	0.045	12.356	0.042	98.02%
PuNp 60th Recycle	12.043	0.043	11.805	0.040	98.03%
PuNpAm 1st Recycle	6.538	0.024	6.409	0.016	98.04%
PuNpAm 10th Recycle	25.839	0.093	25.198	0.080	97.52%
PuNpAm 60th Recycle	25.877	0.093	25.245	0.080	97.56%
PuNpAmCm 1st Recycle	11.120	0.040	10.897	0.022	97.99%
PuNpAmCm 10th Recycle	64.113	0.231	62.441	0.158	97.39%
PuNpAmCm 60th Recycle	64.467	0.232	62.814	0.161	97.44%
PuNpAmCmBkCf 1st Recycle	11.141	0.040	10.897	0.022	97.80%

PuNpAmCmBkCf 10th Recycle	64.110	0.231	62.458	0.158	97.42%
PuNpAmCmBkCf 60th Recycle	64.562	0.232	62.903	0.161	97.43%

Table 6-8. Gamma emission contribution at 50 cm, comparison of a 37 isotope tabulation with the aggregate equivalent calculation (mRem/hour)

	Aggregate	3 Sigma	Tabulation	3 Sigma	Percent of Aggregate
Pu-only 1st Recycle	13.769	0.574	6.138	0.193	44.58%
Pu-only 10th Recycle	14.207	0.690	6.598	0.265	46.44%
Pu-only 60th Recycle	13.989	0.680	4.578	0.249	32.72%
PuNp 1st Recycle	14.988	0.535	4.744	0.147	31.65%
PuNp 10th Recycle	15.199	0.839	4.736	0.367	31.16%
PuNp 60th Recycle	14.809	0.809	4.642	0.350	31.35%
PuNpAm 1st Recycle	185.764	3.232	28.338	0.805	15.25%
PuNpAm 10th Recycle	626.264	9.958	50.114	1.303	8.00%
PuNpAm 60th Recycle	575.335	9.148	49.757	1.296	8.65%
PuNpAmCm 1st Recycle	281.111	4.723	124.822	1.200	44.40%
PuNpAmCm 10th Recycle	1292.558	20.552	772.448	7.723	59.76%
PuNpAmCm 60th Recycle	1315.962	20.924	836.203	7.999	63.54%
PuNpAmCmBkCf 1st Recycle	281.111	4.723	124.822	1.200	44.40%
PuNpAmCmBkCf 10th Recycle	1614.154	25.665	1177.488	7.726	72.95%
PuNpAmCmBkCf 60th Recycle	3232.772	43.642	3251.836	8.103	100.59%

Table 6-9. Total dose at 50 cm, comparison of a dose tabulation method with the aggregate equivalent calculation (mRem/hour)

	Aggregate	3 Sigma	Tabulation	3 Sigma	Percent of Aggregate
Pu-only 1st Recycle	26.206	0.575	18.537	0.817	70.74%
Pu-only 10th Recycle	32.756	0.692	24.943	0.850	76.15%
Pu-only 60th Recycle	32.570	0.682	22.842	0.827	70.13%
PuNp 1st Recycle	24.359	0.536	14.154	0.470	58.10%
PuNp 10th Recycle	35.395	0.841	24.664	1.029	69.68%
PuNp 60th Recycle	34.540	0.810	24.115	0.948	69.82%
PuNpAm 1st Recycle	196.457	3.232	38.891	1.729	19.80%
PuNpAm 10th Recycle	659.920	9.958	83.046	4.657	12.58%
PuNpAm 60th Recycle	609.353	9.148	83.063	4.624	13.63%
PuNpAmCm 1st Recycle	832.151	5.171	674.441	1.755	81.05%

PuNpAmCm 10th Recycle	7126.976	30.477	6557.065	28.639	92.00%
PuNpAmCm 60th Recycle	9032.709	36.449	8491.579	31.023	94.01%
PuNpAmCmBkCf 1st Recycle	832.173	5.171	674.441	1.755	81.05%
PuNpAmCmBkCf 10th Recycle	44107.233	167.452	43317.742	28.639	98.21%
PuNpAmCmBkCf 60th Recycle	216849.944	833.998	215279.105	31.034	99.28%

7. Summary Findings

Isotopic evolution plays an important role in the in-core reactivity and out-of-core fuel manufacturing, handling and transportation safety attributes of recycled fuel. The rate of isotopic evolution as well as the equilibrium fuel concentration is dictated by reactor physics, decay storage time and reprocessing scheme. Not every isotope shares equal importance to overall fuel-cycle performances. Some isotopes are a transmutation gateway to other isotopes which impact heat and dose issues to future radiation workers handling recycled fuel. Many of these gateway isotopes and their transmutation progeny may create Doppler and coolant void issues in the transuranic burner and affect LWRs and SFRs differently.

7.1 Discussion

Gateway isotopes are generally born in LWR UOX and then fed to the thermal or fast burner reactor along with the recycled TRUs from spent LWR fuel. Pu-241 is a gateway into what has been defined in this report as trans-plutonium (i.e., elements heavier than plutonium), as its decay produces americium and its transmutation leads to another gateway, Pu-242, that leads to americium. Pu-242 transmutes into Am-243 which is a gateway into Cm-244. Neither of these isotopes have relatively significant contributions to radiation worker dose or repository related hazards, yet they collectively breed Cm-244 which is contributing to decay heat power and neutron field intensity detriment to fuel handling. Cm-244 is a gateway to a chain of transmutations ultimately ending in Cf-252. Cf-252 is strongly contributing to neutron dose to radiation workers, even in concentrations as low as micro-grams per kilogram of fresh fuel. Almost all trans-plutonium contributes strongly to gamma radiation fields.

Even in fast reactors, the breeding of Cm-244 is significant with equilibrium concentrations per heavy metal comparable to MOX-UE. In fact the buildup of Cm-244 is greater for lower conversion ratio. Lower conversion ratio requires a greater LWR SNF contribution to the SFR fresh fuel. Hence more gateways are introduced into the SFR's fuel cycle.

The equilibration time of Cm-244 is in the range of 50-75 years is comparable between MOX-UE and SFR. If very short spent SFR fuel cooling times are desired, such as might be assumed for on-site reprocessing, the Cm-244 equilibration time is shorter and equilibrium concentration per heavy metal is greater than *both* MOX-UE and SFRs scenarios with cooling times of 10 years.

For Cf-252, the equilibrium concentrations per heavy metal are four orders of magnitude higher for MOX-UE than they are for SFR scenarios of *10 years* cooling time. The MOX-UE scenarios have Cf-252 concentration of only about two orders of magnitude higher than a SFR scenario of *0.8 years* cooling time. Depending on the time allowed for Cf-252 to decay away before recycling (~10 years), the neutron sources of MOX-UE (10 years cooling) can only be about one order of magnitude greater than that of SFR (0.8 years cooling). Because the buildup of Cf-252 in the fuel cycle is slow, the very large

differences between the MOX-UE and the SFR neutron source term only become important after 50-75 years of recycling, depending on the cooling times selected.

Though increasing decay time can potentially decrease the cost of recycling due to the decrease in radiologic source terms, this decay allows for an important fissile isotope to be wasted, Pu-241. The loss of reactivity value to the fresh fuel in both thermal and fast burner reactors can have an impact on the overall amount of electricity that can be produced from the original uranium resource taken from the Earth. Fuel cycle scenarios evaluated that recycled Pu or TRU in MOX allowed for slightly more uranium resource utilization than if the fuel were allowed to sit in spent fuel decay storage for the same amount of time, before recycle in fast reactors. A likely explanation for this is that valuable Pu-241 was lost for the scenario where TRU was decay stored as opposed to recycled in MOX. In the scenarios where TRU was irradiated in MOX before irradiated in the fast reactor, the Pu-241 concentration was sustained by the transuranic conversion achievable in MOX. In fact, the transuranic conversion ratio of the MOX studied was higher than the SFR design selected for the study.

Because most gateway isotopes and their transmutation progeny are non-fissile with threshold fission and neutron capture cross-section properties atypical of current day fuel, their buildup in the fuel cycle ultimately changes the reactor safety performance over time. The timing of these changes is a dynamic evolutionary process that may come into play after only a few recycles or could be a potential non-issue if they require multiple centuries to equilibrate.

In MOX-UE, the multi-recycle of americium leads to a slightly positive void coefficient after approximately 10 recycles. In the scenario evaluated, this number of recycles corresponds to about 150 years. In heterogeneous-IMF, it was found that the number of IMF pins had to be continuously increased with successive recycles to ensure an acceptable level of pin power peaking in the fuel throughout the irradiation.

For SFRs, a method was developed for evaluating certain bounding cases, such as reactor coolant void reactivity worth (an important parameter in gauging reactor safety), as a function of multiple-recycles. A SFR design with oxide fuel and a conversion ratio of CR=0.75 was evaluated for the 1st and the 10th recycle. The small changes in fuel isotopics for this single scenario did not appear to give any significant impact to the void coefficients analyzed. However, this method will be useful to test reactor safety sensitivities over multiple recycles for future scenario studies.

7.2 Recommendations for Future Work

An analysis of sustained multi-recycling in MOX-UE as a burner reactor supporting TRU produced by UOX LWRs was conducted. This analysis is useful for comparing support ratios, fuel value and fuel handling limitations with analogous SFR scenarios. A complimentary study of heterogeneous-IMF is necessary to evaluate the capabilities of inert matrix fuels in the same frame. The current heterogeneous-IMF analysis was intended for creating VISION recipes only. Due to the current calculations' in-series mass balance scheme, they can not be used as an equal comparison to the MOX-UE and SFR studies.

The void coefficient in MOX-UE with recycling PuNpAm was analyzed. This work showed that MOX-UE could have a positive void coefficient at a finite time within bounds of operating this fashion of fuel cycle. Future studies are needed to quantify the physics story causing this phenomenon. To relax the void performance limitations caused by multi-recycling americium in MOX-UE, a study on lumping MAs into target pins is recommended for future work. A target pin approach could also have dual benefits as a burnable poison, which gives a potential for economic benefit.

A methodology for the quick investigations of SFR coolant void reactivity worth over multiple recycles with high MA content was established. This method was only tested for a single SFR scenario. This

scenario had a low MA and high uranium content in the fuel. Thus, the influence of MAs and the recycle-by-recycle evolution of MAs was not very controlling in this single analysis. A more comprehensive study of void coefficients contrasting a range of uranium and MA concentrations in the fuel is recommended for future work.

An analysis of multi-tier reactor deployment (i.e., UOX-MOX-SFR) was conducted. Preliminary testing and calculations using a new "fuel value" method indicated that near term deployment of fuel recycle could be useful for conservation of fissile Pu-241. Extrapolating this conclusion to multi-recycle, leads one to desire short spent fuel cooling times. The assessment of radiologic source term evolution in this report suggests that longer cooling times are beneficial from a fuel handling perspective because of the decrease in Cm-Bk-Cf buildup. Pu-241 conservation and a Cm-244 and Cf-252 decay strategy have opposing optimal cooling time solutions. Therefore, a future trade-study is recommended to evaluate the cost compromise of aging the fuel after every reactor/recycle pass as opposed to quick turnaround scenarios.

An isotope-by-isotope dose contribution library was created for MOX-UE. This library enables tabulation methods to be used for assessing dose issues associated with future MOX-UE scenario studies. An equivalent library is needed for analysis of dose issues regarding SFRs and is recommended for future work. This information will ultimately prove useful for demonstrating bounding cases that indicate when glove-box or hot-cell fuel handling operations are more applicable.

8. References

1. G. Youinou, S. Bays, "A Neutronic Analysis of TRU Recycling in PWRs Loaded with MOX-UE Fuel (MOX with U-235 Enriched U Support)," Idaho National Laboratory, INL/EXT-09-16091, AFCI-SYSA-TRAN-SS-RT-2009-000055, (2009)
2. M. Asgari, B. Forget, S. Piet, R. Ferrer, S. Bays, Computational Neutronics Methods and Transmutation Performance Analyses for Light Water Reactors, Idaho National Laboratory, INL/EXT-07-12472, (2007)
3. M. Pope, S. Bays, S. Piet, R. Ferrer, M. Asgari, B. Forget, "Transmutation Performance Analysis for Inert Matrix Fuels in Light Water Reactors and Computational Neutronics Methods Capabilities at INL," Idaho National Laboratory, INL/EXT-07-12472, Rev. 1, (2009)
4. E. A. Hoffman, W. S. Yang, R. N. Hill, Preliminary Core Design Studies for the Advanced Burner Reactor over a Wide Range of Conversion Ratios, Argonne National Laboratory, ANL-AFCI-177, (2006)
5. E. A. Hoffman, Updated Design Studies for the Advanced Burner Reactor over a Wide Range of Conversion Ratios, Argonne National Laboratory, ANL-AFCI-189, (2007)
6. E. A. Hoffman, FY09 ANL AFCI Transmutation Studies, Argonne National Laboratory, ANL-AFCI-271, (2009)
7. M. D. DeHart, "TRITON: A Two-Dimensional Transport and Depletion Module for Characterization of Spent Nuclear Fuel," Oak Ridge National Laboratory, ORNL/TM-2005/39, Revision 5.1, Vol. I, Book 3, Section T1, (2006)
8. M. D. DeHart, "NEWT: A New Transport Algorithm for Two-Dimensional Discrete Ordinates Analysis in Non-Orthogonal Geometries," Oak Ridge National Laboratory, ORNL/TM-2005-39, Version 5.1, Vol. II, Book 4, Section F21, November, (2006)
9. S. Bays, W. Skerjanc, M. Pope, "Full Core 3-D Simulation of a Partial MOX LWR Core," Idaho National Laboratory, INL/EXT-09-15913, (2009)
10. J. A. Stillman, "Mixed-Oxide Assembly Design for Series 1 Transmutation," Argonne National Laboratory, ANL-AFCI-086, (2003)
11. J. A. Stillman, "Homogeneous Recycling Strategies in LWRs for Plutonium, Neptunium, and Americium Management," Argonne National Laboratory, ANL-AFCI-124, (2004)
12. J. A. Stillman, T. H. Bauer, R. N. Hill, R. A. Wigeland, Follow-up Analyses for the ANTT Review, (2004)
13. B. Forget, M. Asgari, R. Ferrer, S. Bays, "Impact of Including Higher Actinides in Fast Reactor Transmutation Analyses," Idaho National Laboratory, INL/EXT-07-13247, (2007)
14. S. J. Piet, et al, "Description of Transmutation Library for Fuel Cycle System Analyses," Idaho National Laboratory, GNEP-SYSA-PMO-MI-DV-2009-000004, INL/EXT-08-15053, (2008)
15. S. J. Piet, "Selection of Isotopes and Elements for Fuel Cycle Analysis," Proceedings of Advances In Nuclear Fuel Management IV (ANFM-IV), Hilton Head, South Carolina, April 12-15, 2009, INL/CON-08-15050, (2009)
16. International Atomic Energy Agency, Information Circular, INFCIRC/153, (1972)
17. S. Glasstone and A. Sesonske, Nuclear Reactor Engineering: 3rd Edition, Van Nostrand Reinhold Company, New York, New York, pp. 103, (1981).

18. Korea Atomic Energy Research Institute, Table of Nuclides, Retrieved September 13, 2009, from http://atom.kaeri.re.kr/, (2000)

19. S. Bays, P. Medvedev, M. Pope, R. Ferrer, B. Forget, M. Asgari, "Conceptual Design of the Transmutation Targets for Heterogeneous Recycling of Americium and Curium in Fast Spectrum Reactors," Idaho National Laboratory, INL/EXT-08-14831, (2008)

20. I. C. Gauld, S. M. Bowman, J. E. Horwedel, "Origen-ARP: Automatic Rapid Processing for Spent Fuel Depletion, Decay, and Source Term Analysis," Oak Ridge National Laboratory, ORNL/TM-2005/39, Version 5.1, Vol. I, Book 2, Section D1, (2005)

21. KTH Royal Institute of Technology, Division of Reactor Physics, Retrieved September 13, 2009, from http://www.neutron.kth.se/courses/transmutation/Bateman/Bateman.html, (2009)

22. R. Ferrer ; M. Asgari ; S. Bays ; B. Forget, "Fast Reactor Alternative Studies: Effects of Transuranic Groupings on Metal and Oxide Sodium Fast Reactor Designs," Idaho National Laboratory, INL/EXT-07-13236, (2007)

23. "CRC Handbook of Chemistry and Physics: 88th Edition," Taylor and Francis Group, Boca Raton, Florida, United States, (2008)

24. R. M. Ferrer, S. Bays, M. Pope, "Sensitivity Analysis of Reprocessing Cooling Times on Light Water Reactor and Sodium Fast Reactor Fuel Cycles," Idaho National Laboratory, INL/EXT-08-14200, (2008)

25. S. Pillon, J. Somers, S. Grandjean, J. Lacquement, "Aspects of Fabrication of Curium Based Fuels and Targets," Journal of Nuclear Materials, 320, pp. 36-43, (2003)

26. S. Piet, Personal Communication, September, (2009)

27. A. G. Croff, "Origen2: A Versatile Computer Code for Calculating the Nuclide Compositions and Characteristics of Nuclear Materials," Nuclear Technology, 62, pp. 335-352, (1983)

28. B. Dixon, J. Carter, R. Geddes, B. Halsey, M. Nutt, S. Piet, D. Shropshire, R. Weiner, K. Williams, Minor Actinides Trade Study Report, AFCI-SYSA-AI-MI-DV-2009-000077, (2009)

29. D. Shropshire, et al, System Losses and Assessment Trade Study, in preparation

30. S. K. Yee, "Nuclear Fuel Cycle Modeling Approaches for Recycling and Transmutation of Spent Nuclear Fuel," Masters Thesis, Ohio State University, (2008)

31. X-5 Monte Carlo Team, MCNP – A General Monte Carlo N-Particle Transport Code, Version 5. Volume I: Overview and Theory, LA-UR-03-1987, (2003)

32. I. C. Gauld, O. W. Hermann, and R. M. Westfall, ORIGEN-S: Scale System Module to calculate Fuel Depletion, Actinide Transmutation, Fission Product Buildup and Decay, and Associated Radiation Source Terms, Oak Ridge National Laboratory, ORNL/TM-2005/39, Version 5.1, Vol. II, Book 1, Section F7, (2006.)

33. I. C. Gauld, J. E. Horwedel, "OPUS/PLOTOPUS: An Origen-S Post Processing Utility and Plotting Program for SCALE," Oak Ridge National Laboratory, ORNL/TM-2005/39, Version 5.1, Vol. II, Book 3, Section F15, (2006)

34. K. Wirtz, Lectures on Fast Reactors, American Nuclear Society, La Grange Park, Illinoise, pp. 133, (1982)

35. M. Kotschenreuter, P. Valanju, S. Mahajan, E. Schneider, "Fusion-Fission Transmutation Scheme-Efficient destruction of nuclear waste," Fusion Engineering and Design, 84, pp. 83-88, (2009)

36. H. Planchon, R. Singer, D. Mohr, and E. Feldman, “The Experimental Breeder Reactor II Inherent Shutdown and Heat Removal Tests - Results and Analysis,” Nuclear Engineering and Design, **91**, 287-296 (1986).

37. A. L. Reed, “Medical Physics Calculations with MCNP: A Primer,”Boston, MA: Los Alamos National Laboratory, X-3 MCC, LA-UR-07-4133,(2007)

38. D. Harder and K. Hermann, “Tissue-Equivalent Materials and the ICRU Sphere,” Radiation Protection Dosimetry, 12, pp. 125-128, (1985)

39. Nuclear Regulatory Commission, “*Code of Federal Regulations Part 20 Subpart A*,” 10CFR20, (1991)

Appendix A

Exponential Matrix Method of Solving the Bateman Equations

The exponential matrix method provides a simultaneous solution of the generalized Bateman equation for each time step. The generalized burnup equation is given in Eqn A-1.

$$\frac{dNi}{dt} = Y_j \lambda_j N_j + B_j \left(\sum_g \sigma_c^g \phi^g \right) N_j - \lambda_i N_i - \left(\sum_g \sigma_a^g \phi^g \right) N_i \qquad \text{Eqn A-1}$$

Where: N_i is the number of atoms of daughter i, N_j is the number of atoms of parent j, λ is the relevant radioactive decay constant, ϕ is the local neutron flux, σ_c is the capture cross section, σ_a is the total absorption (capture plus fission) cross section, g represents the 33 group neutron flux and cross section set, Y_j is the yield fraction of radioactive decay for isotope j going into i, and B_j is the branching ratio of isotope j going into isotope i. Eqn A-1 is determined for all combinations of i and j to form a list of first order ordinary differential equations for each daughter i. These equations are put into the matrix form shown below in Eqn A-2.

In matrix form, the Yield Fraction and Branching Ratio take on an additional numerical meaning. When i is not the radioactive decay daughter of parent j, then the yield fraction is zero. Similarly when a neutron capture in j does not create i, the branching ratio for j going into i is zero. Otherwise, when i is created by j the yield fraction or branching ratio is determined by the physics characterized by the radioactive decay or neutron reaction, respectively. The vector form of Eqn A-2 is expressed by Eqn A-3.

Given the non-linear behavior of buildup and depletion of isotopes throughout the entire irradiation, the solution can not be solved for in a simple integration, as is done for the scalar form of Eqn A-4. However, if the solution to this equation is assumed to be linear across a small time step, then an accurate approximation can be found for each step. Therefore, the entire radiation time is broken into T time steps. Then the linear solution to Eqn A-4 is found for each step.

$$\begin{bmatrix} \frac{dN_1}{dt} \\ \frac{dN_j}{dt} \\ \cdots \\ \cdots \\ \frac{dN_N}{dt} \end{bmatrix} = \begin{bmatrix} \left[-\lambda_1 N_1 - \left(\sum_g \sigma_a^g \phi^g\right) N_1\right] & \left[Y_j \lambda_j N_j + B_j \left(\sum_g \sigma_c^g \phi^g\right) N_j\right] & \cdots \\ \cdots & \cdots & \cdots \\ \cdots & \cdots & \cdots \\ \cdots & \cdots & \cdots \\ \cdots & \left[Y_j \lambda_j N_j + B_j \left(\sum_g \sigma_c^g \phi^g\right) N_j\right] & \left[-\lambda_N N_N - \left(\sum_g \sigma_a^g \phi^g\right) N_N\right] \end{bmatrix} \begin{bmatrix} N_1 \\ N_j \\ \cdots \\ \cdots \\ N_N \end{bmatrix} \qquad \text{Eqn A-2}$$

$$\frac{d\hat{N}}{dt} = \hat{\Lambda}\hat{N} \qquad \text{Eqn A-3}$$

$$\hat{N}_{t+1} = \hat{N}_t \left[e^{\Lambda(\Delta t)}\right] \qquad \text{Eqn A-4}$$

Where: N_{t+1} is the N_t vector found at time $t+\Delta t$ after t and N_t, found during the previous time interval, and is also the initial condition to Eqn A-4 for the next times step. The exponential matrix is defined through a Taylor series expansion valid for small incremental times of Δt.

$$\left[e^{\Lambda(\Delta t)}\right] = \hat{I} + \hat{\Lambda} t + \frac{1}{2}\hat{\Lambda}^2 t^2 \qquad \text{Eqn A-5}$$

Where: I is an identity matrix and Λ^2 is the vector multiplication of matrix Λ with itself.

Appendix B

Impurity Assessment Data Tables

Table B-1 shows the cross sections and differential reactivity coefficients used in assessing the impact of impurities.

Table B-1. Cross Sections and Differential Reactivity Coefficients

	ORIGEN 2.2		Differential Reactivity Coefficients at End of Cycle [6]		
	LMFBR cross sections	MOX-Pu cross sections	Metal Fuel Fast Reactor CR=0.50	Oxide Fuel Fast Reactor CR=0.50	LWR with MOX-Pu
H (natural)	0.000201	0.016098	-2.623	-2.416	-0.015
H-1	0.000202	0.016100	-2.623	-2.416	-0.015
H-2	0.000000	0.000023	-0.625	-0.586	-0.013
He (natural)	0.000005	0.000078	-0.133	-0.138	-0.005
He-3	3.860000	56.160000	-4.285	-6.413	-23.386
He-4			-0.133	-0.138	-0.005
Li (natural)	0.000012	0.001344	-0.097	-0.111	-0.185
Li-6	0.000020	0.001198	-0.880	-1.081	-2.453
Li-7	0.000011	0.001356	-0.033	-0.032	-0.001
Be (natural, Be-9)	0.000006	0.000390	-0.038	-0.038	0.000
Be-9	0.000006	0.000390	-0.038	-0.038	0.000
B (natural)	0.000103	0.004461	-0.218	-0.316	-1.108
B-10	0.000363	0.021390	-1.011	-1.501	-1.240
B-11	0.000039	0.000256	-0.021	-0.021	-0.001
C (natural)	0.000003	0.000143	-0.018	-0.019	-0.001
C-12	0.000003	0.000144	-0.018	-0.019	-0.001
C-13	0.000002	0.000060			
N (natural)	0.000059	0.003201	-0.023	-0.025	-0.006

N-14	0.000059	0.003213	-0.023	-0.025	0.000
N-15	0.000012	0.000001	-0.010	-0.011	0.000
O (natural)	0.000000	0.000008	-0.010	-0.011	0.000
O-16	0.000000	0.000008	-0.010	-0.011	0.000
O-17	0.000064	0.000000	-0.018	-0.019	-0.002
O-18	0.000001	0.000024			
F (natural, F-19)	0.000028	0.000720	-0.026	-0.025	-0.001
F-19	0.000028	0.000720	-0.026	-0.025	-0.001
Ne (natural)	0.000029	0.001702			
Ne-20	0.000027	0.001583			
Ne-21	0.000503	0.029600			
Ne-22	0.000035	0.002053			
Na (natural, Na-23)	0.001496	0.027050	-0.006	-0.007	-0.001
Na-23	0.001496	0.027050	-0.006	-0.007	-0.001
Mg (natural)	0.000061	0.002920	-0.005	-0.006	0.000
Mg-24	0.000048	0.002379			
Mg-25	0.000179	0.008404			
Mg-26	0.000040	0.001818			
Al (natural, Al-27)	0.000275	0.011400	-0.004	-0.004	0.000
Al-27	0.000275	0.011400	-0.004	-0.004	0.000

	ORIGEN 2.2		Differential Reactivity Coefficients [6]		
	LMFBR cross sections	MOX-Pu cross sections	Metal Fuel Fast Reactor CR=0.50	Oxide Fuel Fast Reactor CR=0.50	LWR with MOX-Pu
Si (natural)	0.000131	0.007483	-0.003	-0.004	0.000
Si-28	0.000126	0.007307			
Si-29	0.000204	0.011980			
Si-30	0.000171	0.005936			
P (natural, P-31)	0.000129	0.007676	-0.003	-0.004	0.000
P-31	0.000129	0.007676	-0.003	-0.004	0.000
S (natural)	0.000373	0.021975	-0.006	-0.007	-0.001
S-32	0.000385	0.022670	-0.005	-0.007	-0.001
S-33	0.000000	0.000000	0.000	0.000	-0.004
S-34	0.000174	0.010270	0.000	0.000	0.000
S-36	0.000109	0.006416	0.000	0.000	0.000
Cl (natural)	0.020919	1.356779	-0.003	-0.004	-0.015
Cl-35	0.027450	1.784000			
Cl-37	0.000494	0.020810			
Ar (natural)	0.000673	0.031529			
Ar-36	0.004037	0.219700			
Ar-38	0.000646	0.035160			
Ar-40	0.000662	0.030890			
K (natural)	0.001512	0.084139	-0.004	-0.005	-0.001
K-39	0.001453	0.084260			
K-40	0.021800	1.283000			
K-41	0.002293	0.080380			
Ca (natural)	0.000317	0.018245	-0.003	-0.005	-0.001
Ca-40	0.000291	0.017110			
Ca-42	0.000468	0.027740			
Ca-43	0.008882	0.328900			
Ca-44	0.000904	0.045360			
Ca-46	0.000517	0.030060			
Ca-48	0.000799	0.047050			
Sc (natural)	0.011640	0.713500			
Sc-45	0.011640	0.713500			
Ti (natural)	0.004817	0.265196	-0.002	-0.002	-0.002
Ti-46	0.000646	0.028720			
Ti-47	0.002907	0.097040			
Ti-48	0.005975	0.338100			
Ti-49	0.002422	0.106100			
Ti-50	0.000191	0.008537			
V (natural)	0.004620	0.229619	-0.002	-0.003	-0.001
V-50	0.108200	3.828000			
V-51	0.004360	0.220600			

	ORIGEN 2.2		Differential Reactivity Coefficients [6]		
	LMFBR cross sections	MOX-Pu cross sections	Metal Fuel Fast Reactor CR=0.50	Oxide Fuel Fast Reactor CR=0.50	LWR with MOX-Pu
Cr (natural)	0.018186	0.241802	-0.002	-0.003	-0.001
Cr-50	0.012270	0.690600			
Cr-52	0.019440	0.162300			
Cr-53	0.014290	0.794000			
Cr-54	0.000291	0.015820			
Mn (natural, Mn-55)	0.070260	0.904000	-0.005	-0.007	-0.008
Mn-55	0.070260	0.904000			
Fe (natural)	0.011069	0.128956	-0.002	-0.003	0.000
Fe-54	0.001938	0.100600			
Fe-56	0.011890	0.131400			
Fe-57	0.002100	0.110400			
Fe-58	0.001922	0.064990			
Co (natural, Co-59)	0.064240	1.363000	-0.005	-0.007	-0.029
Co-59	0.064240	1.363000			
Ni (natural)	0.015415	0.214863	-0.003	-0.004	-0.001
Ni-58	0.021010	0.231400			
Ni-60	0.002422	0.125400			
Ni-61	0.002584	0.118100			
Ni-62	0.010980	0.617000			
Ni-64	0.001777	0.073830			
Cu (natural)	0.006668	0.218780	-0.005	-0.008	-0.002
Cu-63	0.007913	0.260000			
Cu-65	0.003876	0.126300			
Zn (natural)	0.003719	0.089127	0.000	0.000	-0.001
Zn-64	0.002261	0.058020	0.000	0.000	-0.001
Zn-66	0.001292	0.046170			
Zn-67	0.032300	0.692200			
Zn-68	0.004971	0.104500			
Zn-70	0.000060	0.003550			
Ga (natural)	0.034624	0.596854	-0.008	-0.012	-0.003
Ga-69	0.025190	0.420700			
Ga-71	0.048840	0.862300			
Ge (natural)	0.055328	0.295149	-0.003	-0.005	0.000
Ge-70	0.003559	0.153200			
Ge-72	0.051690	0.082340	-0.004	-0.005	0.000
Ge-73	0.355800	2.849000	-0.014	-0.025	0.000
Ge-74	0.030400	0.040050	-0.002	-0.004	0.000
Ge-76	0.020340	0.055660	-0.001	-0.002	0.000
As (natural, As-75)	0.376900	2.164000	-0.019	-0.030	0.000
As-75	0.376900	2.164000	-0.019	-0.030	0.000

	ORIGEN 2.2		Differential Reactivity Coefficients [6]		
	LMFBR cross sections	MOX-Pu cross sections	Metal Fuel Fast Reactor CR=0.50	Oxide Fuel Fast Reactor CR=0.50	LWR with MOX-Pu
Se (natural)	0.094131	0.774796	-0.005	-0.007	0.000
Se-74	0.912500	14.950000	-0.013	-0.019	0.000
Se-76	0.161400	4.050000	-0.008	-0.013	0.000
Se-77	0.368600	2.554000	-0.018	-0.028	0.000
Se-78	0.064540	0.185900	-0.003	-0.006	0.000
Se-79	0.002584	0.166400			
Se-80	0.054450	0.066320	-0.003	-0.005	0.000
Se-82	0.009162	0.007036	-0.001	-0.001	0.000
Br (natural)	0.507962	3.332203	-0.024	-0.037	0.000
Br-79	0.658900	4.776000	-0.030	-0.047	0.000
Br-81	0.352800	1.848000	-0.017	-0.026	0.000
Kr (natural)	0.110819	2.323240	-0.004	-0.006	-0.007
Kr-78	0.008178	0.263900	-0.014	-0.021	0.000
Kr-80	0.198600	2.419000	-0.011	-0.017	0.000
Kr-81	0.000000	0.000000			
Kr-82	0.147600	6.426000	-0.006	-0.008	0.000
Kr-83	0.502000	12.550000	-0.011	-0.017	-0.058
Kr-84	0.054190	0.136600	-0.003	-0.005	0.000
Kr-85	0.038690	0.113000	-0.001	-0.003	0.000
Kr-86	0.003364	0.007867	-0.001	-0.001	0.000
Kr-87	0.436000	25.660000			
Rb (natural)	0.156931	0.207495	-0.008	-0.012	0.000
Rb-85	0.211300	0.256800	-0.010	-0.015	0.000
Rb-86	0.176900	1.006000	-0.007	-0.013	0.000
Rb-87	0.016010	0.079700	-0.002	-0.003	0.000
Rb-88	0.000727	0.042770			
Sr (natural)	0.015296	0.284378	0.000	-0.001	-0.001
Sr-84	0.005496	0.088340	-0.011	-0.016	-0.003
Sr-86	0.073330	0.279800	-0.003	-0.005	-0.001
Sr-87	0.101400	3.649000	-0.004	-0.007	-0.025
Sr-88	0.001135	0.001047	0.001	0.000	0.001
Sr-89	0.021040	0.035320	0.000	-0.001	0.000
Sr-90	0.013020	0.047210	-0.001	-0.002	0.000
Y (natural)	0.022530	0.077170	-0.001	-0.002	0.000
Y-89	0.022530	0.077170	-0.001	-0.002	0.000
Y-90	0.128200	0.288900	-0.007	-0.010	0.000
Y-91	0.041530	0.106400	-0.003	-0.004	0.000

	ORIGEN 2.2		Differential Reactivity Coefficients [6]		
	LMFBR cross sections	MOX-Pu cross sections	Metal Fuel Fast Reactor CR=0.50	Oxide Fuel Fast Reactor CR=0.50	LWR with MOX-Pu
Zr (natural)	0.032904	0.057387	-0.001	-0.002	0.000
Zr-90	0.022910	0.022300	-0.001	-0.001	0.000
Zr-91	0.084330	0.251700	-0.002	-0.005	-0.001
Zr-92	0.039170	0.051940	-0.002	-0.003	0.000
Zr-93	0.095330	1.026000	0.000	0.000	-0.007
Zr-94	0.020830	0.018550	-0.002	-0.003	0.000
Zr-95	0.154600	0.233500	0.000	0.000	-0.022
Zr-96	0.047050	0.197900	-0.001	-0.003	-0.001
Nb (natural)	0.212500	0.402700	-0.010	-0.015	0.000
Nb-93	0.212500	0.402700	-0.010	-0.015	0.000
Nb-93m	0.000000	0.000000			
Nb-94	0.240000	3.857000	-0.010	-0.016	0.000
Nb-95	0.352500	0.871800	-0.013	-0.021	-0.021
Mo (natural)	0.121102	1.080405	-0.007	-0.010	-0.005
Mo-92	0.000840	0.013670	-0.003	-0.004	0.000
Mo-94	0.048630	0.043310	-0.003	-0.005	0.000
Mo-95	0.291800	3.911000	-0.013	-0.019	-0.021
Mo-96	0.059720	0.713100	-0.004	-0.005	-0.004
Mo-97	0.275200	0.654800	-0.012	-0.019	-0.004
Mo-98	0.108200	1.058000	-0.005	-0.008	-0.001
Mo-99	0.468100	1.038000	-0.021	-0.030	0.000
Mo-100	0.079680	0.155400	-0.004	-0.006	0.000
Tc	0.476700	9.447000	-0.023	-0.035	-0.033
Tc-99	0.476700	9.447000	-0.023	-0.035	-0.033
Ru (natural)	0.254730	1.288063	-0.013	-0.019	-0.004
Ru-96	0.010660	0.163100	-0.017	-0.024	0.000
Ru-98	0.005814	0.342200	-0.006	-0.009	0.000
Ru-99	0.484900	4.440000	-0.019	-0.029	0.000
Ru-100	0.163800	0.548400	-0.007	-0.011	-0.002
Ru-101	0.517600	3.041000	-0.029	-0.042	-0.020
Ru-102	0.182500	0.220200	-0.007	-0.010	-0.001
Ru-103	0.425700	2.547000	-0.019	-0.026	-0.081
Ru-104	0.137800	0.269300	-0.006	-0.009	-0.001
Ru-105	0.337200	0.314700	-0.016	-0.022	-0.001
Ru-106	0.078920	0.091880	-0.004	-0.006	0.000
Rh (natural)	0.679000	26.920000	-0.028	-0.040	-0.067
Rh-103	0.679000	26.920000	-0.028	-0.040	-0.067
Rh-104	0.029070	1.711000			
Rh-104m	0.581400	34.220000			
Rh-105	0.552600	596.800000	-0.022	-0.032	0.008
Rh-106	0.000000	0.000000			

	ORIGEN 2.2		Differential Reactivity Coefficients [6]		
	LMFBR cross sections	MOX-Pu cross sections	Metal Fuel Fast Reactor CR=0.50	Oxide Fuel Fast Reactor CR=0.50	LWR with MOX-Pu
Pd (natural)	0.316068	2.886933	-0.015	-0.022	-0.017
Pd-102	0.003488	0.205300	-0.008	-0.012	0.000
Pd-104	0.270600	0.702000	-0.012	-0.017	-0.003
Pd-105	0.802600	3.418000	-0.033	-0.047	-0.019
Pd-106	0.160100	0.295000	-0.010	-0.015	-0.001
Pd-107	0.550300	2.587000	-0.031	-0.045	-0.022
Pd-108	0.170700	7.294000	-0.010	-0.015	-0.046
Pd-110	0.151400	0.279700	-0.007	-0.011	0.000
Ag (natural)	0.589160	21.181178	-0.026	-0.038	-0.055
Ag-107	0.683700	4.831000	-0.025	-0.036	-0.023
Ag-109	0.487400	38.780000	-0.028	-0.041	-0.090
Ag-110	0.059590	3.508000			
Ag-110m	0.059590	3.508000			
Ag-111	0.673300	3.700000	-0.020	-0.034	0.000
Cd (natural)	0.281611	212.328142	-0.011	-0.016	0.001
Cd-106	0.000727	0.042770	-0.010	-0.015	0.000
Cd-108	0.195100	0.233700	-0.008	-0.011	0.000
Cd-109	0.472400	27.800000			
Cd-110	0.261400	1.855000	-0.010	-0.015	-0.009
Cd-111	0.407700	2.599000	-0.016	-0.023	-0.010
Cd-112	0.230900	0.584200	-0.009	-0.013	0.000
Cd-113	0.391900	1730.000000	-0.015	-0.022	0.032
Cd-113m	0.000000	0.000000			
Cd-114	0.289700	0.716200	-0.010	-0.015	0.000
Cd-115	0.693400	0.000000	-0.017	-0.032	0.000
Cd-115m	0.576500	7.465000			
Cd-116	0.109400	0.112600	-0.004	-0.006	0.000
Cd-118	0.000363	0.021390			
In (natural)	0.444590	78.864680	-0.016	-0.023	-0.354
In-113	0.586800	6.860000	-0.023	-0.031	0.000
In-115	0.438200	82.100000	-0.016	-0.023	0.000
In-117	0.003634	0.213900			
In-117m	0.003634	0.213900			
In-119	0.000291	0.017110			
In-119m	0.000291	0.017110			
In-120	0.000097	0.001410			
In-120m	0.000097	0.001410			

	ORIGEN 2.2		Differential Reactivity Coefficients [6]		
	LMFBR cross sections	MOX-Pu cross sections	Metal Fuel Fast Reactor CR=0.50	Oxide Fuel Fast Reactor CR=0.50	LWR with MOX-Pu
Sn (natural)	0.078316	0.230291	-0.003	-0.004	-0.001
Sn-112	0.030330	0.467100	-0.011	-0.015	0.000
Sn-114	0.001938	0.031420	-0.010	-0.013	0.000
Sn-115	0.048330	2.291000	-0.002	-0.004	0.000
Sn-116	0.060640	0.392500	-0.002	-0.003	0.000
Sn-117	0.201200	0.709500	-0.008	-0.011	0.000
Sn-118	0.114500	0.249500	-0.004	-0.006	0.000
Sn-119	0.055730	0.082630	-0.002	-0.004	0.000
Sn-120	0.043770	0.057860	-0.001	-0.002	0.000
Sn-122	0.022610	0.037340	0.000	-0.001	0.000
Sn-123	0.110700	0.119800	-0.003	-0.005	0.000
Sn-124	0.028810	0.239500	-0.001	-0.001	0.000
Sn-125	0.293900	0.583400	-0.005	-0.012	0.000
Sn-126	0.000000	0.000000	0.000	0.000	0.000
Sb (natural)	0.377757	4.843638	-0.011	-0.017	-0.017
Sb-121	0.463000	5.754000	-0.014	-0.021	-0.022
Sb-123	0.262900	3.617000	-0.007	-0.011	-0.011
Sb-124	0.658400	1.173000	-0.022	-0.032	0.000
Sb-125	0.286600	0.721500	-0.009	-0.014	0.000
Sb-126	0.419100	1.765000	-0.011	-0.019	0.000
Te (natural)	0.104382	1.626385	-0.003	-0.005	0.000
Te-120	0.001453	0.085550	-0.015	-0.022	0.000
Te-122	0.342700	2.546000	-0.011	-0.016	0.000
Te-123	0.484100	148.500000	-0.016	-0.024	0.000
Te-124	0.235000	0.554000	-0.008	-0.012	0.000
Te-125	0.354300	0.920100	-0.011	-0.017	0.000
Te-125m	0.000000	0.000000			
Te-126	0.104500	0.419500	-0.003	-0.005	0.000
Te-127	0.365900	0.000000	-0.010	-0.017	0.000
Te-127m	0.346700	1.767000			
Te-128	0.093960	0.116500	-0.003	-0.005	0.000
Te-129	0.119900	0.000000	-0.004	-0.006	0.000
Te-129m	0.114700	0.263900			
Te-130	0.014980	0.023760	0.000	-0.001	0.000
Te-132	0.000398	0.000426	0.000	0.000	0.000
Te-134	0.000073	0.004277			

	ORIGEN 2.2		Differential Reactivity Coefficients [6]		
	LMFBR cross sections	MOX-Pu cross sections	Metal Fuel Fast Reactor CR=0.50	Oxide Fuel Fast Reactor CR=0.50	LWR with MOX-Pu
I (natural)	0.545000	5.097000	-0.017	-0.026	-0.020
I-125	22.170000	351.400000			
I-126	65.570000	1146.000000			
I-127	0.545000	5.097000	-0.017	-0.026	-0.020
I-129	0.375700	2.096000	-0.010	-0.016	-0.007
I-130	0.567700	6.440000	-0.014	-0.025	0.000
I-131	0.142900	0.324000	-0.004	-0.007	-0.070
I-135	0.000598	0.001245	0.001	0.000	-0.003
Xe (natural)	0.189048	8.113447	-0.007	-0.011	-0.023
Xe-124	4.814000	73.470000	-0.015	-0.021	0.000
Xe-125	4.070000	239.500000			
Xe-126	0.057380	0.955400	-0.009	-0.013	0.000
Xe-128	0.170900	0.536100	-0.007	-0.009	-0.002
Xe-129	0.416600	8.142000	-0.014	-0.021	-0.033
Xe-130	0.107400	0.352400	-0.005	-0.007	-0.001
Xe-131	0.213000	27.530000	-0.010	-0.014	-0.070
Xe-132	0.066020	0.089430	-0.003	-0.005	0.000
Xe-133	0.127100	16.590000	-0.003	-0.006	0.000
Xe-134	0.032370	0.035250	-0.002	-0.003	0.001
Xe-135	0.005753	100300.000000	-0.004	-0.002	-0.039
Xe-136	0.002820	0.009644	0.000	-0.001	0.001
Cs (natural, Cs-133)	0.484500	10.630000	-0.014	-0.022	-0.035
Cs-133	0.484500	10.630000	-0.014	-0.022	-0.035
Cs-134	0.536600	10.800000	-0.015	-0.024	-0.007
Cs-134m	0.000945	0.055610			
Cs-135	0.073070	2.160000	-0.003	-0.004	-0.009
Cs-136	0.267000	1.422000	-0.007	-0.011	0.000
Cs-137	0.013030	0.022610	0.000	-0.001	0.001
Cs-141	0.000012	0.000706			
Ba (natural)	0.039767	0.316554	-0.002	-0.002	-0.001
Ba-130	0.197400	3.226000			
Ba-132	0.006177	0.363600			
Ba-134	0.110900	0.854200	-0.004	-0.005	-0.003
Ba-135	0.346800	3.539000	-0.010	-0.016	0.000
Ba-136	0.046670	0.091490	-0.001	-0.002	0.000
Ba-137	0.055730	0.331100	-0.002	-0.003	0.000
Ba-137m	0.000000	0.000000			
Ba-138	0.005692	0.020090	-0.001	-0.001	0.000
Ba-139	0.004360	0.256600			
Ba-140	0.053870	0.504300	0.000	-0.001	0.000

	ORIGEN 2.2		Differential Reactivity Coefficients [6]		
	LMFBR cross sections	MOX-Pu cross sections	Metal Fuel Fast Reactor CR=0.50	Oxide Fuel Fast Reactor CR=0.50	LWR with MOX-Pu
La (natural)	0.040894	0.675720	-0.002	-0.003	-0.001
La-138	0.667000	15.240000			
La-139	0.040330	0.662600	-0.002	-0.003	-0.001
La-140	0.319200	2.328000	-0.008	-0.014	0.000
Ce (natural)	0.019046	0.044478	0.000	-0.001	0.001
Ce-136	0.098240	1.632000			
Ce-138	0.000799	0.047050			
Ce-140	0.017240	0.038440	0.000	-0.001	0.001
Ce-141	0.138200	1.698000	-0.004	-0.006	-0.004
Ce-142	0.032450	0.065290	-0.001	-0.001	0.001
Ce-143	0.273900	1.642000	-0.005	-0.011	0.000
Ce-144	0.052810	0.111100	-0.001	-0.002	0.000
Pr (natural, Pr-141)	0.160700	1.040000	-0.004	-0.006	-0.003
Pr-141	0.160700	1.040000	-0.004	-0.006	-0.003
Pr-142	0.411800	5.131000	-0.010	-0.016	0.000
Pr-143	0.363500	8.612000	-0.009	-0.014	-0.030
Pr-144	0.000000	0.000000			
Pr-144m	0.000000	0.000000			
Nd (natural)	0.145026	2.826925	-0.004	-0.007	-0.007
Nd-142	0.038460	0.865000	-0.001	-0.002	0.000
Nd-143	0.313600	14.330000	-0.008	-0.014	-0.030
Nd-144	0.095630	0.326000	-0.002	-0.004	0.000
Nd-145	0.351100	7.860000	-0.012	-0.018	-0.025
Nd-146	0.123800	0.188800	-0.004	-0.006	0.000
Nd-147	0.700900	19.570000	-0.017	-0.028	-0.087
Nd-148	0.182200	0.829600	-0.006	-0.008	-0.009
Nd-150	0.225500	0.649800	-0.006	-0.008	-0.008
Pm (natural)	0.000000	0.000000	0.000	0.000	0.000
Pm-147	1.282000	61.270000	-0.029	-0.048	-0.074
Pm-148	7.204000	964.700000	-0.088	-0.135	0.010
Pm-148m	3.480000	1294.000000			
Pm-149	3.143000	70.010000	-0.075	-0.118	0.000
Pm-151	0.036870	74.150000	-0.004	-0.005	-0.004

	ORIGEN 2.2		Differential Reactivity Coefficients [6]		
	LMFBR cross sections	MOX-Pu cross sections	Metal Fuel Fast Reactor CR=0.50	Oxide Fuel Fast Reactor CR=0.50	LWR with MOX-Pu
Sm (natural)	0.556551	441.409699	-0.020	-0.031	-0.094
Sm-144	0.000509	0.029940	-0.010	-0.015	-0.003
Sm-145	0.079940	4.705000			
Sm-146	0.000000	0.000000			
Sm-147	0.831000	23.190000	-0.032	-0.049	-0.069
Sm-148	0.341100	1.121000	-0.010	-0.014	-0.013
Sm-149	1.464000	3019.000000	-0.054	-0.087	-0.083
Sm-150	0.412200	11.920000	-0.012	-0.017	-0.095
Sm-151	2.269000	348.500000	-0.057	-0.095	-0.266
Sm-152	0.418800	74.860000	-0.016	-0.022	-0.228
Sm-153	0.062380	82.400000	-0.005	-0.006	0.007
Sm-154	0.215800	1.374000	-0.006	-0.009	-0.012
Eu (natural)	2.967300	222.017960	-0.074	-0.118	-0.250
Eu-151	3.672000	408.800000	-0.091	-0.147	-0.293
Eu-152	4.589000	128.000000	-0.108	-0.168	-0.215
Eu-153	2.322000	50.980000	-0.059	-0.091	-0.210
Eu-154	2.764000	88.530000	-0.064	-0.101	-0.153
Eu-155	2.587000	182.400000	-0.059	-0.095	-0.074
Eu-156	0.062900	52.840000	-0.006	-0.007	-0.035
Eu-157	0.040320	38.390000	-0.002	-0.003	-0.002
Gd (natural)	6.027596	1217.177622	-0.019	-0.030	-0.012
Gd-152	4.845000	105.900000	-0.023	-0.030	-0.192
Gd-153			0.000	0.000	-0.273
Gd-154	0.995600	10.380000	-0.031	-0.046	-0.072
Gd-155	1.986000	1154.000000	-0.056	-0.092	-0.024
Gd-156	0.459100	4.182000	-0.015	-0.022	-0.033
Gd-157	3.883000	4821.000000	-0.031	-0.051	0.009
Gd-158	0.286000	1.917000	-0.009	-0.012	-0.007
Gd-160	0.203000	0.372000	-0.005	-0.007	0.000
Gd-161	22.530000	1326.000000			
Tb (natural, Tb-159)	1.439000	14.730000	-0.037	-0.062	-0.039
Tb-159	1.439000	14.730000	-0.037	-0.062	-0.039
Tb-160	0.147100	45.560000	-0.007	-0.009	0.000
Dy (natural)	1.001413	64.804673	-0.021	-0.035	-0.076
Dy-156	1.550000	23.620000			
Dy-158	0.193800	4.205000			
Dy-160	1.990000	49.540000	-0.045	-0.070	0.000
Dy-161	2.220000	52.290000	-0.041	-0.074	-0.158
Dy-162	0.862200	74.080000	-0.020	-0.031	-0.110
Dy-163	0.976100	42.170000	-0.020	-0.034	-0.071
Dy-164	0.252600	86.360000	-0.009	-0.011	0.000
Dy-165	35.530000	642.600000			

	ORIGEN 2.2		Differential Reactivity Coefficients [6]		
	LMFBR cross sections	MOX-Pu cross sections	Metal Fuel Fast Reactor CR=0.50	Oxide Fuel Fast Reactor CR=0.50	LWR with MOX-Pu
Ho (natural, Ho-165)	1.565000	23.920000	-0.031	-0.053	0.000
Ho-165	1.565000	23.920000	-0.031	-0.053	0.000
Ho-166m	0.000000	0.000000			
Er (natural)	0.516339	37.515499	-0.010	-0.017	-0.018
Er-162	0.775200	11.890000			
Er-164	0.169600	2.886000			
Er-166	0.455500	5.451000	-0.011	-0.016	0.000
Er-167	1.476000	153.700000	-0.028	-0.049	-0.075
Er-168	0.058140	0.908800			
Er-170	0.032300	0.653500	0.000	0.000	-0.009
Er-171	0.203500	11.980000			
Tm (natural,Tm-169)	2.594000	40.800000	0.000	0.000	-0.071
Tm-169	2.594000	40.800000	0.000	0.000	-0.071
Tm-170	0.742900	13.770000			
Tm-171	0.190600	2.918000	0.000	0.000	-0.031
Yb (natural)	0.273082	4.671280	0.000	0.000	-0.004
Yb-168	50.060000	840.200000			
Yb-170	0.484500	7.372000			
Yb-171	0.536200	9.412000	0.000	0.000	-0.028
Yb-172	0.040370	0.629400			
Yb-173	0.629800	9.777000			
Yb-174	0.015580	0.838500			
Yb-176	0.009690	0.218300			
Lu (natural)	0.467121	8.762246	-0.024	-0.038	0.000
Lu-175	0.429900	6.481000	-0.024	-0.038	0.000
Lu-176	1.867000	94.560000	-0.034	-0.051	0.000
Hf (natural)	2.720263	42.474523	-0.017	-0.025	-0.006
Hf-174	0.751000	23.490000	-0.023	-0.037	0.000
Hf-176	1.130000	17.670000	-0.016	-0.023	0.000
Hf-177	11.690000	181.800000	-0.036	-0.061	0.000
Hf-178	1.208000	18.650000	-0.010	-0.014	0.000
Hf-179	0.961600	15.430000	-0.025	-0.041	-0.035
Hf-180	0.069440	1.416000	-0.008	-0.010	-0.004
Hf-181	0.029070	1.711000			
Ta (natural, Ta-181)	1.145979	17.352315	-0.018	-0.029	-0.068
Ta-180	0.969000	36.640000			
Ta-181	1.146000	17.350000	-0.018	-0.029	-0.068
Ta-182	1.615000	287.500000	-0.022	-0.035	0.000

	ORIGEN 2.2		Differential Reactivity Coefficients [6]		
	LMFBR cross sections	MOX-Pu cross sections	Metal Fuel Fast Reactor CR=0.50	Oxide Fuel Fast Reactor CR=0.50	LWR with MOX-Pu
W (natural)	0.568419	8.859902	-0.008	-0.011	-0.032
W-180	0.323000	4.813000			
W-182	0.952800	14.530000	-0.008	-0.011	0.000
W-183	0.557200	8.436000	-0.013	-0.020	0.000
W-184	0.022580	0.386500	-0.006	-0.009	0.000
W-186	0.807500	12.970000	-0.006	-0.009	0.000
W187	4.457000	66.920000			
Re (natural)	1.051448	16.679629	-0.022	-0.035	0.000
Re-185	2.794000	44.260000	-0.023	-0.037	0.000
Re-187	0.010370	0.201900	-0.021	-0.034	0.000
Os (natural)	0.254651	4.094847			
Os-184	2.180000	128.300000			
Os-186	0.000000	0.000000			
Os-187	1.437000	31.730000			
Os-188	0.218000	3.311000			
Os-189	1.211000	18.360000			
Os-190	0.014050	0.330000			
Os-192	0.008656	0.190400			
Ir (natural)	3.555659	65.050490			
Ir-191	6.053000	117.800000			
Ir-193	2.070000	33.670000			
Pt (natural)	0.206158	3.323223			
Pt-190	0.109000	6.416000			
Pt-192	0.113000	2.024000			
Pt-194	0.005975	0.122700			
Pt-195	0.573300	9.212000			
Pt-196	0.012050	0.197500			
Pt-198	0.089780	1.425000			
Au (natural, Au-197)	2.519000	39.840000	-0.013	-0.021	-0.123
Au-197	2.519000	39.840000	-0.013	-0.021	-0.123
Hg (natural)	0.072167	12.838392			
Hg-196	0.667000	108.900000			
Hg-198	0.112000	1.690000			
Hg-199	0.247100	68.000000			
Hg-200	0.043600	2.566000			
Hg-201	0.043600	2.566000			
Hg-202	0.007913	0.272900			
Hg-204	0.000313	0.018390			
Tl (natural)	0.019627	0.392310			
Tl-203	0.063790	1.282000			
Tl-205	0.001130	0.019670			

	ORIGEN 2.2		Differential Reactivity Coefficients [6]		
	LMFBR cross sections	MOX-Pu cross sections	Metal Fuel Fast Reactor CR=0.50	Oxide Fuel Fast Reactor CR=0.50	LWR with MOX-Pu
Pb (natural)	0.000259	0.245799	0.000	0.000	0.001
Pb-204	0.002745	0.061230			
Pb-206	0.000323	0.986800			
Pb-207	0.000646	0.032230			
Pb-208	0.000000	0.000021			
Pb-210	0.000363	0.021390			
Bi (natural, Bi-209)	0.000177	0.003183	0.000	0.000	0.001
Bi-209	0.000177	0.003183			
Ac	0.374300	22.030000			
Ac-227	0.374300	22.030000			
Th (natural, Th-232)	0.382500	2.931000	-0.007	-0.011	-0.004
Th-228	1.636000	27.770000			
Th-229	1.615000	25.240000			
Th-230	0.197000	22.590000	-0.004	-0.006	0.000
Th-232	0.382500	2.931000	-0.007	-0.011	-0.004
Pa					
Pa-231	2.943000	56.950000	-0.039	-0.061	0.000
U (natural)					
U-232	0.653400	9.470000	0.145	0.175	0.000
U-233	0.267900	5.079000	0.131	0.166	0.045
U-234	0.611400	17.190000	0.007	0.004	-0.019
U-235	0.557700	6.398000	0.079	0.102	0.023
U-236	0.551400	8.487000	-0.006	-0.009	-0.015
U-238	0.288400	0.871800	-0.004	-0.006	-0.001
Np					
Np-237	1.516000	24.230000	-0.005	-0.017	-0.040
Pu					
Pu-238	0.730600	15.260000	0.064	0.070	-0.008
Pu-239	0.501800	26.040000	0.107	0.126	0.025
Pu-240	0.513100	43.880000	0.017	0.015	-0.013
Pu-241	0.461900	16.720000	0.139	0.180	0.026
Pu-242	0.426700	25.560000	0.011	0.009	-0.020
Pu-244	0.232300	1.065000	0.012	0.011	0.000
Am					
Am-241	1.387000	57.310000	-0.007	-0.017	-0.046
Am-242m	0.392700	45.840000	0.243	0.331	0.040
Am-243	0.053850	2.100000	-0.003	-0.011	-0.032

	ORIGEN 2.2		Differential Reactivity Coefficients [6]		
	LMFBR cross sections	MOX-Pu cross sections	Metal Fuel Fast Reactor CR=0.50	Oxide Fuel Fast Reactor CR=0.50	LWR with MOX-Pu
Cm					
Cm-242	0.336800	5.341000	0.009	0.007	-0.007
Cm-243	0.244200	7.181000	0.179	0.235	0.075
Cm-244	0.833800	13.840000	0.024	0.022	0.012
Cm-245	0.311000	14.220000	0.219	0.274	0.091
Cm-246	0.235100	2.987000	0.021	0.021	0.000
Cm-247	0.305400	12.020000	0.161	0.181	0.000
Cm-248	0.248100	6.516000	0.024	0.024	0.000
Cm-250	0.001453	0.085550			
Bk					
Bk-249	0.977100	147.300000	0.000	-0.008	0.000
Cf					
Cf-249	0.363500	29.130000	0.223	0.289	0.000
Cf-250	0.420900	293.400000	0.096	0.095	0.000
Cf-251	0.312200	128.800000	0.216	0.263	0.000
Cf-252	0.290500	2.139000	0.061	0.074	0.000